

# **Novel Biosensor Techniques for Analysis of Food Contaminants and Clinical Analytes**

**THESIS**

Submitted in partial fulfillment  
of the requirements for the degree of  
**DOCTOR OF PHILOSOPHY**

By

**GEETESH KUMAR MISHRA**

Under the Supervision of  
**Prof. Sunil Bhand**



**BITS Pilani**  
Pilani | Dubai | Goa | Hyderabad

**BIRLA INSTITUTE OF TECHNOLOGY AND SCIENCE  
PILANI (RAJASTHAN) INDIA**

**2014**

**BIRLA INSTITUTE OF TECHNOLOGY AND SCIENCE  
PILANI (RAJASTHAN)**

**CERTIFICATE**

This is to certify that the thesis entitled “**Novel Biosensor Techniques for Analysis of Food Contaminants and Clinical Analytes**” and submitted by **GEETESH KUMAR MISHRA**, ID No. **2010PHXF816G** for award of Ph.D. Degree of the Institute embodies original work done by him under my supervision.

Signature in full of the Supervisor: \_\_\_\_\_

Name in capital block letters: **Dr. SUNIL BHAND**

Designation: Professor, Department of Chemistry

Date:

## ACKNOWLEDGEMENTS

It is my privilege to take this opportunity to humbly state my gratitude to those people whom I met and interacted with in the course of my Ph.D. thesis.

It has been in our *Vedic* culture that *Guru* (Teacher) holds a supreme purpose in shaping student's life and bonding between them is un-breakable. I have no hesitation in saying that the Prof. Sunil Bhand is an outstanding supervisor for me and well fit for our *Vedic* tradition. Prof. Sunil Bhand has always contributed insightful guidance, thoughtful discussions, and timely encouragement in the due course of my Ph.D. thesis. During my research work, he provided me with high flexibility in various scientific research and creative thinking. He has provided the opportunities to take part in the national/international conferences and discussions. These opportunities have broadened my experience and knowledge in the field of science and technology. I am honored to say thanks to my beloved supervisor Prof. Sunil Bhand for his groundbreaking ideas and firm supports around the clock.

I am extremely grateful to Prof. B. N. Jain (Vice Chancellor, BITS, Pilani), Prof. K. E. Raman (Director, BITS, Pilani - K. K. Birla Goa Campus), Prof. S. K. Verma (Dean, Academic Research, Ph. D. Programme, BITS, Pilani), Prof. Sunil Bhand (Dean, Sponsored Research and Consulting, BITS, Pilani- K. K. Birla Goa campus), and Prof. P. K. Das (Associate Dean, Academic Research, BITS, Pilani - K. K. Birla Goa Campus) for providing me with the facilities to conduct my research work at BITS, Pilani - K. K. Birla Goa Campus.

I express my gratitude to the members of the Doctoral Advisory Committee, Prof. Utpal Roy, Department of Biological Sciences and Prof. N. N. Ghosh, Department of Chemistry for their guidance and co-operation. I also express my sincere thanks to Dr. R. N. Behera, Head, Department of Chemistry, Prof. Bhavana P., Convener, Departmental Research Committee, and members Dr. Halan Prakash, Dr. Mainak Banerjee, and Dr. Anjan Chattopadhyay for their support.

I extend my sincere thanks to Prof. A. P. Koley (Professor of Chemistry and Associate Dean, Instruction Division) for his valuable advice, motivation, and support at various phases of my work.

My gratitude also extends to Prof. Bengt Danielsson, Acromed Invest Lund, Sweden, Prof. Sudhir Chandra, CARE, IIT Delhi, Dr. S. F. D'Souza, Nuclear Agriculture and Biotechnology Division BARC, Mumbai, Dr. B. D. Malhotra, Delhi Technological University, Delhi, Prof. Chanchal K. Mitra, University of Hyderabad and Prof. M. Willander, Linkoping University, Sweden, for scientific interaction and fruitful discussions.

I am very thankful to my collaborators within Biosensor laboratory Dr. Kanchanmala Deshpande, Dr. Rupesh K. Mishra, Mr. Gautam Bacher, Mr. Atul Sharma, and Ms. Pranali for their active collaboration, constant support, and fruitful scientific discussions. I extend my thanks to my other lab mates, Souvik Pal, Dr. Lizy Kanungo, Arun Prusty, Aruna Singh, department colleagues Vikas Kumar, Prasath R., Subhenjit Hazra, and friends Ram K., and Gautam Kumar. I extend sincere thanks to my external collaborators Dr. Hardik Pandya and Dr. Ruchi Tiwari from CARE, IIT Delhi. I am also very thankful to Mr. Rehan Deshmukh (Department of Biological Sciences) for helping me in bacterial culturing and biochemical tests.

I must say without financial support, it would not be possible for me to carry out my research study. Therefore, I take this opportunity to thank National Agricultural Innovation Project (Senior Research Fellowship from March 2009-June 2011 and Research Associate Fellowship from July 2011-June 2014); BITS, Pilani- K. K. Birla Goa Campus (July 2014 – Sep 2014); CORE WWEM BITS Pilani (Oct 2014 onwards) for their financial support.

No words can express my gratefulness towards my grandparents Late Shri Badri Prasad Mishra and Late Smt. Sadarani Mishra; my parents Shri Onkar Nath Mishra and Smt. Bharti Mishra; my uncle Dr. Nirankar Nath Mishra and aunty Smt. Hema Mishra; my elder brother Dr. Rupesh Kumar Mishra and sister-in-law Smt. Krati Mishra; younger brother Neetesh and my sister Priyanka for their constant support, motivations, and love throughout my doctoral work.

I thank to the Almighty Lord for all the wonderful things and surrounding life he is giving to me every moment and hope his blessing will be continue on my journey.

**Geetesh Kumar Mishra**

## CONTENTS

	<b>Page No.</b>
Acknowledgement	iii
Abstract	vi
Table of Content for Chapters	x
List of Figures	xv
List of Tables	xxi
List of Abbreviations & Symbols	xxii
References	122
List of Publications	Appendix i
Brief Biography of Candidate	Appendix ii
Brief Biography of Supervisor	Appendix iii
Reprint of Publications	Appendix iv

## ABSTRACT

Public health standard depends on the quality of food products. Apart from beneficial constituents, food products also contain contaminants that are toxic in nature and can cause infections and diseases. Defining human exposure to various contaminants like chemicals (urea), biochemical (antibiotics), or biological (bacteria) is an enormous task. Conventional techniques are not capable of providing high-throughput and sensitive detection of these contaminants, especially in milk, water and clinical analytes *i.e.* urine. Current analytical techniques do not provide any reliable platform, capable of analyzing complex food matrix such as milk. Hence, there is a need for reliable detection technique to quantify the analytes in the given matrix. Biosensors have proved to be extremely reliable tools in complementing existing analytical methodologies in the detection and monitoring of an ever-increasing number of contaminants in food and water. Therefore, development of novel biosensor techniques capable of detecting the contaminants below or within permissible limits in these matrices is important (Chapter 1).

Adulteration of milk with synthetic chemicals is a serious concern for human health. Urea is commonly used as an adulterant, which decreases the nutritive value of the milk. Adulteration of milk with urea is hazardous and cause irreversible damage to the organs. Thus, regulatory authorities like Food Safety and Standards Authorities of India (FSSAI) have set permissible limit of 18–40 mg/dL for urea in the milk. Among the reported biosensor techniques, thermal biosensors are good alternative devices owing to their simplicity of operation and long-term stability. Availability of numerous enzymes and their well-defined specificity combines with the exothermic nature of many enzymatic reactions make it possible to develop thermal biosensor for detecting a wide range of biomolecules. Among the various reported transducers, enzyme thermistor (ET) has been extensively used over past 4 decades and acknowledged as one of the most widely developed heat measurement based biosensor. However, development of ET based biosensor for milk sample detection was unexplored thus, provided the opportunity for further development. Chapter 2 of this thesis presents the development of a flow injection analysis-enzyme thermistor (FIA-ET) biosensor for detection of urea adulterated in milk. The biosensor is based on the specific heat measurement resulting from the hydrolysis of urea present in milk by enzyme urease. The urease was immobilized on controlled pore glass (CPG) particles as carrier

and packed into a column to constitute an immobilized enzyme reactor mounted as an up-flow packed reactor. Using the developed FIA-ET biosensor, urea was measurable up to 250 mM in the milk in semi-automated mode and up to 500 mM in an automated mode. An excellent stability of the immobilized enzyme column (IEC) was observed up to 18 months during milk urea analysis. The developed biosensor has potential for deployment in dairy processing plants to monitor urea adulteration.

Chapter 3 of this thesis presents further development of the FIA-ET biosensor for clinical analysis *i.e.* urea in urine. Urea is an important biomarker that is routinely monitored to determine the functional ability of the renal system. Recommended range of urea in urine is 20 mg/dl. Elevated levels of urea in urine are indicative of renal dysfunction, urinary tract obstruction, dehydration, diabetes, and gastrointestinal bleeding. In order to achieve urea detection in urine suitable matrix matching protocols were developed. Urease was immobilized onto a novel material (aminated silica gel) to reduce the cost of column and subsequently to reduce the cost per sample analysis. The FIA-ET biosensor showed an excellent dynamic range for the urea present in spiked urine in the range 10–1000 mM with a good linearity and a minimum detection limit was found to be 10 mM. The immobilized urease column showed excellent stability over 7 months for urea analysis in urine. Excellent recoveries were obtained in the range 92.26–99.80 % in the spiked urine samples. The FIA-ET biosensor has been automated for real time analysis with response time of 90 sec.

Chapter 4 of the thesis presents the development of FIA-EQCN biosensor for antibiotic residue analysis in the milk. Occurrence of antibiotic residues in the milk carries the risk of increasing the number of resistant bacteria and transferring antibiotic resistance genes to human pathogens. Indiscriminate use of antibiotics may produce residues in milk, and subsequently induce allergic reactions in humans. Monitoring of antibiotics is very important for safety of milk or milk products for human consumption. Several regulation agencies have fixed maximum residual limits for the antibiotic residues in milk. The United States Food and Drug Administration (USFDA) have set limit of 125 ng/mL for streptomycin (SRT) in the milk. European Union (EU) has fixed the limit at 200 ng/mL (200 ppb) for SRT in the milk whereas for sulfadiazine (SDZ) it is 100 ng/mL. The chapter is described in two parts; the first part deals

with the development of the FIA-EQCN system for analysis of the SDZ residues in milk. SDZ was chosen as a model analyte to perform the residual testing as a proof of concept. Second part of the chapter describes about the development of FIA-EQCN biosensor for ultrasensitive detection of SRT in milk samples. Obtained calibration for SDZ (10-200 ng/mL) and SRT (0.3-300 ng/mL) supports the applicability of the developed biosensor in the milk sample analysis. The obtained recoveries for SDZ (98.6-100.5%) and SRT (98-99.33%) spiked milk samples also encourage the application of developed biosensor towards the quantification of these antibiotic residues in milk samples. Developed biosensor exhibited promising results and could be adopted for analysis of antibiotics in the milk. Validation of the presented biosensor against commercial ELISA kit supports that the developed biosensor is sensitive for detection of antibiotic residues in the milk.

Chapter 5 of the thesis presents development of a novel immunosensor for rapid bacterial detection in water. Detection of contaminated water by pathogenic microorganism is an important concern for ensuring water safety, security, and public health. *Escherichia coli* (*E.coli*) is a natural inhabitant of the intestinal tracts of humans and warm-blooded animals. Presence of this bacterium in water indicates the fecal contamination of water thus, World Health Organization (WHO) have set the limit of zero bacteria in 100 mL water sample. The developed immunosensor comprised a two-electrode setup functionalized with specific antibodies against *E. coli* as bioreceptor. Optimal binding of the bacteria to the receptor antibody was achieved *via* screening of various cross linkers and quantified using electrochemical impedance spectroscopy (EIS). A linear trend of increasing impedance was obtained when the *E. coli* concentration increased. The developed immunosensor was able to detect  $10^2$ – $10^8$  CFU/mL *E. coli* bacteria in water samples. The developed immunosensor is sensitive for detection of *E. coli*. The sensor does not require any additional reagents such as fluorescent or enzyme labels for sensor response and showed stable signals.

In brief, biosensors for analysis of food contaminants (urea, antibiotic residues, and bacteria) and clinical analytes (urea in urine) has been developed under this thesis work. The major highlights of this work include development of;



- FIA-ET biosensor technology for urea analysis in adulterated milk and its validation with commercial kit and AOAC method
- FIA-ET biosensor for urea analysis in urine samples, preparation of the low cost non-porous column material and successful measurements to reduce the cost of per sample analysis; without compromising the biosensor performance
- FIA-EQCN biosensor for antibiotic residue analysis in milk, validation of the biosensor against commercial ELISA kit and application of the developed biosensor in dairy industries with automated analysis, and
- EIS based label-free immunosensor for rapid measurement of *E. coli* in water and specificity of the developed immunosensor

## Table of Content for Chapters

Chapters	Page No.
<b>1. Introduction</b>	
1.1 Scope of the research	2
1.1.1 Milk as food matrix	2
1.2 Introduction to biosensor	2
1.2.1 Bio-recognition elements used in biosensor development	3
1.2.1.1 Enzyme based biosensor	3
1.2.1.2 Antibody based biosensors	4
1.3 Transducers in biosensor	4
1.3.1 Thermal biosensor	4
1.3.2 Piezoelectric (mass sensitive) biosensor	5
1.3.3 Impedimetric (electrochemical) biosensor	5
1.4 Generation of biosensors	6
1.5 Performance criteria of biosensor	7
1.6 Analytical figures of merit	7
1.7 Immobilization of the bio-recognition element	8
1.8 State of the art for food contaminants and clinical analytes	9
1.8.1 Biosensors for urea analysis	9
1.8.2 Biosensors for antibiotic residues analysis	10
1.8.3 Biosensors for bacterial detection	11
1.9 Gaps in the existing research	12
1.10 Objective of the present research	12
1.11 Thesis structure	13
<b>2. Development of flow injection analysis-enzyme thermistor (FIA-ET) biosensor for urea analysis in adulterated milk</b>	
2.1 Introduction	17
2.1.1 Urea as adulterant in milk	17
2.1.2 State of the art for analysis of urea in milk	18

2.1.3	FIA-ET technique	19
2.1.4	Objective	19
2.1.5	Working principle of enzyme thermistor	19
2.1.6	Mechanism of urea hydrolysis by urease	20
2.2	Experimental Section	21
2.2.1	Chemicals and biochemicals	21
2.2.2	Solution preparation	21
2.2.3	Instrumentation for FIA-ET biosensor	21
2.2.4	Immobilization of urease on CPG	22
2.3	Result and Discussion	23
2.3.1	Optimization of the experimental variables for FIA-ET biosensor	23
2.3.1.1	Optimization of the pH, ionic strength and flow rate	23
2.3.1.2	Optimization of sample volume	25
2.3.2	Calibration of biosensor for urea analysis in buffer	26
2.3.3	Matrix matching for milk sample analysis	27
2.3.4	Urea analysis in milk	28
2.3.5	Calibration of biosensor for urea analysis in spiked milk	29
2.3.6	Urea recovery studies from spiked milk samples	31
2.3.7	Stability of the urease immobilized CPG column	31
2.3.7.1	Operational stability of the column	32
2.3.7.2	Storage stability and shelf life of the column	33
2.3.8	Validation of FIA-ET milk urea biosensor	34
2.3.8.1	Using FIA-ET urea biosensor	35
2.3.8.2	Using urea enzymatic assay kit	36
2.3.8.3	Using AOAC method	37
2.3.8.4	Recovery studies from spiked commercial milk samples	38
2.3.9	Precision of the biosensor for milk urea analysis	40
2.4	Conclusion	41
<b>3.</b>	<b>Development of FIA-ET biosensor for urea analysis in urine</b>	
3.1	Introduction	44

3.1.1	Urea as clinical analyte in urine	44
3.1.2	State of the art for analysis of urea in urine	44
3.1.3	Objective	46
3.2	Experimental Section	46
3.2.1	Chemicals and biochemicals	46
3.2.2	Solution preparation	46
3.2.3	Instrumentation for FIA-ET biosensor	46
3.2.4	Immobilization of urease on aminated silica gel	47
3.2.5	Surface Characterization of the Silica gel Matrix	48
3.3	Result and Discussion	50
3.3.1	Optimization of the experimental variables for FIA-ET biosensor	50
3.3.1.1	Optimization of the pH, ionic strength and flow rate	50
3.3.2	Calibration of biosensor for urea analysis in buffer	52
3.3.3	Matrix matching for urine sample analysis	53
3.3.4	Analysis in urine	54
3.3.5	Calibration of biosensor for urea analysis in spiked urine	54
3.3.6	Urea recovery studies from spiked urine samples	56
3.3.7	Operational stability of the urease immobilized silica gel column	57
3.3.8	Precision of the biosensor for urea analysis in urine	58
3.4	Conclusion	60
<b>4.</b>	<b>Development of flow injection analysis – electrochemical quartz crystal nanobalance (FIA-EQCN) biosensor for analysis of antibiotic residues in milk</b>	
4.1	Introduction	62
4.1.1	Occurrence of antibiotic residues in milk	62
4.1.2	State of the art for antibiotic detection in milk	63
4.1.3	Working principle of EQCN	66
4.1.4	Self-assembled monolayers	67
4.1.5	Objective	68
4.2	Experimental Section	68
4.2.1	Chemicals and biochemicals	68

4.2.2	Instrumentation for FIA-EQCN biosensor	69
4.2.3	Microfluidic of the flow cell	70
4.2.3	FIA-EQCN biosensor for SDZ residue analysis in milk	71
	4.2.3.1 Immobilization of anti-sulfadiazine antibodies	71
	4.2.3.2 Solution preparation	72
4.2.4	Matrix matching for milk sample analysis	72
4.3	Results and Discussion for SDZ analysis	73
4.3.1	Optimization of the FIA-EQCN system for SDZ analysis	73
	4.3.1.1 Effect of influential parameters of FIA system	73
	4.3.1.2 Optimization of antibody dilutions for pAb-SDZ	75
4.3.2	Characterization of pAb-SDZ immobilized gold crystal	76
4.3.3	Calibration of SDZ in buffer and milk	77
4.3.4	Cross reactivity of SDZ	79
4.3.5	Recovery studies from SDZ spiked milk samples	79
4.3.6	Cross validation and comparison	80
4.4	FIA-EQCN biosensor for SRT residue analysis in milk	81
4.4.1	Immobilization of anti-streptomycin antibodies	81
4.4.2	Solution preparation	82
4.4.3	Matrix matching for milk sample analysis	82
4.5	Results and Discussion for SRT analysis	83
4.5.1	Optimization of the FIA-EQCN system for SRT analysis	83
	4.5.1.1 Effect of influential parameters of FIA system	83
	4.5.1.2 Optimization for surface modification	85
	4.5.1.3 Optimization of antibody dilutions for mAb-SRT	86
4.5.2	Characterization of mAb-SRT immobilized gold crystal	87
4.5.3	Calibration for SRT in buffer and milk	89
4.5.4	Cross reactivity of SRT	92
4.5.5	Recovery studies for SRT spiked milk samples	93
4.5.6	Cross validation and comparison	93
4.5.7	Precision of the FIA-EQCN biosensor	94
4.6	Conclusion	95

<b>5.</b>	<b>Rapid label-free immunosensor for bacterial detection in water</b>	
5.1	Introduction	97
5.1.1	Label-free detection using electrochemical impedance spectroscopy	98
5.1.2	State of the art for bacterial detection	98
5.1.2.1	Conventional methods for bacterial detection	99
5.1.2.2	Biosensors for bacterial detection	99
5.1.3	Objective	101
5.1.4	Working principle of EIS	101
5.2	Experimental section	102
5.2.1	Reagents and instrumentation	102
5.2.2	Immobilization of pAb- <i>E.coli</i> on Ag-wire electrode	103
5.2.3	Experimental setup of the EIS immunosensor	104
5.2.4	Preparation of solutions, bacterial culture and dilutions	104
5.2.5	Confirmation of <i>E.coli</i> with IMViC test	105
5.3	Result and Discussion	106
5.3.1	Optimization of the Immunosensor	108
5.3.1.1	Optimization of antibody concentration	108
5.3.1.2	Influence of applied frequency	109
5.3.1.3	Influence of applied potential	109
5.3.2	Selection of SAMs for binding of <i>E. coli</i>	110
5.3.3	Surface characterization of pAb- <i>E.coli</i> modified electrodes	111
5.3.4	EIS studies for <i>E. coli</i> binding	112
5.3.5	Calibration of immunosensor for <i>E. coli</i> detection in water	114
5.3.6	Actual water sample analysis	115
5.3.7	Sensing specificity of the immunosensor	116
5.4	Conclusion	116
<b>6.</b>	<b>Conclusion and future scope of work</b>	<b>118-121</b>

## List of Figures

S. No.	Figure	Page No.
1.1	A schematic representation of biosensor components.	3
1.2	Different transduction methods for biosensor.	6
1.3	Flowchart detailing the different stages of the thesis work.	13
2.1	Molecular structure of urea.	17
2.2	Mechanism for hydrolysis of urea by urease.	20
2.3	Schematic set-up for FIA-ET for urea analysis.	22
2.4	Schematic representation of immobilization of urease on CPG.	23
2.5	Effect of pH of the PB on the response of FIA-ET biosensor for 0.1 mL injection of 100 mM urea.	24
2.6	Effect of ionic strength of PB on the response of FIA-ET biosensor for 0.1 mL injection of 100 mM urea.	24
2.7	Effect of flow rate of PB on the response of FIA-ET biosensor for 0.1 mL injection of 100 mM urea.	25
2.8	Effect of sample volume on the response of FIA-ET biosensor for injection of 100 mM urea.	26
2.9	Calibration plot obtained for urea using urease column in 100 mM PB, pH 7.2 for 0.1 mL of sample injection, flow rate 0.5 mL/min at 30°C ( $R^2 = 0.99$ , % RSD = 0.96, line equation $y = 0.42x + 2.08$ ).	27
2.10	Effect of dilution of PB and milk on the response of FIA-ET biosensor for 0.1 mL injection of 100 mM urea.	28
2.11	Calibration plot obtained for urea using urease column in milk with 0.5%, 1.5% and 3.5% fat. (Inset: linear range obtained for 0.5% fat milk urea). ( $R^2 = 0.99$ , % RSD = 0.95, line equation $y = 0.4x + 1.8$ ).	30
2.12	Response signal recorded for two different milk urea concentrations (50 mM and 100 mM) using FIA-ET biosensor. Sample volume 0.1 mL, flow rate 0.5 mL/min acquired using data acquisition system with Chart recorder.	30

2.13	Analytical performance of different urease immobilized CPG column against 100 mM urea in milk samples.	32
2.14	Operational stability of FIA-ET milk urea biosensor, response to 0.1 mL, 100 mM urea, observed for 206 days at 30°C and up to 300 days after storage at 4°C. Samples were injected randomly during the period.	33
2.15	Comparison of storage stability of urease immobilized CPG column at low temperature (4°C) and room temperature (25°C).	34
2.16	Calibration plot obtained for urea spiked milk samples using FIA-ET biosensor in 100 mM PB, pH 7.2 for 0.1mL of sample injection, flow rate 0.5 mL/min at 30°C ( $R^2 = 0.99$ , % RSD= 0.007, line equation $y= 0.0094x+0.134$ ).	35
2.17	Calibration plot obtained for urea analysis by commercial kit (absorbance at 620 nm) at 30°C, ( $R^2= 0.98$ , % RSD = 0.049) for validation of FIA-ET urea biosensor ( $R^2 = 0.99$ , % RSD = 0.007).	36
2.18	Calibration plot obtained for urea analysis by AOAC method (absorbance at 450 nm) at 30°C, ( $R^2= 0.97$ , % RSD =0.048) for validation of FIA-ET urea biosensor ( $R^2 = 0.998$ , % RSD = 0.007).	37
3.1	Schematic representation of the experimental setup of the automated FIA-ET biosensor for urea analysis in urine. A-buffer reservoir, B-automated injection valve, C-reference probe, D-thermistor, E-immobilized urease column, F-heat exchanger.	47
3.2	Schematic representation of immobilization of urease on aminated silica gel matrix.	48
3.3	SEM micrographs of bare and enzyme coupled silica matrix at magnification 400X.	49
3.4	FT-IR characterization of (1) aminated silica matrix (2) glutaraldehyde activated silica matrix and (3) immobilized urease on silica matrix. Inset: (1a, 1b, 2a and 3a) represents the corresponding FT-IR characteristic peaks.	50
3.5	Effect of pH of PB on the response of FIA-ET biosensor for 0.1 mL injection of 200 mM urea.	51



3.6	Effect of ionic strength of PB on the response of FIA-ET biosensor for 0.1 mL injection of 200 mM urea.	51
3.7	Effect of flow rate of PB on the response of FIA-ET biosensor for 0.1 mL injection of 200 mM urea.	52
3.8	Calibration plot obtained for urea using FIA-ET biosensor in 100 mM PB, pH 7.2 for 0.1mL of sample injection, flow rate 0.5mL/min at 30°C ( $R^2 = 0.99$ , % RSD = 0.02, line equation $y = 0.0098x+0.048$ ).	53
3.9	Effect of dilution of PB and urine on the response of FIA-ET biosensor for 0.1 mL injection of 200 mM urea.	54
3.10	Calibration plot obtained for urea spiked urine samples using FIA-ET biosensor in 100 mM PB, pH 7.2 for 0.1mL of sample injection, flow rate 0.5mL/min at 30°C ( $R^2 = 0.99$ , RSD=0.741, $y = 1.72x+0.14$ ).	55
3.11	Real time responses obtained from urea spiked urine samples (10-1000 mM) using FIA-ET biosensor in 100 mM PB, pH 7.2 for 0.1mL of sample injection, flow rate 0.5mL/min at 30°C.	56
3.12	Operational stability of FIA-ET urine urea biosensor, response to 0.1 mL, 200 mM urea over the period of 30 weeks at room temperature, inset: real time triplicate response obtained from FIA-ET urea biosensor against 200 mM urea of initial week and 30 <sup>th</sup> week of operation.	58
3.13	Real time triplicate sensor signal recorded from FIA-ET urea biosensor for 0.1mL sample of 200 mM urea, flow rate 0.5 mL/min at 30°C.	59
4.1	Molecular structures of some cross-reactive sulfonamides and aminoglycosides antibiotics.	63
4.2	Schematic of FIA-EQCN biosensor for antibiotic residue analysis in milk.	69
4.3	Schematic for the microfluidics of FIA-EQCN biosensor. R- Buffer reservoir, P- Peristaltic pump, and V- 6-port injection valve.	70
4.4	Schematic representation of immobilization procedure for anti-sulfadiazine polyclonal antibody (pAb-SDZ) on cystamine chloride.	71
4.5	Effect of dilution of PBS and milk on the response of FIA-EQCN biosensor for 100 ng/mL SDZ.	72

4.6	Effect of pH of PBS on the response of FIA-EQCN biosensor for 100 ng/mL SDZ. PBS 100 mM, flow rate 0.5 mL/min.	73
4.7	Effect of ionic strength of PBS on the response of FIA-EQCN biosensor for 100 ng/mL SDZ, flow rate 0.5 mL/min.	74
4.8	Effect of flow rate of PBS on response of FIA-EQCN biosensor for 100 ng/mL SDZ. PBS 100 mM, pH 7.4.	75
4.9	Effect of antibody dilution on the response of FIA-EQCN biosensor for 100 ng/mL SDZ. Carrier buffer- PBS (100 mM), pH 7.4, flow rate 0.5 mL/min.	76
4.10	SEM analysis of (i) bare gold crystal and (ii) gold crystal with immobilized antibody at 5000X magnification.	76
4.11	Calibration graph for analysis of SDZ in PBS. Inset: linear fit data representation for SDZ analysis in PBS ( $R^2 = 0.98$ , % RSD (n =3) 0.83, line equation $y = 1.3x + 215$ ).	77
4.12	Calibration graph for analysis of SDZ in milk. Inset: linear fit data representation for SDZ analysis in milk ( $R^2 = 0.98$ , % RSD (n=3) 0.80, line equation $y = 1.3x + 196$ ).	78
4.13	Comparison of the results for SDZ concentration obtained with the FIA-EQCN biosensor and commercial ELISA kit.	80
4.14	Schematic representation of immobilization procedure for anti-streptomycin monoclonal antibody (mAb-SRT) on 11-MUA.	81
4.15	Effect of dilution of the PBS and milk on the response of FIA-EQCN biosensor for 10 ng/mL SRT.	82
4.16	Effect of pH of the PBS on the response of FIA-EQCN biosensor for 10 ng/mL SRT. PBS 100 mM, flow rate 0.1 mL/min.	83
4.17	Effect of ionic strength of the PBS on the response of FIA-EQCN biosensor for 10 ng/mL SRT, flow rate 0.1 mL/min.	84
4.18	Effect of flow rate of the PBS on the response of FIA-EQCN biosensor for 10 ng/mL SRT. PBS 100 mM, pH 7.4.	85
4.19	Optimization of different self assembled monolayers. Inset: representation of different thiols attached to the gold quartz crystal.	86

4.20	Real time binding response for antibody dilutions for analysis of streptomycin. Inset: Binding capacity of the gold crystal through different layers of antibody. Carrier buffer- PBS (100 mM), pH 7.4, flow rate 0.1 mL/min.	87
4.21	FT-IR characterization of immobilized antibody on modified gold crystal.	88
4.22	Calibration graph for analysis of SRT in PBS. Inset: linear fit data representation for SRT analysis in PBS ( $R^2 = 0.99$ , % RSD 0.23-2.13 n=3, line equation $y = 67.05x + 202.64$ ).	89
4.23	Calibration graph for analysis of SRT in milk. Inset: linear fit data representation for SRT analysis in milk ( $R^2 = 0.99$ , % RSD 0.13-1.10 n=3, line equation $y = 64.024x + 205.40$ ).	90
5.1	Schematic representations for surface modification of Ag-wire electrode and immobilization of <i>E.coli</i> antibody with experimental setup of EIS immunosensor.	104
5.2	Metallic green colonies of <i>E. coli</i> on EMB agar medium.	106
5.3	IMViC test results of <i>E.coli</i> .	107
5.4	Impedance values at 10 Hz for dilutions of pAb- <i>E. coli</i> antibody with PBS (0.1 M, pH 7.4) for $10^4$ CFU/mL <i>E.coli</i> .	108
5.5	Impedance values for various concentration of <i>E. coli</i> at 1 Hz, 10 Hz and 100 Hz.	109
5.6	Voltage-current waveform at 10 mV applied potential.	110
5.7	Percentage impedance change for different SAMs (Cysteaminium, L-Cysteine and 11- MUA) for different concentrations of <i>E. coli</i> ( $10^2$ – $10^8$ CFU/mL). EIS: 1-100 KHz applied frequency and 10 mV applied potential.	111
5.8	Surface characterization of pAb- <i>E. coli</i> modified electrodes using fluorescence microscopy (a) image of control Ag-wire electrode, inset: non-subtracted background image of Ag-wire electrode (b) image of pAb- <i>E.coli</i> coupled Ag-wire electrode attached with FITC labeled secondary <i>E.coli</i> antibody, inset: non-subtracted background image of Ag-wire electrode.	112

5.9	Impedance spectra for PBS and <i>E. coli</i> ( $10^2$ CFU/mL) in water. EIS: 1-100 KHz applied frequency and 10 mV applied potential.	113
5.10	Calibration curve obtained for label-free impedimetric immunosensor for <i>E. coli</i> in water (SD=0.802, $R^2=0.99$ , line equation $y= 4.73x+13.31$ ) EIS: 1-100 KHz applied frequency and 10 mV applied potential.	114
5.11	Nyquist plot for sensing specificity of the functionalized Ag-wire immunosensor validated for <i>E. coli</i> against <i>Streptococcus pyogenes</i> . Concentrations of bacterial suspensions are $10^4$ CFU/mL. EIS: 1-100 KHz applied frequency and 10 mV applied potential.	116

## List of Tables

S. No.	Tables	Page No.
1.1	Analytical figures of merit for biosensor.	8
1.2	Methods of immobilization of the biological component.	9
2.1	Summary of reported biosensors for analysis of urea in milk.	18
2.2	Determination of % recovery from urea spiked commercial milk samples.	31
2.3	Recovery studies for urea from FIA-ET, commercial kit and AOAC method.	39
2.4	Intra-day and Inter-day analysis result for FIA-ET biosensor for urea analysis in milk.	40
2.5	Comparison of analytical features and figure of merit of all three method used FIA-ET, commercial kit and AOAC method.	41
3.1	Summary of reported biosensors for analysis of urea in urine.	45
3.2	Determination of % recovery from urea spiked urine samples.	57
3.3	Intra-day and inter-day reliability of FIA-ET biosensor for urea analysis in urine.	59
4.1	Summary of reported biosensor techniques for detection of SDZ and SRT in milk samples.	65
4.2	Cross reactivity of SDZ with other antibiotics.	79
4.3	Recovery studies of SDZ from spiked milk samples.	80
4.4	Real time mass change ( $\Delta m$ ) values for SRT analysis in milk sample.	91
4.5	Cross reactivity of SRT with other antibiotics.	92
4.6	Recovery studies of SRT from spiked milk samples.	93
4.7	Comparison of FIA-EQCN SRT biosensor with commercial ELISA kit.	94
4.8	Reproducibility and precision of FIA-EQCN biosensor.	95
5.1	Summary of reported biosensor techniques using EIS for detection of <i>E.coli</i> in water.	100
5.2	IMViC test results of some common bacterial species of water.	107
5.3	Impedance values for blank and different <i>E. coli</i> concentrations at 10 Hz.	114
5.4	Analytical results for actual water samples.	115

## List of Symbols & Abbreviations

<b>Symbols</b>	<b>Description</b>
$ Z $	Absolute impedance
$\Delta H$	Enthalpy change
$\Delta m$	Mass change
$\mu\text{g}$	Micro gram
$\mu\text{l}$	Micro liter
Ag	Silver
Hz	Hertz
IU	International unit
$K_d$	Dissociation constant
$K_g$	Kilo gram
$K_m$	Michaelis constant
MHz	Mega hertz
mL	Mili liter
mM	Mili molar
mV	Mili volt
ng	Nano gram
nm	Nano meter
pH	Acidity measurement unit
ppm	Part per million
$Z'$	Real impedance
$Z''$	Imaginary impedance

### **Abbreviations**

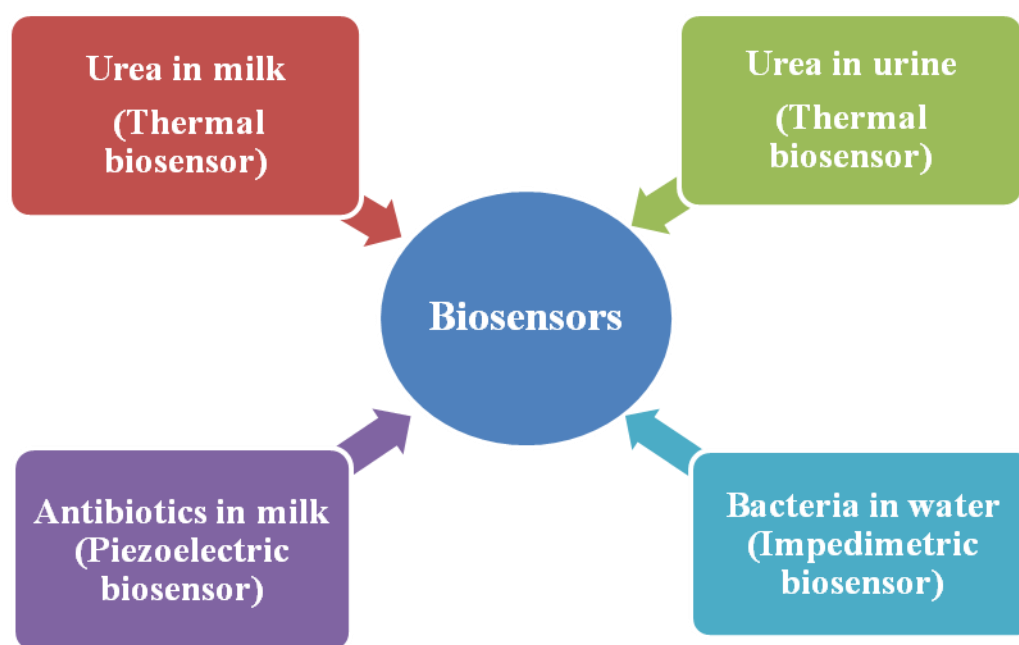
11-MUA	11-mercaptoundecanoic acid
Ab	Antibody
AC	Alternating current
ADC	Analog to digital converter

Ag	Antigen
ATR	Attenuated total reflectance
BSA	Bovine serum albumin
CFU	Colony forming unit
CNT	Carbon nanotubes
CPG	Control pore glass
DAQ	Data acquisition system
DC	Direct current
DHSRT	Dihydrostreptomycin
DNA	Deoxyribonucleic acid
<i>E. coli</i>	<i>Escherichia coli</i>
EDC	1-ethyl-3-[3-dimethylaminopropyl] carbodiimide hydrochloride
EIS	Electrochemical impedance spectroscopy
ELISA	Enzyme linked immuno sorbent assay
EMB	Eosin methylene blue
EQCN	Electrochemical quartz crystal nanobalance
ET	Enzyme thermistor
EU	European Union
FIA	Flow injection analysis
FITC	Fluorescein isothiocyanate
FSSAI	Food safety and standards authority of India
FTIR	Fourier transform infrared
GC	Gas chromatography
GENTA	Gentamycin
GLISA	Gold labeled immuno sorbent assay
HPLC	High performance liquid chromatography
IMViC	Indole Methyl Red Voges-Proskauer Citrate test
IUPAC	International Union of Pure and Applied Chemistry
KAN	Kanamycin

LC	Liquid chromatography
LOD	Limit of detection
LOQ	Limit of quantification
mAb	Monoclonal antibodies
MEMS	Micro electromechanical systems
MRL	Maximum residue limit
MR-VP	Methyl red–Voges-Proskauer
MS	Mass spectroscopy
MTCC	Microbial type culture collection
NEO	Neomycin
NHS	N-hydroxy succinimide
NTC	Negative temperature coefficient
OD <sub>600</sub>	Optical density at 600 nm
pAb	Polyclonal antibodies
PB	Phosphate buffer
PBS	Phosphate buffer saline
PCR	Polymerase chain reaction
QCM	Quartz crystal microbalance
RSD	Relative standard deviation
RNA	Ribonucleic acid
rpm	Revolution per minute
RT	Room temperature
S.D.	Standard deviation
SAMs	Self-assembled monolayers
SDZ	Sulphadiazine
SEM	Scanning electron microscopy
SPR	Surface plasmon resonance
SRT	Streptomycin
US FDA	United States food and drug administration
UV	Ultra violet



**Chapter 1**  
**Introduction**



*Graphical abstract of the thesis contents*

## 1.1 Scope of the research

Reliable and cost effective analytical methods are increasingly needed in the food and clinical diagnostic industry for determination of specific chemical compounds in foods and clinical analytes. The need arises from increased regulatory action and heightened consumer and patient's health concern about food composition and health safety. The monitoring and detection of contaminants in milk/food products and clinical samples (*i.e.* urine and serum) are the key to prevent and identify problems related to human health and safety. The conventional techniques as well as current wet chemistry and analytical practices are time consuming and may require highly skilled technicians and expensive equipment. The food and clinical industries need rapid, reliable, and affordable techniques for food quality control and prognosis as well as diagnosis of clinical analytes. The application of the biosensor in food analysis and clinical diagnostics is a growing field with increasing demand for reliable biosensors (Bhand *et al.*, 2010).

### 1.1.1 Milk as food matrix

The dietary habits of people throughout the world are different depending on the availability, ethnicity, cultural influences and the preparation and preferences for food. Access to high quality food and water is a basic need in our community. Among the various food matrices milk has gained immense importance due to its nutritional value and extensive usage. Milk is an ideal food not only for the young ones, but also for the aged ones and convalescents alike. It is an excellent source of energy, proteins, minerals and vitamins (Noyhouzer *et al.*, 2009), due to the presence of all these nutrients, milk is considered as nearest complete food. Food products may contaminate during production, processing, and handling, these contaminants are of preliminary chemicals (urea), biochemical (antibiotics), or biological (bacteria) in nature. Their source might be different, but their ultimate impacts are very severe on the society. Thus, monitoring of these contaminants in food matrix such as milk and water is very important.

## 1.2 Introduction to biosensor

A rapid proliferation of biosensors and their diversity has led to a lack of rigor in defining their performance criteria. Although each biosensor can only truly be evaluated for a particular application, it is still useful to examine how standard protocols for performance criteria may be

defined in accordance with standard IUPAC (International Union of Pure and Applied Chemistry) protocols or definitions. According to the IUPAC definition “a device that uses specific biochemical reactions mediated by isolated enzymes, immunosystems, tissues, organelles or whole cells to detect chemical compounds usually by electrical, thermal or optical signals (Compendium of Chemical Terminology, 2nd edition (the Gold Book))”. The transducer converts the biochemical signal, into a quantifiable electronic signal, which is proportional to the concentration of a specific analyte or group of analytes present. Biosensors are characterized by a high level of specificity generated by the biocomponents, which specifically reacts with a given analyte or substrate. The combination of this specificity, with a sensitive transducer, gives to biosensors their unique and unrivaled characteristics for the detection of a variety of analytes, even when they occur in complex matrices. The different components of a biosensor are shown in Figure 1.1.

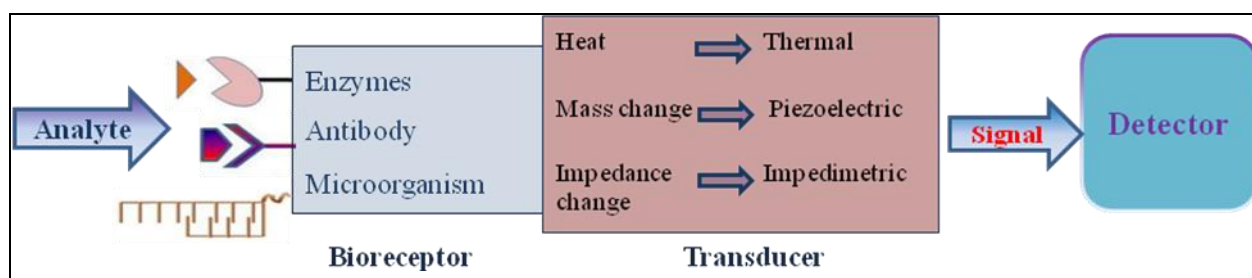


**Figure 1.1** Schematic representation of biosensor components.

## 1.2.1 Bio-recognition elements used in biosensor development

### 1.2.1.1 Enzyme based biosensor

These biosensors use enzymes as their bio-recognition element. Enzymes are the most common and extensively used bio-recognition elements in biosensors. Advantage of enzyme-based biosensor is to modify catalytic properties or substrate specificity by genetic engineering. If the enzyme metabolizes the analyte, the analyte concentration can be determined by measuring the enzymatic product or generated heat. The high substrate specificity that enzymes exhibit, makes them especially well suited for bioanalytical determinations. In particular with thermal biosensors, the ease with which enzymes can be immobilized, and their ability to cycle catalysis, makes them ideally suited particularly in thermal biosensing. Expanding interest in biodiversity

will most certainly lead to the identification of numerous enzymes with both new and variable substrate specificities that will spur the development of a never ending cascade of new biosensors (Danielsson, 1980).

### **1.2.1.2 Antibody based biosensors (Immunosensors)**

These biosensors employ interaction between an antibody and an antigen. Immunosensors are affinity ligand-based biosensor solid-state devices in which the immunochemical reaction is coupled to a transducer. The fundamental basis of all immunosensors is the specificity of the molecular recognition of antigens by antibodies to form a stable complex. This is similar to the immunoassay methodology. Immunosensors can be categorized based on the detection principle applied. The main developments are electrochemical, optical, and micro gravimetric immunosensors. In contrast to immunoassay, modern transducer technology enables the label-free detection and quantification of the immune complex (Luppa *et al.*, 2001).

## **1.3 Transducers in biosensor**

Biosensors can also be classified according to their method of signal transduction. The transducer is an important component in a biosensor through which the measurement of the target analyte is achieved by selective interaction of a bio-molecule and analyte into a quantifiable signal. Based on the type of transducers used, biosensors may be classified as optical, electrochemical, thermal, and piezoelectric. This thesis is focused on three transducers, which are described here;

### **1.3.1 Thermal biosensor**

Thermal biosensors measure the changes in temperature in the reaction between an enzyme molecule and a suitable analyte. The total heat produced or consumed in a reaction is proportional to the molar enthalpy and the number of moles produced. These temperature changes are reflected in the reaction medium. Temperature changes are recorded sensitively using thermistors. Among the various thermal transducers, thermistors comprise a major share for biosensor development. The other thermal transducers are thermocouples and resistance thermometers. A thermistor is a thermally sensitive resistor that exhibits a change in electrical resistance with a change in its temperature. Enzyme thermistor (ET) coupled with flow injection

analysis (FIA) system have advantages such as reusability of the biocatalyst, the possibility of continuous flow operation, inertness to optical and electrochemical interference, and simple operating procedures employing a small column, with the enzyme immobilized on a suitable support. The majority of thermistors have negative temperature coefficient (NTC) as the resistance decreases when the temperature rises. The temperature coefficient can change to several percentages per degree centigrade. This allows thermistors to measure small changes in temperature. Thermistors typically work over a relatively small temperature range, compared to other temperature sensors and can be very accurate and precise within that range. They are inexpensive, easily obtainable, easy to use and adaptable. Biosensors comprising of thermal transducers are robust, highly reproducible, and free from interference due to the optical or electrochemical nature of reaction constituent. Many researchers (Danielsson *et al.*, 1979; Ramnathan and Danielsson 2001; Yakovleva *et al.*, 2013) reviewed the principle and applications of thermal biosensors.

### **1.3.2 Piezoelectric (mass sensitive) biosensor**

These biosensors are based on mass-sensitive measurements and can detect small mass changes caused by chemical binding to small piezoelectric crystals. The piezoelectric biosensor is thought to be one of the most sensitive analytical instruments developed to date, being capable of detecting antigens in the picogram range. Moreover, this type of device is believed to have the potential to detect antigens in the gas phase as well as in the liquid phase. The general approach, to take advantage of the piezoelectric effect, is to coat a piezoelectric crystal with biological materials such as antibodies or enzymes, etc.; compounds that have high selectivity for the target molecule. When the coated crystal is exposed to the particular substance of interest, adsorption occurs, causing a frequency/mass change that can be used to determine the amount of material absorbed. This type of biosensor has great potential for the direct detection of different analytes such as antibiotic residues and pathogens.

### **1.3.3 Impedimetric (electrochemical) biosensor**

The third and most commonly used transducers are electrochemical. Different types of the electrochemical transducers have been employed in the development of biosensors. The main

electrochemical transducers are amperometric (measuring of current), potentiometric (measuring of electrode potential or voltage differences), and conductometric/impedometric (measuring of change in conductivity or resistance/impedance). The current produced can be correlated to either the concentration of the electro-active species present or its rate of production or consumption (Joshi et al., 2005). Capacitance measurements can also be used to develop a biosensor. Among the reported electrochemical biosensors, electrochemical impedance spectroscopy (EIS) has emerged as sensitive techniques for biosensor detection due to multiple advantages, such as fast response, low cost, and capability of miniaturization. EIS based sensors are particularly attractive since they allow label-free detection with high sensitivity. In EIS, traditionally, macro sized metal rods or wires were used as electrodes immersed in the medium to measure impedance and it is suitable to analyze the electrical properties of the modified electrodes. Figure 1.2 represents a schematic illustration for classification of biosensors based on transducers.

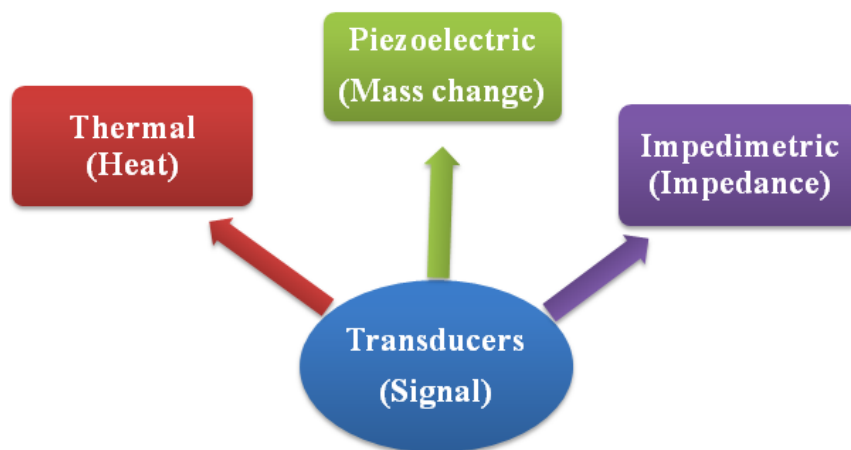


**Figure 1.2** Different transduction methods for biosensor.

#### 1.4 Generation of biosensors

Biosensors can be classified into three generations according to the degree of integration of the separate components, *i.e.* the method of attachment of the bio recognition molecule (bio-receptor) to the base indicator (transducer) element. In the first generation of biosensors, the bio receptor is retained in the vicinity of the base sensor behind a dialysis membrane, while in the subsequent generations; immobilization is achieved *via* cross-linking reagents or bi-functional

reagents at a suitably modified transducer interface or by incorporation into a polymer matrix at the transduction surface. In the second generation, the individual components remain essentially distinct (*e.g.* Control electronics-electrode-bio-molecule), while in the third generation, the bio-receptor molecule becomes an integral part of the base sensing element. It is in the second and third generations of these families that the major development effort can now be seen (Andreescu and Marty 2006).

### 1.5 Performance criteria of biosensor

The performance of a biosensor is evaluated based on various parameters. Parameters significant in evaluating biosensor performance are listed below:

- 1. Specificity:** Ability of a method to detect one element in the presence of another element.
- 2. Sensitivity:** The slope of the calibration curve. If the curve is in fact a 'curve', rather than a straight line, then of course sensitivity will be a function of analyte concentration or amount.
- 3. Precision:** Measure of instrument reproducibility, which is the ability to obtain the same value with repeated measurements of a process variable.
- 4. Stability and lifetime:** The operational stability of a biosensor may vary according to the sensor geometry, method of preparation, as well as on the applied enzyme or transducer. Storage stability is the stability of biosensor if it is stored under optimum conditions. This gives an idea of the lifetime of biosensor.
- 5. Response time:** The time required for the detector output to go from the initial value to a percentage (*e.g.* 99%) of the final value.
- 6. Sample throughput:** The number of results that is produced by an instrument divided by time of operation.

### 1.6 Analytical figures of merit

Performance of any biosensing technique is generally determined based on the analytical figures of the merits of a biosensor, which are listed below in Table 1.1.

**Table 1.1** Analytical figures of merits for biosensor

<b>Parameters</b>	<b>Biosensor Performance</b>
Dynamic range	The concentration range over which signal varies in a monotonic manner with analyte concentration.
Linearity	The relationship of signal to amount of analyte over a range of concentration of analyte with a constant proportionality factor.
Limit of detection (LOD)	The lowest concentration of the analyte which can be measured at a specific confidence level.
Limit of quantification (LOQ)	The lowest concentration level at which a measurement is quantitatively meaningful. Normally more than LOD.
Limit of linearity	The upper limit of quantification where calibration curve tends to become non-linear.
Reaction time	Time for enzyme –substrate or antigen- antibody reaction.

### 1.7 Immobilization of the bio-recognition element

The biocomponent specifically recognizes the analyte and the physiochemical changes caused by the interaction between the bio-component and the analyte such as change of light absorption or electrical charge or frequency of oscillation, etc. The key part in the preparation of biosensor is immobilization of the biocomponent or bio-recognition element. For immobilization of the biocomponent, several types of immobilization procedures are used. These are entrapment and encapsulation, covalent binding, cross-linking and adsorption. In general, the choice of procedure depends on the nature of the biological element, the type of transducer used, the physicochemical properties of the analyte and the operating conditions in which the biosensor is to function, and overriding all these considerations is the necessity for the biological element to exhibit maximum activity in its immobilized microenvironment. Table 1.2 enlists some of the advantages and disadvantages of these procedures.



**Table 1.2** Methods of immobilization of the biological component

Methods	Advantages	Disadvantages	References
Entrapment and encapsulation	No direct chemical modification. Specificity of biocatalyst and analyte interaction retained.	Applicable for small analyte detection. High diffusion barrier to both substrate and product transport. Continuous loss of biocatalyst.	Malhotra <i>et al.</i> , 2006; Sassolas, <i>et al.</i> , 2012; Verma and Singh, 2008
Covalent binding	Low diffusional resistance. Strong binding force between biocatalyst and matrix. Not affected by adverse conditions of pH, ionic strength.	May involve harsh/toxic chemicals. Matrix not regenerable. Frequently occurring loss of activity.	Sassolas, <i>et al.</i> , 2012; Petri <i>et al.</i> , 2004
Cross-linking	Used in conjunction with entrapment to reduce loss of biocomponent activity.	Harsh treatment with toxic chemicals. Covalent linkages formed amongst protein molecules rather than matrix and protein.	Sassolas, <i>et al.</i> , 2012; Barsan and Brett, 2009
Adsorption	Gentle treatment of biocatalyst. No modification of biological component. Matrix can be regenerated. Maximal retention of activity.	Very weak bonds. Susceptible to changes in pH, temperature, ionic strength.	Choi, 2004; Sassolas, <i>et al.</i> , 2012

## 1.8 State of the art for food contaminants and clinical analytes

### 1.8.1 Biosensors for urea analysis

Different detection strategies have employed for these contaminants in milk. The requirements, both in terms of time and costs, of most traditional analytical methods *e.g.* High Performance Liquid Chromatography (HPLC), Gas Chromatography/Mass Spectroscopy (GC/MS), Enzyme Linked Immuno Sorbent Assay (ELISA), Spectroscopy, Electrophoresis, etc. often makes the main impediment for their application on a regular basis. Commonly used microbial techniques

are sensitive, but it takes at least 5–7 days for results, by that time, most of the foods such as milk have been distributed or consumed. These methods are time consuming, laborious, and need large volume of samples. Thus, there is a demand for fast and simple methods, which can analyze the sample rapidly (Salman *et al.*, 2008). Current analytical techniques do not provide any reliable platform, capable of analyzing complex food matrix such as milk. Hence, there is a need for reliable detection techniques to quantify the analyte in the given matrix. Biosensors have proved to be extremely reliable tools in complementing existing analytical methodologies in the detection and monitoring of an ever-increasing number of food contaminants. Numerous biosensors have reported in recent years for milk urea analysis, such as manometric biosensor (Jenkins and Delwiche, 2002; Renney *et al.*, 2005) and potentiometric biosensor (Verma and Singh, 2003; Trivedi *et al.*, 2009). Some of these reported biosensors have a very narrow detection limit and short operational stability, which renders them unfit for routine analysis.

### **1.8.2 Biosensors for antibiotic residue analysis**

Wide varieties of antibiotics have used to treat or prevent bacterial infection in food producing animals. The use of antibiotics can effectively control the occurrence of disease and maintain the growth of animals. However, with increasing use of antibiotics, the sanitary issues, including drug residues in edible tissues of food-producing animals and the bacterial resistance been transferred from animals to human, have occurred significantly. In order to protect the consumer's health, some regulatory agencies like United States Food and Drug Administration (US FDA) and the European Union (EU) has established maximum residue limit (MRL) for antibiotics, which is around 5 $\mu$ g/kg to 200 $\mu$ g/kg in milk and milk products depending upon the group of antibiotics. Different detection strategies have employed for the determination of antibiotics levels. These include adsorptive stripping voltammetry (Alghamdi *et al.*, 2009), SPR-based Immuno-sensor (Rebe Raz *et al.*, 2009; Fernandez *et al.*, 2010), HPLC using ultraviolet adsorption or fluorescence detection and ELISA with UV–vis spectrometry (Adrian *et al.*, 2009; Rodríguez *et al.*, 2009). Among these, the lowest detection limit of antibiotic was 0.1 ng/ml, obtained with the ELISA method with fluorescence detection. ELISA is a sensitive, fast, and specific method for the detection of antibiotics in the dairy field by means of the interaction of an antigen and an antibody. However, in indirect competitive ELISA methods, experimental

procedures such as the preparation of antigen or antibody-enzyme conjugates and the reaction of enzymes with their specific substrates are complicated and time-consuming. In conclusion, biosensors form an interesting part of food and clinical analysis, and they have achieved a notable success. However, they have not yet reached their full potential and new products are being under development stage.

### **1.8.3 Biosensors for bacterial detection**

Traditional methods for the detection of bacteria involve plating and culturing, enumeration methods, biochemical testing, and microscopic examination. Although these conventional methods are reliable but they are time consuming and laborious. Some newer methods that have applied for detecting bacteria are ELISA (Magliulo *et al.*, 2007), polymerase chain reaction (PCR), multiplex and real-time PCR (Kawasaki *et al.*, 2010; Zemanick *et al.*, 2010), fluorescence in situ hybridization and DNA microarrays (Kostić *et al.*, 2010). Several label-free methods also applied, including surface plasmon resonance (SPR) and use of electrochemical impedance immunosensor (Borghol *et al.*, 2010). However, many of these methods have associated disadvantages; for example, they are expensive, complicated, and time consuming, and have low sensitivity (Shen *et al.*, 2010). In recent years, biosensors have explored for their application in the detection of pathogenic bacteria. More recently, automated platforms for flow cytometry capable of rapid detection of bacteria have been developed and widely adopted by centralized laboratories. Although rapid, these technologies do not provide microbiological diagnosis and susceptibility information, which remains the cornerstone of diagnosis and particularly in settings of complicated bacterial infections (Mach *et al.*, 2011; Pieretti *et al.*, 2010). Recently an out-break of the food borne illness in Europe being caused by a new strain of the *Escherichia coli* (*E. coli*) bacteria that is resulting in a higher incident of kidney failure, the bacteria have killed at least 17 people in Germany and Sweden and sickened about 1614 persons in 10 countries in Europe (Noam and Henry, 2011). Development of the rapid and label-free biosensor for bacterial detection in water and the sensitive detection will be very helpful for indication and update of this kind of bacterial outbreaks as well as it will help in the prognosis of the bacterial contaminations.

### **1.9 Gaps in the existing research**

Although thousands of articles are published in the field of biosensors for food and clinical analytes every year due to its vast potential, some areas that still can be explored. The areas that need special and immediate attention are:

- From the existing literature survey, it is evident that Urea is toxic when present in high concentrations. Reported biosensor techniques do not meet higher standards for monitoring their levels in milk and urine. Thus, there is a need for highly sensitivity yet with a broad working range, stable and continues monitoring biosensor to determine the level of adulteration in milk as well as in urine to appraise the renal function.
- It is evident from the existing literature that even the presence of minute amount of antibiotics can also trigger the potential health hazards, so there is a need for biosensor that can detect sensitive levels of antibiotic residues with broad range and gives stable and reproducible results without much sample preparation.
- Bacterial populations are major risk agents when present as infection. Reported biosensors do not meet the requirement to trace them rapidly. Thus, there is a need for a biosensor detection system that can provide rapid yet sensitive determination of bacteria in water samples.

### **1.10 Objective of the present research**

The present research work aims at:

1. Development of flow injection analysis-enzyme thermistor (FIA-ET) based biosensor for determination of urea adulteration in milk and urine.
2. Development of novel biosensing techniques for analysis of antibiotic residues in milk using flow injection analysis-electrochemical quartz crystal nanobalance (FIA-EQCN) based biosensor.
3. Development of novel biosensor techniques for analysis of bacterial contamination in water using electrochemical impedance spectroscopy (EIS) based biosensor.

## 1.11 Thesis structure

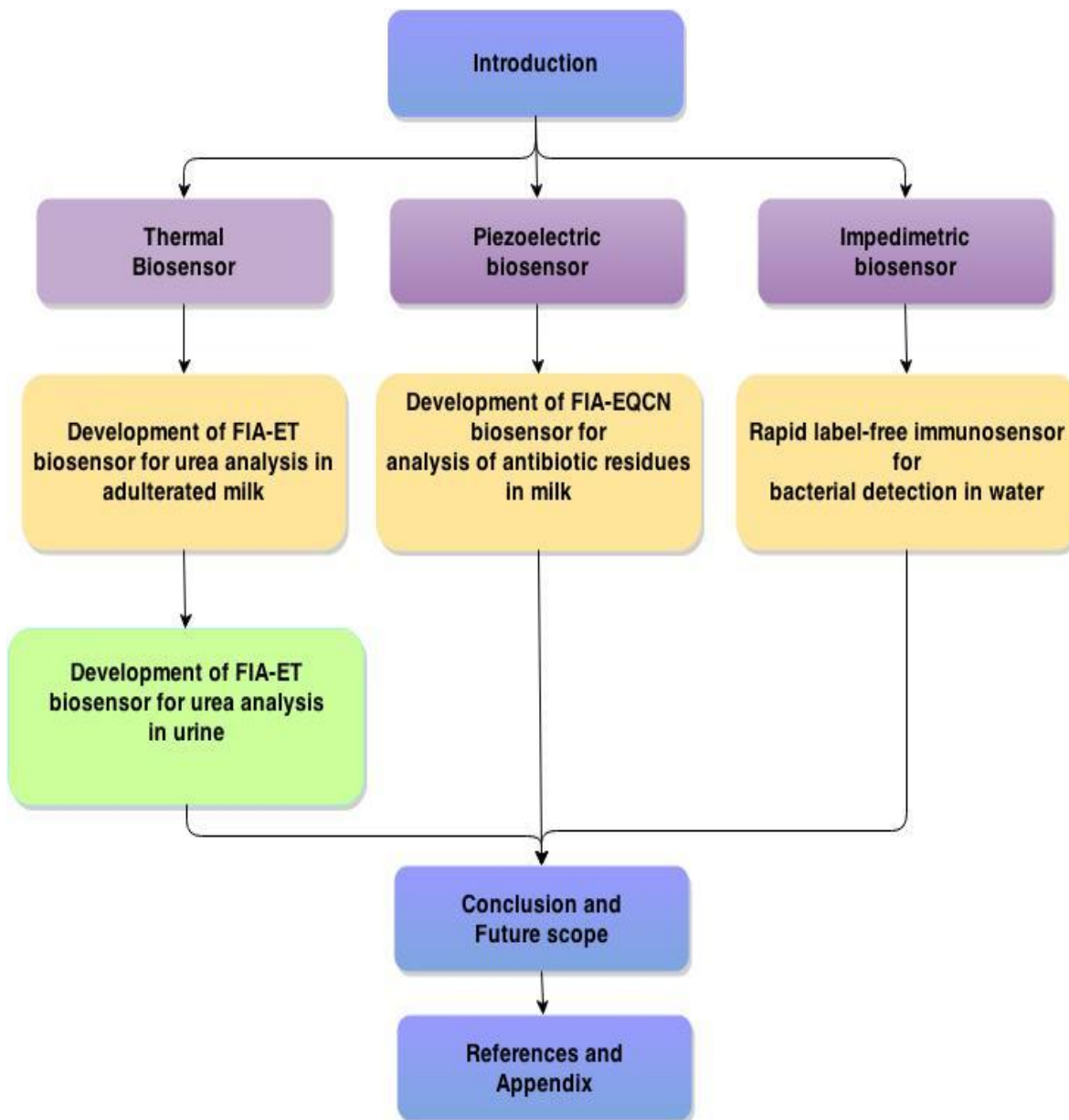


**Figure 1.3** Flowchart detailing the different stages of the thesis work.

The thesis comprises in six chapters and each of these chapters has been detailed below:

### **1.11.1 Chapter 1: Introduction**

This chapter gives a description about biosensors, classification of biosensors, transducers, various aspects of biosensors, performance criteria of biosensors, different immobilization techniques for bio-recognition elements, state of art for food samples and clinical analytes including urea, antibiotic residues, and bacterial contamination. The chapter also discusses about gaps in the existing research and objective of the proposed doctoral work and finally about the thesis structure.

### **1.11.2 Chapter 2: Development of flow injection analysis-enzyme thermistor (FIA-ET) biosensor for urea analysis in adulterated milk**

This chapter gives a detail account for the development of FIA-ET based biosensor for analysis of urea in adulterated milk. This also describes the novel sample pre-treatment procedures for investigation in milk, optimization of the FIA system, immobilization of enzyme and the stability of the biosensor. Detailed study of the enzyme column performance, stability and analytical performance of the biosensor. Measurements of milk samples with different fat percentages and validation against AOAC method and a commercial kit are discussed in details. Applicability of the broad dynamic range of the biosensor for urea analysis in milk for dairy industries is also discussed in this chapter. Being a flow injection technique, FIA-ET biosensor has potential for automated measurements in the dairy industry.

### **1.11.3 Chapter 3: Development of FIA-ET biosensor for urea analysis in urine**

This chapter gives an detail account for the development of the FIA-ET based biosensor for analysis of urea in urine samples. In this chapter, we have demonstrated further development of FIA-ET biosensor for urea analysis in urine samples. Preparation of the low cost non-porous column material and successful measurements are described. Furthermore, the broad dynamic range of the developed biosensor and precision in the biosensor performance are described. Application for monitoring of urine samples to check the functional ability of the renal system are also discussed in this chapter.

#### **1.11.4 Chapter 4: Development of flow injection analysis-electrochemical quartz crystal nanobalance (FIA-EQCN) biosensor for analysis of antibiotic residues in milk**

This chapter describe about the development of FIA-EQCN biosensor for antibiotic residue analysis in milk samples. This chapter described in two parts; first part deals with the development of the FIA-EQCN system for analysis of the sulfadiazine residues in milk. Sulfadiazine was chosen as a model analyte to perform the residual testing as a proof of concept. This part of the chapter also describes about the optimization of FIA system including matrix matching for milk sample analysis and immobilization of the biomolecule (antibody) on the crystal surface in a semi-automated mode. The broad detection range and obtained recovery from the developed biosensor is also described in this chapter. In the second part of the chapter, development of FIA-EQCN biosensor for ultrasensitive detection of streptomycin is described. Detailed studies on optimization of flow system, selection of the self-assembly for immobilization of the biomolecule and characterization of the immobilized surface is described. Attempts were made to do the automated analysis of milk samples, and the applicability of biosensor in the dairy industry is described for streptomycin residues. Validation of the developed FIA-EQCN biosensor with a commercial ELISA kit and precision and reproducibility of the biosensor is described before the concluding remarks.

#### **1.11.5 Chapter 5: Rapid label-free immunosensor for bacterial detection in water**

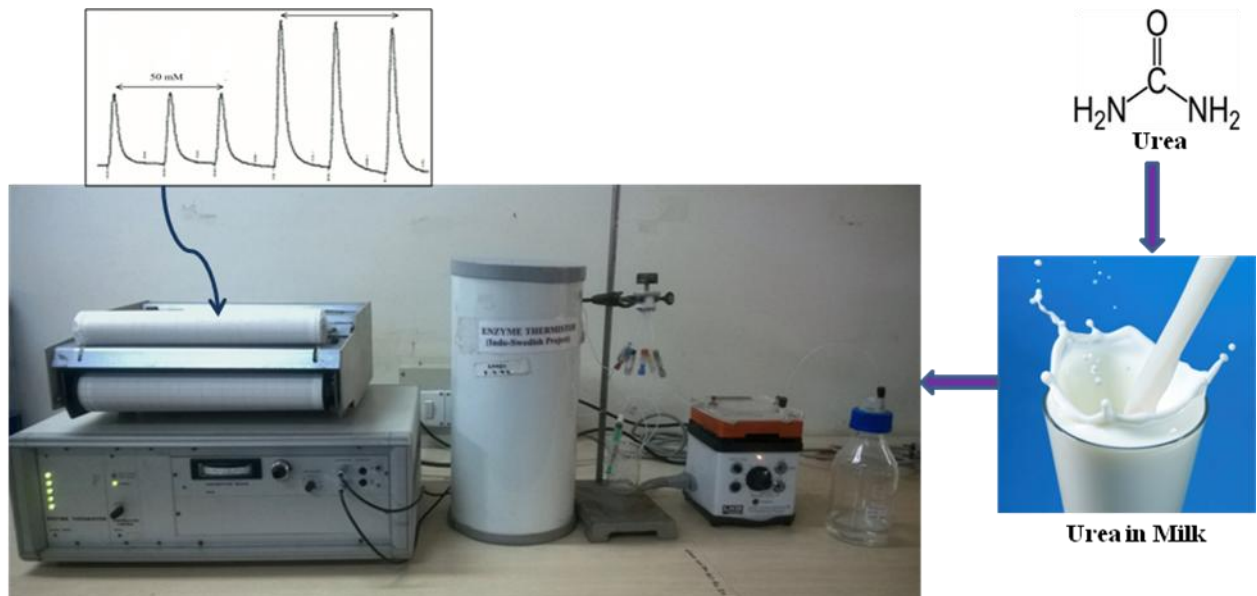
This chapter describes the development of a rapid label-free impedance based immunosensor for bacterial detection in water. Silver wires were used as two-electrode setup for electrochemical impedance analysis. Immunosensor construction was carried out using specific antibodies against *E. coli* development. The developed immunosensor is rapid and sensitive for detection of *E. coli* in water.

#### **1.11.6 Chapter 6: Conclusion and future scope of work**

This chapter gives a review of all the five chapters, conclusions and proposes the future scope of work followed by references and appendix.

## Chapter 2

### Development of flow injection analysis-enzyme thermistor (FIA-ET) biosensor for urea analysis in adulterated milk



*Graphical abstract of chapter content*



## 2.1. Introduction

### 2.1.1. Urea as adulterant in milk

Determination of urea has numerous applications in a wide range of fields such as clinical diagnostics, environmental monitoring and food science. Adulteration of natural milk with synthetic chemicals is a serious concern for human health. Milk is an excellent source of energy, protein, minerals and vitamins (Noyhouzer *et al.*, 2009). In India, Urea [CO(NH<sub>2</sub>)<sub>2</sub>] is commonly used as an adulterant for milk. Adulteration of milk with urea decreases the nutritive value of the milk. Urea is also a normal constituent of milk. The typical concentration of urea in milk is 18-40 mg/dL (Jonker *et al.*, 1998). A cut off limit for urea concentration in milk is normally accepted at 70 mg/dL. It also forms a major part (55%) of the non-protein nitrogen of milk (Sharma *et al.*, 2008). Urea being relatively cheap and rich in nitrogen is an economical choice to adulterate the milk. Urea is used as an adulterant of milk to increase the thickness and viscosity of the milk as well as to preserve it for a longer period. The most common reason given for adulteration is the difference between demand and supply of milk. In order to meet the demand, the suppliers usually adulterate the milk and increase the quantity. These adulterants are hazardous and cause irreversible damage to the organs. The immediate effect of drinking urea adulterated milk is gastroenteritis, but the long term effects are known to be far more serious. According to a survey on milk adulteration conducted by Food Safety and Standards Authority of India (FSSAI) about 65-70% of milk samples were reported to be adulterated with urea, detergents, water, skimmed milk; among that about 17% samples comprised packaged milk from dairy industries (FSSAI,2012). Hence, the demand for estimation of urea adulteration in milk is of great significance. Figure 2.1 represents the molecular structure of urea.

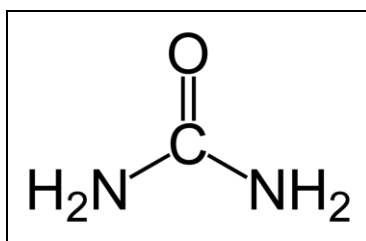


**Figure 2.1** Molecular structure of urea.

### 2.1.2 State of the art for analysis of urea in milk

Several methods have been reported in recent years for urea analysis in milk. Conventional techniques such as differential pH technique (Luzzana and Giardino, 1999) and spectrophotometric and conductometric detection (Reis Lima *et al.*, 2004), were widely reported for analysis of urea in milk. The conventional techniques as well as current wet chemistry and analytical practices are time consuming and may require highly skilled workers and expensive equipment (Luong *et al.*, 1991). The food and dairy industries need rapid, reliable and affordable techniques for quality control of milk, thus biosensors come into the practice. Numerous biosensors have been reported in recent years for milk urea analysis, such as manometric biosensor (Jenkins and Delwiche, 2002; Renny *et al.*, 2005) and potentiometric biosensor (Verma and Singh, 2003; Trivedi *et al.*, 2009). Some of these reported biosensors have a very short detection limit and low operational stability, which renders them unfit for routine analysis. There is a need for economical, reliable, robust and reproducible biosensors specifically for urea analysis in milk. Thus, thermal biosensors are good alternative devices owing to their simplicity of operation and long-term stability (Pirvutoiu *et al.*, 2002). The reported biosensors for analysis of urea in milk samples are summarized in Table 2.1.

**Table 2.1** Summary of reported biosensors for analysis of urea in milk

<b>Biosensor/ Transducer</b>	<b>Linear range</b>	<b>Detection limit</b>	<b>Response time</b>	<b>Stability</b>	<b>References</b>
Manometric	2-11 mM	2 mM	5 min	1Month/25°C	Jenkins and Delwiche, 2002
Potentiometric	1.66-16.6 mM	1.66 mM	2 min	Disposable	Verma and Singh, 2003
Manometric	0-5.55 mM	-	3 min	-	Renny <i>et al.</i> , 2005
Potentiometric	1.30-4.180 mM	0.025 mM	30 sec	7-8 days/RT	Trivedi et al, 2009

### 2.1.3 FIA-ET technique

The availability of numerous enzymes and their well-defined specificity combines with the exothermic nature of many enzymatic reactions makes it possible to develop thermal or calorimetric based biosensor for detecting a wide range of biomolecules. In the case of thermal biosensor, these reactions are detected by measuring temperature changes caused by the enthalpy change. Among the various thermal transducers, enzyme thermistor (ET) has been extensively used for last 40 years and acknowledged as one of the most widely developed type of heat measurement based sensor (Yakovleva *et al.*, 2013). The thermistor based calorimeter was designed to cover a broad range of applications which includes determination of metabolites, monitoring of enzyme reactions, bioprocess monitoring, characterization of immobilized biocatalyst, bio-separation, reaction in non-aqueous medium, environmental control and ionic interactions (Xie *et al.*, 2000). ET combined with FIA commonly known as FIA-ET provides the excellent platform for analysis over 40 analytes till now (Bhand *et al.*, 2010). In this chapter, a FIA-ET biosensor was explored to develop a major application for analysis of urea in milk samples. The immense need of online monitoring techniques for analysis of urea in milk in the dairy industries is the sole reason to undertake this development.

### 2.1.4 Objective

The aim of this work was to develop a biosensor with broad detection range for analysis of urea in adulterated milk samples using FIA-ET technique. Enzyme urease was chosen as a biocomponent for the biosensor construction.

### 2.1.5 Working principle of enzyme thermistor

The evolution of heat is a general property accompanying biochemical transformations. The total heat evolution is proportional to the molar enthalpy change and to the total number of moles of product molecules created in the reaction:

$$Q = - n_p (\Delta H) \quad (2.1)$$

where Q – total heat,  $n_p$  – moles of product, and  $\Delta H$  – molar enthalpy change.

The resulting temperature change ( $\Delta T$ ) is dependent on the total heat capacity ( $C_S$ ) of the system including the heat capacity of the solvent. Thus the change in temperature recorded by the thermal biosensors can be defined by:

$$\Delta T = - (n_p \Delta H) / C_S \quad (2.2)$$

The enthalpy changes for enzymatic catalysis is around  $-10$  to  $-200 \text{ kJ mol}^{-1}$  which is adequate for the determination of the substrate concentrations at interesting levels for a range of metabolites.

### 2.1.6 Mechanism of urea hydrolysis by urease

In this work, analysis of urea in adulterated milk samples was based on the principle of hydrolysis of urea by urease. For development of FIA-ET Biosensor, enzyme urease was used in an immobilized column reactor. Urease catalyzes the hydrolysis of urea into ammonia and carbamate, which spontaneously decomposes to form carbon dioxide and a second molecule of ammonia. Urea is very stable in aqueous medium and its hydrolysis rate is accelerated  $10^{14}$  to  $10^{32}$  times by the action of urease, one of the more proficient enzymes known so far (Krajewska, 2009).

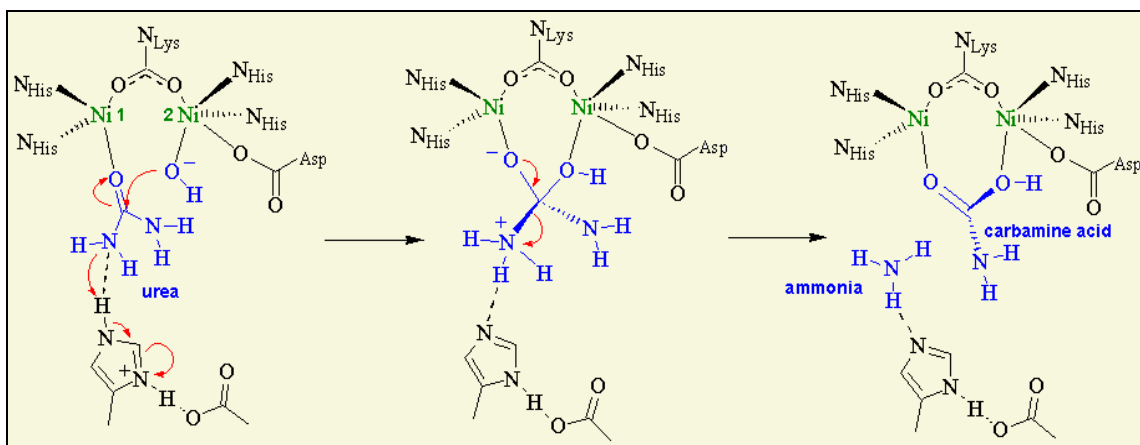


**Figure 2.2** Mechanism for hydrolysis of urea by urease (adopted from: Carter *et al.*, 2009)

The supposed mechanism, as shown in Figure 2.2 is a cooperative interaction between the two Ni ions. One Ni ion (Ni 1) acts as a Lewis acid. The metal ion polarizes the carbonyl group of

urea and activates it toward nucleophilic attack. In the process, two H<sub>2</sub>O molecules are replaced by urea. The other Ni ion (Ni<sup>2+</sup>) binds a hydroxide ion. The OH<sup>-</sup> ion attacks the partially positive carbonyl carbon of the urea molecule. One of the two NH<sub>2</sub> groups of urea is protonated. Histidine is postulated to be the acid. The reactions result in the formation of ammonia and carbamate acid (Karplus *et al.*, 1997; Carter *et al.*, 2009). The hydrolysis reaction is presented as equation 2.3



## 2.2 Experimental Section

### 2.2.1 Chemicals and biochemicals

Enzyme urease (Jack beans lyophilized 5 IU/mg, EC 3.5.1.5), urea, sodium dihydrogen phosphate monohydrate (NaH<sub>2</sub>PO<sub>4</sub>·H<sub>2</sub>O), disodium hydrogen phosphate monohydrate (Na<sub>2</sub>HPO<sub>4</sub>·H<sub>2</sub>O), glutaraldehyde solution 25%, and tri-ethanol amine were obtained from Merck, Germany. Amino silanized control pore glass (CPG) spherical beads (Trisoperl, size 125–140 μm, pore size 50 nm) were purchased from VitraBio (Germany). Maxsignal® urea enzymatic assay kit was purchased from BIOO SCIENTIFIC, USA. All other chemicals used in the study were GR grade.

### 2.2.2 Solution preparation

Phosphate buffer (PB) 100 mM, pH 7.2 was prepared by mixing 100 mM of sodium dihydrogen phosphate monohydrate and 100 mM of disodium hydrogen phosphate monohydrate in double distilled water. PB was degassed before analysis. A stock solution of urea (400 mM) was prepared by dissolving 2.4024 gm in 100 mL of PB (100 mM, pH 7.2). Working solution of urea was prepared daily prior to use.

### 2.2.3 Instrumentation for FIA-ET biosensor

The set-up for FIA-ET biosensor for urea analysis is presented as Figure 2.3. The experimental setup consists of a peristaltic pump (Gilson Minipuls Evolution II, France), an injection valve (type-50 from Rheodyne, Cotati, USA), sample loop (0.1 mL), enzyme thermistor, Wheatstone bridge equipped with a chopper-stabilized amplifier and conventional chart recorder were used.

PTFE tubing's (0.8 mm id) were used for the connection. 100 mM PB, pH 7.2 was used as the carrier buffer.

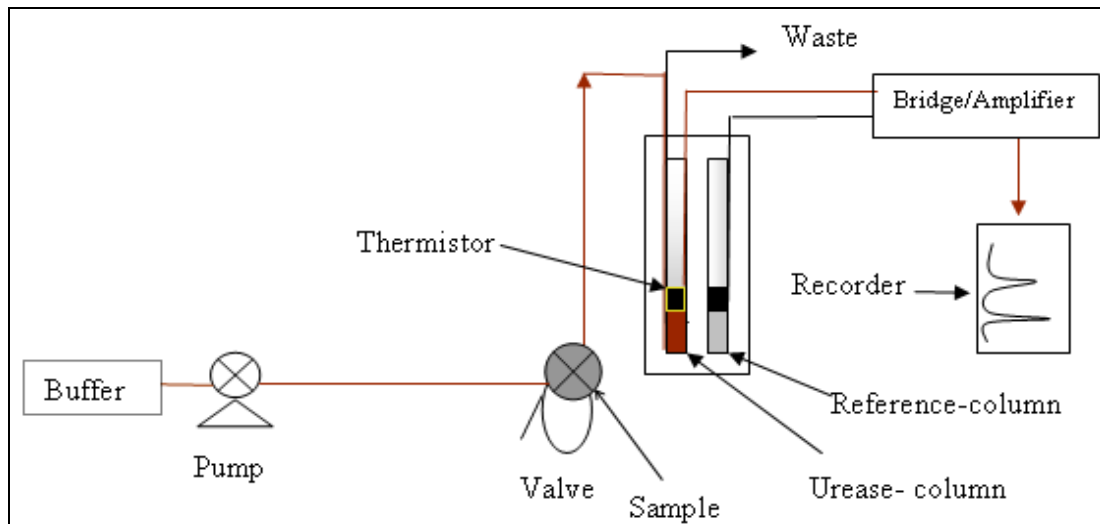


**Figure 2.3** Schematic set-up for FIA-ET biosensor for urea analysis.

#### 2.2.4 Immobilization of urease on CPG

Enzyme immobilization on amino silanized CPG was achieved by glutaraldehyde cross-linking. Urease was covalently immobilized on CPG according to the following procedure: 250 mg CPG was activated with 2.5% glutaraldehyde in 100 mM PB, pH 7.2. The reaction was allowed to take place for at least 1h inside the desiccators, under reduced pressure. The activation of column support was confirmed by the presence of brick red color (formation of Schiff's base). Activated CPG was successively washed with double distilled water and PB. Urease 200 mg (1000 IU) dissolved in 1mL PB was added to the wet activated CPG. The coupling reaction was allowed to proceed for 30 min at room temperature and overnight at 4°C. The enzyme preparation was washed with PB. Tri-ethanolamine (200 mM) was added to terminate all the unreacted groups and then washed with 100 mM PB, pH 7.2. The immobilized urease was finally packed into a delrin column by a slurry packing method. Schematic representation for immobilization of enzyme urease on CPG is shown as Figure 2.4.

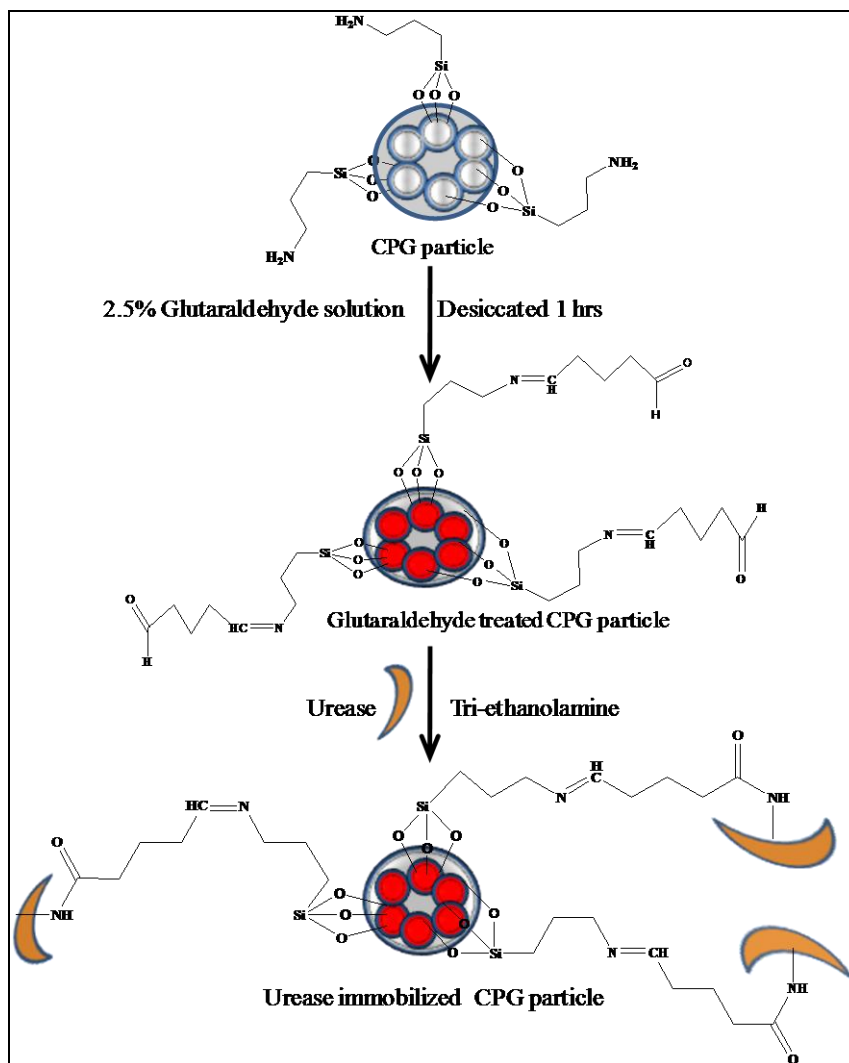


Figure 2.4 Schematic representation of immobilization of urease on CPG.

## 2.3 Result and Discussion

### 2.3.1 Optimization of the experimental variables for FIA-ET biosensor

#### 2.3.1.1 Optimization of the pH, ionic strength and flow rate

A series of experiments were performed to determine the influence of pH and ionic strength of PB and the effect of flow rate on the activity of enzyme urease and the sensitivity of the biosensor for determination of urea in adulterated milk samples. Measurements were carried out in the flow system with varying pH (6.8, 7.0, 7.2 and 7.4) and ionic strength (10, 50, 100 and 200 mM) of PB for 100 mM urea. Figure 2.5 clearly suggests that urease exhibit maximum activity at pH 7.2.

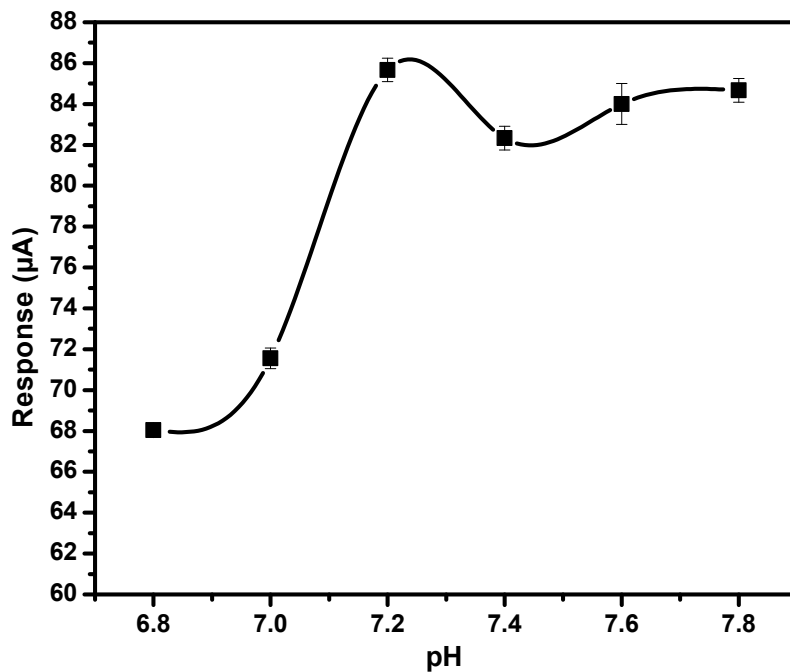


**Figure 2.5** Effect of pH of the PB on the response of FIA-ET biosensor for 0.1 mL injection of 100 mM urea.

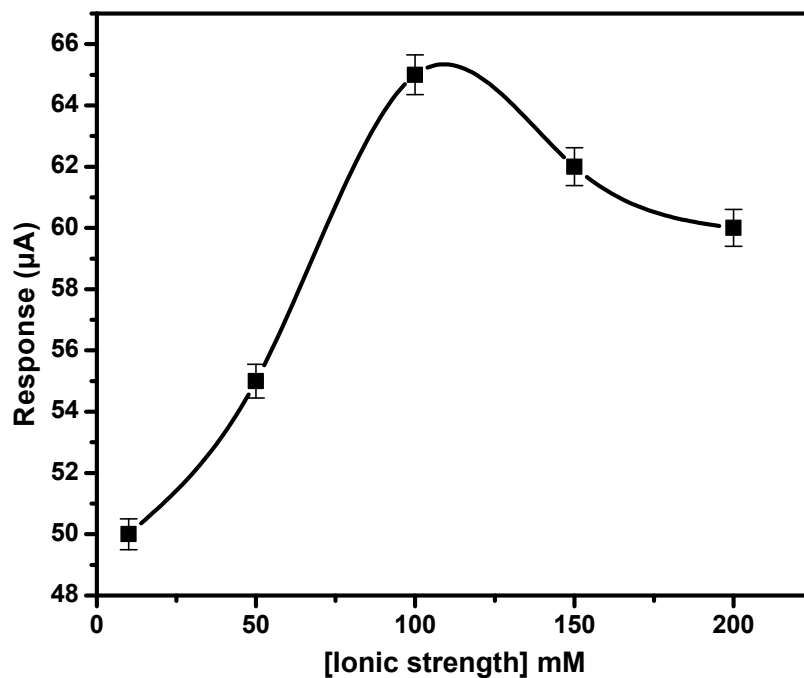


**Figure 2.6** Effect of ionic strength of PB on the response of FIA-ET biosensor for 0.1 mL injection of 100 mM urea.



It is evident from Figure 2.6 that with an increase in the ionic strength of PB, response signal increases upto 100 mM, and then the signal starts decreasing. Thus, further experiments were carried out with 100 mM PB. Flow rates of 0.25, 0.5, 0.75, and 1.0 mL/min were investigated against 100 mM urea. As presented in Figure 2.7, the results indicate that the flow rate of 0.5 mL/min provides sufficient contact time between the enzyme and substrate for hydrolysis of urea. The FIA-ET performance was highly reproducible under the optimized conditions of PB (Ionic strength 100 mM, pH 7.2, flow rate 0.5 mL/min).

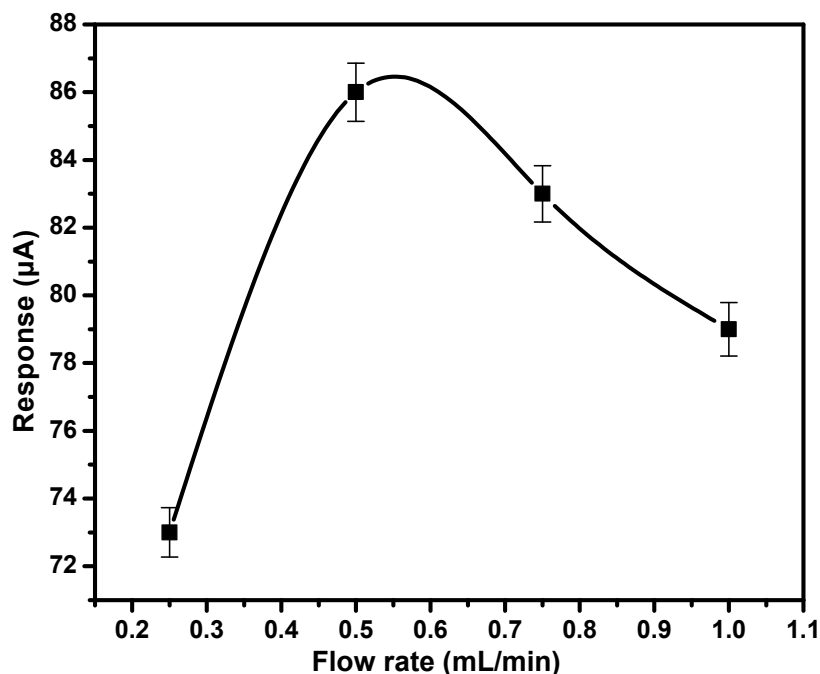


**Figure 2.7** Effect of flow rate of PB on the response of FIA-ET biosensor for 0.1 mL injection of 100 mM urea.

### 2.3.1.2 Optimization of sample volume

Experiments were performed to check the effect of sample volume of the analyte (urea) on the response of FIA-ET biosensor. Sample loops of 0.05 and 0.1 mL volume were tested. As evident from Figure 2.8, sample loop of 0.1 mL volume showed the higher response as compared to 0.05 mL. Further experiments were carried out using the optimized sample volume of 0.1 mL.

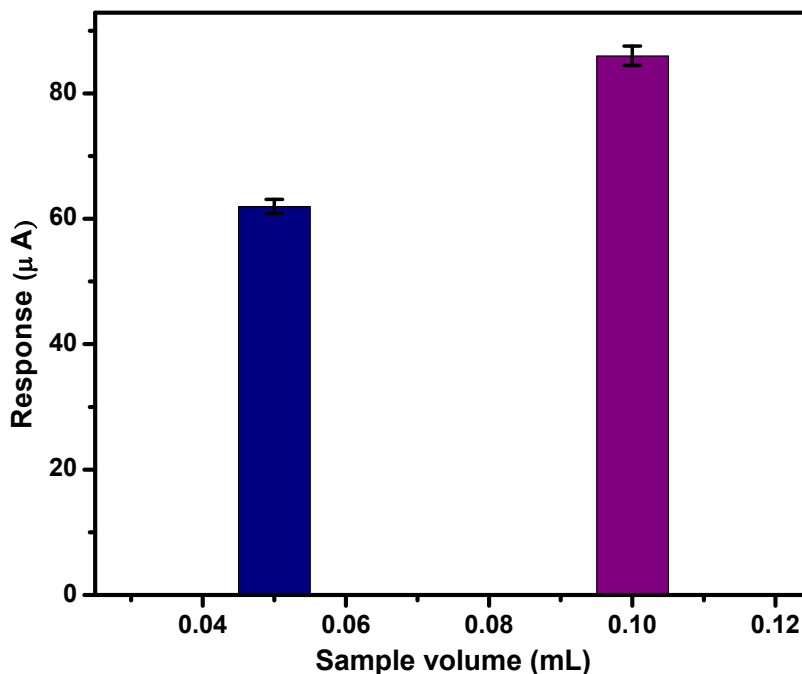


**Figure 2.8** Effect of sample volume on the response of FIA-ET biosensor for injection of 100 mM urea.

### 2.3.2 Calibration of biosensor for urea analysis in buffer

The immobilized urease column was kept inside the thermistor and allowed to equilibrate overnight. The buffer solution was filtered, degassed and pumped *via* FIA manifold, until a constant baseline is achieved. Urea standard solutions 0.1, 1, 10, 50, 100, 150, 200, 250 mM were prepared in carrier buffer and injected into the flow stream. Response signals were recorded using a data acquisition system connected to Wheatstone bridge and plotted as current ( $\mu\text{A}$ ) vs. urea (mM). All samples were injected in triplicates. The Michaelis constant,  $K_m$  for urea was calculated using Lineweaver–Burk plot. The  $K_m$  was found to be 100 mM. A good linear response was obtained for urea hydrolysis in the range of 1–200 mM with minimum detection limit of 0.1mM (6.06 ppm), which is presented in Figure 2.9. The linear fit of data shows a good correlation between urea and immobilized urease ( $R^2 = 0.99$ , % RSD = 0.96).

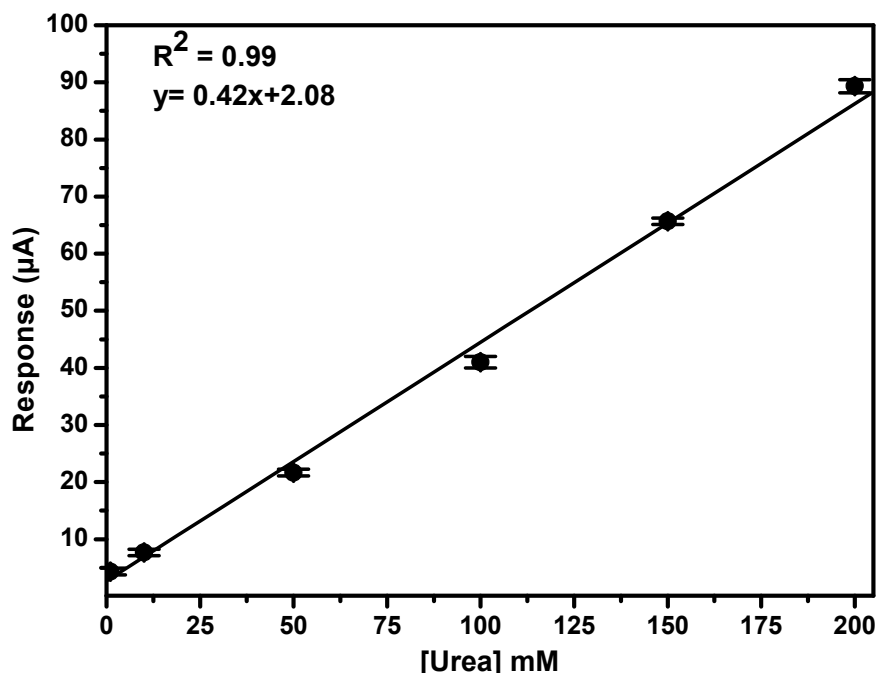


**Figure 2.9** Calibration plot obtained for urea using urease column in 100 mM PB, pH 7.2 for 0.1 mL of sample injection, flow rate 0.5 mL/min at 30°C.

### 2.3.3 Matrix matching for milk sample analysis

For milk urea analysis, commercial milk samples of different fat content (0.5%, 1.5%, and 3.5%) were purchased from the local market of Goa, India. The matrix effect in the analysis of urea in milk samples was investigated. In FIA system, fat present in milk may lead to matrix related quenching and block the flow in FIA, which can decrease the device sensitivity or completely clog the column. Various sample pre-treatment techniques such as combination of centrifugation, filtration and dilution were tested to select the optimum pretreatment procedure for milk urea analysis. Milk samples were centrifuged at 10,000 rpm for 10 min at room temperature. The centrifuged milk samples were diluted with PB to obtain different ratios of milk: PB and further spiked with known amount of urea. It was observed from the Figure 2.10 that 1:4 dilution of milk and PB was most responsive to urea analysis. To obtain the calibration curve for urea in spiked milk samples, a simple strategy was worked out to remove the fat and to obtain a suitable dilution to avoid clogging of the urease column. In brief, milk samples were centrifuged, diluted

and filtered through 0.45 and 0.22  $\mu\text{m}$  filter (Whatman, USA). Milk analysis was carried out within the same day after sample preparation.

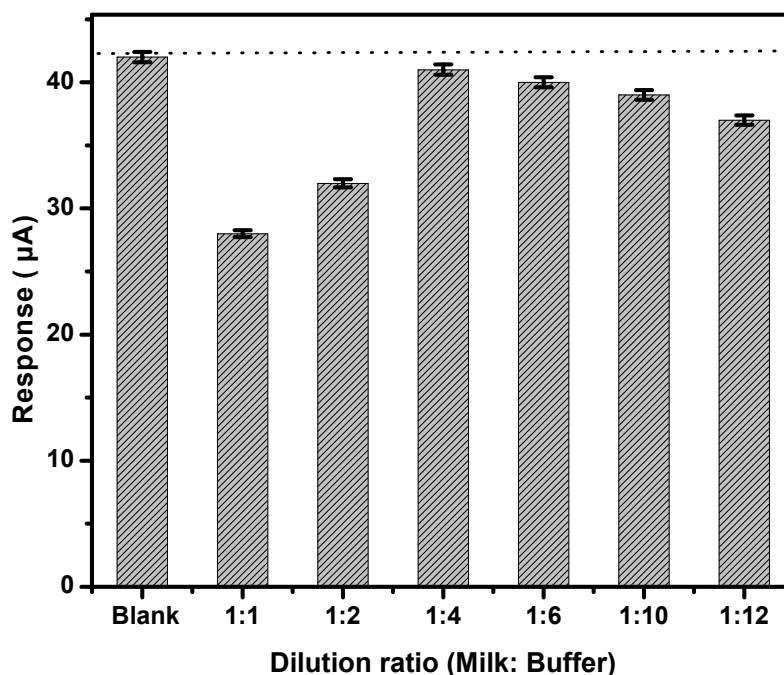


**Figure 2.10** Effect of dilution of PB and milk on the response of FIA-ET biosensor for 0.1 mL injection of 100 mM urea.

### 2.3.4 Urea analysis in milk

For urea analysis, calibration standards were prepared by dilution of urea stock solution in 100 mM PB, pH 7.2. The immobilized urease column was mounted inside ET and was allowed to equilibrate with the surrounding. The degassed carrier buffer was passed through the column initially at a higher flow rate (0.9 mL/min). Subsequently, the flow rate was brought down to the optimum value of 0.5 mL/min at which a stable baseline was achieved. Spiked samples were injected and data were collected using a data acquisition system connected to the Wheatstone bridge. All measurements were carried out by injection of 100  $\mu\text{L}$  samples at a flow rate of 0.5 mL/min. After each sample analysis, the sample loop was thoroughly rinsed with PB. The milk samples were spiked with known amounts of urea after appropriate filtration and dilution and injected into the system.

Commercial milk samples of different fat content (0.5 %, 1.5 %, and 3.5 %) were purchased from the local market of Goa, India. The matrix effect in the analysis of urea in milk samples was investigated. In FIA system, fat present in milk may lead to matrix related quenching and block the flow in FIA, which can decrease the device sensitivity or completely clog the column. Various sample pre-treatment techniques such as combination of centrifugation, filtration and dilution were tested to select the optimum pre-treatment procedure for milk urea analysis. Milk samples were centrifuged at 10000 rpm for 10 minutes at room temperature. The centrifuged milk samples were diluted with PB to obtain a different ratio of milk: PB and further spiked with known amount of urea. It was observed that 1:4 dilution of milk: PB was most responsive to urea analysis. To obtain the calibration curve for urea in spiked milk samples, a simple strategy was worked out to remove the fat and to obtain a suitable dilution to avoid clogging of the urease column. In brief, milk samples were centrifuged, diluted and filtered through 0.45 $\mu$  and 0.22 $\mu$  filter (Whatman, USA). Milk analysis was carried out within the same day after sample preparation.

### **2.3.5 Calibration of biosensor for urea analysis in spiked milk**

Spiked milk urea standard solutions (0.1–250 mM) of different fat content (0.5%, 1.5% and 3.5%) were injected into the flow stream, and response signals were recorded. The FIA-ET biosensor showed an excellent dynamic range for milk urea in the range 0.1–250 mM with a good linearity (1–200 mM). The results are presented in Figure 2.11 ( $R^2 = 0.99$ , % RSD = 0.95). A broad linear range, 0.1–200 mM was obtained with the lower limit of detection 0.1mM (6.06 ppm). The upper limit of detection as high as 200 mM was achieved with sensitivity of 4.17% per mM for buffer urea. For milk urea, a broad linear range, 0.1–200 mM was obtained with the upper limit of detection 250 mM and sensitivity of the signal 4.58%  $\text{mM}^{-1}$ . The reported heat of reaction for urea hydrolysis by urease is  $-61 \text{ kJ mol}^{-1}$ . In our case the calculated heat of reaction in diluted milk urea samples was found to be  $-46.81 \text{ kJ mol}^{-1}$ . The broad dynamic range obtained for milk urea makes the biosensor highly suitable for analysis of adulterated milk samples. An actual sensor signal recorded using conventional chart recorder for triplicate measurement of 50 and 100 mM spiked milk urea samples is presented in Figure 2.12.

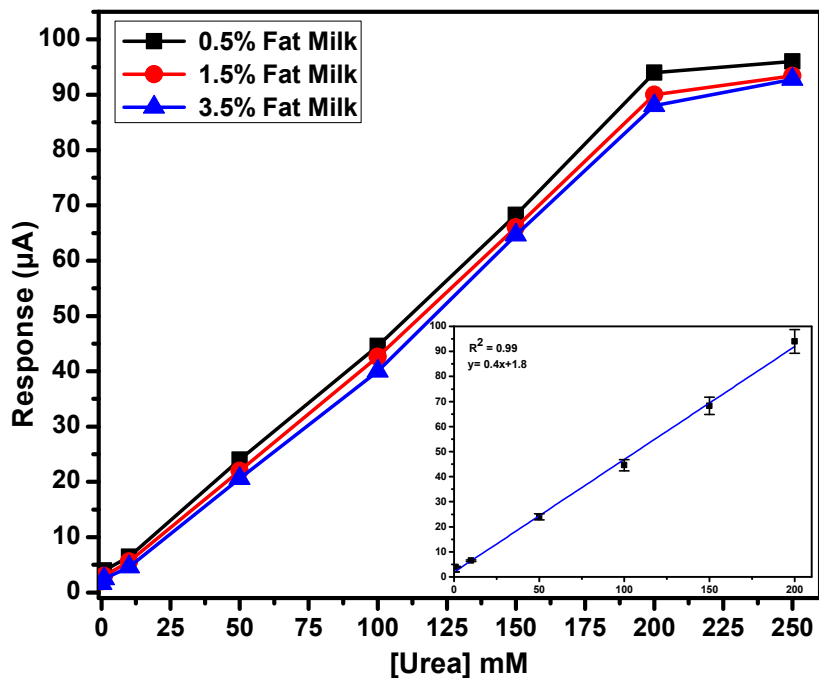


**Figure 2.11** Calibration plot obtained for urea using urease column in milk with 0.5%, 1.5% and 3.5% fat. (Inset: linear range obtained for 0.5% fat milk urea).

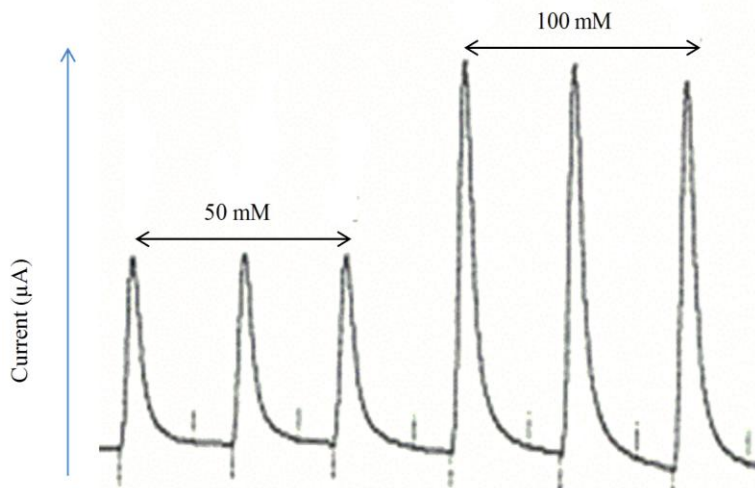


**Figure 2.12** Response signal recorded for two different milk urea concentrations (50 mM and 100 mM) using FIA-ET biosensor. Sample volume 0.1 mL, flow rate 0.5 mL/min acquired using a data acquisition system with Chart recorder.

### 2.3.6 Urea recovery studies from spiked milk samples

To perform recovery studies from milk samples, a known amount of urea standard solution was added to centrifuged, diluted and filtered milk and analyzed in FIA-ET. Based on the response signal, recoveries were calculated. Table 2.2 shows the recovery results obtained for milk urea. Excellent recoveries in the range of 97.56–108.70% were obtained for urea in milk. This ensures the reproducibility of the presented biosensor for urea analysis of adulterated milk samples.

**Table 2.2** Determination of % recovery from urea spiked commercial milk samples

Milk sample	Urea added (mM) (n=3)	Urea found (mM) (n=3)	% Recovery	Mean $\pm$ S.D.	% RSD
Sample 1	41	44.6	108.7	44.6 $\pm$ 0.4	0.89
Sample 2	41	42.6	103.9	42.6 $\pm$ 0.4	0.93
Sample 3	41	40	97.56	40.0 $\pm$ 0.5	1.25

### 2.3.7 Stability of the urease immobilized CPG column

Analytical performance of the urease immobilized CPG column was studied over the period of 24 months. Total four columns were prepared in the entire duration. Urea measurements in milk samples were carried out randomly over the entire period. As presented in Figure 2.13, column 2 retains the highest activity up to 300 days when used for urea analysis. Whereas, loss in activity of column 1 was observed within the 108 days of installation. Similarly, column 3 and 4 showed good enzyme retention, i.e. 65% and 50% when used continuously for 180 and 168 days respectively. Furthermore, the operational stability, storage stability and shelf life of the column were studied against 100 mM milk urea standards.

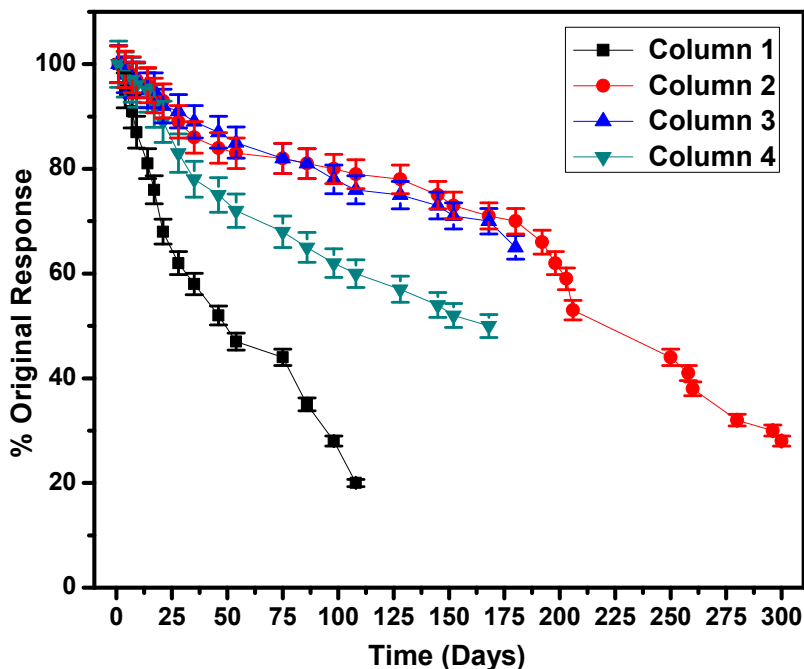


**Figure 2.13** Analytical performance of different urease immobilized CPG column against 100 mM urea in the milk samples.

### 2.3.7.1 Operational stability of the column

The operational stability of the urease immobilized CPG column was monitored over the period of 300 days. About 15 measurements were made every week for 0.1 mL, 100 mM urea. The operational stability is over the studied period is presented in Figure 2.14. The immobilized urease inside the thermistor presented excellent stability, over the first 30 days the enzyme activity was found 90% of the original response and there was no appreciable loss of activity. However, after a period of 45 days operation, about 16% decay in response was observed. Similarly the response was monitored after 75, 150, 180, 198 and 206 days and signals recorded were respectively 82%, 73% ,70%, 62% and 53% of the original response. The column was stored at 4°C for about 45 days and again used for urea analysis in milk. After the 250 days original response was found about 44% of the original response. Similarly, the response was recorded after 268, 280, and 300 days and signals recorded were respectively 38%, 32% and 30% of the original response.



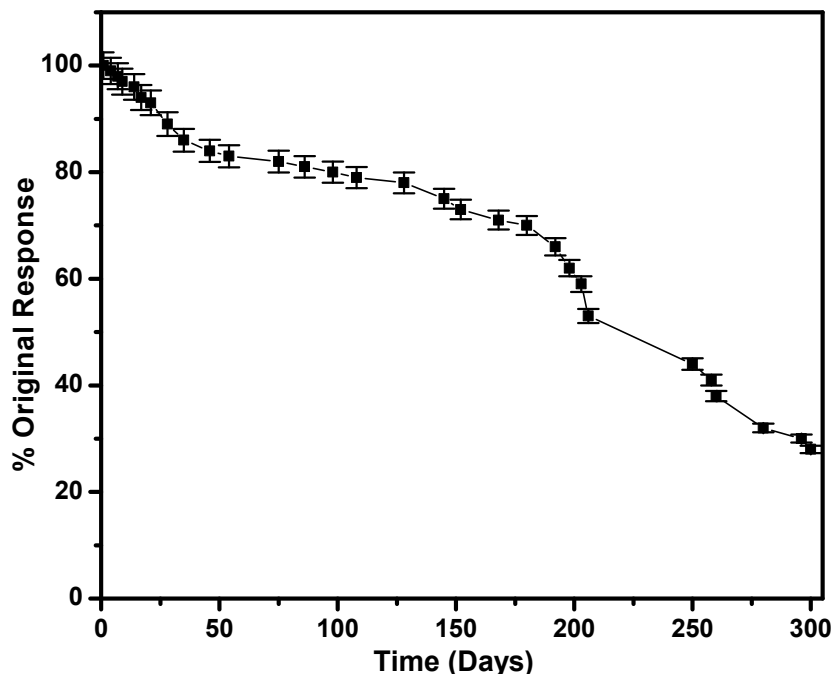


**Figure 2.14** Operational stability of FIA-ET milk urea biosensor, response to 0.1 mL, 100 mM urea, observed for 206 days at 30°C and up to 300 days after storage at 4°C. Samples were injected randomly during the period.

### 2.3.7.2 Storage stability and shelf life of the column

Most enzymes lose their activity when not stored in the refrigerator, and therefore, storage at low temperatures is one of the most important parameters to retain the stability of enzyme-based biosensors (Trivedi *et al.*, 2009). Moreover, in order to attain high water content in the immobilized layer, the column was kept in a closed bottle with PB (100 mM, pH 7.2) and minimal amount of sodium azide to prevent from the fungal growth. The operational stability of a biosensor response may vary considerably depending upon the sensor storage, method of preparation, biological recognition reactions. Figure 2.15 compares the storage stability of the two enzyme columns stored at two different temperatures *i.e.* room temperature (RT) (25°C) and refrigerator (4°C). The studies were carried out randomly over the period of 62 days. As observed from the Figure 2.15, performance of the urease immobilized CPG column stored at low temperature is higher. Over the first week, no appreciable loss in activity was observed in both the columns. Whereas, after 27 days of usage column stored at low temperature showed 87% retention in the original response as compared to column stored at RT which showed 75%

retention in the original response. After 62 days of studies column of low temperature showed 70% of the original response, whereas, the column at RT showed 50% of the original response.

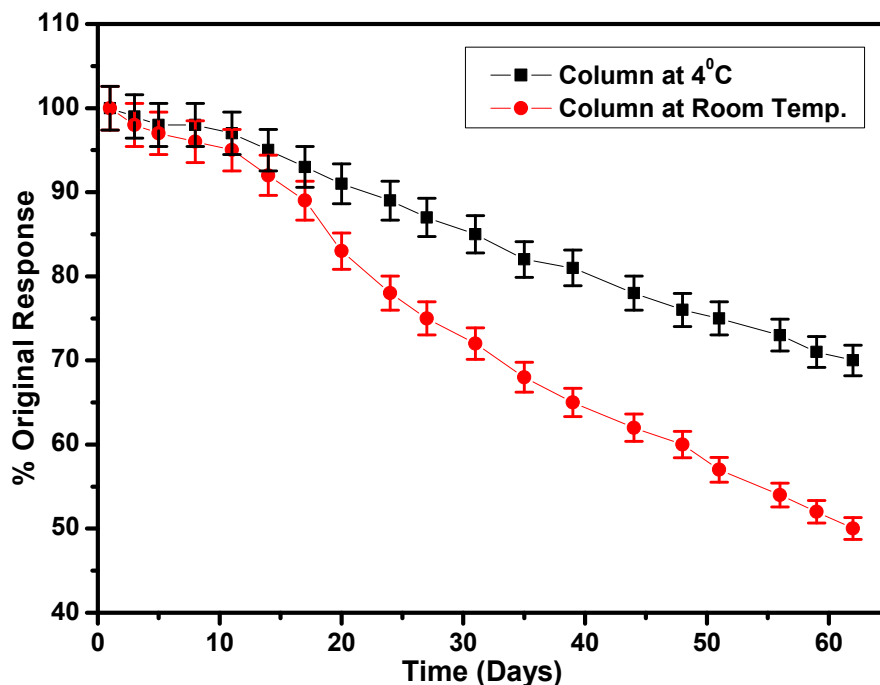


**Figure 2.15** Comparison of storage stability of urease immobilized CPG column at low temperature (4°C) and room temperature (25°C).

### 2.3.8 Validation of FIA-ET milk urea biosensor

For validation of developing FIA-ET urea biosensor, a survey was conducted to find the adulteration of urea in commercial milk samples of Goa, India. Milk samples of different brands of low fat content (3.0%) were purchased from the local market of Goa, India. The measurements were carried out with FIA-ET biosensor in semi-automated mode. To quantify the adulteration of urea in milk as recommended by the regulatory agencies milk samples were artificially adulterated with some known amount of urea. The spiked milk urea samples were analyzed using FIA-ET biosensor and further validated against commercial kit (BIOO Scientific, USA) and the Association of Analytical Communities (AOAC) method for confirmation of the urea adulteration in milk.

The matrix effect in the analysis of urea in milk sample was investigated and optimized for various measurements of ionic strength and pH of milk samples for appropriate dilutions with PB. In the validation work, we observed that 1:6 dilution of milk sample with PB was most

responsive for the urea analysis as compared to earlier reported 1:4. In the validation of FIA-ET urea biosensor conventional chart recorded was replaced by an online picodata logger thus, we could able to detect higher concentrations of milk urea (500 mM)

### 2.3.8.1 Using FIA-ET urea biosensor

For urea analysis, calibration standards (1-500 mM) were prepared by dilution of urea stock solution (500 mM) in 100 mM PB, pH 7.2. The immobilized urease column was mounted inside ET and allowed to equilibrate with the surrounding. The degassed carrier buffer was passed at an optimum flow rate of 0.5 mL/min at which a stable baseline was achieved. The spiked milk samples were injected and data were recorded in real time using a data acquisition system connected to the Wheatstone bridge.

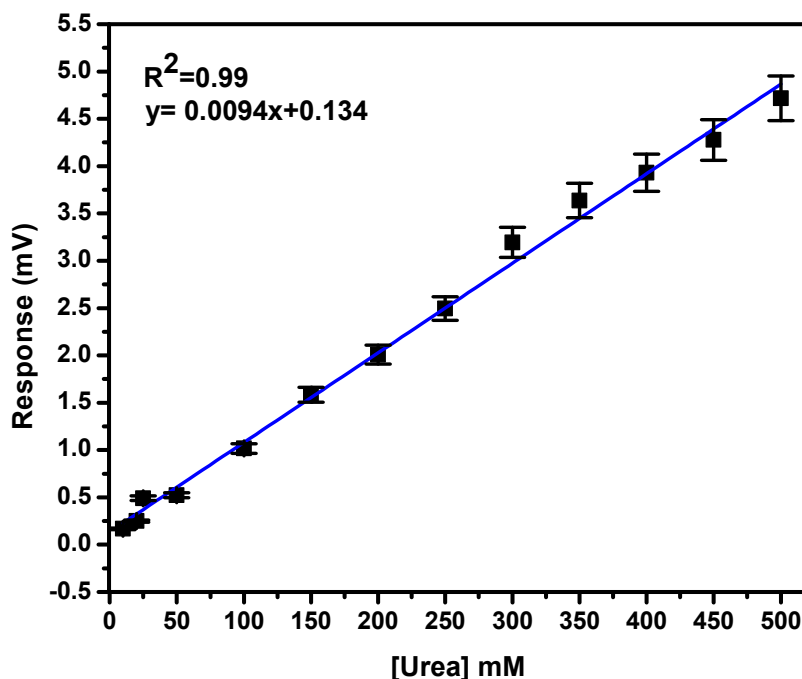


**Figure 2.16** Calibration plot obtained for urea spiked milk samples using FIA-ET biosensor in 100 mM PB, pH 7.2 for 0.1mL of sample injection, flow rate 0.5 mL/min at 30°C.

All measurements were carried out by injection of 0.1 mL sample at a flow rate of 0.5 mL/min. After each sample analysis, the sample loop was thoroughly rinsed with buffer (PB). The milk samples were spiked with known amounts of urea after matrix matching. Appropriate dilutions

were injected into the FIA-ET system. Milk sample spiked with urea standard solutions (10-500 mM) were injected into the flow stream and response signal was recorded. The FIA-ET biosensor showed an excellent dynamic range for urea present in spiked milk (10–500 mM) with a good linearity. The minimum detection limit was found to be 1 mM. The Michaelis constant,  $K_M$  for urea was calculated using Line weaver–Burk plot and found to be 248.9 mM. The result is presented as Figure 2.16 ( $R^2 = 0.99$ , % RSD = 0.007,  $n=3$ ).

### 2.3.8.2 Using urea enzymatic assay kit

To validate the developed FIA-ET urea biosensor, the milk samples were analyzed by using the commercial colorimetric kit. The analytical features and figures of merit of the biosensor were compared with Maxsignal® Urea enzymatic assay kit (BIOO SCIENTIFIC USA). The kit measures the concentration of urea using the urease enzyme, which converts urea to ammonia. An alkaline hypochlorite solution is then added to the reaction mixture.

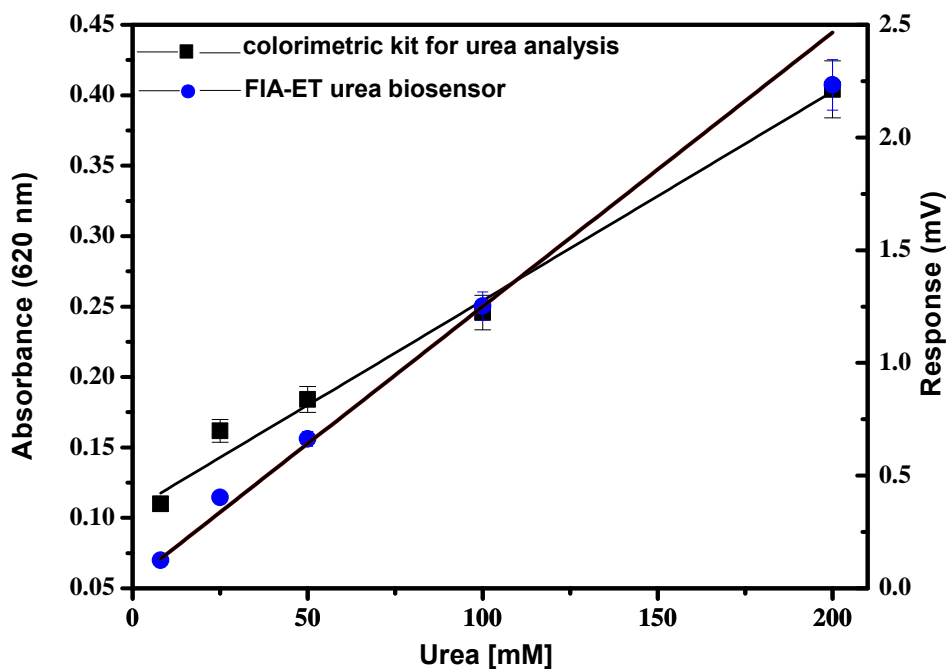


**Figure 2.17** Calibration plot obtained for urea analysis by commercial kit (absorbance at 620nm) at 30°C, ( $R^2 = 0.98$ , % RSD = 0.049) for validation of FIA-ET urea biosensor. ( $R^2 = 0.99$ , % RSD = 0.007).

The colour produced from the reaction is measured using a colorimetric multi-plate reader at 620 nm. The limit of detection of urea in milk using the commercial kit is 40 ppm. The kit is

provided with reagents and a 96 well plate to perform the assay (catalogue no.:1051). Spiked milk urea samples corresponding to 8, 25, 50, 100 and 200 ppm were analyzed simultaneously using the FIA-ET and the colorimetric assay. The obtained result is presented in Figure 2.17. For colorimetric measurements Multilabel plate reader Victor X4, Perkin Elmer, USA was deployed with 620 nm filter. The dynamic range and the upper limit of detection for the milk urea using the kit were found much lower as against presented biosensor, which offers a manifold higher linear range 10-500 mM. The analysis time for the thermal biosensor is less than 2 min per sample with throughput of 30/hrs, whereas with commercial kit, up to 72 samples can be analyzed within an hrs. For FIA-ET biosensor, a higher sensitivity was observed. As many as 1500 samples were analyzed with the single urease column over the period of 300 days.

### 2.3.8.3 Using AOAC method

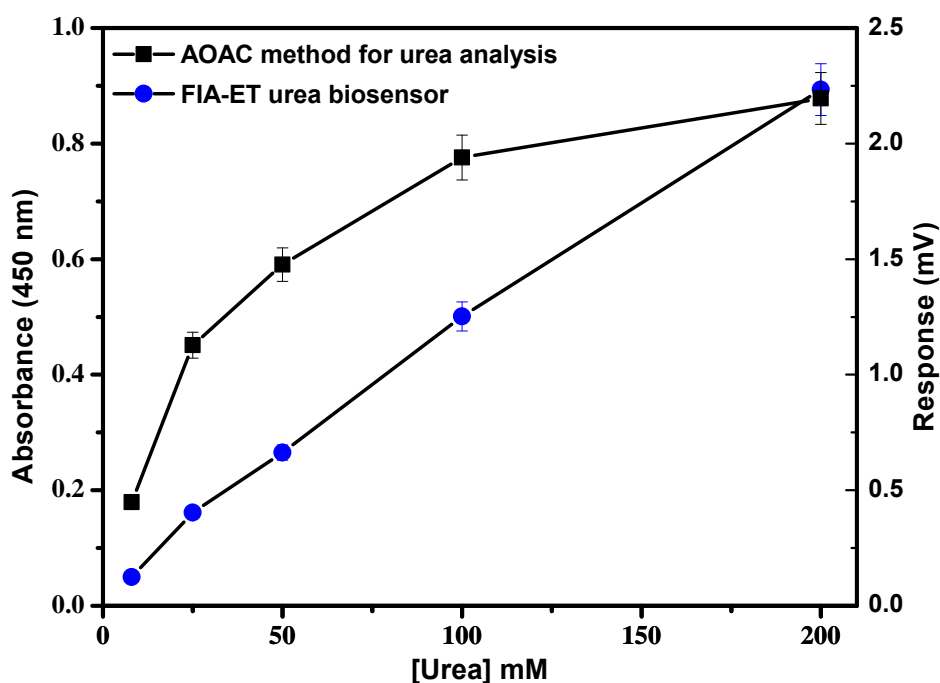


**Figure 2.18** Calibration plot obtained for urea analysis by AOAC method (absorbance at 450nm) at 30°C, ( $R^2 = 0.97$ , % RSD = 0.048) for validation of FIA-ET urea biosensor ( $R^2 = 0.998$ , % RSD = 0.007).

The developed FIA-ET urea biosensor was further validated with AOAC approved method (AOAC, 2000). Measurement was based on colorimetric reaction of p-Dimethyl amino benzaldehyde solution with milk sample denatured by trichloroacetic acid (24% w/v). All measurements were done using spectrophotometer at 420 nm. A calibration curve for competitive assay by AOAC method as per protocol was obtained and shown in Figure 2.18 ( $R^2 = 0.97$ , % RSD = 0.048, n=5). A concentration dependent increase in percentage absorption for milk urea adulteration was found by AOAC method.

#### **2.3.8.4 Recovery studies from spiked commercial milk samples**

A known amount of urea standard (200 mM) was spiked to diluted unknown milk sample and analyzed in FIA-ET urea biosensor. Recoveries were calculated from the obtained response signals. Excellent recoveries were obtained (98.96–105.15%) from FIA-ET urea biosensor in the spiked milk samples. Recovery studies were further validated with commercial kit and AOAC method. Good recoveries were found from both the methods (98.48-103.40% for commercial kit and 98.93-105.13 % for AOAC method). The results obtained from the above methods confirm the reliability of the developed method. The results for all the methods used are summarized as Table 2.3.

**Table 2.3** Recovery studies for urea from FIA-ET, Commercial kit and AOAC method

Milk	Urea added [mM]	Urea Found (mean, n=3)			± S. D. (n= 3)			% RSD			% Recovery		
		FIA-ET	Kit	AOAC	FIA-ET	Kit	AOAC	FIA-ET	Kit	AOAC	FIA-ET	Kit	AOAC
S1	200	204.03	200.70	201.66	±0.1	±1.4	±1.8	0.58	0.30	0.35	102.01	100.35	100.83
S2	200	204.40	201.88	204.40	±0.2	±1.6	±1.6	0.08	0.15	0.29	102.20	100.94	102.20
S3	200	201.73	200.66	201.50	±0.1	±1.8	±1.9	0.33	0.27	0.35	100.86	100.33	100.75
S4	200	210.30	204.66	210.27	±0.2	±1.9	±1.7	0.22	0.24	0.19	105.15	102.33	105.13
S5	200	197.93	198.00	197.86	±0.3	±1.8	±1.6	0.21	0.30	0.21	98.96	99.00	98.93
S6	200	208.13	206.80	207.73	±0.2	±1.1	±1.8	0.15	0.42	0.20	104.06	103.40	103.86
S7	200	198.73	196.97	198.67	±0.4	±1.5	±1.5	0.25	0.25	0.21	99.36	98.48	99.33

S1-S7: Milk samples

### 2.3.9 Precision of the biosensor for milk urea analysis

Precision of the developed biosensor was determined by measuring the known concentrations of urea at different time interval ranging from hrs to days. Four concentrations of urea (10, 50, 100 and 200 mM) were selected from the calibration range. The response of urea was recorded 3 times in a day for seven consecutive days. The precision and reproducibility of the method was evaluated in terms of % RSD As observed from the Table 2.4, very good reproducibility was obtained for urea concentration with % RSD 0.50- 1.42 (n=3) for intraday analysis and % RSD 0.05-2.57 (n=3) for interday analysis. The obtained results confirm the reproducibility of the sensor response.

**Table 2.4** Intra-day and Inter-day analysis result for FIA-ET biosensor for urea analysis in milk.

Intra-day reliability				Inter-day reliability			
Urea (mM)	Intra-day mean (mV) n = 3	Mean $\pm$ S.D.	% RSD	Day's	Inter-day mean (mV) n = 3	Mean $\pm$ S.D.	%RSD
10	0.1407	0.14 $\pm$ 0.002	1.42	Day-1	2.0306	2.03 $\pm$ 0.044	2.16
50	0.5963	0.59 $\pm$ 0.005	0.85	Day-2	2.0462	2.74 $\pm$ 0.033	1.20
100	1.1267	1.12 $\pm$ 0.015	1.34	Day-3	2.0417	2.04 $\pm$ 0.001	0.05
200	2.0100	2.01 $\pm$ 0.010	0.50	Day-4	2.0284	2.02 $\pm$ 0.014	0.69
				Day-5	2.0393	2.03 $\pm$ 0.051	2.51
				Day-6	2.0470	2.04 $\pm$ 0.044	2.15
				Day-7	2.0632	2.06 $\pm$ 0.053	2.57

Analytical figures of merit of the developed FIA-ET urea biosensor was compared with the other techniques used namely commercial enzymatic assay kit and AOAC method for urea determination. The results are compared and summarized as Table 2.5



**Table 2.5** Comparison of analytical features and figure of merit of all three method used FIA-ET, Commercial kit and AOAC method.

<b>Techniques</b>	<b>FIA-ET Biosensor</b>	<b>Commercial Enzymatic Assay Kit</b>	<b>AOAC method</b>
Method	Thermal Biosensor-immobilized Enzyme based	Colorimetric-Enzyme based	Colorimetric/spectrophotometric
Stability	Up to 2 year	6 Months	Not mentioned
Format	Enzymatic	Enzymatic	Liquid/Chemical based
Instrument	Enzyme thermistor	Multiplate reader	Spectrophotometer
Sensitivity	1 mM	20 ppm	25 mM
Limit of detection	1 mM	8 ppm	8 mM
Precision	Intra/Inter-assay % RSD typically <3%	Intra/Inter-assay % RSD typically < 3%	Intra/Inter-assay % RSD typically < 3%
R <sup>2</sup>	0.99	0.98	0.97
Reference	Our method	Bioscientific USA, catalogue no.:1051, 2009	FSSAI, AOAC method of urea analysis, 2012

## 2.4 Conclusion

The objective of this work was to develop a FIA-ET based urea biosensor for the determination of urea in adulterated milk samples. The developed biosensor can analyze concentration of urea up to 250 mM with semi-automated mode and up to 500 mM with automated mode in adulterated milk samples. Developed FIA-ET biosensor have potential for online monitoring in the dairy industries with some automation. The analytical signal is practically unaffected by matrix at optimized dilution with PB. Being specific in nature, it does not require separation of the reaction products, as would be necessary for other detection techniques. There is a

considerable rise in the sampling rate as there is no need of assay blanks thus serving as high throughput technique. When suitably treated, the enzyme reactor was used for years, thus eliminating the repeated use of costly enzyme, *i.e.* urease. The system has been used for months and the column is working excellent. The FIA-ET presented here is suitable for the rapid measurement of urea, maintaining the same sensitivity and accuracy of the enzymatic spectrophotometric and electrochemical methods with the typical advantages of the use of an immobilized biosensor such as reusability of the enzyme, no use of additional reagents, and the possibility to measure turbid samples without any much pretreatment. Thus, the biosensor presented in this study maintains the qualities required for further development into an on-line urea biosensor in the dairy processing plants.

## Chapter 3

### Development of FIA-ET biosensor for urea analysis in urine



*Graphical abstract of chapter content*

### **3.1 Introduction**

#### **3.1.1 Urea as clinical analyte in urine**

Being a waste product of the kidney, urea is an important biomarker that is routinely monitored to determine the functional ability of the renal system (Alizadeh and Akbari, 2013; Gutierrez et al, 2008). Urea serves an important role in the metabolism of nitrogen-containing compounds by animals and is the main nitrogen-containing substance in the urine of mammals. Urea is synthesized in the body of many organisms as part of the urea cycle, either from the oxidation of amino acids or from ammonia. In this cycle, amino groups donated by ammonia and L-aspartate are converted to urea, while L-ornithine, citrulline, L-argininosuccinate, and L-arginine act as intermediates. Urea production occurs in the liver and is regulated by N-acetylglutamate. Urea then dissolves into the blood and further transported and excreted by the kidney as a component of urine. The normal range of urea in urine and blood is between 8 and 20 mg/dL. The handling of urea by the kidneys is a vital part of mammalian metabolism. Besides its role as a carrier of waste nitrogen, urea also plays a role in the countercurrent exchange system of the nephrons, which allows for re-absorption of water and critical ions from the excreted urine. Elevated urea levels in serum and urine are indicative of renal dysfunction, urinary tract obstruction, dehydration, diabetes, shock, burns, and gastrointestinal bleeding. However, the reduced urea level may cause hepatic failure, nephritic syndrome, and cachexia (Sumana et al, 2010).

#### **3.1.2 State of the art for analysis of urea in urine**

Several analytical methods such as reverse phase ultra-fast liquid chromatography (Czauderna *et al.*, 2012), colorimetric method based on the reaction of urea and diacetyl-monoxime derivatives (Goeyens *et al.*, 1998), infrared spectrometry (Jensen *et al.*, 2004), and high performance liquid chromatography (Clark *et al.*, 2007) have been utilized for urea determination. Furthermore, biosensor techniques such as potentiometry, conductimetry, and amperometry have also been extensively studied for the detection of urea by urease-catalyzed hydrolysis products (Koncki *et al.*, 2000; Jdanova *et al.*, 1996; Pizzariello *et al.*, 2001). The growing demand for clinical diagnostics in relation to kidney diseases has stipulated the development of new methods for the rapid and accurate measurement of urea in samples like urine and serum. Thermal biosensors

have been considered to be a practical alternative due to their robustness, simplicity, low cost, and extended stability. Another advantage of thermal biosensors is the universal detection principle that has been combined with the specificity of biological reactions. A number of enzymatic reactions for the analysis of urea, glucose, lactate, cholesterol, heavy metals, and fructose have been studied by thermal biosensors among which urea detection was studied extensively in serum and milk (Yakovleva *et al.*, 2013). The reported biosensors for analysis of urea in urine samples are summarized in Table 3.1.

**Table 3.1** Summary of reported biosensors for analysis of urea in urine.

<b>Biosensor/ Transducer's</b>	<b>Dynamic range</b>	<b>Detection limit</b>	<b>Response time</b>	<b>Stability</b>	<b>References</b>
Capacitance biosensor	0.1 pM–10 mM	3.7 pM	-	-	Alizadeh and Akbari, 2013
Potentiometric	1-1000 mM	1 mM	1-2 min	20 days	Gutierrez et al, 2007
Colorimetric	0.17-0.44 M	1 nM	2 min 29 sec	20 days at 4°C	Verma <i>et al.</i> , 2012
Amperometric	10-250 μM	10 μM	-	3 months	Pizzariello <i>et al.</i> , 2001
Enzyme based biosensor	0-714.3 mM	0.066 mM	10 min	-	Morishita <i>et al.</i> , 1997
Enzyme based biosensor	0-100 mM	0.047 mM	-	-	Orsonneau <i>et al.</i> , 1992
Amperometric Biosensor	0.1-35 mM	0.1 mM	3 sec	-	Tiwari <i>et al.</i> , 2009

### **3.1.3 Objective**

The aim of this work was to develop a biosensor with broad detection range for analysis of urea in urine samples using FIA-ET technique. Another objective of this work was to reduce the cost of column material for immobilization of the enzyme urease.

## **3.2 Experimental Section**

### **3.2.1 Chemicals and biochemicals**

Enzyme urease (Jack beans lyophilized 5 U mg<sup>-1</sup>, EC 3.5.1.5), urea, sodium dihydrogen phosphate monohydrate, disodium hydrogen phosphate monohydrate, glutaraldehyde solution 25 %, and tri-ethanol amine were obtained from Merck, Germany. Functionalized silica gel (amino-3, ca. 1.4 mmol, particle size 40–83 μm) was procured from Across Organics, NJ, USA. All other chemicals used were of GR grade.

### **3.2.2 Solution preparation**

Phosphate buffer (PB) 100 mM, pH 7.2, was prepared by mixing 100 mM of sodium dihydrogen phosphate monohydrate and 100 mM of disodium hydrogen phosphate monohydrate in double distilled water. PB was degassed before the analysis. A stock solution of urea (1,000 mM) was prepared by dissolving an appropriate amount of urea in 100 mL of PB (100 mM, pH 7.2). The working solution of urea was freshly prepared prior to use.

### **3.2.3 Instrumentation for FIA-ET biosensor**

For urea analysis in urine samples, automated FIA-ET biosensor was used. The schematic setup for the FIA-ET biosensor is presented in Figure 3.1. The experimental setup consists of a peristaltic pump (Gilson Minipuls Evolution II, France), an automated six-port injection valve (Rheodyne, Cotati, USA), sample loop (0.1 mL), enzyme thermistor, Wheatstone bridge equipped with a chopper-stabilized amplifier, and pico logger data recorder (Picotech, UK). PTFE tubing's (0.8 mm i.d.) were used for the connection. PB (100 mM, pH 7.2) was used as the carrier buffer.

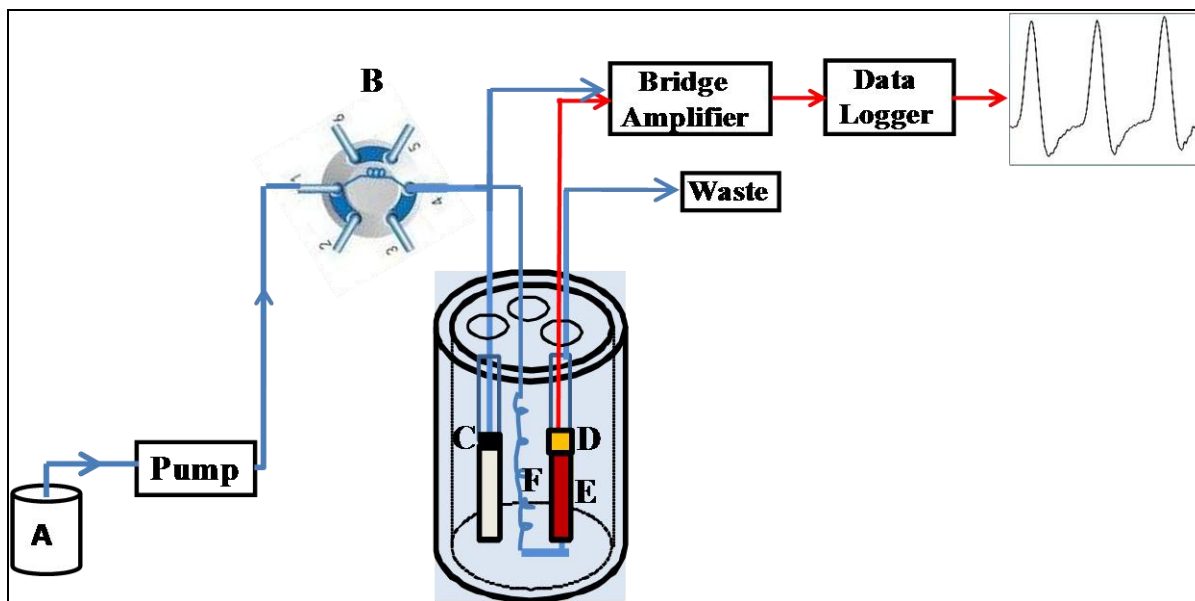


**Figure 3.1** Schematic representation of the experimental setup of automated FIA-ET biosensor for urea analysis in urine. A-buffer reservoir, B-automated injection valve, C-reference probe, D-thermistor, E-immobilized urease column, and F-heat exchanger.

### 3.2.4 Immobilization of urease on aminated silica gel

Enzyme immobilization on amine-functionalized silica gel was achieved by glutaraldehyde cross-linking as reported earlier with slight modifications as presented in Figure 3.2. In brief, urease were covalently immobilized on amine-functionalized silica gel according to the following procedure: 250 mg aminated silica gel was activated with 2.5 % glutaraldehyde in 100 mM PB, pH 7.2. The reaction was allowed to take place for at least 1 hrs inside the desiccators, under reduced pressure. The activation of the aminated silica gel support was confirmed by the presence of a brick red color (formation of Schiff base). Activated silica gel was successively washed with double distilled water and PB. Urease 200 mg (1,000 IU) dissolved in 1 mL PB was added to the wet activated silica gel. The coupling reaction was allowed to proceed for 30 min at room temperature and overnight at 4°C. The enzyme preparation was washed with PB. Tri-ethanolamine (200 mM) was added to terminate all the unreacted groups and then washed with 100 mM PB, pH 7.2. The immobilized urease was finally packed into a delrin column by a slurry packing method.

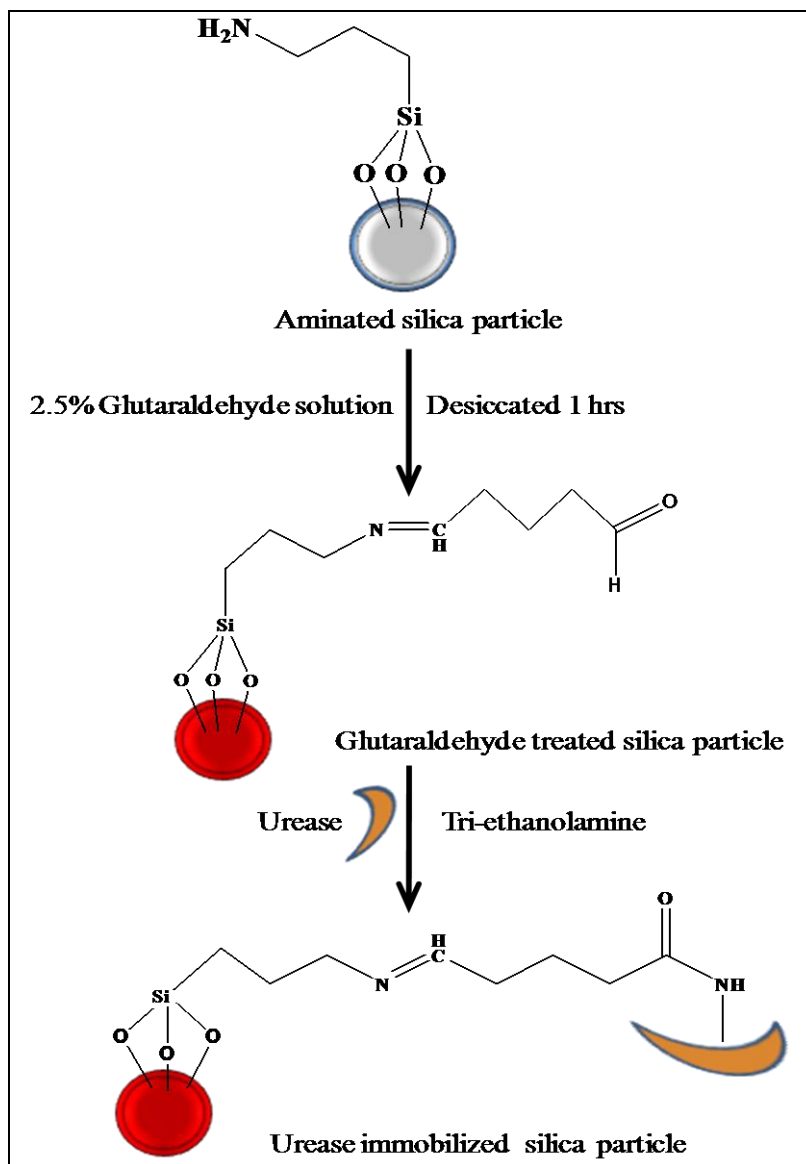


**Figure 3.2** Schematic representation of immobilization of urease on aminated silica gel.

### 3.2.5 Surface Characterization of the Silica gel Matrix

The surface of the aminated silica matrix was characterized using JEOL JSM6360 LV scanning electron microscope (SEM) at 400X magnification as presented in Figure 3.3 (A) and (B). Figure 3.3 (A) shows the bare surface of the silica particle and enlarge section shows the clear surface of the silica. Figure 3.3 (B) shows the enzyme molecule attached to the silica matrix. Furthermore, Fourier transform infra red (FTIR) spectroscopy was also applied to measure the surface properties of the aminated silica matrix coupled to an enzyme. The surface was characterized



before and after immobilizing the enzyme to the silica particles. Spectra were recorded using IR Affinity1 (SHIMADZU, Japan) with attenuated total reflectance (ATR) attachment specac diamond ATR AQUA using 40 scans at  $4\text{ cm}^{-1}$  resolution collected under vacuum condition. The ATR FT-IR spectra are shown in Figure 3.4. The insets in Figure 3.4 (1a, 1b and 1c) showing the result for amine functionalized silica surface. In Figure 3.4 (1a) presence of two peaks at  $2963$  and  $2858\text{ cm}^{-1}$  represent the  $as\text{CH}_2$  and  $s\text{CH}_2$  vibration. In Figure 3.4 (1b) four different peaks at  $1562$ ,  $1506$ ,  $1488$  and  $1471\text{ cm}^{-1}$  is due to the asymmetric and symmetric bending of primary amine. The presence of one peak at  $669\text{ cm}^{-1}$  with two associated peaks at  $686$  and  $648\text{ cm}^{-1}$  confirms the presence of  $-\text{Si}-\text{C}-$  bond in amine functionalized silica (not shown in inset). In Figure 3.4 (2a) the formation of Schiff's base after treatment with glutaraldehyde is confirmed by the appearance of two different peaks at  $1702$  and  $1651\text{ cm}^{-1}$  for  $-\text{C}=\text{N}-$  and  $-\text{CO}$  of free aldehyde group. In Figure 3.4 (3a) the presence of peak at  $1641\text{ cm}^{-1}$  is attributed to  $-\text{C}=\text{O}$  of peptide bond between immobilized urease enzyme and glutaraldehyde activated silica particle. In Figure 3.4 (3a) presence of peaks at  $1528$  and  $1477\text{ cm}^{-1}$  with two associated peaks at  $1459$  and  $1443\text{ cm}^{-1}$  are due to asymmetric and symmetric bending vibration of  $-\text{NH}-$  of secondary amide. The peaks appear at  $1234$  and  $1076\text{ cm}^{-1}$  are due to  $-\text{C}-\text{N}-$  and  $-\text{Si}-\text{O}-\text{Si}$  bond. A broad band from  $3257\text{ cm}^{-1}$  may be attributed to  $-\text{NH}-$  stretching vibration.

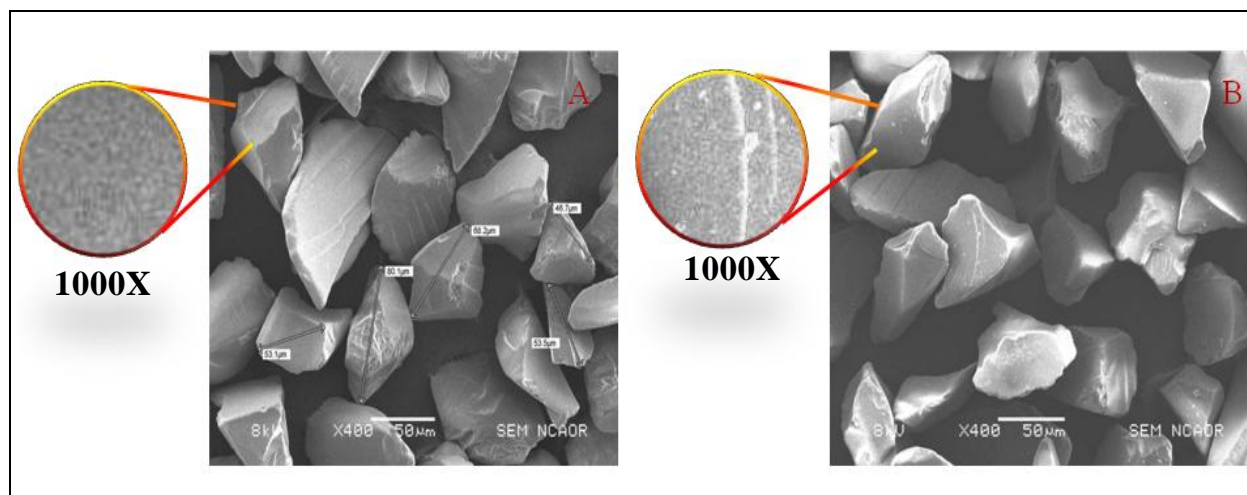


**Figure 3.3** SEM micrographs of bare and enzyme coupled silica matrix at magnification 400X.

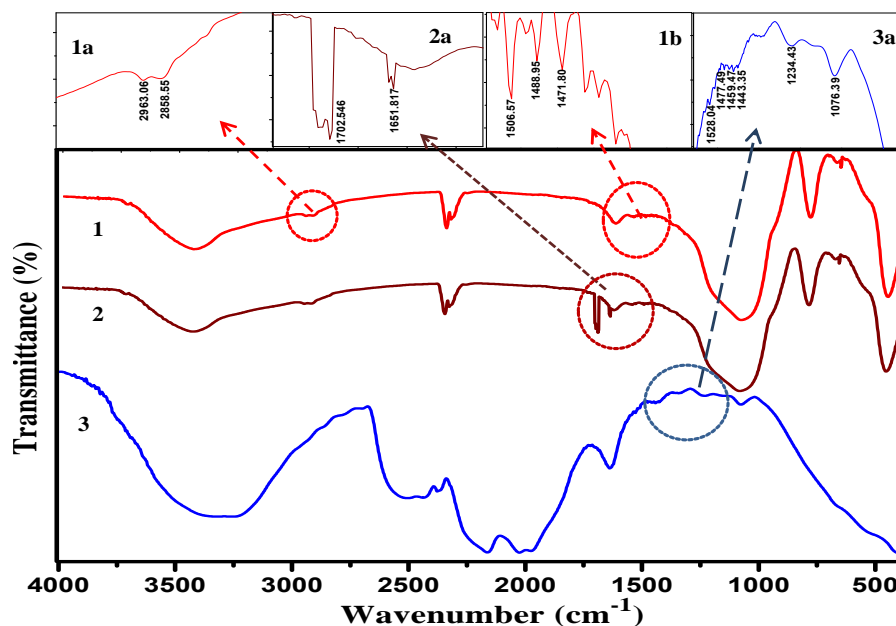


**Figure 3.4** FT-IR characterization of (1) aminated silica matrix (2) glutaraldehyde activated silica matrix and (3) immobilized urease on silica matrix. Inset: (1a, 1b, 2a and 3a) represents the corresponding FT-IR characteristic peaks.

### 3.3 Result and Discussion

#### 3.3.1 Optimization of the experimental variables for FIA-ET biosensor

##### 3.3.1.1 Optimization of the pH, ionic strength and flow rate

For determination of urea in urine samples, measurements for optimization of flow system were carried out. A series of experiments were performed for varying pH (6.8–7.4) and ionic strength (10, 50, 100 and 200 mM) for PB. As presented in Figure 3.5 and Figure 3.6, it is clear that the FIA-ET gives maximum response at pH 7.2 and 100 mM ionic strength of the PB against 200 mM urea. Flow rates of 0.25, 0.5, 0.75, and 1.0 mL/min was investigated against 200 mM urea. As presented in Figure 3.7, maximum response was observed at a flow rate of 0.5 mL/min. These results indicate that the performance of the FIA-ET was highly reproducible under optimized conditions of PB (pH 7.2, ionic strength 100 mM and flow rate of 0.5 mL/min).

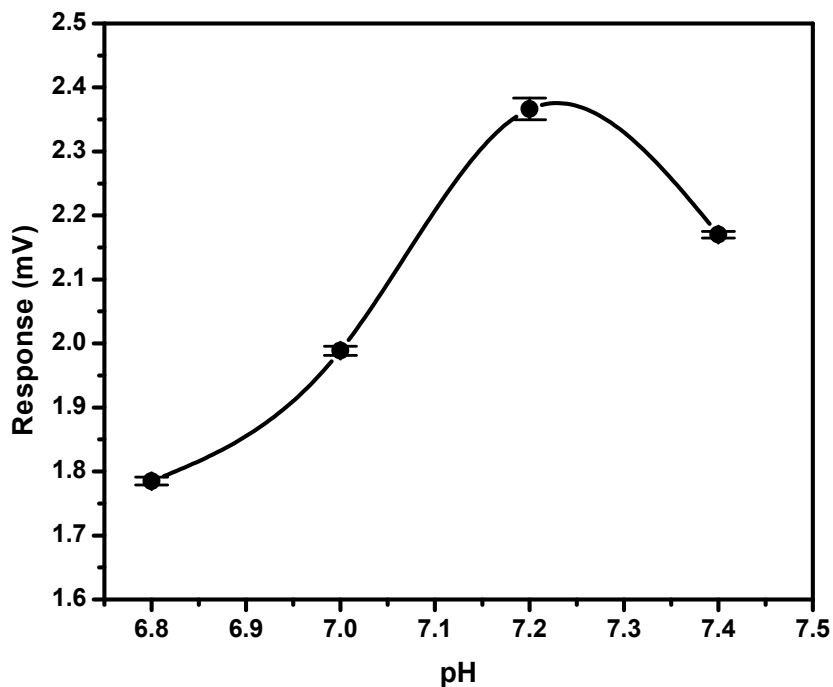


**Figure 3.5** Effect of pH of PB on the response of FIA-ET biosensor for 0.1 mL injection of 200 mM urea.

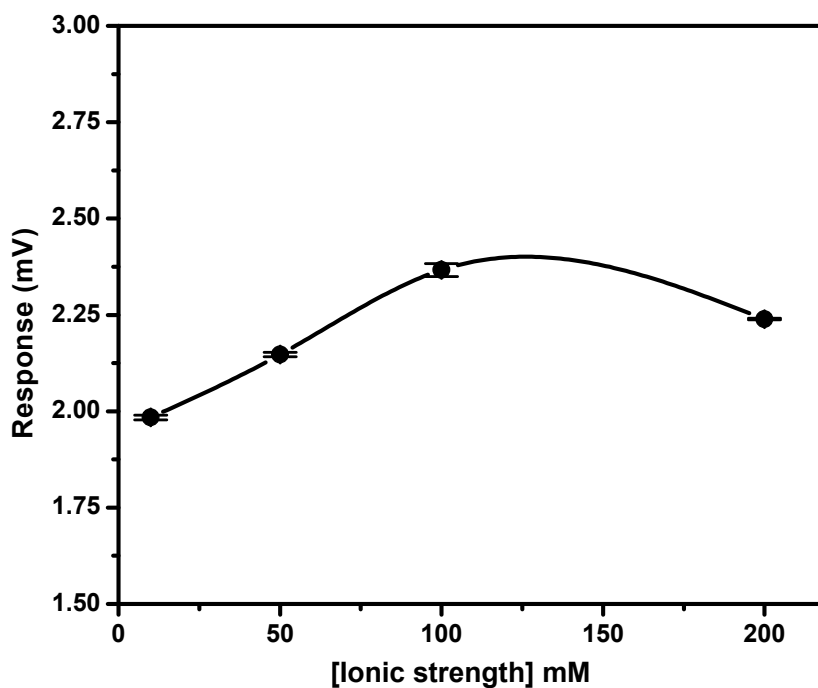


**Figure 3.6** Effect of ionic strength of PB on the response of FIA-ET biosensor for 0.1 mL injection of 200 mM urea.

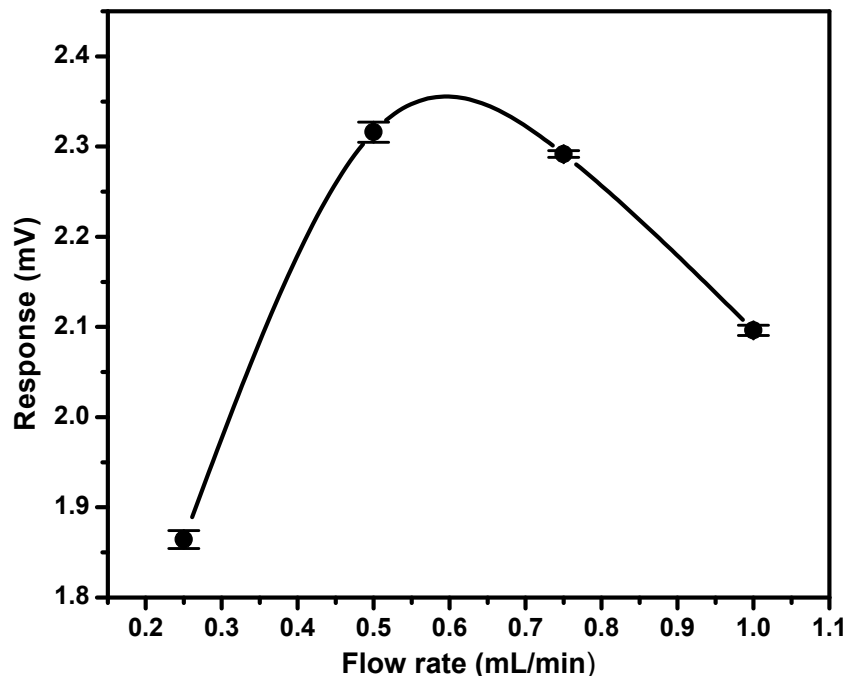


**Figure 3.7** Effect of flow rate of PB on the response of FIA-ET biosensor for 0.1 mL injection of 200 mM urea.

### 3.3.2 Calibration of biosensor for urea analysis in buffer

The packed column with immobilized urease enzyme was installed inside the thermistor and allowed to equilibrate with the carrier buffer. The filtered and degassed PB was pumped manifold via FIA until a constant baseline was achieved. Mock urea standard solutions in the range 10- 1000 mM were prepared in PB and injected in to the flow stream. Response signals were recorded using a data logger acquisition system connected to Wheatstone bridge and plotted as current (mV) vs. urea (mM). All samples were measured in triplicates. The Michaelis constant,  $K_M$  for urea was calculated using Line weaver–Burk plot and found to be 448 mM. A good linear response was obtained for urea hydrolysis in the range of 10–1000 mM, which is presented in Figure 3.8. The linear fit of data shows a good correlation between urea and immobilized urease ( $R^2 = 0.99$ , % RSD = 0.02).

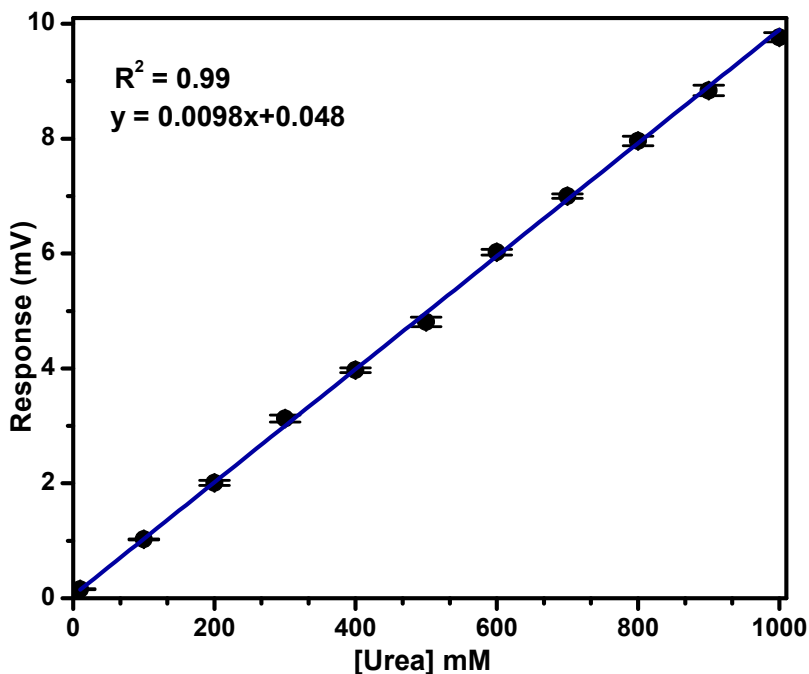


**Figure 3.8** Calibration plot obtained for urea using FIA-ET biosensor in 100 mM PB, pH 7.2 for 0.1mL of sample injection, flow rate 0.5mL/min at 30°C.

### 3.3.3 Matrix matching for urine sample analysis

For urea analysis in urine, samples of different individuals were collected and the matrix effect in the analysis of urea in urine sample was investigated. Various measurements on ionic strength and pH of urine samples were performed for appropriate dilutions of urine with PB. It was observed from Figure 3.9, that 1:4 dilution of urine sample with PB was most responsive to urea analysis. To obtain the calibration curve for urea in spiked urine samples, a simple dilution strategy worked out to avoid the effect of ionic strength and pH on urease column. Urine analysis was carried out within the same day after sample preparation.

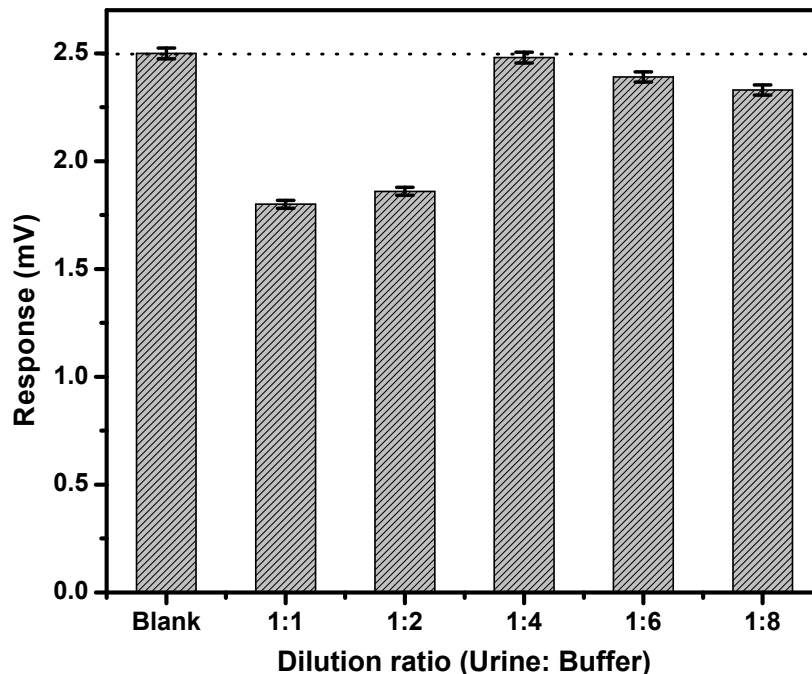


**Figure 3.9** Effect of dilution of PB and urine on the response of FIA-ET biosensor for 0.1 mL injection of 200 mM urea.

### 3.3.4 Analysis in urine

For urea analysis in urine samples, calibration standards (10-1000 mM) were prepared by dilution of urea stock solution (1000 mM) in 100 mM PB, pH 7.2. The immobilized urease column was mounted inside ET and was allowed to equilibrate with the surrounding. The degassed carrier buffer was passed at an optimum flow rate of 0.5 mL/min at which a stable baseline was achieved. Samples were injected and data collected using a data acquisition system connected to the Wheatstone bridge. All measurements were carried out by injection of 0.1 mL sample at a flow rate of 0.5 mL/min. After each sample analysis, the sample loop was thoroughly rinsed with PB. The urine samples were spiked with known amounts of urea and after matrix matching with appropriate dilutions were injected into the FIA-ET system.

### 3.3.5 Calibration of biosensor for urea analysis in spiked urine

Urine samples spiked with urea standard solutions (10-1000 mM) were injected into the flow stream and response signal was recorded. The FIA-ET biosensor showed an excellent dynamic range for the urea present in spiked urine in the range 10–1000 mM with a good linearity and

minimum detection limit was 10 mM. The results are presented as Figure 3.10 ( $R^2 = 0.99$ , % RSD = 0.741).

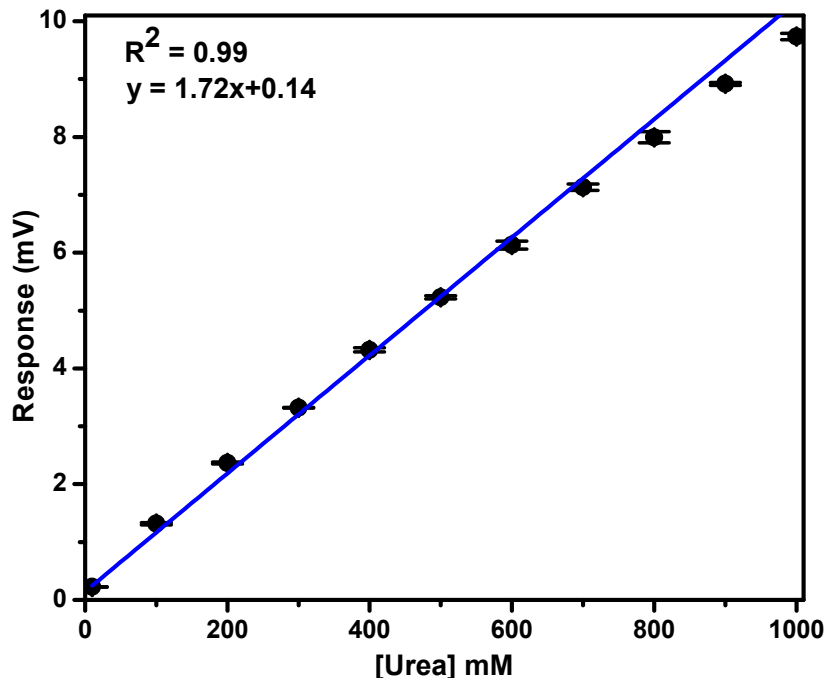


**Figure 3.10** Calibration plot obtained for urea spiked urine samples using FIA-ET biosensor in 100 mM PB, pH 7.2 for 0.1mL of sample injection, flow rate 0.5mL/min at 30°C.

Various biosensors are reported in the literature for analysis of urea and most of the biosensors used urease as biorecognition element and have a good detection range. However, the presented FIA-ET urea biosensor is capable of detecting urea in urine sample in a broad dynamic range (10-1000 mM) that covers the requirement of clinical industries to determine the functional ability of the renal system. A real time response obtained from FIA- ET urea biosensor for urea concentration 10-1000 mM is shown as Figure 3.11.

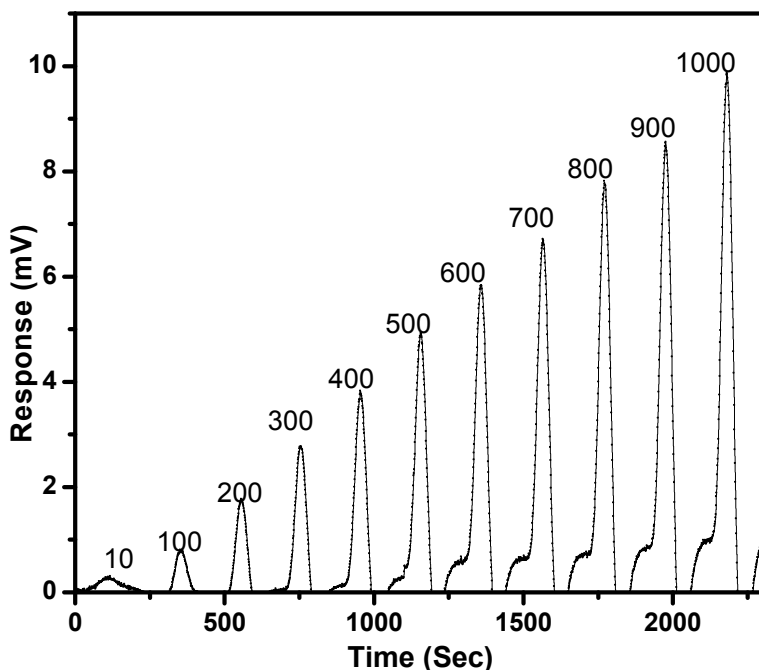


**Figure 3.11** Real time responses obtained from urea spiked urine samples (10-1000 mM) using FIA-ET biosensor in 100 mM PB, pH 7.2 for 0.1mL of sample injection, flow rate 0.5mL/min at 30°C.

### 3.3.6 Urea recovery studies from spiked urine samples

To perform recovery studies in urine samples, a known amount of urea standard was spiked to dilute urine sample and analyzed in FIA-ET biosensor. Recoveries were calculated from the obtained response signal. Table 3.2 shows the recovery results obtained for urine urea. Excellent recoveries were obtained in the range 92.26–99.80 % in the spiked urine samples. This ensures the reproducibility and sustainability of the developed biosensor.



**Table 3.2** Determination of % recovery from urea spiked urine samples.

Urine Samples	Urea added (mM) (n= 3)	Urea found (mM) (n=3)	% Recovery	Mean $\pm$ S.D.	%RSD
Sample-1	0.5328	0.5219	97.97	0.97 $\pm$ 0.016	1.64
Sample-2	1.0237	0.9445	92.26	0.94 $\pm$ 0.012	1.28
Sample-3	2.0086	1.9767	98.41	1.97 $\pm$ 0.071	3.60
Sample-4	3.1277	2.9511	94.36	2.95 $\pm$ 0.016	0.54
Sample-5	3.9692	3.9613	99.80	3.96 $\pm$ 0.016	0.40
Sample-6	4.8124	4.7315	98.32	4.73 $\pm$ 0.022	0.46
Sample-7	6.0250	5.7695	95.76	5.77 $\pm$ 0.034	0.59
Sample-8	6.9983	6.7612	96.61	6.76 $\pm$ 0.021	0.31
Sample-9	7.9598	7.6810	96.50	7.68 $\pm$ 0.106	1.38
Sample-10	8.8393	8.5633	96.88	8.56 $\pm$ 0.123	0.14
Sample-11	9.7647	9.3846	96.11	9.38 $\pm$ 0.022	0.23

### 3.3.7 Operational stability of the urease immobilized silica gel column

Stability of the developed FIA-ET urea biosensor was investigated by making repetitive measurements over a period of 30 weeks. The sensor showed a good operational stability when continuously monitored at room temperature. Amine-functionalized silica gel micro particle (particle size 40-83  $\mu\text{m}$ ) was used as a column matrix to reduce the cost of the column and the cost per sample analysis. To check the stability of the developed urea biosensor about 20 measurements were made every week against 200 mM urea. The operational stability of immobilized urease column is presented as Figure 3.12. The immobilized urease column showed excellent stability over the initial 5 weeks with no appreciable loss of enzyme activity. After the 15 weeks of continuous use, enzyme activity was found about 90% of the original response. However, after a period of 20 weeks operation, about 14% decay in response was recorded. Similarly, the response was monitored within 25, and 30 weeks and signals recorded were respectively 85%, and 80% of the original response.

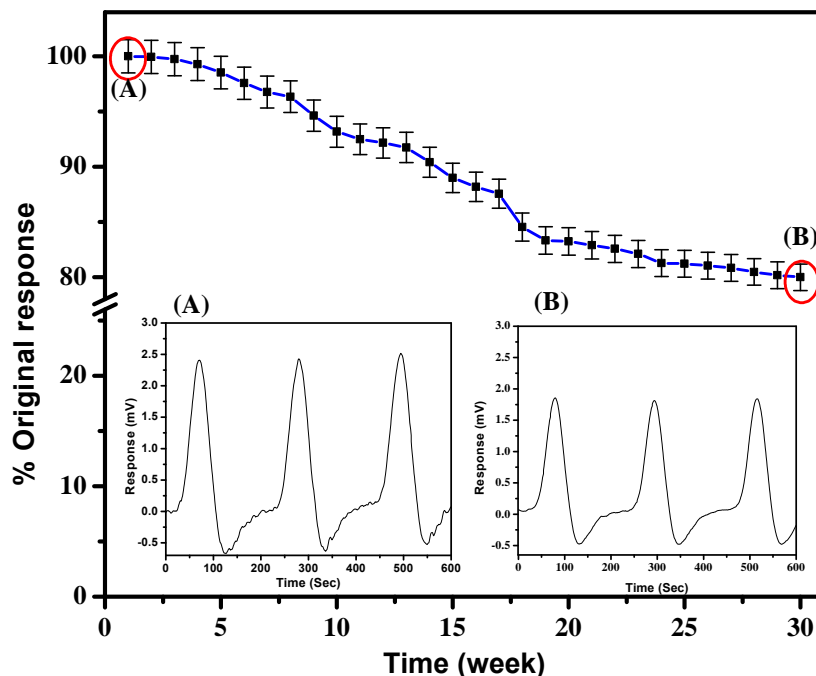


**Figure 3.12** Operational stability of FIA-ET urine urea biosensor, response to 0.1 mL, 200 mM urea over the period of 30 weeks at room temperature, inset: real time triplicate response obtained from FIA-ET urea biosensor against 200 mM urea of initial week and 30<sup>th</sup> week of operation.

### 3.3.8 Precision of the biosensor for urea analysis in urine

Precision of the developed biosensor was determined by measuring the known concentrations of urea at different time interval ranging from hrs to days. Three concentrations of urea (100, 200 and 500 mM) were selected from the calibration range. The response of urea was recorded 3 times in a day for five consecutive days. The precision and reproducibility of the method were evaluated in terms of % RSD As observed from the Table 3.3, very good reproducibility was obtained for urea concentration with % RSD 0.49- 1.29 (n=3) for intraday analysis and % RSD 0.08-0.89 (n=3) for interday analysis. Furthermore, in order to determine the reliability of the developed urea biosensor, several triplicate measurements were performed on urea spiked urine samples. Figure 3.13 shows the real time triplicate sensor signal recorded from FIA-ET urea biosensor for 200 mM urea spiked urine sample. The obtained signal confirms reproducibility of the sensor response.

**Table 3.3** Intra-day and inter-day reliability of FIA-ET biosensor for urea analysis in urine.

Intra-day reliability				Inter-day reliability			
Urea(mM)	Mean (mV) (n = 3)	Mean ± S.D.	% RSD	Day's	Mean (mV) (n = 3)	Mean ± S.D.	%RSD
100	1.3145	1.31 ± 0.017	1.29	Day-1	2.3721	2.37± 0.021	0.89
200	2.3664	2.36 ± 0.016	0.67	Day-2	2.3605	2.36± 0.019	0.80
500	5.2284	5.22 ± 0.026	0.49	Day-3	2.3479	2.34± 0.015	0.65
				Day-4	2.3518	2.35± 0.002	0.10
				Day-5	2.3305	2.33± 0.002	0.08

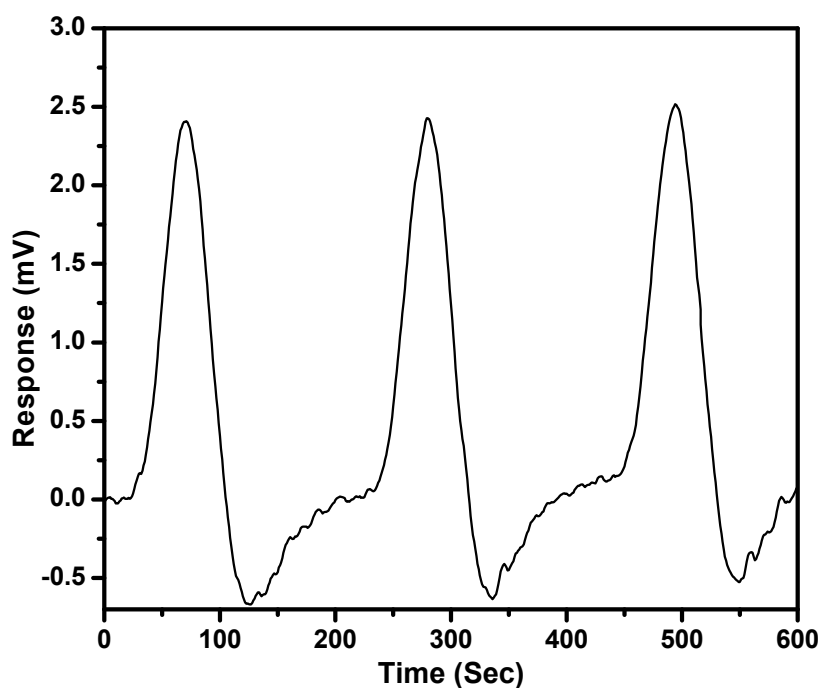


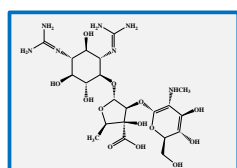
**Figure 3.13** Real time triplicate sensor signal recorded from FIA-ET urea biosensor for 0.1mL sample of 200 mM urea, flow rate 0.5 mL/min at 30°C.

### **3.4 Conclusion**

The objective of this work was to develop a FIA-ET based urea biosensor for the determination of urea in urine samples. A low cost urease immobilized aminated silica gel column matrix has been tested successfully for analysis of urea present in the urine samples, without compromising the operational stability. This significantly reduces the cost of analysis per sample. The FIA-ET biosensor showed an excellent dynamic range for urea present in spiked urine in the range 10–1000 mM with a good linearity and minimum detection limit was 10 mM. Results indicate that the developed biosensor is highly stable, simple, and economical. The system has been automated for real time analysis with response time of 90 sec. Developed biosensor can facilitate the regular monitoring of abnormal urea concentrations to keep track of functional ability of the renal system.

## Chapter 4

### Development of flow injection analysis–electrochemical quartz crystal nanobalance (FIA-EQCN) biosensor for analysis of antibiotic residues in milk



Streptomycin



*Graphical abstract of chapter content*

## **4.1 Introduction**

### **4.1.1 Occurrence of antibiotic residues in the milk**

Antibiotics are one of the most important bioactive and chemotherapeutic groups of compounds. In veterinary medicine, antimicrobial drugs are routinely used to treat mastitis in dairy cows but the efficiency of antibiotics as growth enhancers also has led to their use as supplements in animal feed. Sulphonamides and aminoglycosides are the family of chemotherapeutic that are widely used for therapeutic and prophylactic purposes in animal diseases. Antibiotics are being in use either individually or in combination with other drugs for the treatment of inflammatory diseases or as feed additives. Toxicological data show that some antibiotics have antithyroid effects in both animals and humans (Velasco-Garcia and Mottram, 2003). **Streptomycin (SRT)**, a member of aminoglycoside, finds wide application in modern agriculture and dairy for treatment of mastitis in cattle's (Haasnoot *et al.*, 2003). **Sulfadiazine (SDZ)** is a member of the sulfonamide or the sulpha drug family, which plays an important role in veterinary medicine by controlling many bacterial and protozoan diseases (Murtazina *et al.*, 2004). The occurrence of these antibiotic residues in food carries the risk of increasing the number of resistant bacteria and transferring antibiotic resistance genes to human pathogens. Indiscriminate use of antibiotics may produce residues in the milk, and subsequently induce allergic reactions in humans. Monitoring of antibiotics is very important for safety of milk or milk products for human consumption, since the presence of these residues even in minute amount can trigger potential health hazard such as allergic reactions in hypersensitive individuals, toxicity, or they can be act as potential carcinogens (Conzuelo *et al.*, 2012). Apart from the consequences for public health, economic reasons have also led to a control of antimicrobial residues in food. Several regulatory agencies have set the maximum residual limit (MRL) for antibiotics in the milk for consumer protection. In particular, the European Union (EU) has fixed the limit at 200 ng/mL (200 ppb) for SRT in the milk whereas for SDZ it is 100 ng/mL. In The United States, the tolerance limit for SRT in the milk is 125 ng/mL. The Codex Committee has set a combined MRL of 200 ng/mL for SRT and dihydro-streptomycin (DHSRT) (Commission Regulation (EU) No 37/2010, 2009; Baxter *et al.*, 2001). The molecular structures of some cross reactive sulfonamides and aminoglycosides are shown as Figure 4.1.

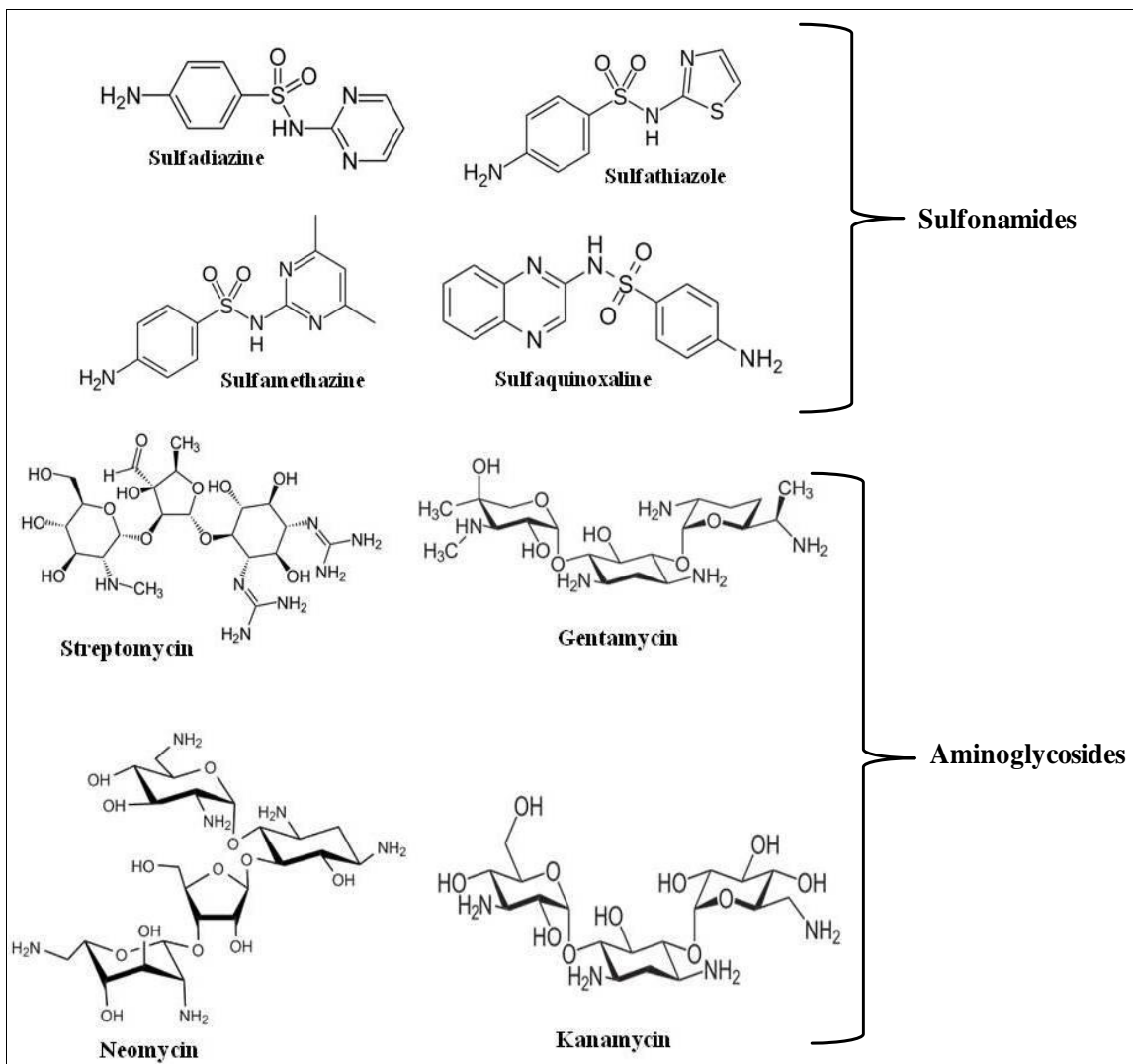


**Figure 4.1** Molecular structures of some cross-reactive sulfonamides and aminoglycosides antibiotics.

#### 4.1.2 State of the art of antibiotic detection in the milk

Various analytical methods have been reported for the analysis of antibiotics in the last decade. Traditional methods usually involve methods such as microbial inhibition assays or enzymatic colorimetric assays along with immunoassay methods. Usually, milk samples will be examined using rapid screening methods that may only indicate whether antibiotics are present and not the levels and types of antibiotics. Samples that fail to pass the screening tests will then be examined

using more complex instrumental methods, such as high-performance liquid chromatography (HPLC) and gas chromatography–mass spectrometry (GC–MS). Several analytical techniques such as HPLC (Stoev and Michailova, 2000; Furusawa, 2003) GC–MS (Reeves, 1999) and enzyme-linked immuno sorbent assay (ELISA) (Cliquet *et al.*, 2003) are reported for the detection of sulfonamides in different matrices. HPLC and GC–MS are sensitive and specific, but are very laborious and expensive. They are suitable for confirming but not for screening a large number of samples (Wang *et al.*, 2007). More recently, immunoassay type methods have been developed, which are faster and more specific than traditional screening methods. These ELISA can identify and quantify a wide range of antibiotics and can be specific to a single or a group of antibiotics (Adrian *et al.*, 2008). However, ELISA do require modification of the antibodies used in the assay and can become laborious and time consuming when large numbers of samples are to be analyzed. Therefore, there has been an interest in the development of biosensors for antibiotics that do not require extensive chemical modification or pretreatment steps and that are rapid, quantitative, and selective. This has led to investigations into the use of immunosensors for the detection of antibiotics (Davis and Higson, 2010). Biosensors are a recent addition to analytical instrumentation capable of performing residue testing and offer the potential for rapid, quantitative high-throughput analysis. More recently, several biosensors techniques have also been reported addressing clinical, environmental, and food safety for antibiotic residue analysis, one such testimony for sulfonamide detection is surface plasmon resonance (SPR) based biosensors (Situ *et al.*, 2010; Fernandez *et al.*, 2011). However, there are very few biosensor reported for the detection of sulfadiazine particularly in the milk samples

A wide range of analytical methods currently exist for the detection and quantitative measurements of SRT. Microbial inhibition assay (Currie *et al.*, 1998), enzyme immunoassay (Abuknesha *et al.*, 2005) ELISA (Heering *et al.*, 1998) and microplate array based techniques (Ye *et al.*, 2008) are commonly employed as screening tests. Conventional analytical techniques such as liquid chromatography and liquid chromatography-mass spectroscopy (LC-MS) (Zhu *et al.*, 2008) have been described for confirmatory analysis. An effective monitoring technique for regulation of these antibiotics require specific sensitivity, rapid, reliable and economical methods able to detect them at or below the MRL levels (Conzuelo *et al.*, 2013).



**Table 4.1** Summary of reported biosensor techniques for detection of SDZ and SRT in the milk samples.

Analyte	Biosensor/ Transducers	Detection limit	Reference
Sulfadiazine	Flow cytometry Immunoassay	1 ng/mL	Keizer <i>et al.</i> , 2008
	Immunoassay	10 ng/mL	Bjurling <i>et al.</i> , 2000
Streptomycin	Electrochemical	7 pg/mL	Que <i>et al.</i> , 2013
	Electrochemical immunoassay	5pg/mL	Liu <i>et al.</i> , 2011
	Immunoassay	4.5 ug/L	Bilandzic <i>et al.</i> , 2011
	ELISA	2ng/mL	Wu <i>et al.</i> , 2010
	iSPR Immunosensor	1.2 ng/ml	Raz <i>et al.</i> , 2009
	ELISA	3.0 ng/mL	Samsonova <i>et al.</i> , 2005
	Immunoassays	5.06 ug/L	Knecht <i>et al.</i> , 2004
	Immunochemical	3.2ng/mL	Strasser <i>et al.</i> , 2003
	Immunoassay	65ng/mL	Haasnoot <i>et al.</i> , 2003
	Optical biosensor	30 µg/kg	Ferguson <i>et al.</i> , 2002
	Optical immunobiosensor	4.1ng/mL	Baxter <i>et al.</i> , 2001

Several biosensor techniques have also been reported recently for SRT detection in the milk. One such testimony is Surface plasmon resonance (SPR) based optical biosensor (Baxter *et al.*, 2001). Some biosensor techniques are summarized in Table 4.1 for detection of SDZ and SRT.

Compared with expensive and complicated optical instrumentation of SPR, quartz crystal microbalance (QCM) is more suitable for wide generalization and applications. Owing to its simplicity, convenience, and real time response, QCM has been increasingly explored in many fields of biological studies (Yang *et al.*, 2009; Yang *et al.*, 2009). QCM has the advantages of minimal electrical requirements, adaptability to microfluidic techniques, inexpensive fabrication, utility in a flow cell, and label-free detection. QCM biosensor integrated in a flow injection analysis (FIA-QCM) system has the advantages in terms of reproducibility, speed of analysis, control of contact time and concentration profiling in kinetic studies (Malitesta *et al.*, 2011).

#### 4.1.3 Working principle of EQCN

The principle of QCM detection is based on the frequency changes of the crystal that is proportional to the mass changes to the crystal surface. The quantitative relationship between the frequency shifts and the mass changes of the crystal is given by the well-known Sauerbrey equation (Sauerbrey, 1959)

$$\Delta f = \frac{-2\Delta m f_0^2}{A\sqrt{\rho_q \mu_q}} \quad (4.1)$$

Where,  $\Delta f$  is frequency change (Hz),  $\Delta m$  is the mass change (gm) on the sensor surface,  $f_0$  is the fundamental frequency (Hz),  $A$  the electrode surface area, and  $\rho_q$  and  $\mu_q$  are the density ( $\text{cm}^3$ ) and the shear modulus ( $\text{gm cm}^{-1}\text{s}^{-2}$ ) of the QCM sensor, respectively.

The EQCN is a measurement system for monitoring, extremely small variation in the mass of a working electrode attached to a vibrating quartz single crystal. Thin wafers cut from a quartz crystal at a specific orientation ( $35^\circ 15'$  angle) and with precise thickness (0.166 mm), which oscillates at a characteristic fundamental frequency of 10 MHz. The working electrode is in the form of a thin metal film evaporated on one side of a quartz crystal wafer, which is then sealed to the side opening in an electrochemical cell. Any change in the mass rigidly attached to the working electrode results in the change of the quartz crystal oscillation frequency. The frequency of the working quartz crystal is measured and compared to the frequency of the standard reference quartz crystal. Hence, the frequency measurements are differential, *i.e.* the frequency

of the reference crystal is subtracted from the frequency of the working crystal. The obtained frequency difference is then converted to an analog voltage using a frequency-to-voltage converter and measured using a 16-bit analog-to-digital converter (ADC). The frequency shift is proportional the mass change of the working electrode. The EQCN experiments are completely computer controlled with the data logger DAQ-716 with real-time VOLTSCAN data acquisition and control system (based on a 16-bit D/A converter and 16-bit A/D converters). All the data processing, graphing, and spreadsheet reporting are done with Voltscan 5.0 software. Calculations of frequency to mass change is calculated as per the following equation:

$$\Delta m = \frac{-\Delta f \times A \times \sqrt{\mu_q \rho_q}}{2(f_q^2)} \quad (4.2)$$

Where,

$\Delta m$  = Mass Change (gm)

$\Delta f$  = Resonant Frequency Change (Hz),

$A$  = Piezoelectric active surface for reaction (0.25 cm<sup>2</sup>)

$\mu_q$  = AT-cut quartz constant (2.947x10<sup>11</sup> gm cm<sup>-1</sup> s<sup>-2</sup>)

$\rho_q$  = Quartz crystal density (2.65g cm<sup>3</sup>)

$f_q$  = Reference frequency or Resonant Frequency (Hz),

In the EQCN 700 system, resonant frequency of the gold crystal was 10MHz (10 x 10<sup>6</sup> Hz) and calculated change of 1 Hz equals to 1.1040 ng.

#### 4.1.4 Self-assembled monolayers

To implement a FIA-QCM biosensor, biomolecules need to be immobilized on the crystal surface to capture target analyte. Various immobilization methods, including thiolation, silanization, and immobilization *via* cross-linking are used for binding of the biomolecules on the crystal surface. Recently antibody immobilization by way of self-assembled monolayers (SAMs) of thiolated antibody, exploiting carboxyl amine coupling of the antibody over the SAMs of different thiols or sulphide compounds have been demonstrated (Park *et al.*, 2004). SAMs of

organic molecules are molecular assemblies formed spontaneously on surfaces by adsorption and organized into more or less large ordered domains. SAMs are created by the chemisorptions of head groups onto a substrate from either the vapor or liquid phase followed by a slow organization of tail groups. The head groups assemble on the substrate, while the tail groups assemble far from the substrate. Areas of close packed molecules nucleate and grow until the surface of the substrate is covered in a single monolayer. Moreover, SAMs provide versatility and novel properties of surfaces and interfaces by conjugating biomolecules to facilitate a low-cost method of fabricating biosensor devices with improved activity, stability and selectivity (Ulman, 1996).

#### **4.1.5 Objective**

The aim of this work was to develop a highly sensitive and broad range biosensor for determination of antibiotic residues in the milk samples using FIA-EQCN based biosensor using specific antibodies against these antibiotics as a biocomponent.

### **4.2 Experimental Section**

#### **4.2.1 Chemicals and biochemicals**

Anti- Streptomycin monoclonal antibody-IgG fraction isolated from Mouse was purchased from abcam (UK). Streptomycin sulfate was procured from MP biomedical (France) and the streptomycin ELISA kit was procured from Biooscientific (USA). Anti-sulfadiazine polyclonal antibody Ig fraction isolated from sheep, sulfadiazine and sulfadiazine ELISA kit were purchased from Randox (UK). Sodium dihydrogen phosphate monohydrate, disodium hydrogen phosphate monohydrate, sodium chloride, 11-mercaptoundecanoic acid (11-MUA), 1-ethyl-3-[3-dimethylaminopropyl] carbodiimide hydrochloride (EDC), N-hydroxy succinimide (NHS), glutaraldehyde solution 25%, sodium chloride, glycine and cysteamine chloride were obtained from Merck (Germany). L-cysteine hydrochloride was procured from Himedia labs India. For sample handling, micropipettes (Eppendorf®, Germany) were used. Centrifugation of milk sample was done by minispin (Eppendorf®, Germany). All the solutions were prepared in a 0.22µm membrane filtered Milli-Q system RO water (Millipore, USA), Seven Multi pH meter

(Mettler Toledo, Switzerland) was used for pH measurements. All other chemicals used were of analytical grade and used as received.

#### 4.2.2 Instrumentation for FIA-EQCN biosensor

EQCN system integrated with flow cell model FC-6 (Elchema, USA) was deployed for construction of FIA biosensor. The gold quartz crystal (10 MHz, AT cut) was connected to the frequency-measuring unit, which contains a reference crystal with the same characteristics as the measuring crystal. A peristaltic pump (Gilson, France) was connected through a 6-port injection valve (Rheodyne, USA) to the flow-cell. The output from the oscillator was measured by the frequency unit, which calculated the mass by using a conversion factor (1Hz equivalent to 1ng). A personal computer controlled the data acquisition. The flow cell was placed in a faraday cage to shield the crystal from external electromagnetic sources. The experimental setup used for the study is shown as Figure 4.2.

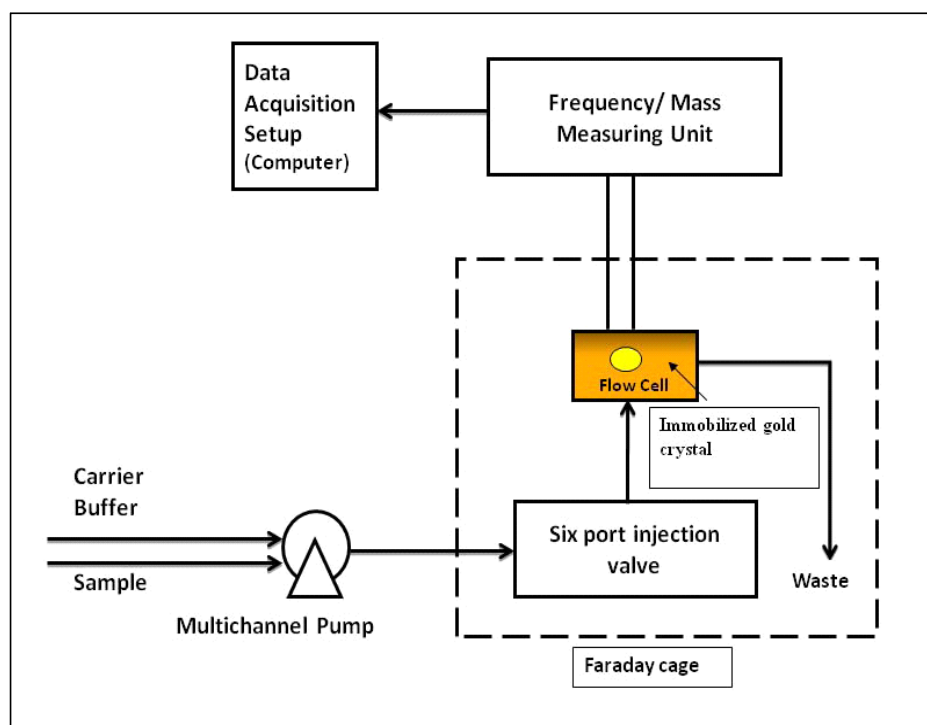


**Figure 4.2** Schematic of FIA-EQCN biosensor for antibiotic residue analysis in milk.

#### 4.2.2.1 Microfluidic of the flow cell

The gold quartz crystal was placed in a plexiglass flow cell, sandwiched between two O-rings, with its upper electrode in contact with the liquid and its lower electrode in the air. The diameter of the quartz wafer is 14 mm and the diameter of the working electrode is 5 mm. The volume of the flow cell was 50  $\mu\text{L}$  ( $\text{O} = 8\text{mm}$  and height = 1mm). The pump was connected in such a way that it reduced the pressure exerted on the crystal. Samples were filled in the 6-port injection valve and injected into the carrier buffer through 100  $\mu\text{L}$  sample loop. The sample was passed on the flow cell through the peristaltic pump with the flow rate of 0.5 mL/min in static mode and 0.1 mL/min in semi-automated mode. Real time response was recorded till the sample equilibrium. To reach the steady state equilibrium about 2 ml of sample was used at the flow rate of 0.1mL/min. The capacity of the working area (area under O ring) of the flow cell is 40  $\mu\text{L}$  at equilibrium. Figure 4.3 represents the schematic setup of the FIA-EQCN system with microfluidic of the flow cell.

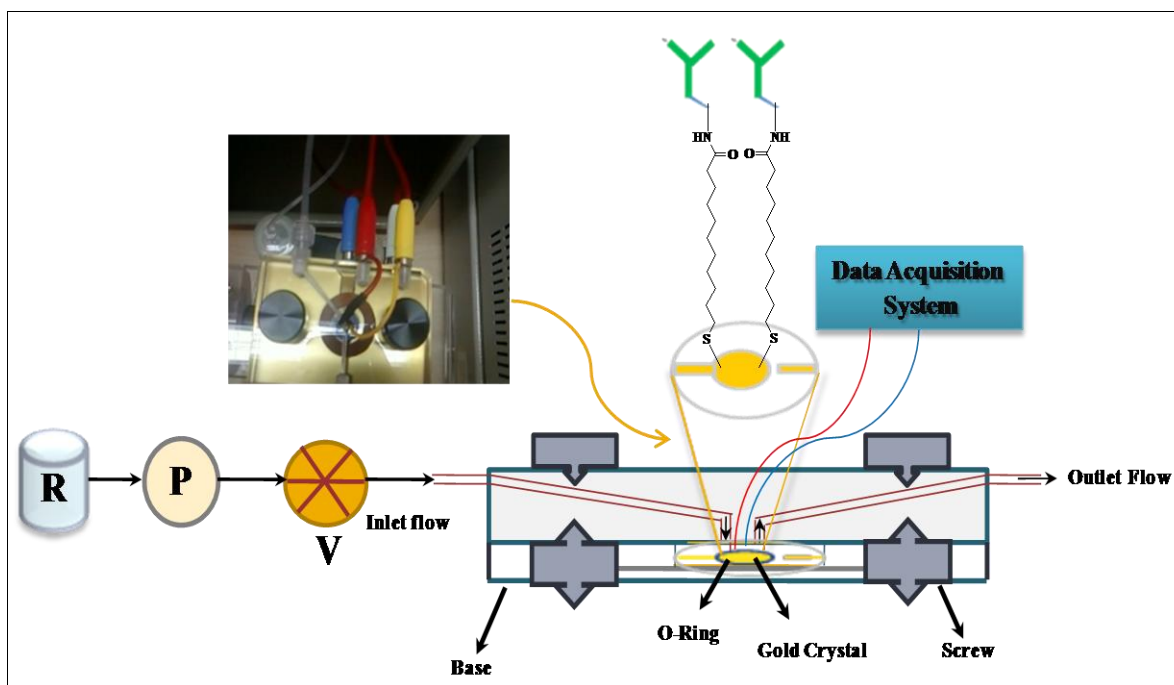


**Figure 4.3** Schematic for the microfluidics of FIA-EQCN biosensor. R- Buffer reservoir, P- Peristaltic pump, V- 6-port injection valve.

### 4.2.3 FIA-EQCN biosensor for SDZ residue analysis in the milk

#### 4.2.3.1 Immobilization of anti-sulfadiazine antibodies

The methodology employed for anti-sulfadiazine polyclonal antibody (pAb-SDZ) immobilization was based on multilayer assembling on the gold surface of the piezoelectric transducer gold quartz crystal. The cleaned gold quartz crystal was incubated for 12 hrs in an aqueous solution with 15 mM cystamine chloride (CYST). The crystal was then washed with double distilled water and was incubated in glutaraldehyde solution (2.5% v/v for 30 min.). Subsequently, the crystal was washed with PBS to remove residual glutaraldehyde molecules. The crystal was finally exposed to the pAb-SDZ solution (1:500 dilutions of 10  $\mu\text{g}/\text{ml}$ ) for 1 hrs and then rinsed with PBS. To block remanent aldehyde groups the modified crystal surface was exposed to glycine solution (4% w/v for 30 min) and washed with PBS. Schematic for immobilization of pAb-SDZ is shown as Figure 4.4.

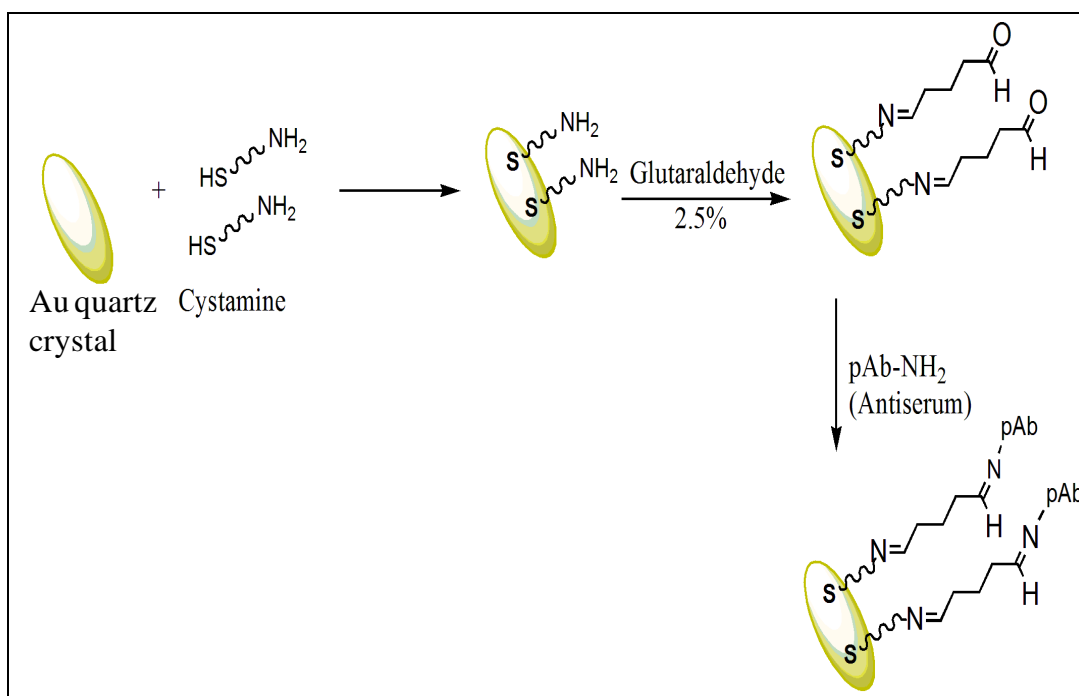


**Figure 4.4** Schematic representation of immobilization procedure for anti-sulfadiazine polyclonal antibody (pAb-SDZ) on cystamine chloride.

#### 4.2.3.2 Solution preparation

Phosphate buffered saline (PBS, 100 mM) was prepared by dissolving appropriate amount of  $\text{Na}_2\text{HPO}_4$  and  $\text{NaH}_2\text{PO}_4$  containing 137 mM NaCl and 27 mM KCl in membrane filtered RO water. The pH of the buffer was adjusted to 7.4 before use. For preparation of standards, known amount of SDZ was dissolved in PBS and further diluted to meet the calibration standards. For analysis in the milk, samples were centrifuged and diluted (1:4) in PBS. A stock solution of SDZ (250 ng/mL) was prepared and further diluted to meet the calibration standards in the range of 10-200 ng/mL. All the solutions were freshly prepared before the experiment and stored at 4°C when not in use.

#### 4.2.4 Matrix matching for milk sample analysis

The commercial milk sample of 3.0% fat was procured from the local market of Goa, India. The matrix effect on the analysis of SDZ in the milk samples was investigated. In FIA system, fat present in the milk may lead to clogging of the fluidic channels and thus, can decrease the biosensor performance.

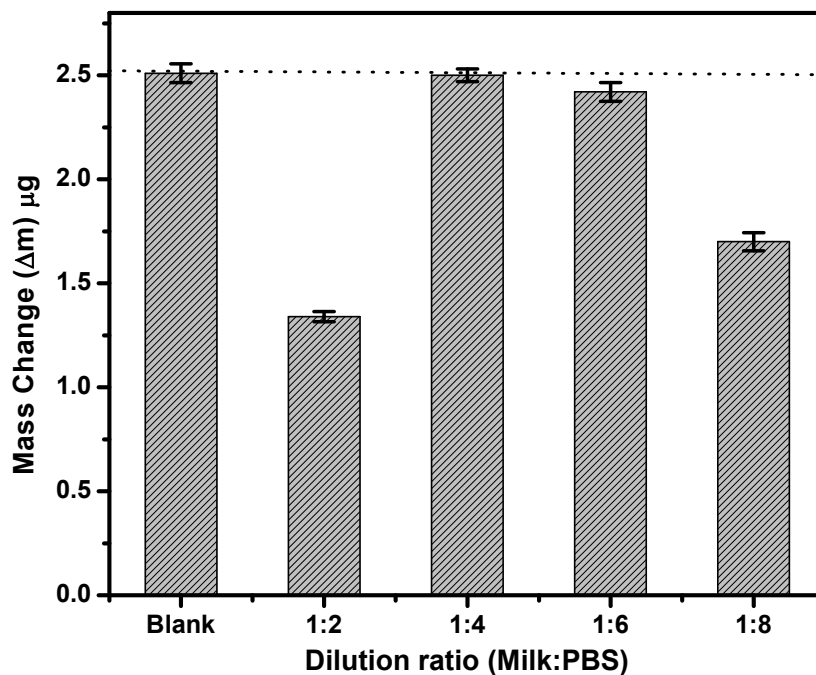


**Figure 4.5** Effect of dilution of PBS and milk on the response of FIA-EQCN biosensor for 100 ng/mL SDZ.



To avoid such problems, a simple strategy was worked out to obtain the calibration curve for SDZ in spiked milk samples. A combination of several sample pre-treatment techniques such as centrifugation, filtration, and dilution of milk with PBS was done. In brief, the milk samples were centrifuged at 6000 rpm for 20 min at room temperature and filtered with 0.22  $\mu\text{m}$  filter (Whatman, USA) and diluted with PBS to obtain different ratios of milk and PBS (1:2, 1:4, 1:6, 1:8). A known amount of SDZ (100 ng/mL) was spiked in the diluted milk sample and it was observed that 1:4 dilution of milk sample with PBS showed maximum binding for SDZ with immobilized antibody on the modified crystal surface as presented in Figure 4.5.

### 4.3 Results and Discussion for SDZ analysis

#### 4.3.1 Optimization of the FIA-EQCN system for SDZ analysis

##### 4.3.1.1 Effect of influential parameters of FIA system

Different parameters like pH, ionic strength of the carrier buffer and flow rate of the FIA system were optimized before the experiment was performed. Measurements were carried out with different pH (6.8-7.6) and ionic strength (10, 50, 100 and 200 mM) of PBS for 100 ng/mL SDZ.

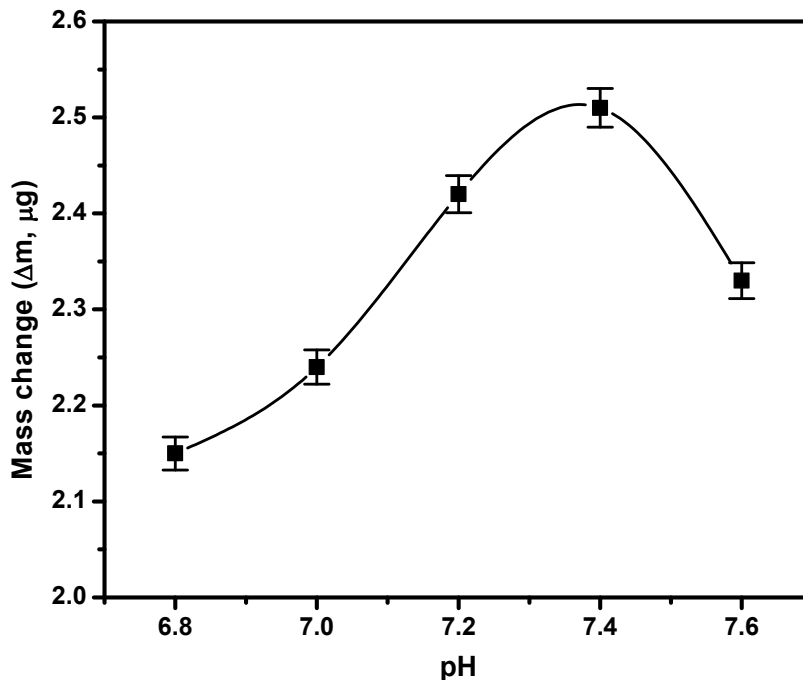


**Figure 4.6** Effect of pH of PBS on the response of FIA-EQCN biosensor for 100 ng/mL SDZ. PBS 100 mM, flow rate 0.5 mL/min.

It is evident from Figure 4.6 that the 100 ng/mL SDZ showed the maximum binding at pH 7.4. Similarly, it was observed that the maximum binding of SDZ to pAb-SDZ was found at 100 mM PBS as presented in Figure 4.7.

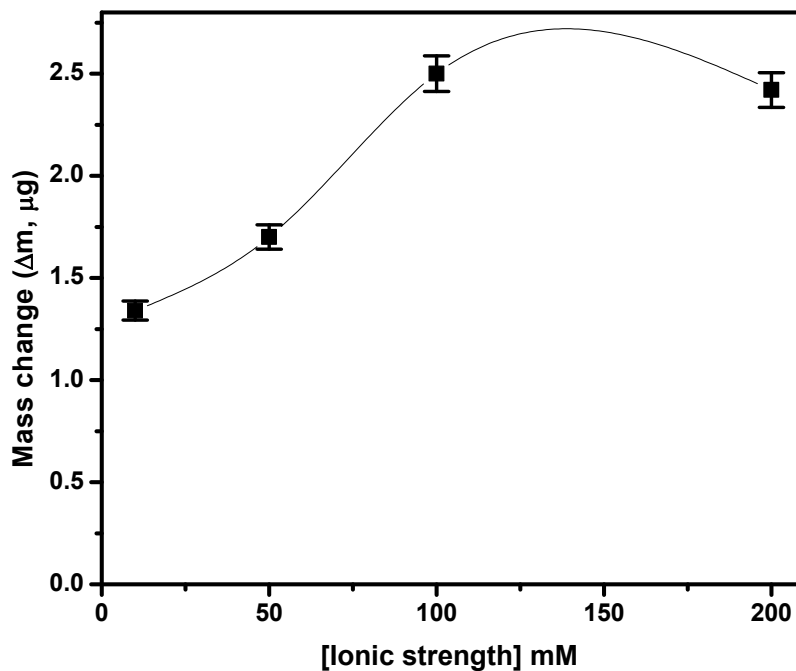


**Figure 4.7** Effect of ionic strength of PBS on the response of FIA-EQCN biosensor for 100 ng/mL SDZ, flow rate 0.5 mL/min.

The effect of flow rate on the binding of SDZ with the immobilized antibody on modified crystal surface was tested. The known amount of SDZ standard (100 ng/mL) was passed over the mounted crystal in different flow rates (0.01, 0.1, 0.5 and 1 mL/min). As shown in Figure 4.8 flow rate of 0.5 mL/min provides sufficient contact time for binding of SDZ to the immobilized antibody on the gold crystal, thus gives the maximum response. These optimized parameters (pH 7.4, Ionic strength 100 mM, and flow rate 0.5 mL/min) were used throughout the experiment for analysis of SDZ.

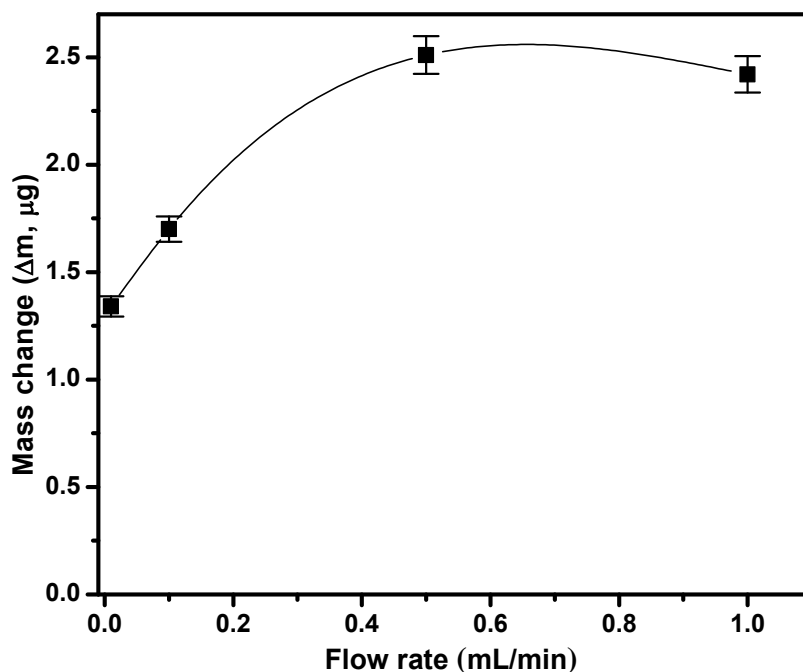


**Figure 4.8** Effect of flow rate of PBS on the response of FIA-EQCN biosensor for 100 ng/mL SDZ. PBS 100 mM, pH 7.4.

#### 4.3.1.2 Optimization of antibody dilutions for pAb-SDZ

It is very important to optimize the concentration of antibody (bioreceptors), which critically affects their conjugation onto the electrodes as well as their ease of access toward analytes with minimum physical steric hindrance (Ahmed et al., 2013). To determine the optimum antibody concentration and to check the maximum binding efficiency, different dilutions of pAb-SDZ were injected into the FIA system on the different SAMs modified crystal surface. The pAb-SDZ antibodies were diluted with PBS as 1:100, 1:500 and 1:1000. As shown in Figure 4.9, it was found that 1:1000 dilution of pAb-SDZ showed the maximum binding on the optimized monolayer surface. Hence, further experiments were carried out using 1:1000 dilutions of antibodies. However, antibody dilution of 1:100 and 1:500 showed less binding which agrees with the hypothesis that too high a density of bioreceptors can actually hinder binding due to steric hindrance at high concentration

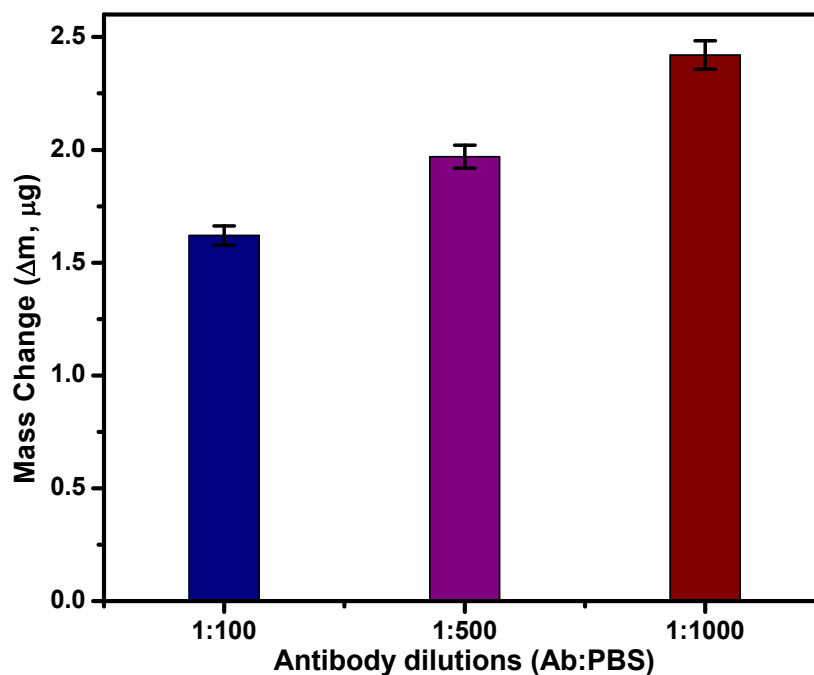


**Figure 4.9** Effect of antibody dilution on the response of FIA-EQCN biosensor for 100 ng/mL SDZ. Carrier buffer- PBS (100 mM), pH 7.4, flow rate 0.5 mL/min.

#### 4.3.2 Characterization of pAb-SDZ immobilized gold crystal

The surface of the gold quartz crystal before and after coupling to pAb-SDZ were characterized by scanning electron microscopy (SEM) by Zeiss EVO-50 (Germany).

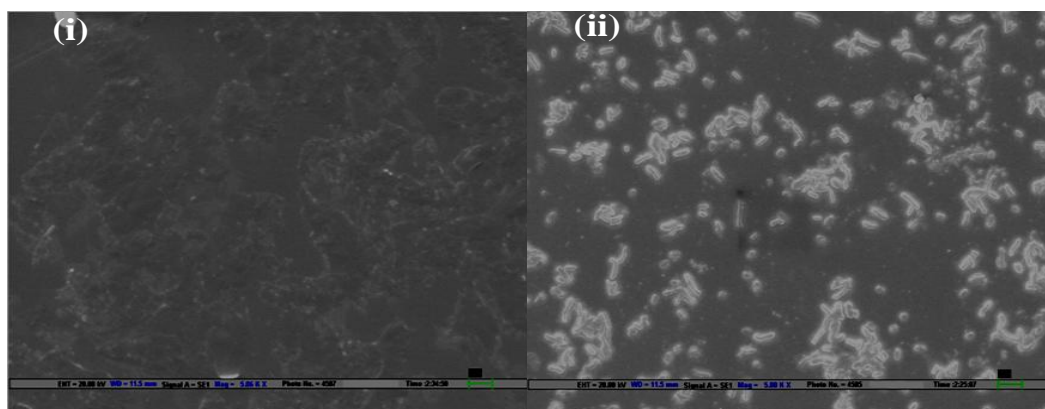


**Figure 4.10** SEM analyses of (i) bared gold crystal and (ii) gold crystal with immobilized antibody at 5000X magnification.

Figure 4.10 shows the SEM micrograph of the bare gold quartz crystal and pAb-SDZ immobilized gold quartz crystal at 5000X magnification. Plain and uniform morphology can be seen in the SEM image of gold quartz crystal surface in Figure 4.10 (i). However, the transformation to dense globular morphology with bright streaks is observed after immobilization of pAb-SDZ on to gold quartz crystal surface as presented in Figure 4.10 (ii). Both the images confirm the binding of pAb-SDZ on the gold quartz crystal surface.

### 4.3.3 Calibration of SDZ in buffer and milk

The pAb immobilized gold quartz crystal was kept in a plexiglas flow-cell, sandwiched between two O-rings and degassed PBS solution was pumped via FIA manifold, until a constant baseline was achieved. SDZ standard solutions from 10 to 200 ng/mL were prepared in carrier buffer and injected into the FIA-EQCN system.

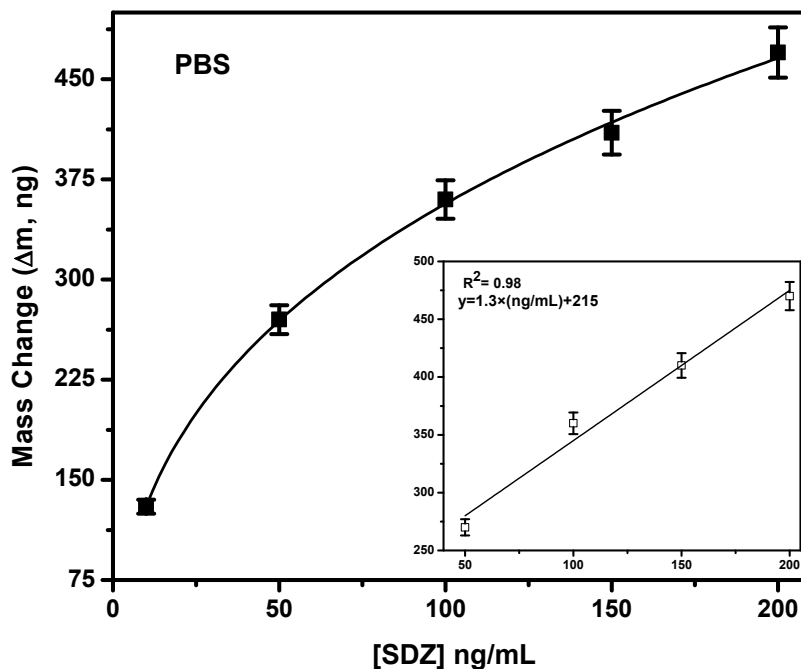


**Figure 4.11** Calibration graph for analysis of SDZ in PBS. Inset: linear fit data representation for SDZ analysis in PBS.

Response signals were recorded using a data acquisition system connected to resonator and plotted as mass change vs. concentration of SDZ. All samples were injected in triplicates. A good linear response was obtained for SDZ binding in the range of 50–200 ng/mL. The results are presented as Figure 4.11. The linear fit of data shows a good correlation between immobilized pAb and SDZ ( $R^2 = 0.98$ , % RSD ( $n=3$ ) 0.83). Furthermore, the usefulness of the developed biosensor was also evaluated in the milk samples by analyzing 1:4 diluted milk with PBS. Known concentrations of SDZ (10 to 200 ng/mL) were spiked in the diluted milk samples to construct a calibration graph. A good dynamic range was obtained from 10 to 200 ng/mL with a linear range of 50-200 ng/mL. The correlation coefficient ( $R^2$ ) of the developed biosensor in the milk was found to be 0.98, with % RSD ( $n=3$ ) 0.80. The minimum limit of detection for SDZ in PBS and milk was found to be 10 ng/mL. The obtained results are presented as Figure 4.12.

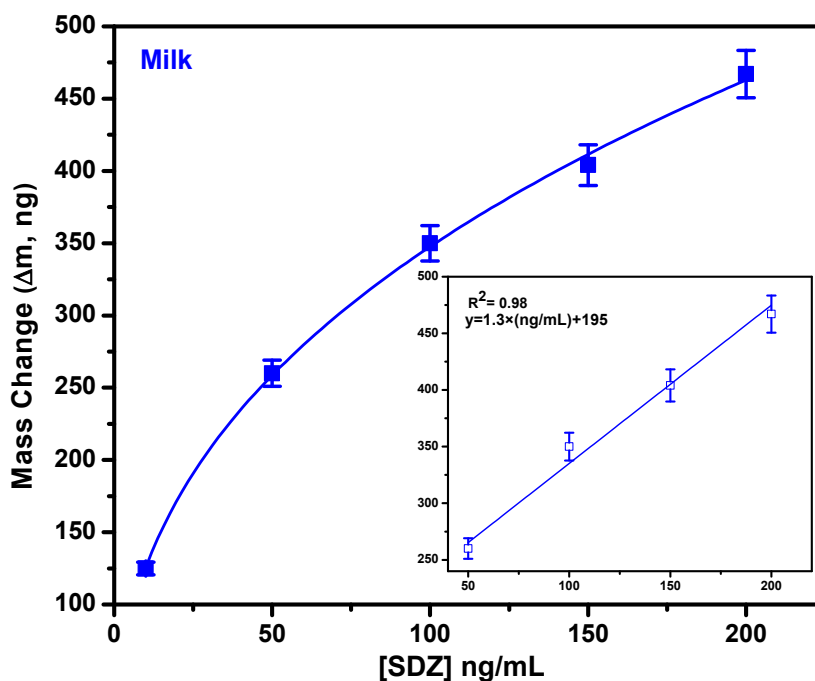


**Figure 4.12** Calibration graph for analysis of SDZ in the milk. Inset: linear fit data representation for SDZ analysis in the milk.

#### 4.3.4 Cross reactivity of SDZ

Cross-reactivity studies were performed in PBS using standard solutions (100 ng/mL) of different sulfonamides. Most common sulfonamides like sulfadiazine, acetyl-sulfadiazine, sulfathiazole, sulfamethazine, sulfaquinoxaline, and sulfamethoxazole are tested for cross reactivity with sulfadiazine specific pAb. Very high cross-reactivity was obtained for sulfadiazine and acetyl sulfadiazine, which contains more related structures with sulfadiazine, are recognized by the antiserum with a cross-reactivity of 100% and 92%, respectively. sulfathiazole and sulfamethazine shows cross reactivity of 1.2% and 0.2% respectively. sulfaquinoxaline and sulfamethoxazole shows less than 0.1% cross reactivity. Apart from sulphonamides, 1 aminoglycoside *e.g.* streptomycin (SRT, 100 ng/mL) was also tested for cross reactivity with SDZ and no cross reactivity observed. Results are shown in Table 4.2.

**Table 4.2** Cross reactivity of SDZ with other antibiotics

<b>Sulphonamides</b>	<b>% Cross Reactivity</b>
Sulfadiazine	100
Acetyl-sulfadiazine	92
Sulfathiazole	1.2
Sulfamethazine	0.2
Sulfaquinoxaline	<0.1
Sulfamethoxazole	<0.1
<b>Aminoglycosides</b>	
Streptomycin	0.00

#### 4.3.5 Recovery studies from SDZ spiked milk samples

The potential application of the developed FIA-EQCN system for detection of SDZ in the milk was tested. All milk samples were initially assumed as SDZ free. A known amount of the SDZ standard solution was added to centrifuged, diluted and filtered milk and analyzed in the FIA-EQCN system. Based on the response signal, recoveries were calculated. Table 4.3 shows the recovery results obtained from milk samples. Recoveries in the range of 98.6–100.5% were

obtained. This ensures the potential application of the developed biosensor for SDZ analysis in the milk samples.

**Table 4.3** Recovery studies of SDZ from spiked milk samples

SDZ Added (ng/mL)	SDZ Found (ng/mL) mean (n=3)	Mean $\pm$ S.D.	% RSD	% Recovery
100	98.06	98.06 $\pm$ 0.40	1.10	98.6
100	99.02	99.02 $\pm$ 0.26	0.96	99.2
100	100.05	100.05 $\pm$ 0.10	0.21	100.5

#### 4.3.6 Cross validation and comparison

The results obtained from the FIA-EQCN measurements were cross validated against commercial ELISA kit. Validation experiments against ELISA method confirmed the reliability of the FIA-EQCN biosensor test. In EQCN measurements, mass changes increases with an increase in the concentration of SDZ whereas in the ELISA measurements, optical density of the reactant decreases with increase in the concentration.

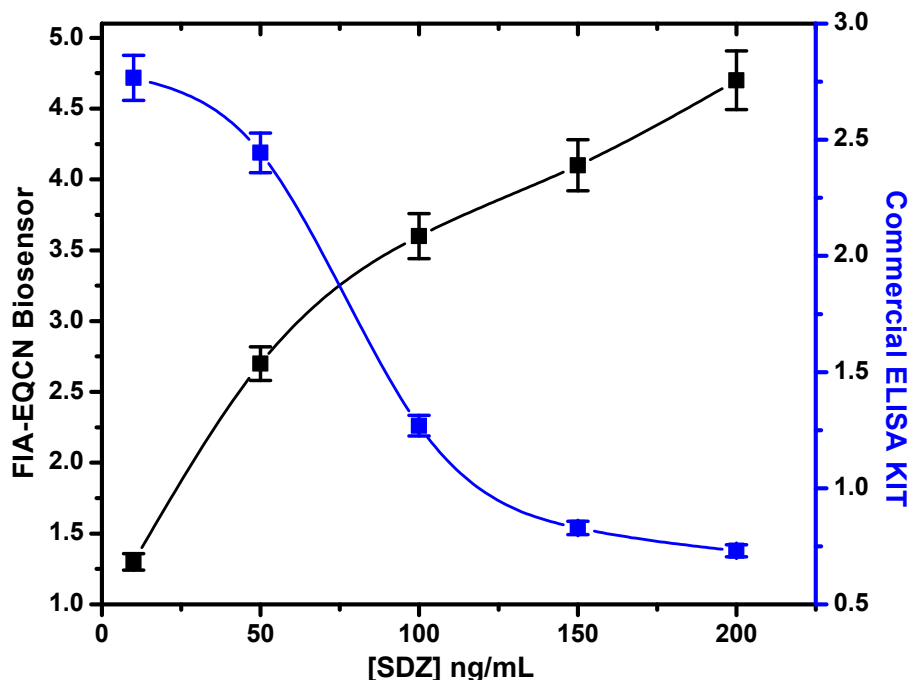


**Figure 4.13** Comparison of the results for SDZ concentration obtained with FIA-EQCN biosensor and commercial ELISA kit.



It is clear from the Figure 4.13, that one technique is supplementary to another technique as the results are inversely proportional. The obtained results from both the methods show good correlation in terms of sensitivity and reproducibility. The % RSD obtained shows the difference of  $\pm 0.5\%$  by both methods. In addition, the methods show linearity in the same range as from 50 - 150 ng/mL.

#### 4.4 FIA-EQCN biosensor for SRT residue analysis in the milk

##### 4.4.1 Immobilization of anti-streptomycin antibodies

The methodology employed for immobilization of anti-streptomycin monoclonal antibodies (mAb-SRT) was based on multilayer assembling on the surface of gold quartz crystal. In brief, a clean gold quartz crystal was immersed overnight in 4 mM ethanolic solution of 11-MUA under ambient condition. The gold quartz crystal was gently washed with absolute ethanol to remove unbound 11-MUA residues and dried with nitrogen stream before use. For coupling of the mAb-SRT antibody, the carboxyl group of SAM on modified electrode was activated by 1:1 EDC/NHS (100 mM each) mixture for 2 hrs. Subsequently, the crystal was washed with membrane filtered water to remove excess EDC/NHS. Finally, solution of 10 mg mL<sup>-1</sup> (1:1000 in PBS) mAb-SRT was added carefully over the activated surface of SAM followed by overnight (8-12 hrs) incubation at 4°C. The coupled gold crystal was washed to remove unbound antibody and mounted on the flow cell to use in FIA mode. Schematic for immobilization of mAb-SRT is shown as Figure 4.14.

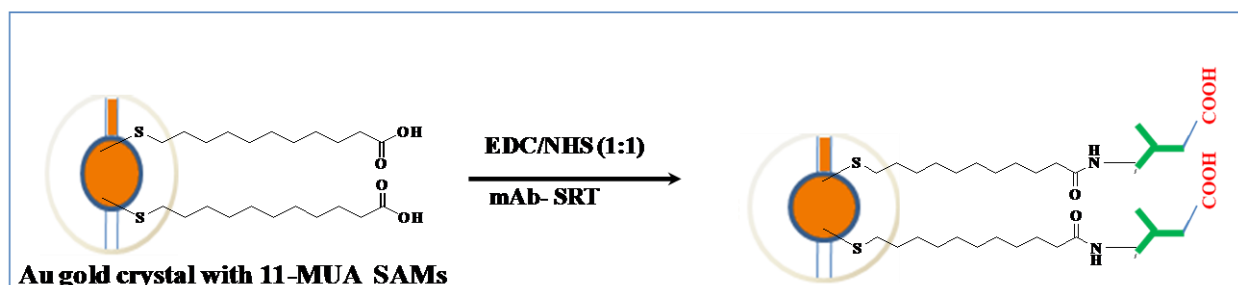


**Figure 4.14** Schematic representation of immobilization procedure for anti-streptomycin monoclonal antibody (mAb-SRT) on 11-MUA.

#### 4.4.2 Solution preparation

Phosphate buffered saline (PBS, 100 mM) was prepared by dissolving appropriate amount of  $\text{Na}_2\text{HPO}_4$  and  $\text{NaH}_2\text{PO}_4$  containing 137 mM NaCl and 27 mM KCl in membrane filtered RO water. The pH of the buffer was adjusted to 7.4 before use. For preparation of standards, known amount of SRT was dissolved in PBS and further diluted to meet the calibration standards. For analysis in the milk, samples were centrifuged and diluted (1:4) in PBS. A stock solution of SRT (300 ng/mL) was prepared and further diluted to meet the calibration standards in the range of 0.001 to 300 ng/mL. All the solutions were freshly prepared before the experiment and stored at 4°C when not in use.

#### 4.4.3 Matrix matching for milk sample analysis

The commercial milk sample of 3.0% fat was procured from the local market of Goa, India. The matrix effect on the analysis of SRT in the milk samples was investigated.

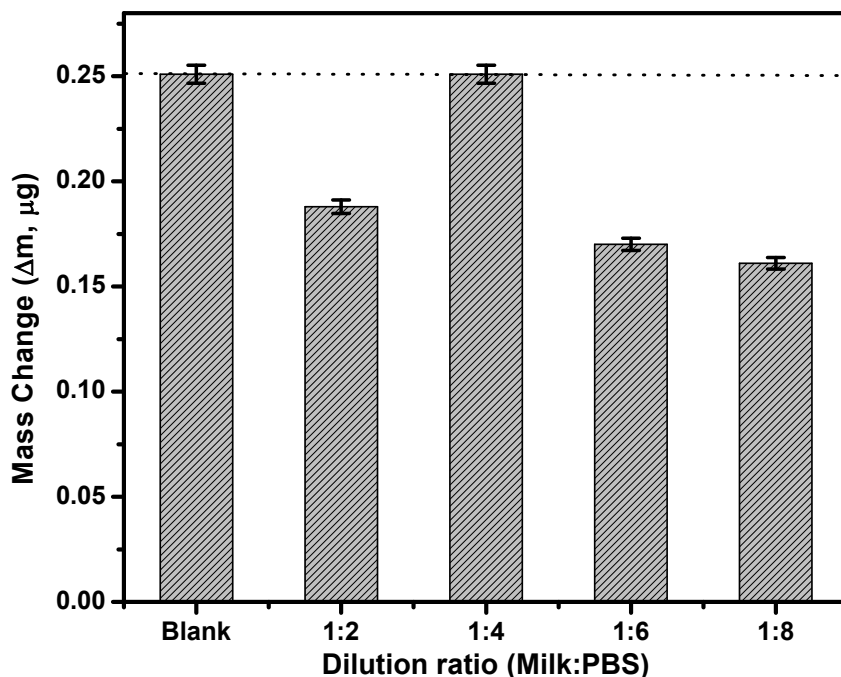


**Figure 4.15** Effect of dilution of PBS and milk on the response of FIA-EQCN biosensor for 10 ng/mL SRT.

A combination of several sample pre-treatment techniques such as centrifugation, filtration, and dilution of milk with PBS was done. In brief, the milk samples were centrifuged at 6000 rpm for 20 min at room temperature and filtered with 0.22  $\mu\text{m}$  filter (Whatman, USA) and diluted with PBS to obtain different ratios of milk and PBS (1:2, 1:4, 1:6, 1:8). A known amount of SRT (10 ng/mL) was spiked in the diluted milk sample and it was observed that 1:4 dilution of milk sample with PBS showed maximum binding for SRT with immobilized antibody on the modified crystal surface as shown in Figure 4.15.

#### 4.5 Results and Discussion for SRT analysis

##### 4.5.1 Optimization of the FIA-EQCN system for SRT analysis

###### 4.5.1.1 Effect of influential parameters of FIA system

Different influential parameters like pH, ionic strength of the carrier buffer and flow rate of the FIA system were optimized before the experiment was performed. Measurements were carried out with different pH (6.8-7.6) and ionic strength (10, 50, 100 and 200 mM) of PBS for 10 ng/mL SRT.

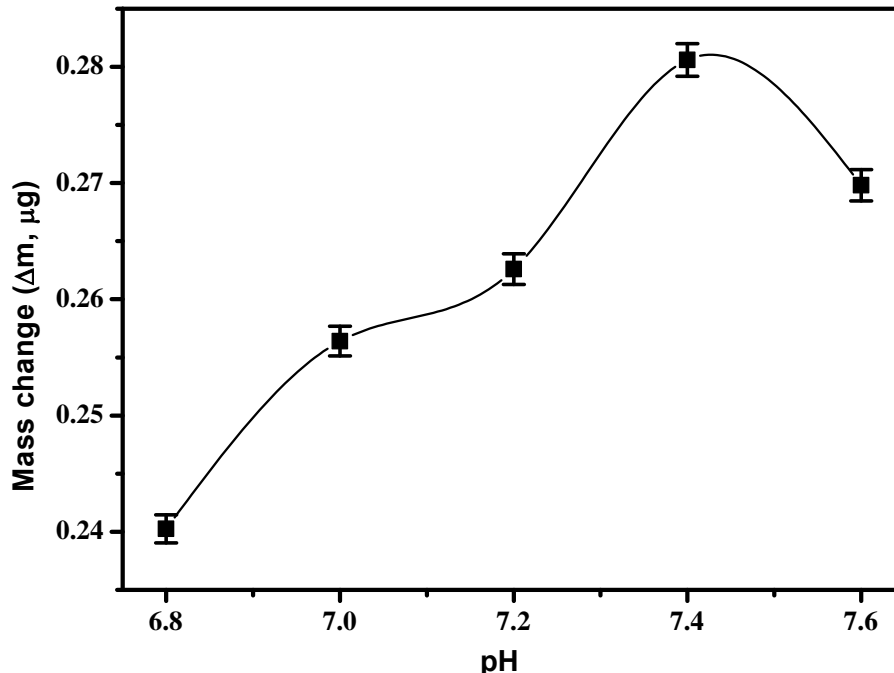


**Figure 4.16** Effect of pH of PBS on the response of FIA-EQCN biosensor for 10 ng/mL SRT. PBS 100 mM, flow rate 0.1 mL/min.

It is evident from Figure 4.16 that the 10 ng/mL SRT showed the maximum binding at pH 7.4. Similarly, 100 mM PBS showed the maximum binding for mAb-SRT and SRT as presented in Figure 4.17.

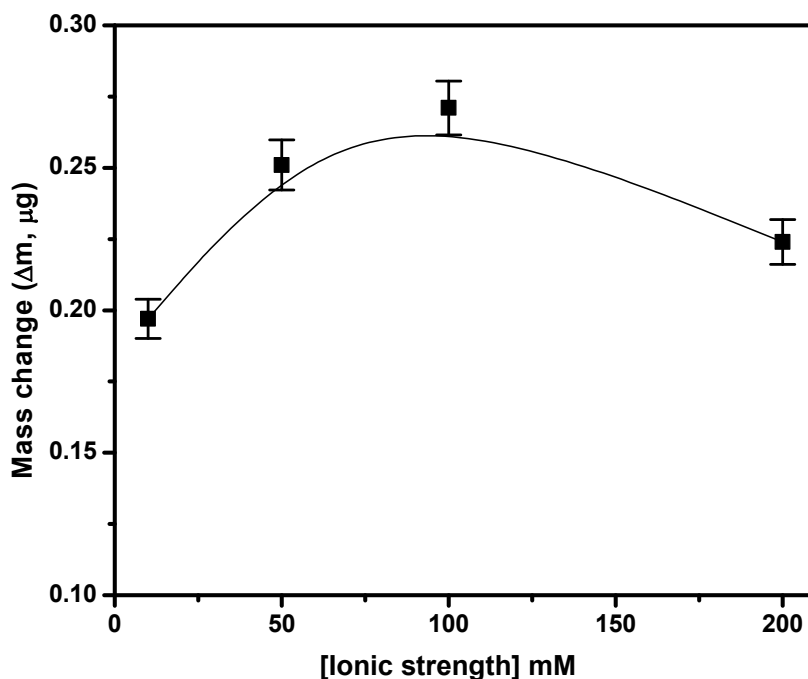


**Figure 4.17** Effect of ionic strength of PBS on the response of FIA-EQCN biosensor for 10 ng/mL SRT, flow rate 0.1 mL/min.

The effect of flow rate on the binding of SRT with the immobilized antibody on modified crystal surface was tested. The known concentration of SRT standard (10 ng/mL) was passed over the mounted crystal in different flow rates (0.01, 0.1, 0.5 and 1 mL/min). As shown in Figure 4.18, flow rate of 0.1 mL/min provides sufficient contact time for binding of SRT to the immobilized antibody on the gold crystal, thus gives the maximum response. These optimized parameters (pH 7.4, ionic strength 100 mM and flow rate 0.1 mL/min) were used throughout the experiment for analysis of SRT.

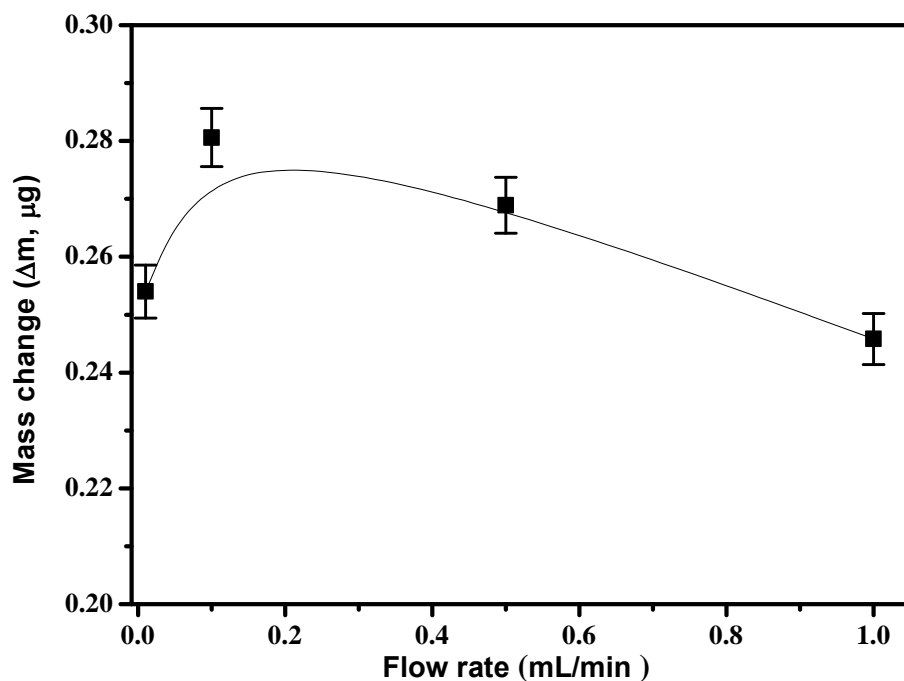


**Figure 4.18** Effect of flow rate of PBS on the response of FIA-EQCN biosensor for 10 ng/mL SRT. PBS 100 mM, pH 7.4.

#### 4.5.1.2 Optimization for surface modification

SAMs provide a robust and reproducible method for the immobilization of biomolecules where some control over the orientation and distribution is possible. Thiols and sulfides in solution can spontaneously adsorb onto the surface of gold, silver, platinum and copper with regular organization and high thermal, mechanical and chemical stability. Gold-coated crystals are most frequently used for QCM biosensors due to their stability. Some earlier reported protocols for SAMs were used for optimization of surface modification to immobilize mAb-SRT on gold quartz crystal, with slight modifications. 11-MUA (4 mM) (Park *et al.*, 2004), cysteaminium chloride (10 mM) (Silva *et al.*, 2010) and L-cysteine (10 mM) (Zhang *et al.*, 2009) were tested for immobilization of mAb-SRT on the gold quartz crystal surface. The concentrations of different surface modifiers and cross-linkers were optimized and mAb-SRT antibody was attached to the surface. The SAMs based on 11-MUA showed the maximum mass change against mAb-SRT coupled gold quartz crystal for SRT standard which confirms the maximum

binding. Thus, further experiments were carried out using 11-MUA. Figure 4.19 represents the binding responses obtained with different SAM's.

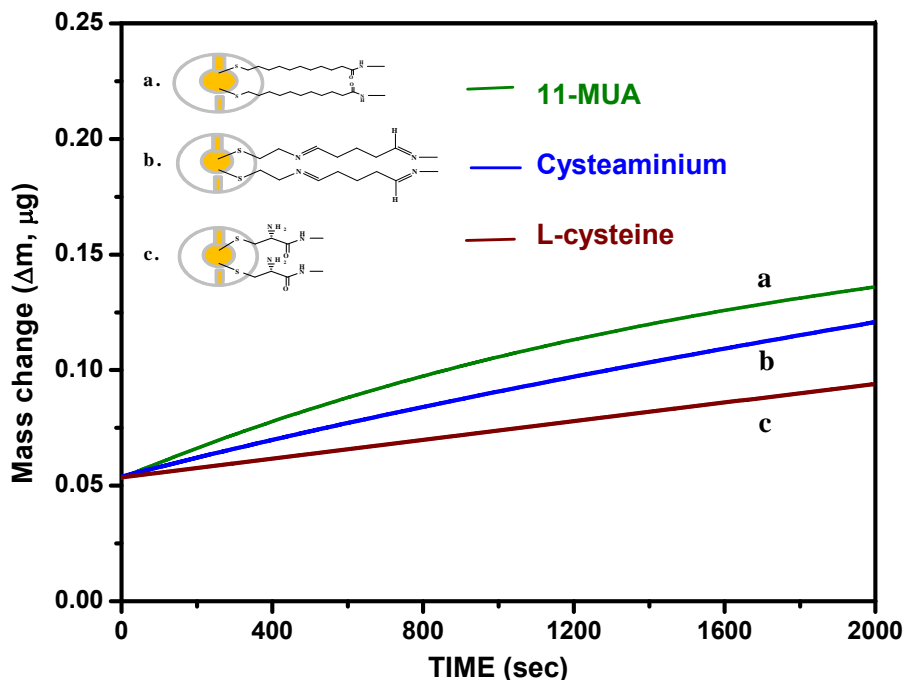


**Figure 4.19** Optimization of different self assembled monolayers. Inset: representation of different thiols attached to the gold quartz crystal.

#### 4.5.1.3 Optimization of antibody dilutions for mAb-SRT

To determine optimum antibody concentration and to check the maximum binding efficiency, different dilutions of mAb-SRT were injected into the FIA system on the SAMs modified crystal surface. The mAb-SRT antibody was diluted with PBS as 1:100, 1:500 and 1:1000. As shown in Figure 4.20, it was found that 1:1000 dilution of mAb-SRT showed the maximum binding on the optimized monolayer surface. However, antibody dilution of 1:100 and 1:500 showed less binding which agrees with the hypothesis that too high a density of bioreceptors can actually hinder binding because of steric hindrance at high concentration. Recently, Holford et al has also demonstrated that a high concentration of antibody decreased biosensor sensitivity, as it did not facilitate bioreceptor binding on the surface, probably due to steric hindrance (Holford *et al.*, 2013). Hence, all the further experiments were carried out using 1:1000 dilutions.

Simultaneously, experiments were carried out to study the maximum binding capacity of modified crystal with mAb-SRT. Optimized dilution of antibody solution in buffer was passed to the modified crystal surface and the real time binding response was recorded. Saturation of the modified SAMs layer on crystal surface was observed during the second run of antibody as evident from the inset of Figure 4.20.

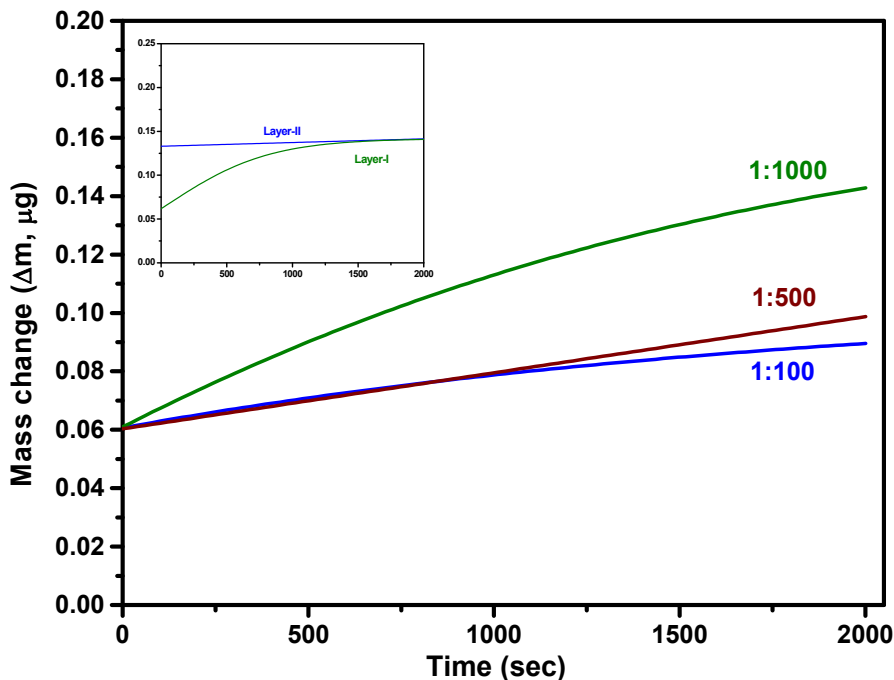


**Figure 4.20** Real time binding response for antibody dilutions for analysis of SRT. Inset: Binding capacity of the gold crystal through different layers of antibody. Carrier buffer- PBS (100 mM), pH 7.4, flow rate 0.1 mL/min.

#### 4.5.2 Characterization of mAb-SRT immobilized gold crystal

Fourier transform infra red (FT-IR) spectroscopy was applied to measure the surface properties of the AT-cut gold quartz crystal coupled through 11-MUA SAMs via the carbodiimide cross-linking reaction. The surface was characterized before and after coupling of mAb-SRT at each step during the experiment. Spectra were recorded using IR Affinity-1 (M/s SHIMADZU Corp., Kyoto, Japan) with attenuated total reflectance (ATR) attachment specac diamond ATR AQUA. The spectra were recorded using 40 scans at  $4\text{ cm}^{-1}$  resolution collected under vacuum condition.

The FT-IR spectra are shown in Figure 4.21. FT-IR spectrum of bared gold surface is shown as Figure 4.21 (a). Spectrum of gold surface treated with 11-MUA is shown as Figure 4.21 (b) where it showed the C-H Stretches in asymmetric and symmetric mode at  $2925\text{ cm}^{-1}$  and  $2848\text{ cm}^{-1}$ . The broad region from  $2500\text{--}3500\text{ cm}^{-1}$  with out-of-plane bending for O-H at  $935\text{ cm}^{-1}$  confirming the presence of COOH group of 11-MUA. The broad region with asymmetric and symmetric Stretches at  $1676$  and  $1619\text{ cm}^{-1}$  confirm the presence of C=O of acid. Two-associated peak for C-H deformation (scissoring) was found to be at  $1488$  and  $1448\text{ cm}^{-1}$ . Three associated peak for long chain carbon of 11-MUA appears at  $684$ ,  $635$  and  $537\text{ cm}^{-1}$ . As shown in Figure 4.21 (c), after immobilization of Ab on gold crystal, new absorption bands appears at  $1645$  and  $1552\text{ cm}^{-1}$  which confirm the presence of the amide bond (CO-NH) in between 11-MUA and mAb-SRT. The presented FT-IR spectra confirms the attachment of mAb-SRT to the modified surface of gold quartz crystal.

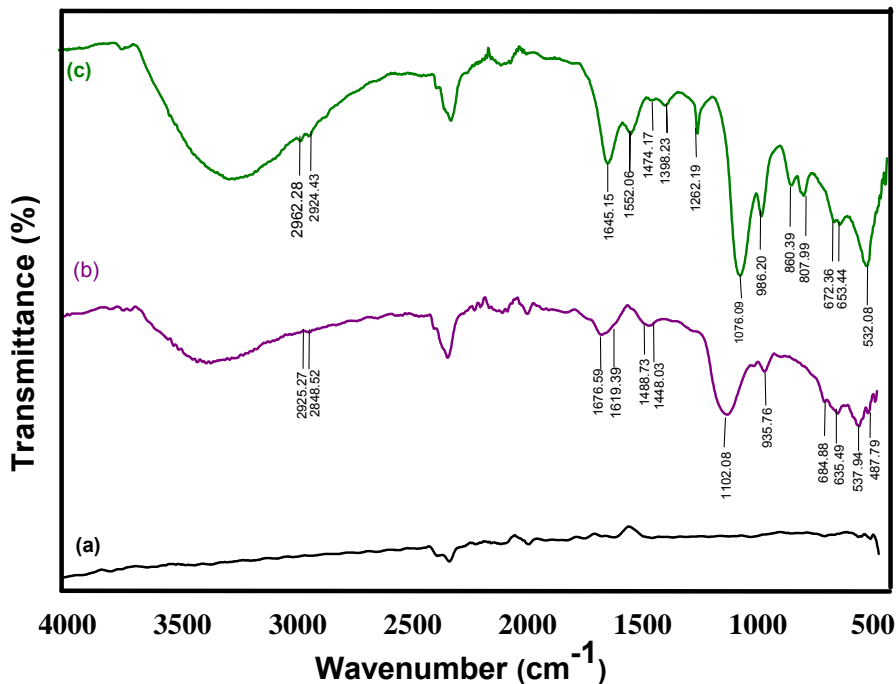


**Figure 4.21** FT-IR characterization of immobilized SRT antibody on modified gold crystal.



### 4.5.3 Calibration of SRT in buffer and milk

The mAb-SRT immobilized gold quartz crystal was mounted in plexiglas flow-cell and degassed PBS was passed until the constant baseline was achieved. Freshly prepared SRT standard in PBS (0.001-300 ng/mL) were injected into the FIA-EQCN system, starting from lower to higher concentration. The response signals of different concentration were recorded using the data acquisition system (DAQ-716) and plotted as mass change ( $\Delta m$ ) vs. concentrations. The obtained data from the Voltscan 5 software was treated using OriginPro 8 software and the data of best fit was plotted. In the developed FIA-EQCN biosensor, results were obtained as mass change resulting from the real time binding of SRT to the mAb-SRT immobilized via the SAMs on the quartz crystal. The mass change ( $\Delta m$ ) is converted into ng to impart more clarity in the calibration graph. The background value (50 ng/mL) is exhibited from the interaction of the antibody coupled quartz crystal with the carrier buffer (PBS 100 mM, pH 7.4) at a flow rate of 0.1 mL/min.

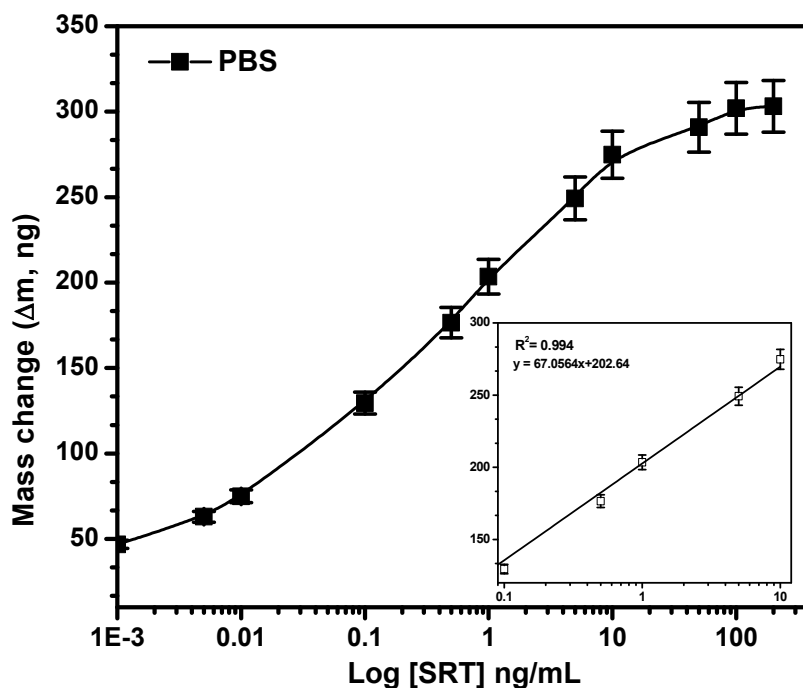


**Figure 4.22** Calibration graph for analysis of SRT in PBS. Inset: linear fit data representation for SRT analysis in PBS.

As presented in Figure 4.22, good dynamic range was obtained for SRT in PBS from 0.3 to 300 ng/mL with a linear range of 0.3-10 ng/mL. The correlation coefficient ( $R^2$ ) of the biosensor performance on PBS was 0.99 with % RSD (n=3) 0.23 to 2.13 and the linear equation was  $y = 67.0564x \text{ (ng/mL)} + 202.64$ . Furthermore, the usefulness of the developed biosensor was also evaluated in the milk sample by analyzing 1:4 diluted milk with PBS.

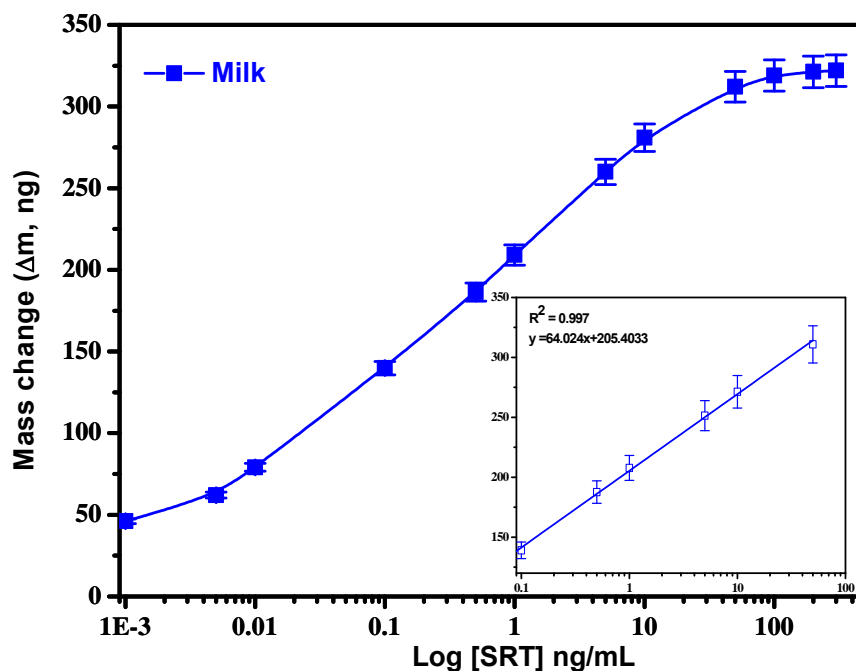


**Figure 4.23** Calibration graph for analysis of SRT in the milk. Inset: linear fit data representation for SRT analysis in the milk.

Known concentrations of SRT (0.001 to 300 ng/mL) were spiked in the diluted milk samples to construct a calibration graph. A good dynamic range was obtained from SRT spiked milk from 0.3 to 300 ng/mL with a linear range of 0.3-50 ng/mL. The correlation coefficient of the developed biosensor in the milk was found to be 0.997, with % RSD (n=3) 0.13 to 1.10 and the linear equation was  $y = 64.024x \text{ (ng/mL)} + 205.4033$ . Based on the calculation of baseline peak to peak noise root mean square (RMS) *i.e.* 6.7 and the sensitivity of the calibration curve, *i.e.* 67.0564 ng/mL for PBS and 64.024 ng/mL of milk, the minimum limit of detection for SRT in PBS and milk was determined to be 0.3 ng/mL. The obtained result is presented as Figure 4.23. Sensitivity and the detection range of the developed biosensor is attributed to the affinity

interaction between the antibodies and the antigen, since the specific monoclonal antibody against SRT was immobilized on the SAMs surface which selectively graft the target analyte (SRT). Obtained real time mass change ( $\Delta m$ ) and cumulative mass change values for baseline (functionalized gold crystal and mAb-SRT immobilized crystal) and SRT (0.001, 0.005, 0.01, 0.1, 0.5 and 1 ng/mL) spiked milk have been presented as Table 4.4. The dissociation constant ( $K_d$ ) for SRT spiked in PBS and milk with immobilized mAb-SRT on the modified gold crystal was determined using ligand binding kinetics in sigma plot 11.0.0 and found to be  $1.33 \times 10^{-10}$  M and  $1.161 \times 10^{-10}$  M for PBS and milk respectively.

**Table 4.4** Real time mass change ( $\Delta m$ ) values for SRT analysis in the milk

Steps	Interaction's	Step-wise average mass change ( $\Delta m$ ) ng $\pm$ S.D.	Cumulative mass change ( $\Delta m$ ) ng
1.	Baseline of functionalized gold crystal	0.00 $\pm$ 6.7	0.00
2.	The response of mAb-SRT on functionalized gold crystal	39.80 $\pm$ 1.9	39.80
3.	The response of SRT (0.001 ng/mL) spiked milk on mAb-SRT immobilized crystal	41.09 $\pm$ 2.1	80.89
4.	The response of SRT (0.005 ng/mL) spiked milk on mAb-SRT immobilized crystal	23.61 $\pm$ 1.1	104.70
5.	The response of SRT (0.01 ng/mL) spiked milk on mAb-SRT immobilized crystal	14.78 $\pm$ 1.9	119.48
6.	The response of SRT (0.1 ng/mL) spiked milk on mAb-SRT immobilized crystal	59.56 $\pm$ 1.3	179.04
7.	The response of SRT (0.5 ng/mL) spiked milk on mAb-SRT immobilized crystal	48.56 $\pm$ 0.9	227.60
8.	The response of SRT (1.0 ng/mL) spiked milk on mAb-SRT immobilized crystal	21.92 $\pm$ 0.74	249.52

#### 4.5.4 Cross reactivity of SRT

Cross-reactivity studies were performed to check the group specificity of the developed biosensor against the most structurally similar molecule dihydrostreptomycin (DHSRT) and other three non-targeted aminoglycosides namely gentamycin (GENTA), neomycin (NEO) and kanamycin (KAN). Apart from aminoglycosides, one sulfonamide *e.g.* sulfadiazine (SDZ) was also tested for cross reactivity, which is commonly used in veterinary medicine and may present in the milk. Cross-reactivity was tested in 1:4 diluted milk samples using 10 ng/mL standard solutions of above mentioned antibiotics. mAb-SRT immobilized crystal was fixed on flow cell and solutions of different antibiotics were passed individually through the FIA system at the flow rate of 0.1mL/min . As shown in Table 4.4, very high cross-reactivity was obtained for SRT and DHSRT (100% and 93.8%, respectively) on mAb-SRT immobilized gold crystal, which contains more related structures with SRT. Other aminoglycosides *e.g.* GENTA, KAN and NEO showed no significant cross reactivity with mAb-SRT antibody and obtained results were less than 0.1% for all the three aminoglycosides. Similarly, no cross-reactivity was observed with SDZ. Obtained results demonstrate that there is no significant interference produced by any other non-targeted antibiotics, which may commonly be present in the milk. The results indicate the remarkable specificity of the developed FIA-EQCN biosensor for SRT detection in the milk.

**Table 4.5** Cross reactivity of SRT with other antibiotics

<b>Aminoglycosides</b>	<b>% Cross-reactivity</b>
Streptomycin	100
Dihydro-streptomycin	93.8
Gentamycin	≤ 0.1
Kanamycin	≤ 0.1
Neomycin	≤ 0.1
<b>Sulphonamides</b>	
Sulfadiazine	0.00

#### 4.5.5 Recovery studies for SRT spiked milk samples

The potential application of developed FIA-EQCN biosensor has been tested for the detection of SRT in the diluted milk samples. Initially, all the milk samples were assumed to be free of SRT. A known amount of SRT (1 ng/mL) was spiked in the diluted milk samples from the prepared stock solution. Based on the response signals recorded from FIA-EQCN biosensor, recoveries were calculated. Table 4.6 shows the % recovery obtained for SRT spiked milk samples. The recoveries obtained (98- 99.33%) from the developed biosensor indicates the potential application of the FIA-EQCN biosensor for the ultra sensitive detection of SRT in the milk samples.

**Table 4.6** Recovery studies of streptomycin from spiked milk samples

Milk Sample	SRT added [ng/mL]	SRT Found [ng/mL]			Mean ± S.D. (n=3)	% RSD	%Recovery
		R1	R2	R3			
Milk-1	1.0	1.00	0.96	0.98	0.98 ± 0.02	2.04	98.00
Milk-2	1.0	0.99	0.98	1.01	0.99 ± 0.01	1.51	99.33
Milk-3	1.0	0.99	0.97	1.00	0.98 ± 0.01	1.52	98.67
Milk-4	1.0	0.96	1.02	0.99	0.99 ± 0.03	3.03	99.00

**R1-R3:** Response in FIA-EQCN biosensor

#### 4.5.6 Cross validation and comparison

The results obtained from the FIA-EQCN measurements were cross-validated against commercial ELISA kit. Different diluted milk samples were spiked with a known amount of SRT and analyzed through the developed biosensor and commercial ELISA kit. Analysis was performed to determine % recovery for obtaining results. The recoveries obtained from the FIA-EQCN biosensor (99.7-101.3%, % RSD (n=3) 0.60- 1.50) was more or less similar to the results obtained from the ELISA kit (98.7-101.1%, % RSD (n=3) 1.28-1.78). It is evident from the Table 4.7 that the obtained results from both the methods show good correlation in terms of

sensitivity and reproducibility. The developed biosensor is reliable and as precise as the commonly used ELISA method.

**Table 4.7** Comparison of FIA-EQCN biosensor with commercial ELISA kit

SRT added (ng/mL)	SRT Found (ng/mL) (n=3)		Mean $\pm$ S.D. (ng/mL) (n=3)		% RSD		% Recovery	
	FIA- EQCN	Kit	FIA-EQCN	Kit	FIA- EQCN	Kit	FIA- EQCN	Kit
10.0	9.97	9.87	9.97 $\pm$ 0.15	9.87 $\pm$ 0.13	1.50	1.31	99.70	98.7
10.0	10.03	10.02	10.03 $\pm$ 0.06	10.02 $\pm$ 0.16	0.60	1.59	100.3	100.2
10.0	10.13	10.11	10.13 $\pm$ 0.14	10.11 $\pm$ 0.13	1.38	1.28	101.3	101.1

#### 4.5.7 Precision of FIA-EQCN biosensor

Precision of developed biosensor was tested by determining intra and inter run analysis on the same modified gold quartz crystal immobilized with mAb-SRT antibody and with the diverse sets of immobilized crystals. A known amount of SRT concentration (10 ng/mL) was spiked in the diluted milk sample and successively analyzed for biosensor performance (n= 5). The baseline was corrected before each analysis and mass change ( $\Delta m$ ) was calculated based on the obtained responses. The biosensor showed a good reproducibility with standard deviation of  $280.11 \pm 0.98$  and calculated % RSD (n=5) 0.35 within the same crystal. Similarly, the biosensor performance was tested on diverse sets of immobilized crystals. Satisfactory results were obtained for SRT analysis in diluted milk samples when analyzed using different sets of biosensor. The % RSD (n=5) was found in the range of 0.278-0.558. The obtained results were summarized in the Table 4.8. These results indicate the precision and reproducibility of the biosensor thus can be used as a potential tool for analysis of SRT in the milk samples.

**Table 4.8** Reproducibility and precision of FIA-EQCN biosensor

<b>Intra-batch reproducibility performance of FIA-EQCN biosensor for SRT</b>							
<b>Concentration (ng/mL)</b>	<b>R1</b>	<b>R2</b>	<b>R3</b>	<b>R4</b>	<b>R5</b>	<b>S.D. ± Mean (n=5)</b>	<b>% RSD</b>
10	279.4	280.94	280.1	278.9	281.2	280.108 ± 0.98	0.35
<b>Inter-batch reproducibility performance of FIA-EQCN biosensor for SRT</b>							
<b>Crystals</b>	<b>Concentration (ng/mL)</b>	<b>R-1</b>	<b>R-2</b>	<b>R-3</b>	<b>S.D. ± Mean (n=3)</b>	<b>% RSD</b>	
Crystal-1	10	279.40	280.94	280.10	280.15 ± 0.77	0.278	
Crystal-2	10	280.65	281.20	279.64	280.48 ± 0.79	0.282	
Crystal-3	10	279.60	280.34	281.34	280.43 ± 0.87	0.310	
Crystal-4	10	281.56	280.40	280.00	280.65 ± 0.81	0.289	
Crystal-5	10	279.84	281.78	282.94	281.52 ± 1.57	0.558	

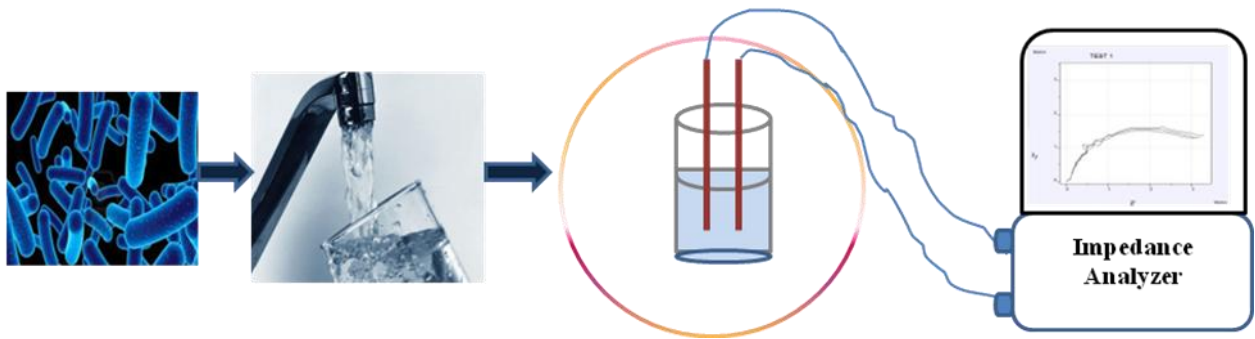
**R1-R5:** Response in FIA-EQCN biosensor

#### 4.6 Conclusion

The objective of this work was to develop a broad detection range biosensor with sensitive detection and which gives highly stable results for determination of antibiotic residues in the milk samples using FIA-EQCN based biosensor. A FIA-EQCN biosensor for SDZ and SRT residue analysis in the milk was developed. Obtained calibration for SDZ (10-200 ng/mL) and SRT (0.3-300 ng/mL) supports the applicability of the developed biosensor in the milk sample analysis. The obtained recoveries for SDZ (98.6-100.5%) and SRT (98-99.33%) spiked milk samples also encourage the application of developed biosensor towards the quantification of these antibiotic residues in the milk samples. Validation of the presented biosensor against commercial ELISA kit (BioScientific, USA) supports that the developed biosensor provides much sensitive detection (0.3 ng/mL) as compared to the analysis of commercial kit (5 ng/mL) for SRT detection. The developed biosensor could complete the analysis in less than 17 min and exhibited a great potential for automated analysis in dairy industries.

## Chapter 5

### Rapid label-free immunosensor for bacterial detection in water



*Graphical abstract of chapter content*

*Note: Development of a novel application for bacterial detection using impedimetric immunosensor was envisaged under collaborative mode. The bioelectronic aspects including electrical characterization and equivalent circuit has been reported elsewhere (Bacher et al., 2012).*



## 5.1 Introduction

Detection of contaminated water by pathogenic microorganism is an important concern for ensuring water safety, security, and public health. A clean and treated water supply to each house may be the norm in Europe and North America, but in developing countries, access to both clean water and sanitation are not in the prime focus thus waterborne infections are common. Two and a half billion people have no access to improved sanitation, and more than 1.5 million children die each year from water borne diarrheal diseases (Fenwick, 2006). According to the World Health Organization (WHO), the mortality of water associated diseases exceeds 5 million people per year. From these, more that 50% are microbial intestinal infections (Cabral, 2010). *Escherichia coli* (*E. coli*) is a natural inhabitant of the intestinal tracts of humans and warm-blooded animals. The presence of this bacterium in water indicates that fecal contamination may have occurred and consumers might be exposed to enteric pathogens when consuming water. Hence, *E. coli* is often preferred as an indicator organism because it is specifically stands for fecal contamination (Min and Baeumner, 2002). Rapid and reliable detection of *E. coli* is critical for the management of the waterborne diseases threatening human lives worldwide. The occurrence of potential *E. coli* is extensively studied in water resources in the developing world, since it is an important health concern as a large population depends on both processed and unprocessed surface waters for drinking and domestic purposes (Ram *et al.*, 2006). Despite the potential public health threat from waterborne *E. coli*, there are no accepted methods for the rapid, accurate detection in surface waters. Current measures of microbial water quality rely exclusively on “indicators” of fecal pollution (*e.g.* fecal coliform bacteria or generic *E. coli*). However, there are no established correlations between the prevalence or concentration of these “indicators” and specific pathogens (Shelton *et al.*, 2006). Conventional methods for bacterial identification usually involves various culturing techniques and different biochemical tests which are very time consuming and usually requires 2-4 days. Hence, there is a need for adequate monitoring technologies targeting representative pathogenic bacteria like *E. coli* at low levels within hours to prevent mortality and morbidity caused by waterborne outbreaks. The effective testing of bacteria requires methods of analysis that meet a number of challenging criteria. Analysis time and sensitivity are the most important limitations related to the usefulness of bacterial testing. An extremely selective detection methodology is also required, because low

numbers of pathogenic bacteria are often present in a complex biological environment along with many other non-pathogenic bacteria (Maalouf *et al.*, 2007).

### 5.1.1 Label-free detection using electrochemical impedance spectroscopy

Immunosensors are often classified as label-based and label-free techniques. Label-based detection is widely used due to the common availability of reagents and simple instrument requirements. Most of the labeled detection such as fluorescence, chemiluminescence, and radioactive labeling strategies have synthetic challenges, multiple label issues and may exhibit interference with the binding site. However, these labeling strategies often alter surface characteristics and natural activities of the target molecule. Moreover, the labeling procedure is laborious, lengthy and limits the number and types of target molecules that can be studied. Therefore, the development of sensitive, reliable, high-throughput, label-free detection techniques are now attracting significant attention. Many label-free techniques such as surface plasmon resonance (SPR), carbon nano-tubes (CNTs) and nanowires, nanohole arrays etc. have been successfully integrated with bioanalysis and are emerging rapidly as a potential complement to labeling methods (Yu *et al.*, 2006). The label-free detection techniques are progressing rapidly. Standard label-free techniques such as imaging with surface plasmon resonance (SPR) quartz crystal microbalance (QCM) and electrochemical impedance spectroscopy (EIS) are reported for label-free detection of the different biomolecules (Yu *et al.*, 2006). EIS is an effective and reliable method to investigate antibody–antigen interactions on electrode surfaces. The basic approach for EIS is to apply small amplitude sine wave perturbations to an electrochemical system over a wide range of frequencies, and measure the responding signals (e.g. current) as a function of frequencies. The Nyquist plot is one of the most popular formats for interpretation of EIS data. A typical Nyquist plot is generated by comparing an imaginary part of impedance ( $Z''$ ) versus a real part of impedance ( $Z'$ ). Several studies have reported that attachment of bacterial cells to the electrode surface could form a blocking layer that inhibits the current flow and thus increases the impedance of the electrode. EIS based biosensors have received particular attention in biomedical and environmental fields during the last years due to their multiple advantages, such as fast response, low cost, mass production, and

capability of miniaturization and they allow label-free detection with high sensitivity (Bogomolova et al., 2009).

## **5.1.2 State of the art for bacterial detection**

### **5.1.2.1 Conventional methods for bacterial detection**

Conventional bacterial testing methods rely on specific media to enumerate and isolate viable bacterial cells. These methods are very sensitive, inexpensive and can give both qualitative and quantitative information on the number and the nature of microorganisms present in the sample (Doyle, 2001). Conventional methods for the detection of bacteria involve the following basic steps: pre-enrichment, selective enrichment, selective plating, biochemical screening, and serological confirmation (Downes *et al.*, 2001). Hence, a complete series of tests is often required before any identification can be confirmed. These conventional methods require several days to give results because they rely on the ability of the organisms to multiply to visible colonies. Moreover, culture medium preparation, inoculation of plates and colony counting makes these methods labor intensive. Conventional methods generally regarded as the golden standard often takes days to complete the identification of viable pathogens. Conventional methods for the detection of bacteria involve plating and culturing, enumeration methods (Rompre *et al.*, 2002), biochemical testing and microscopic examination (Flores Abuxapqui *et al.*, 1999). Some newer methods that have applied for detecting bacteria are ELISA (Magliulo et al., 2007), polymerase chain reaction (PCR), multiplex and real-time PCR (Kawasaki et al., 2010; Zemanick et al., 2010), fluorescence in situ hybridization and DNA microarrays (Kostić et al., 2010). DNA-based techniques require efficient DNA extraction and need DNA amplification using PCR as bacterial cells contain a low copy number of DNA (Liao and Ho, 2009; Heo and Hua, 2009).

### **5.1.2.2 Biosensors for bacterial detection**

In recent years, several biosensors techniques have played important roles in detection of pathogenic bacteria in different matrices. Among them immunosensors and DNA-based biosensors are mostly used. A variety of immunosensors have been developed based on the antibody of the target bacteria, which utilizes fluorescence (Heyduk and Heyduk, 2010), EIS (Lu

*et al.*, 2013; Barreiros dos Santos *et al.*, 2013), QCM (Guo *et al.*, 2012) and SPR (Baccar *et al.*, 2010). However, these biosensors lack in practical applications because of their single use nature and instability of antibodies in unfavorable conditions. Among the reported biosensors, EIS has emerged as sensitive techniques for bacterial detection due to multiple advantages, such as fast response, low cost, and capability of miniaturization. In EIS, traditionally, macro sized metal rods or wires were used as electrodes immersed in the medium to measure impedance and it is suitable to analyze the electrical properties of the modified electrode, *i.e.* when an antibody coupled to the electrode reacts with the antigen of interest (Berggren *et al.*, 1998; Felice *et al.*, 1999).

**Table 5.1** Summary of reported biosensor techniques using EIS for detection of *E. coli* in water.

Detection Technique	Detection range	Detection limit	Analysis time	Reference
MEMS based microimpedance	$10^0$ - $10^7$ CFU/mL of <i>E. coli</i> K 12	$10^5$ CFU/mL	5 Min.	Radke <i>et al.</i> , 2004
Aptamer-based impedance biosensor	$1 \times 10^{-7}$ - $2 \times 10^{-6}$ M of <i>E. coli</i> OMPs	-	NR	Queirós <i>et al.</i> , 2013
EIS based immunobiosensor chip	$6 \times 10^4$ - $6 \times 10^7$ CFU/mL of <i>E. coli</i> O157:H7	$6 \times 10^3$ cells/mL	NR	Ruan <i>et al.</i> , 2002
IDE based impedance biosensor	$7.1 \times 10^1$ - $7.1 \times 10^7$ CFU/mL of <i>E. coli</i> O157:H7	-	NR	Settu <i>et al.</i> , 2013
EIS immunosensor	$3.0 \times 10^3$ - $3.0 \times 10^7$ CFU/mL of <i>E. coli</i>	$1.0 \times 10^3$ CFU/mL	NR	Geng <i>et al.</i> , 2008

NR- Not Reported

Table 5.1 summarized some EIS based biosensor techniques for detection of *E. coli* in water. Radke et al reported an impedimetric biosensor with micro electromechanical systems (MEMS) technology integrated with biosensing methods to detect whole *E. coli* bacterial cells in food and water (Radke and Alocilja, 2004). More recently, Queirós et al developed a label-free DNA aptamer biosensor incorporated in a biochip and used for in situ detection of *E. coli* outer membrane protein (OMPs) in water samples (Queirós et al., 2013). Lu et al achieved LOD of  $10^3$  CFU/mL for *E. coli* K12 using gold-tungsten micro-wire based three electrode EIS system with  $10^3$ - $10^8$  CFU/mL linear range (Lu et al., 2013). Li et al achieved LOD of  $10^3$  CFU/mL of *E. coli* 0157:H7 using ferrocene -peptide conjugates based three-electrode EIS system with  $10^3$ - $10^7$  CFU/mL linear range (Li et al., 2014). The lowest LOD for *E. coli* 0157:H7 reported by Barreiros dos Santos et al is 2 CFU/mL using three electrode EIS system using gold disc as working electrode, they have achieved linear range of  $3 \times 10^0$ - $3 \times 10^4$  CFU/mL. Settingington and Alocilja described a novel approach for detection of *E. coli* 0157:H7 using cyclic voltammetry in combination with immunomagnetic separation and achieved LOD of 6 CFU/mL from the pure culture in concentration range  $10^0$ - $10^2$  CFU/mL (Settingington and Alocilja, 2012). These reported techniques supports the fact that the EIS with label-free approach is cost-effective because it does not require any labels, expensive instrumentation and allows portability.

### 5.1.3 Objective

The aim of this work was to develop a rapid, cost effective, label-free impedimetric immunosensor for detection of *E. coli* in water using two-electrode EIS setup.

### 5.1.4 Working principle of EIS

EIS is an alternating current (AC) method that describes the response of an electrochemical cell to small amplitude sinusoidal voltage signal as a function of frequency. The resulting current sine wave differs in time (phase shift) with respect to the perturbing (voltage) wave, and the ratio  $V(t)/I(t)$  is defined as the impedance ( $Z$ ). The most popular formats for evaluating electrochemical impedance data are the Nyquist and Bode plots. In the former format, the imaginary impedance component ( $Z''$ , out-of-phase) is plotted against the real impedance component ( $Z'$ , in-phase) at each excitation frequency, whereas in the latter format, both the

logarithm of the absolute impedance,  $|Z|$  and the phase shift ( $\theta$ ) are plotted against the logarithm of the excitation frequency. Capacitive immunosensors exploit the change in dielectric properties and/or thickness of the dielectric layer at the electrolyte–electrode interfaces, due to the antibody–antigen (Ab–Ag) interaction, for monitoring this process. An electrolytic capacitor (working electrode/dielectric/electrolyte; the second plate is represented by the electrolyte) allows the detection of an analyte specific to the receptor that has been immobilized on the insulating dielectric layer, which has previously been deposited on the surface of the working electrode. Ideally, this configuration resembles a capacitor in its ability to store charge and thus, the electric capacitance between the working electrode and the electrolyte is given by equation 5.1.

$$C = \epsilon_0 \epsilon A/d \quad (5.1)$$

where,

$\epsilon$  - Dielectric constant of the medium between the plates

$\epsilon_0$  - Permittivity of free space (8.85419 pF/m)

A - Surface area of the plates ( $m^2$ ), and

d - Thickness of the insulating layer (m)

## 5.2 Experimental section

### 5.2.1 Reagents and instrumentation

Ag-wire (diameter = 0.25 mm) and Bovine serum albumin (BSA) was procured from ACROS Organics, USA. Polyclonal antibody to *E. coli* raised from goat (2 mg/mL) (*pAb-E. coli*) and fluorescein isothiocyanate (FITC) labeled polyclonal antibody against *E. coli* raised from rabbit (0.75 mg/ml) was purchased from AbCam, UK. Sodium dihydrogen phosphate monohydrate, disodium hydrogen phosphate monohydrate, sodium chloride, 11-mercaptoundecanoic acid (11-MUA), 1-ethyl-3-[3-dimethylaminopropyl] carbodiimide hydrochloride (EDC), N-hydroxy succinimide (NHS), ethyl alcohol 200 proof was used (TEDIA, USA). Glutaraldehyde solution 25%, sodium chloride, glycine and cysteamine hydrochloride were obtained from Merck (Germany). L-cysteine hydrochloride was procured from Himedia labs India. For sample handling,

micropipettes from eppendorf®, Germany were used. All the solutions were prepared in a 0.22 µm membrane filtered Milli-Q system RO water (Millipore, Bedford, MA, USA), Seven Multi pH meter (Mettler Toledo, 8603, Switzerland) was used for pH measurements. All other chemicals used were of analytical grade and used as received. Certified ultra high pure nitrogen (99.9%), pH meter (Seven Multi Mettler Toledo, 8603, Switzerland) were used. Fluorescence images were taken on inverted fluorescence microscope (IX-71, Olympus, Japan). Impedance measurements were carried out using IVIUM CompactStat impedance analyzer (IVIUM, Netherland). All the bacterial sample handling and dilutions were done under biosafety cabinet class II type B2 (NuAire, USA).

### 5.2.2 Immobilization of pAb-*E. coli* on Ag-wire electrode

Initially the surfaces of the bare Ag-wire electrodes was washed ultrasonically in membrane filtered RO water for 5 min to remove inorganic particles. Following this, the electrodes were immersed into piranha solution ( $\text{H}_2\text{O}_2/\text{H}_2\text{SO}_4$ , 30/70 v/v) for 30 sec. The electrodes were washed with distilled water followed by drying under ultra pure nitrogen stream. This cleaning procedure was repeated before every step. The *pAb-E. coli* was covalently coupled on Ag-wire electrode through SAMs. Firstly, the concentration of cysteaminium (CYST) was optimized and a set of clean Ag-wire electrode were immersed overnight into a solution of 10 mM CYST in 0.1 M phosphate buffer saline (PBS, pH 7.4) under ambient condition. The electrodes covered by SAMs were gently washed with RO water to remove any unbounded CYST residues. The electrodes were dried with nitrogen stream before use. For coupling the *pAb-E. coli*, the carboxyl group of SAMs on modified electrode was activated by incubated in glutaraldehyde solution (2.5% v/v) for 30 min. Subsequently, the electrodes were washed with PBS to remove residual glutaraldehyde molecules. Finally, *pAb-E. coli* was attached to the electrode by carefully spreading the solution (1:1000 in PBS) over the activated surface followed by overnight incubation at 4°C. To block reminiscent aldehyde groups the modified electrode surface was exposed to glycine solution (4% w/v) for 30 min and washed with PBS. The unused antibody coupled electrodes were washed and stored at 4°C for future use. The schematic for immobilization of antibody to Ag-wire surface is presented in Figure 5.1 together with the schematic of experimental set-up.

### 5.2.3 Experimental setup of the EIS immunosensor

The experimental set-up consist of a pair of pre-functionalized Ag-wire electrode immersed in the single well of 384 polystyrene well plate (NUNC, USA) (capacity 120  $\mu\text{L}$ /well) containing 90  $\mu\text{L}$  bacterial suspensions of different concentration. The operation of presented sensor was based on the pair of Ag-wire as an electrical transducer.

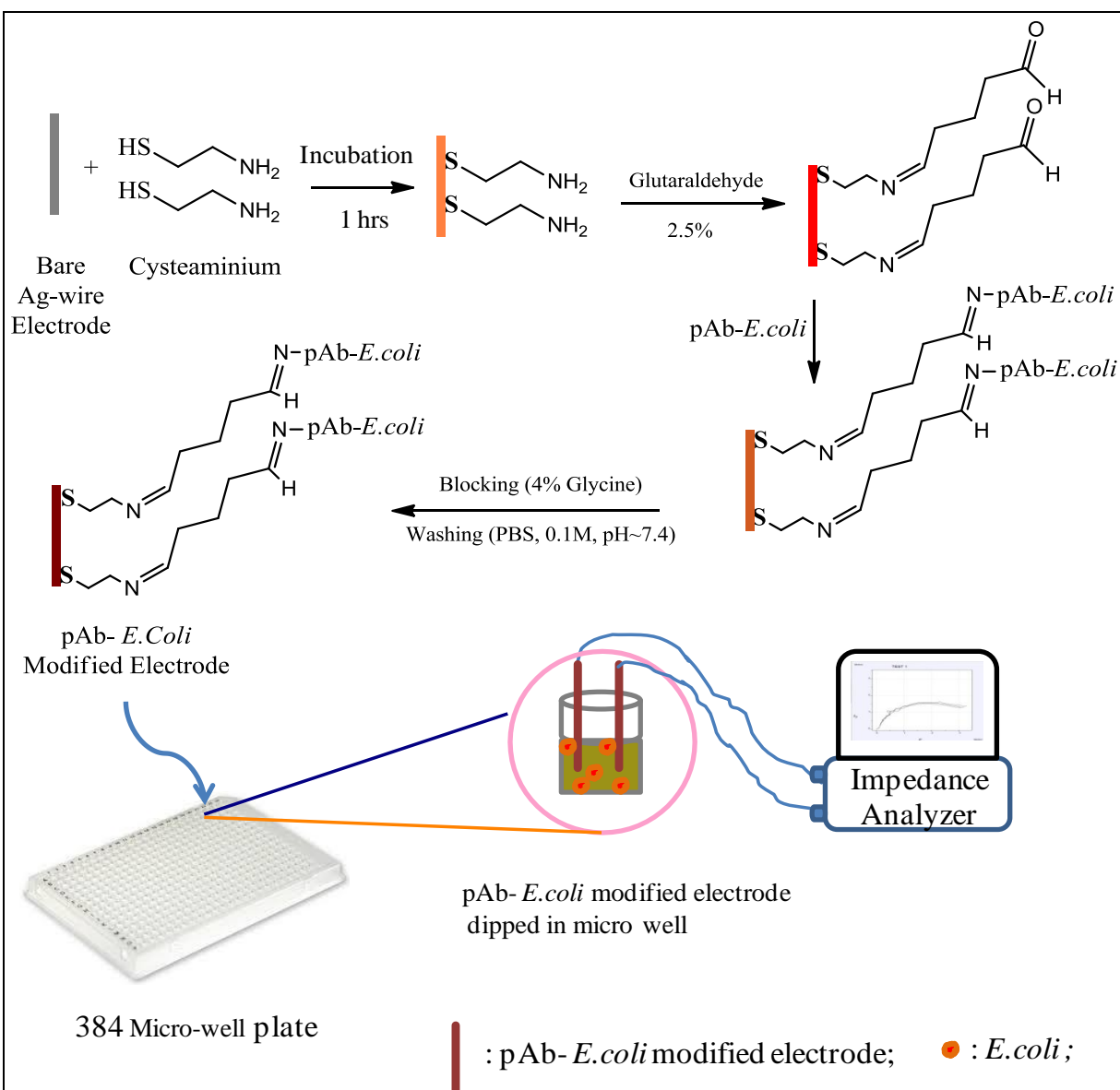


**Figure 5.1** Schematic representations for surface modification of Ag-wire electrode and immobilization of *E. coli* antibody with experimental setup of EIS immunosensor.



The effective surface area of the Ag-wire electrode was calculated and found to be 7.85 mm<sup>2</sup>. The Ag-wire surface was functionalized with attached *pAb-E. coli* over the self-assembled monolayers (SAMs), to form a biological transducer. The binding of the bacterial cells to the biological transducer causes the change in impedance. This interaction was measured using two electrode set-up. The electrode set-up and the well plate were placed in a custom-made faraday cage to shield the electrodes from external electromagnetic sources. The schematic of experimental set-up is presented as Figure 5.1. In the presented set-up, the two pre-functionalized Ag-wire electrodes were dipped in to the micro well plate. The functionalized Ag-wire electrodes were connected to IVIUM CompactStat impedance analyzer in 4-electrode mode controlled through software (IVIUM soft). In the 4-electrode mode, the first electrode was configured as working electrode (working and sense electrode combined together) and second electrode was reference electrode (reference and counter combined together). The impedance change caused by antigen–antibody interactions at the electrode surface was measured at 1-100 KHz applied frequency and 10 mV applied potential.

#### 5.2.4 Preparation of solutions, bacterial culture, and dilutions

0.1 M phosphate buffered saline (PBS) was prepared by dissolving appropriate amount of Na<sub>2</sub>HPO<sub>4</sub>, NaH<sub>2</sub>PO<sub>4</sub> containing 0.0027 M potassium chloride and 0.137 M sodium chloride. The pH of the buffer was adjusted to 7.4. All buffer solutions were stored at 4°C when not in use. The bacterial culture of *E. coli* (MTCC 723) and *Streptococcus pyogenes* (MTCC 1928) used in the present study were procured from the microbial type culture collection and gene bank, IMTECH Chandigarh, India. The strains were grown aerobically for 16 h at 37°C in Brain Heart Infusion broth, pH 7.40 ± 0.2 (BHI broth, Hi-Media, India). The bacterial cultures were maintained as frozen stock at -80 °C in BHI broth containing 15% (v/v) glycerol when not in use. The initial concentrations of the bacterial cultures were obtained using serial dilutions and plate counting methods. The concentration of *E. coli* (MTCC 723) is also confirmed by taking optical density at 600 nm (OD<sub>600</sub>) and found corresponding to bacteria concentration of 1.16 ×10<sup>9</sup> CFU/mL. The stock solution of bacterial concentration diluted serially in PBS to achieve the concentrations of calibration plot (1.16 ×10<sup>2</sup> to 1.16 ×10<sup>8</sup> CFU/mL).

### 5.2.5 Confirmation of *E. coli* with IMViC test

Before development of the immunosensor confirmation test of *E. coli* was carried out in the spiked water samples by using the IMViC (Indole methyl red Voges-Proskauer citrate) test. This test is frequently employed in the water testing laboratories for the identification of *E. coli* and other coliforms, which includes microorganisms such as *Klebsiella* and *Enterobacter* (Niemi *et al.*, 2003). First, the water samples were spiked with a loop full stock culture of *E. coli* (MTCC 723) and streaking was done on Eosin methylene blue (EMB) agar and incubated at 37°C for 24 hrs. After 24 hrs, characteristic colonies of *E. coli* (metallic green colonies) were observed on EMB agar plate. The obtained result is presented as Figure 5.2.

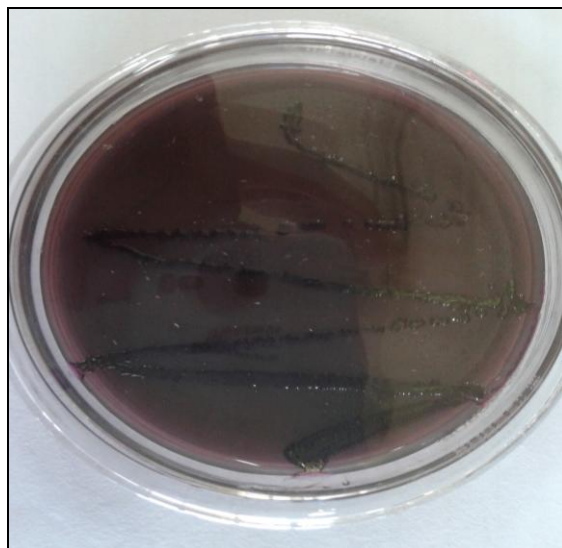


**Figure 5.2** Metallic green colonies of *E. coli* on EMB agar medium.

From the isolated colonies IMViC test were performed for further confirmation of *E. coli*. Table 5.2 summarized the IMViC test results of some common bacterial species of water. Indole test is performed on tryptophan broth. Result is read after adding Kovac's reagent. The positive result is indicated by the red layer at the top of the tube after the addition of Kovács reagent. Methyl red test and Voges-Proskauer test both are done in methyl red–Voges-Proskauer (MR-VP) broth. Positive methyl red test are indicated by the development of red color after the addition of methyl red reagent. Negative test of VP is indicated by lack of color change after the addition of Barritt's A and Barritt's B reagents. For citrate utilization test Simmons citrate agar is used.

Negative citrate utilization test is indicated by the lack of growth and no change of color from green to blue in the tube. Figure 5.3 represents the IMViC test results for *E. coli*.

**Table 5.2** IMViC test results of some common bacterial species of water.

Species	Indole	Methyl Red	Voges-Proskauer	Citrate
<i>E. coli</i>	Positive	Positive	Negative	Negative
<i>Salmonella spp.</i>	Negative	Positive	Negative	Positive
<i>Klebsiella spp.</i>	Negative	Negative	Positive	Positive
<i>Enterobacter spp.</i>	Negative	Negative	Positive	Positive



**Figure 5.3** IMViC test results of *E. coli*.

## 5.3 Result and Discussion

### 5.3.1 Optimization of the Immunosensor

Following parameters are optimized for the preparation of the EIS based immunosensors:

#### 5.3.1.1 Optimization of antibody concentration

The binding of the *E. coli* and *anti-E. coli* antibody on the electrodes directly affects the sensitivity of the immunosensor.

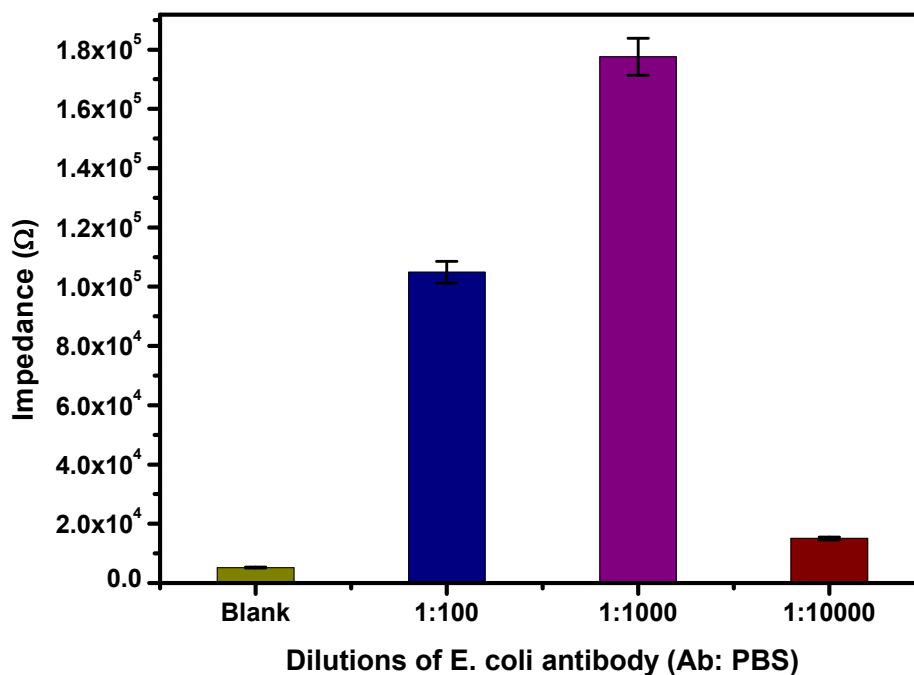


**Figure 5.4** Impedance values at 10 Hz for dilutions of *pAb-E. coli* antibody with PBS (0.1 M, pH 7.4) for 10<sup>4</sup> CFU/mL *E. coli*.

The amount of *anti-E. coli* antibody plays an important role in this process. The change in impedance of the immunosensor depends upon antigen- antibody binding and incubation time. Hence, the effect of both the parameters has been investigated. Several *anti-E. coli* dilution ratios with PBS were evaluated (1:100, 1:1000 and 1:10000) and the maximum change in impedance was recorded for dilution of 1:1000 as shown in Figure 5.4. Incubation time of 5 min was found to be optimal for impedance measurements. Thus, these optimized parameters were used for further investigations.

### 5.3.1.2 Influence of applied frequency

Antigen–antibody interaction results in impedance change at the electrode and the electrode/electrolyte interface, known as interface impedance, which can be measured at different frequency ranges. The impedance measurement is conducted in the range of 1 Hz to 100 KHz. Since electrode impedance is dominated at low frequency, we have investigated the impedance change at 1 Hz, 10 Hz and 100 Hz. Impedance change for antigen–antibody was found to be maximum at 10 Hz as shown in Figure 5.5. Thus 10 Hz was chosen for quantitative analysis of *E. coli*.

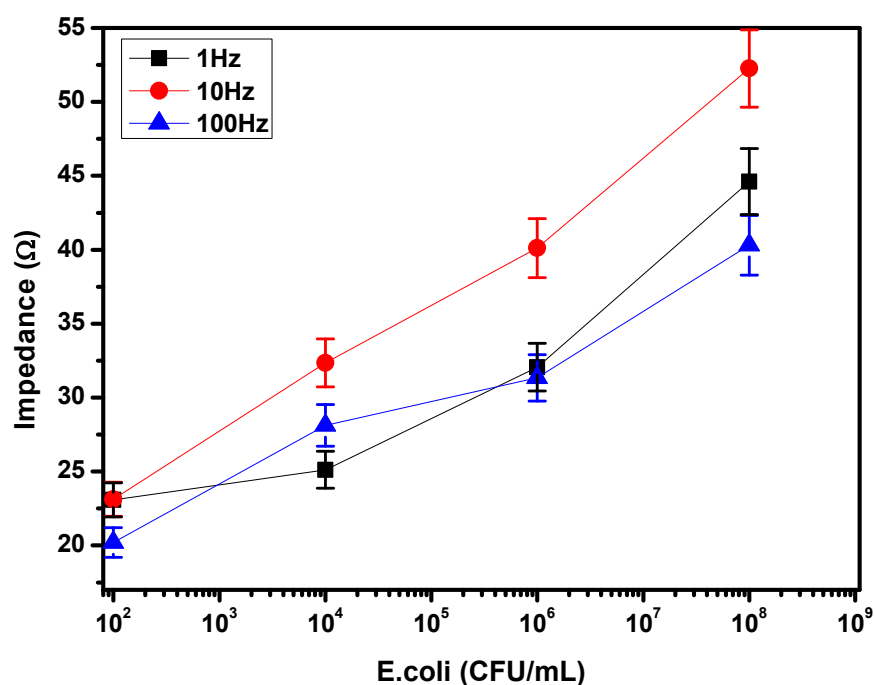


**Figure 5.5** Impedance values for various concentration of *E. coli* at 1 Hz, 10 Hz and 100 Hz.

### 5.3.1.3 Influence of applied potential

In impedance immunosensor the applied voltage/Potential should be quite small, usually 10 mV or lesser since the current voltage relationship is often linear for small perturbations (Barbero *et al.*, 2005). The impedance measurements were conducted for different applied potential from 0.1 mV to 10 mV. It was observed that at low applied potential, the current voltage waveform is distorted, whereas a better response was found at 10 mV applied potential as depicted in Fig 5.6.

Stable and non-distorted waveform at 10 mV, validate fruitful impedance measurement. Thus, this applied potential was chosen for impedance measurement for quantitative analysis of *E. coli* bacteria in water.

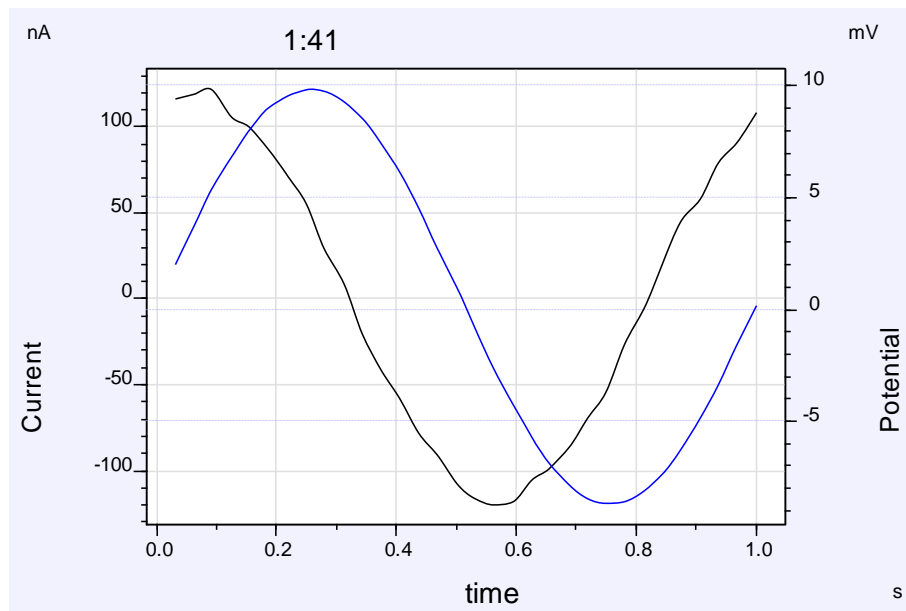


**Figure 5.6** Voltage-current waveform at 10 mV applied potential.

### 5.3.2 Selection of self assembled monolayer's (SAM's) for binding of *E. coli*

To implement an EIS immunosensor, biomolecules need to be immobilized on the surface of electrode to capture target analyte. Well-established protocols for SAMs were used for optimization of surface modification to immobilize *pAb-E. coli* on the Ag-wire electrode surface, with slight modifications. 11-MUA (Park *et al.*, 2004), CYST (Pedroso *et al.*, 2008) and L-cysteine (Zhang *et al.*, 2009) SAMs were tested for the immobilization of *pAb-E. coli* on the electrode surface. The concentrations of different surface modifiers and cross-linkers were optimized and *pAb-E. coli* antibody was attached to the surface. The SAM based on CYST showed the maximum % Impedance change for the binding of *E. coli* to *pAb-E. coli* antibody, thus the further experiments were carried out using CYST. Figure 5.7 represents the % Impedance change with respect to different *E. coli* concentrations obtained with different SAM's.

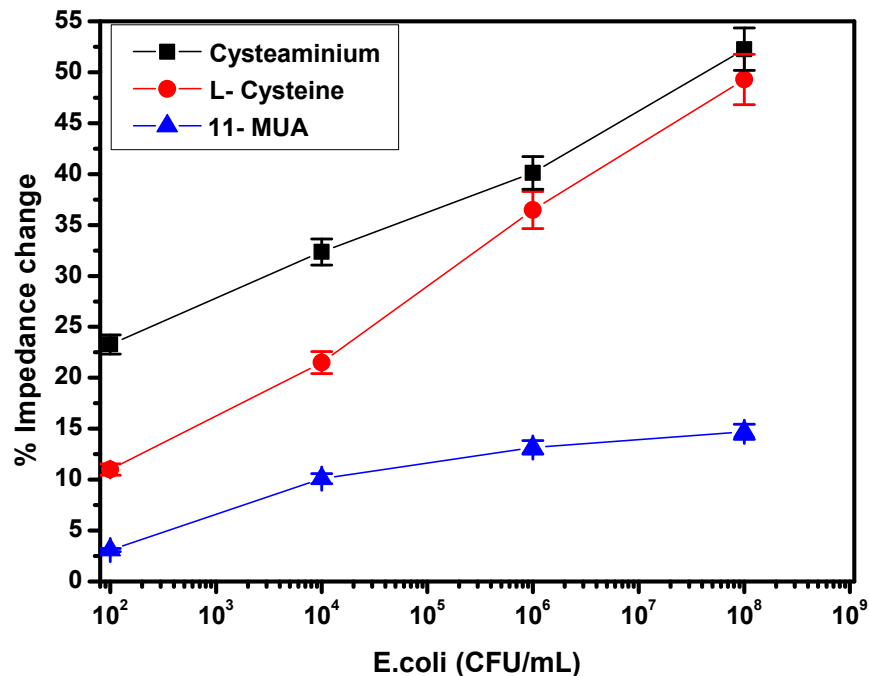


**Figure 5.7** Percentage impedance change for different SAMs (Cysteaminium, L-Cysteine and 11- MUA) for different concentrations of *E. coli* ( $10^2$ – $10^8$  CFU/mL). EIS: 1-100 KHz applied frequency and 10 mV applied potential.

### 5.3.3 Surface characterization of *pAb-E. coli* modified electrodes

The binding of *pAb-E. coli* to Ag-wire electrodes was confirmed by fluorescence microscopy using IX71 inverted microscope (Olympus, Japan). Two functionalized Ag-wires (reference wire without *pAb-E. coli* and sample wire coupled with *pAb-E. coli*) were incubated with FITC labeled secondary antibody against *E. coli* (pAb-FITC) (1:1000) for 2 hrs at room temperature. Before excitation, both reference and the sample wire were rinsed with 0.1 M PBS to remove unbound pAb-FITC. Figure 5.8 (a) shows fluorescence image of reference and (b) the sample Ag wire, after excitation. It can be observed; the labeled secondary antibody specifically recognized the anti-*E. coli*, demonstrating an optimal immobilization of the primary capture antibodies to the activated SAM. The binding of the pAb-FITC to the *pAb-E. coli* of the thiolated Ag-wire is clearly distinguished from the fluorescence images.

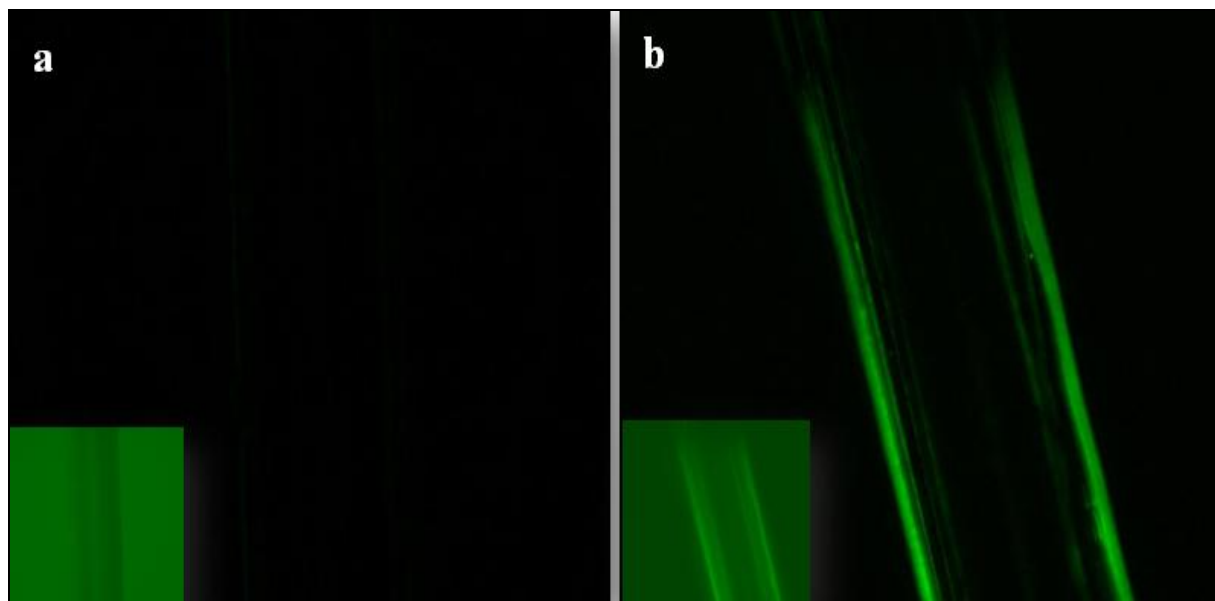


**Figure 5.8** Surface characterization of pAb-*E. coli* modified electrodes using fluorescence microscopy (a) image of control Ag-wire electrode, inset: non-subtracted background image of Ag-wire electrode (b) image of pAb-*E. coli* coupled Ag-wire electrode attached with FITC labeled secondary *E. coli* antibody, inset: non-subtracted background image of Ag-wire electrode.

### 5.3.4 EIS studies for *E. coli* binding

The antigen–antibody interaction of *E. coli* and pAb-*E. coli* immobilized Ag-wire electrode surface was studied using EIS. Figure 5.9 shows the impedance spectra for PBS as blank and *E. coli* ( $10^2$ CFU/mL) in water resulted from interaction of antigen–antibody on functionalized electrode surface. EIS is a useful technique to capture such interaction. This interaction results in change of electrical properties such as capacitance and resistance at the electrode surface allowing for label-free biosensing (Guan *et al.*, 2004). The Impedance/capacitance change is commonly used as indicator of antigen–antibody interaction for non-faradic biosensor (Danielsa and Pourmand, 2007). In the EIS measurement, pAb-*E. coli* interactions create a new charged layer as a capacitance that is in series with the double layer capacitance. A decreased double layer capacitance and increased impedance were observed at the lower frequency.



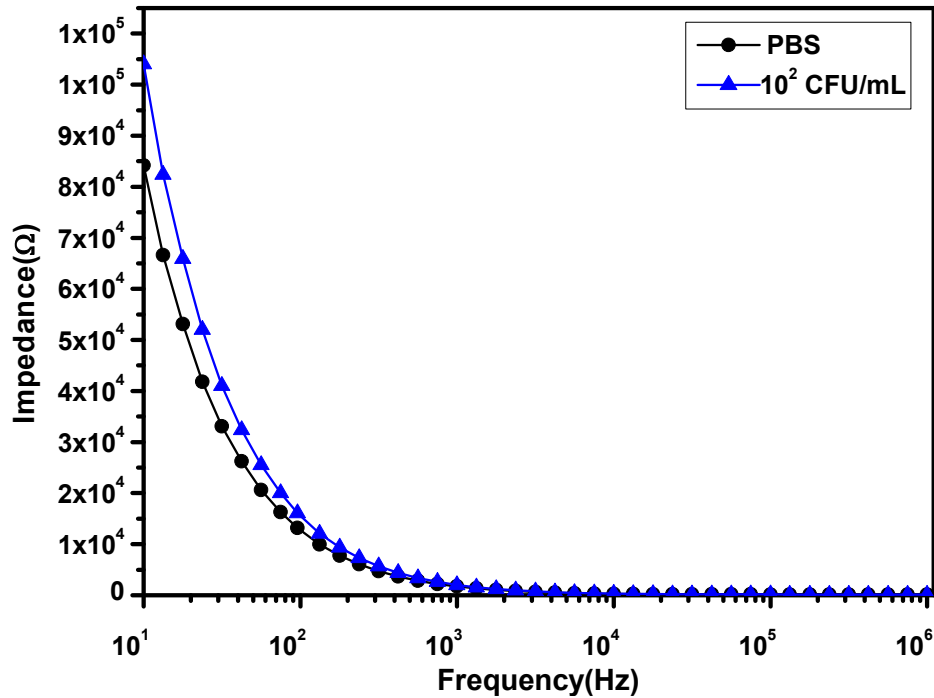


**Figure 5.9** Impedance spectra for PBS and *E. coli* ( $10^2$  CFU/mL) in water. EIS: 1-100 KHz applied frequency and 10 mV applied potential.

Impedance values of blank (PBS) and different *E. coli* concentration ( $10^2$ - $10^8$ CFU/mL) are shown in Table 5.3. For comparison the impedance value at 10 Hz were considered. This confirms that the change in impedance is resulting from binding of the antigen (*E. coli*). It is also clear from figure that the total impedance decreases linearly with the increasing frequency in the low frequency range from 10 Hz to 1 KHz, while it becomes independent of the frequency in the high frequency range from 1 KHz to 100 KHz. At low frequencies (<1 KHz), since the double layer capacitance offers essentially high impedance, it becomes the main component contributing to the total impedance, such that the medium resistance can be neglected. This region is defined as the double layer capacitive region in which the electrode impedance can be detected. In the higher frequency region (10 Hz to 100 KHz) it was observed that impedance remains constant. A significant change was measurable in the low frequency region (10–1 KHz) with highest impedance change observed at 10 Hz.

**Table 5.3** Impedance values for blank and different *E. coli* concentrations at 10 Hz.

Samples	Impedance ( $\Omega$ )
Blank	$6.67 \times 10^4$
<i>E. coli</i> MTCC 723 $10^2$ CFU/mL	$8.43 \times 10^4$
<i>E. coli</i> MTCC 723 $10^4$ CFU/mL	$9.08 \times 10^4$
<i>E. coli</i> MTCC 723 $10^6$ CFU/mL	$9.58 \times 10^4$
<i>E. coli</i> MTCC 723 $10^8$ CFU/mL	$10.6 \times 10^4$

### 5.3.5 Calibration of immunosensor for *E. coli* detection in water

The *E. coli* samples were spiked in water to meet the calibration standards. Before spiking the standards, water was filtered through the bacteriological membrane filter (0.22  $\mu\text{m}$ ) and tested for presence of any other *E. coli* strain *i.e.* *E. coli* O157:H7 using Singlepath® *E. coli* O157, a gold labeled immuno sorbent assay (GLISA) rapid test (obtained from Merck-Millipore, Germany).

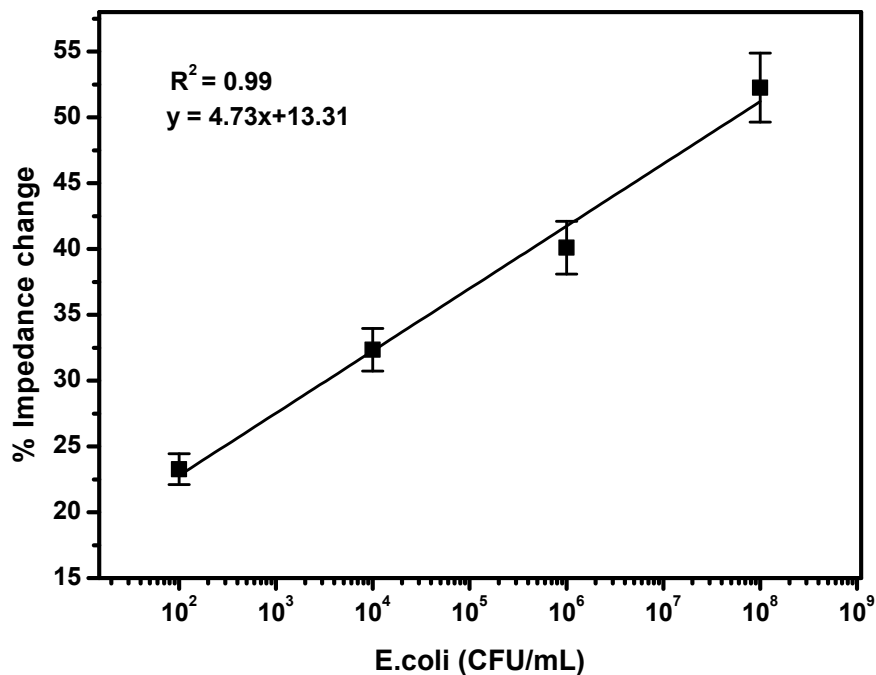


**Figure 5.10** Calibration curve obtained for label-free impedimetric immunosensor for *E. coli* in water (SD=0.802) EIS: 1-100 KHz applied frequency and 10 mV applied potential.

Impedance data were recorded for the functionalized electrodes after exposing it to increasing *E. coli* concentration ( $10^2$ – $10^8$  CFU/mL) in water. A frequency of 10 Hz at applied potential 10 mV was selected for analysis since at this frequency significant change in impedance response was observed. The specific interaction of *pAb-E. coli* and *E. coli* gave rise to an overall increase in impedance change from baseline response at the electrode/solution interface for *E. coli* concentrations. The % impedance change was calculated corresponding to different concentrations of *E. coli*. The resulting calibration curve in water is shown as Figure 5.10. A linear range for *E. coli* detection  $10^2$ – $10^8$  CFU/mL with SD=0.802 and  $R^2=0.99$  was achieved with line equation  $y = 4.73x+13.31$ . Limit of detection (LOD) of the biosensor was  $10^2$  CFU/mL and sensitivity of the immunosensor is found to be 4.73.

### 5.3.6 Actual water sample analysis

Actual water samples were tested for the presence of *E. coli* using the developed immunosensor and compared with the spiked water sample with different concentrations of *E. coli* (MTCC 723) as presented in Table 5.4. For comparison the impedance value at 10 Hz were considered. It is clear from the obtained impedance values that all the tested water samples showed values less than the value of blank thus; all the water samples were determined to be free of *E. coli*.

**Table 5.4** Analytical results for actual water samples.

Tested Samples	Impedance ( $\Omega$ )
Blank	$6.68 \times 10^4$
<i>E. coli</i> MTCC 723 $10^2$ CFU/mL	$8.42 \times 10^4$
<i>E. coli</i> MTCC 723 $10^4$ CFU/mL	$9.06 \times 10^4$
<i>E. coli</i> MTCC 723 $10^6$ CFU/mL	$9.57 \times 10^4$
<i>E. coli</i> MTCC 723 $10^8$ CFU/mL	$10.4 \times 10^4$
Water sample I	$3.88 \times 10^4$
Water sample II	$1.51 \times 10^4$
Water sample III	$1.966 \times 10^4$
Water sample IV	$2.056 \times 10^4$

### 5.3.7 Sensing specificity of the immunosensor

The specificity of the immunosensor towards *E. coli* was tested against *Streptococcus pyogenes*. All the bacterial suspensions were taken at  $10^4$  CFU/mL. The impedance measurements were carried out at frequency range of 10 Hz to 100 KHz using EIS at 10 mV applied potential. In the optimized condition, the response signal for pAb-*E. coli* binding with bacterial suspension was measurable in 10 min. Obtained results are presented as Nyquist plot in Figure 5.11. From the Nyquist plot, it is clear that the imaginary part (Capacitive reactance) increased by 20% for binding of *E. coli* with pAb-*E. coli* as compared to *Streptococcus pyogenes*. The response of *Streptococcus pyogenes* with pAb-*E. coli* is may be due to non-specific adsorption on to the Ag-wire electrode surface.

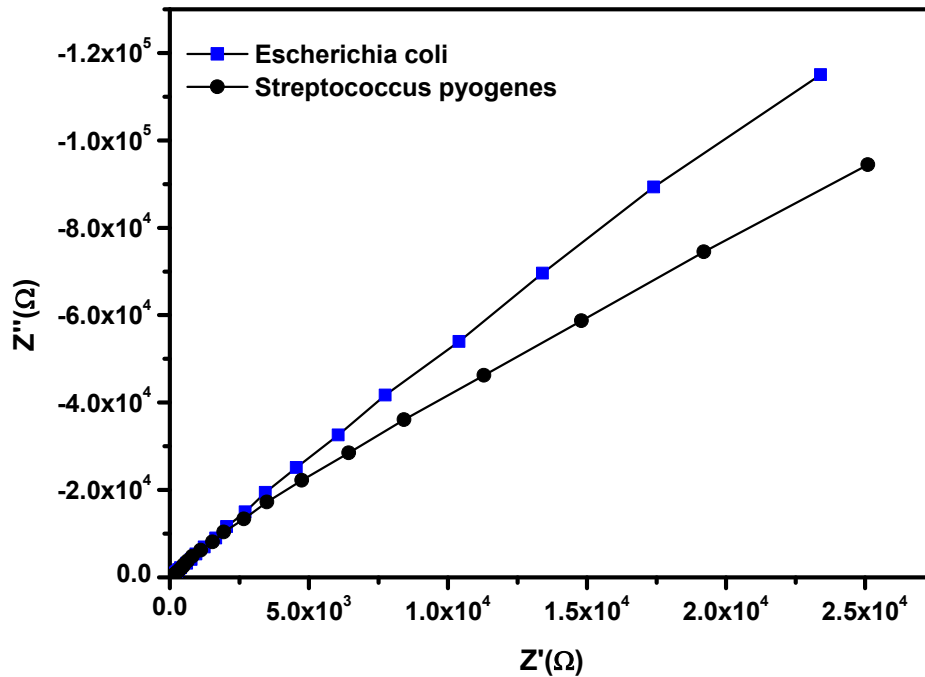


**Figure 5.11** Nyquist plot for sensing specificity of the functionalized Ag-wire immunosensor validated for *E. coli* against *Streptococcus pyogenes*. Concentrations of bacterial suspensions are  $10^4$  CFU/mL. EIS: 1-100 KHz applied frequency and 10 mV applied potential.

### 5.4 Conclusion

In this chapter, label-free impedemetric immunosensor for rapid detection of *E. coli* (MTCC 723) in water sample is developed and demonstrated. The analysis time of the developed

immunosensor was found to be 10 min. For biosensor development, polyclonal antibody against *E. coli* was immobilized over the SAMs of cysteaminium. Sensitivity and specificity of the developed immunosensor were evaluated by monitoring the changes in electrochemical impedance of the Ag-wire after bacterial cells were deposited on its surface. A linear trend of increasing impedance was obtained when the *E. coli* concentration increased from  $10^2$ – $10^8$  CFU/mL. EIS analysis has proved that the developed immunosensor was able to detect  $10^2$ – $10^8$  CFU/mL *E. coli* bacteria in water samples. The developed immunosensor is specific for detection of *E. coli*. The sensor does not require any additional reagents such as fluorescent or enzyme labels for sensor response and showed stable signals. Development of the presented immunosensor also supports that the label-free approaches may become practical for routine analysis of bacterial contamination in water.

## Chapter 6

### Conclusions

The main objectives of this doctoral research were to develop a robust biosensing technology for contaminated milk, urine and water. Contamination like urea and antibiotic residues in the milk can cause severe health and economic impact. Urea, a significant clinical analyte, often measured in the urine samples to appraise the functional ability of the renal system. The water, a key ingredient of the life, is often contaminated with bacteria, also need a rapid and cost effective biosensing technique for the bacterial detection. Our developed biosensing technology uses EIS based two-electrode immunosensor system for the detection of bacterial contamination in the samples. The significance of this research work lies in the development of high-throughput, sensitive, rapid, cost effective biosensors for determination of urea, antibiotic residues, and bacterial contamination. Extensive experiments were carried out for optimizing flow systems for enzyme activity, immobilization of enzymes, optimization of optimal antibody dilutions, selection of the self-assemblies, cross reactivity with structurally similar analytes, analysis of real samples and monitor biosensor performance. During the course of study, significant observations were noted. The overall conclusions are summarized chapter-wise below:

**1. Introduction (Chapter 1):** This chapter gave a detail description about biosensors, classification of biosensors, types of transducers with special emphasis on thermal, piezoelectric and electrochemical biosensors, various aspects of biosensors, performance criteria of biosensors, various components, different immobilization techniques used for bio-recognition elements, state of art for food samples and clinical analytes including urea, antibiotic residues and bacterial contamination. The chapter has also discussed about gaps in the existing research and objective of the proposed doctoral work and thesis structure.

**2. Development of flow injection analysis-enzyme thermistor (FIA-ET) biosensor for urea analysis in adulterated milk (Chapter 2):** This chapter gave a detailed account for the development of FIA-ET based biosensor for analysis of urea in adulterated milk. This also describes the novel sample pre-treatment procedures for investigation into milk, optimization of the FIA system, immobilization of enzyme and the stability of the biosensor. Detailed study of the enzyme column performance, stability and analytical performance of the biosensor are

described. The developed biosensor can analyze the concentration of urea up to 250 mM with semi-automated mode and up to 500 mM with an automated mode in adulterated milk samples. Excellent recoveries in the range of 97.56–108.70% were obtained for urea in milk. Very good reproducibility was obtained for urea concentration with % R.S.D. 0.50- 1.42 (n=3) for intraday analysis and % R.S.D. 0.05-2.57 (n=3) for interday analysis. The obtained results confirm the reproducibility of the sensor response. Measurements of milk samples with different fat percentages and validation against AOAC method and a commercial kit was carried out successfully. Being a flow injection technique FIA-ET biosensor has potential for automated measurements and it shows the applicability of the developed biosensor in the dairy industry for continuing monitoring of the milk urea.

**3. Development of flow injection analysis-enzyme thermistor (FIA-ET) biosensor for urea analysis in urine (Chapter 3):** This chapter described about the development of FIA-ET based biosensor for analysis of urea in urine samples. To achieve urea detection in urine suitable matrix matching protocols were developed. Urease was immobilized onto a novel material (aminated silica gel) to reduce the cost of column and subsequently to reduce the cost per sample analysis. The FIA-ET biosensor showed an excellent dynamic range for urea in urine in the range of 10–1000 mM with good linearity. The obtained minimum detection limit was found to be 10 mM. The immobilized urease column showed excellent stability over 7 months for urea analysis in urine. Excellent recoveries were obtained in the range 92.26–99.80% in the spiked urine samples. The FIA-ET biosensor is automated for real time data acquisition using automated injection valve. Obtained results support that the developed biosensor is highly stable, simple, and economical for urea analysis in urine samples.

**4. Development of flow injection analysis-electrochemical quartz crystal nanobalance (FIA-EQCN) biosensor for analysis of antibiotic residues in milk (Chapter 4):** This chapter detailed about the development of FIA-EQCN biosensor for antibiotic residue analysis in milk samples. This chapter was described in two parts; the first part deals with the development of the FIA-EQCN system for analysis of the SDZ residues in milk. SDZ was chosen as a model analyte to perform the residual testing as a proof of concept. This part of the chapter also describes about the optimization of the FIA system including matrix matching for milk sample analysis and immobilization of the biomolecule (antibody) on the crystal surface in a semi-automated mode.

In the second part of the chapter, development of the FIA-EQCN biosensor for ultrasensitive detection of SRT was described. Detailed studies on optimization of the flow system, selection of the self-assembly for immobilization of the biomolecule and characterization of the immobilized surface is described. A FIA-EQCN biosensor for SDZ and SRT residue analysis in milk was developed. Obtained calibration for SDZ (10-200 ng/mL) and SRT (0.3-300 ng/mL) supports the applicability of the developed biosensor in the milk sample analysis. The obtained recoveries for SDZ (98.6-100.5%) and SRT (98-99.33%) spiked milk samples also encourage the application of developed biosensor towards the quantification of SDZ and SRT in milk samples. Validation of the presented biosensor against commercial ELISA kit supports that the developed biosensor provides sensitive detection. Attempts were made to do the automated analysis of milk samples for streptomycin residues, and the developed biosensor exhibited a great potential for advance-automated analysis in dairy industries.

**5. Rapid label-free immunosensor for bacterial detection in water (Chapter 5):** This chapter described about the development of EIS based label-free immunosensor for rapid detection of *E. coli* in water samples. Ag-wires were used as two-electrode setup for impedance analysis. For biosensor development, polyclonal antibody against *E. coli* was immobilized over the SAMs of cysteaminium. Sensitivity and specificity of the developed immunosensor were evaluated by monitoring the changes in electrochemical impedance of the Ag-wire after bacterial cells were deposited on its surface. A linear trend of increasing impedance was obtained when the *E. coli* concentration increased from  $10^2$ – $10^8$  CFU/mL. EIS analysis has proved that the developed immunosensor was able to detect  $10^2$ – $10^8$  CFU/mL *E. coli* bacteria in water samples. The developed immunosensor is specific for detection of *E. coli*. The sensor does not require any additional reagents such as fluorescent or enzyme labels for sensor response and showed stable signals.



### **Future scope of the work**

- The developed FIA-ET urea biosensor technology can be deployed at dairy industry or milk collection centers with some advance automation.
- FIA-ET technology can be extended for analysis of other matrices.
- Novel column materials can be investigated for immobilization of enzymes and subsequently can be developed to a commercial product.
- FIA-EQCN technique can be fully automated for antibiotic residue analysis in dairy industries.
- Other antibiotic residues can be analyzed by exploring FIA-EQCN biosensor.
- Developed label-free impedimetric immunosensor can be extended to develop a portable/ field deployable biosensor.

- Abuknesha, R. A., and Luk, C. (2005) Enzyme immunoassays for the analysis of streptomycin in milk, serum and water: development and assessment of a polyclonal antiserum and assay procedures using novel streptomycin derivatives, *Analyst* 130, 964-970.
- Adrian, J., Pasche, S., Diserens, J.-M., Sánchez-Baeza, F., Gao, H., Marco, M., and Voirin, G. (2009) Waveguide interrogated optical immuno sensor (WIOS) for detection of sulfonamide antibiotics in milk, *Biosensors and Bioelectronics* 24, 3340-3346.
- Adrian, J., Pinacho, D. G., Granier, B., Diserens, J.-M., Sánchez-Baeza, F., and Marco, M.-P. (2008) A multianalyte ELISA for immunochemical screening of sulfonamide, fluoroquinolone and  $\beta$ -lactam antibiotics in milk samples using class-selective bioreceptors, *Analytical and Bioanalytical Chemistry* 391, 1703-1712.
- Ahmed, A., Rushworth, J. V., Wright, J. D., and Millner, P. A. (2013) Novel Impedimetric Immunosensor for Detection of Pathogenic Bacteria *Streptococcus pyogenes* in Human Saliva, *Analytical Chemistry* 85, 12118-12125.
- Alghamdi, A. H., Alghamdi, A. F., and Alomar, M. A. (2009) A study of stripping voltammetric behavior of cefadroxil antibiotic in the presence of cu (II) and its determination in pharmaceutical formulation, *Portugaliae Electrochimica Acta* 27, 645-655.
- Alizadeh, T., and Akbari, A. (2013) A capacitive biosensor for ultra-trace level urea determination based on nano-sized urea-imprinted polymer receptors coated on graphite electrode surface, *Biosensors and Bioelectronics* 43, 321-327.
- Andreescu, S., and Marty, J.-L. (2006) Twenty years research in cholinesterase biosensors: From basic research to practical applications, *Biomolecular Engineering* 23, 1-15.
- Baccar, H., Mejri, M., Hafaiedh, I., Ktari, T., Aouni, M., and Abdelghani, A. (2010) Surface plasmon resonance immunosensor for bacteria detection, *Talanta* 82, 810-814.
- Bacher, G., Pal, S., Kanungo, L., and Bhand, S. (2012) A label-free silver wire based impedimetric immunosensor for detection of aflatoxin M1 in milk, *Sensors and Actuators B: Chemical* 168, 223-230.

Bang-Ce, Y., Songyang, L., Peng, Z., and Xiao-hong, L. (2008) Simultaneous detection of sulfamethazine, streptomycin, and tylosin in milk by microplate-array based SMM-FIA, *Food Chemistry* 106, 797-803.

Barbero, G., and Alexe-Ionescu, A. (2005) Role of the diffuse layer of the ionic charge on the impedance spectroscopy of a cell of liquid, *Liquid Crystals* 32, 943-949.

Barreiros dos Santos, M., Agusil, J., Prieto-Simón, B., Sporer, C., Teixeira, V., and Samitier, J. (2013) Highly sensitive detection of pathogen *Escherichia coli* O157: H7 by electrochemical impedance spectroscopy, *Biosensors and Bioelectronics* 45, 174-180.

Barsan, M. M., and Brett, C. (2009) A new modified conducting carbon composite electrode as sensor for ascorbate and biosensor for glucose, *Bioelectrochemistry* 76, 135-140.

Baxter, G., Ferguson, J., O'Conno, M., and Elliott, C. (2001) Detection of streptomycin residues in whole milk using an optical immunobiosensor, *Journal of Agricultural and Food Chemistry* 49, 3204-3207.

Berggren, C., Bjarnason, B., and Johansson, G. (1998) An immunological Interleukine-6 capacitive biosensor using perturbation with a potentiostatic step, *Biosensors and Bioelectronics* 13, 1061-1068.

Bhand, S. G., Soundararajan, S., Surugiu-Wärnmark, I., Milea, J. S., Dey, E. S., Yakovleva, M., and Danielsson, B. (2010) Fructose-selective calorimetric biosensor in flow injection analysis, *Analytica Chimica Acta* 668, 13-18.

Bilandžić, N., Solomun Kolanović, B., Varenina, I., and Jurković, Z. (2011) Concentrations of veterinary drug residues in milk from individual farms in Croatia, *Mljekarstvo* 61, 260-267.

Bjurling, P., Baxter, G. A., Caselunghe, M., Jonson, C., O'Connor, M., Persson, B., and Elliott, C. T. (2000) Biosensor assay of sulfadiazine and sulfamethazine residues in pork, *Analyst* 125, 1771-1774.

Bogomolova, A., Komarova, E., Reber, K., Gerasimov, T., Yavuz, O., Bhatt, S., and Aldissi, M. (2009) Challenges of electrochemical impedance spectroscopy in protein biosensing, *Analytical Chemistry* 81, 3944-3949.

Borghol, N., Mora, L., Jouenne, T., Jaffézic-Renault, N., Sakly, N., Duncan, A. C., Chevalier, Y., Lejeune, P., and Othmane, A. (2010) Monitoring of *E. coli* immobilization on modified gold electrode: A new bacteria-based glucose sensor, *Biotechnology Bioprocess E 15*, 220-228.

Cabral, J. P. S. (2010) Water Microbiology. Bacterial Pathogens and Water, *International Journal of Environmental Research and Public Health 7*, 3657-3703.

Carter, E. L., Flugga, N., Boer, J. L., Mulrooney, S. B., and Hausinger, R. P. (2009) Interplay of metal ions and urease, *Metallomics 1*, 207-221.

Choi, M. M. F. (2004) Progress in Enzyme-Based Biosensors Using Optical Transducers, *Microchimica Acta 148*, 107-132.

Clark, S., Francis, P. S., Conlan, X. A., and Barnett, N. W. (2007) Determination of urea using high-performance liquid chromatography with fluorescence detection after automated derivatisation with xanthidrol, *Journal of Chromatography A 1161*, 207-213.

Cliquet, P., Cox, E., Haasnoot, W., Schacht, E., and Goddeeris, B. (2003) Extraction procedure for sulfachloropyridazine in porcine tissues and detection in a sulfonamide-specific enzyme-linked immunosorbent assay (ELISA), *Analytica Chimica Acta 494*, 21-28.

Commission Regulation (EU) No 37/2010, 22 December 2009. *Official Journal of European Union L15/1*.

Conzuelo, F., Campuzano, S., Gamella, M., Pinacho, D. G., Reviejo, A. J., Marco, M. P., and Pingarrón, J. M. (2013) Integrated disposable electrochemical immunosensors for the simultaneous determination of sulfonamide and tetracycline antibiotics residues in milk, *Biosensors and Bioelectronics 50*, 100-105.

Conzuelo, F., Gamella, M., Campuzano, S., G Pinacho, D., Reviejo, A. J., Marco, M. P., and Pingarrón, J. M. (2012) Disposable and integrated amperometric immunosensor for direct determination of sulfonamide antibiotics in milk, *Biosensors and Bioelectronics 36*, 81-88.

Currie, D., Lynas, L., Kennedy, D. G., and McCaughey, W. J. (1998) Evaluation of a modified EC Four Plate Method to detect antimicrobial drugs, *Food Additives & Contaminants 15*, 651-660.

- Czauderna, M., and Kowalczyk, J. (2012) Simple, selective, and sensitive measurement of urea in body fluids of mammals by reversed-phase ultra-fast liquid chromatography, *Czech. journal Animal Science* 57, 19-21.
- Daniels, J. S., and Pourmand, N. (2007) Label-Free Impedance Biosensors: Opportunities and Challenges, *Electroanalysis* 19, 1239-1257.
- Danielsson, B. (1982) The enzyme thermistor, *Applied Biochemistry Biotechnology* 7, 127-134.
- Danielsson, B., Lundström, I., Mosbach, K., and Stibler, L. (1979) On a New Enzyme Transducer Combination: The Enzyme Transistor, *Analytical Letters* 12, 1189-1199.
- Davis, F., and Higson, S. P. (2010) Label-free immunochemistry approach to detect and identify antibiotics in milk, *Pediatric Research* 67, 476-480.
- de Keizer, W., Bienenmann-Ploum, M. E., Bergwerff, A. A., and Haasnoot, W. (2008) Flow cytometric immunoassay for sulfonamides in raw milk, *Analytica Chimica Acta* 620, 142-149.
- Downes, F. P., Ito, K., and Association, A. P. H. (2001) *Compendium of Methods for the Microbiological Examination of Foods*, American Public Health Association.
- Doyle, M.P. (2001) *Food Microbiology: Fundamentals and Frontiers*. 2<sup>nd</sup> Edn. ASM Press, Washington.
- Felice, C. J., Madrid, R. E., Olivera, J. M., Rotger, V. I., and Valentinuzzi, M. E. (1999) Impedance microbiology: quantification of bacterial content in milk by means of capacitance growth curves, *Journal of Microbiological Methods* 35, 37-42.
- Fenwick, A. (2006) Waterborne Infectious Diseases—Could They Be Consigned to History?, *Science* 313, 1077-1081.
- Ferguson, J., Baxter, G., McEvoy, J., Stead, S., Rawlings, E., and Sharman, M. (2002) Detection of streptomycin and dihydrostreptomycin residues in milk, honey and meat samples using an optical biosensor, *Analyst* 127, 951-956.

Fernández, F., Hegnerová, K., Piliarik, M., Sanchez-Baeza, F., Homola, J., and Marco, M. (2010) A label-free and portable multichannel surface plasmon resonance immunosensor for on site analysis of antibiotics in milk samples, *Biosensors and Bioelectronics* 26, 1231-1238.

Fernández, F., Pinacho, D. G., Sánchez-Baeza, F., and Marco, M. P. (2011) Portable surface plasmon resonance immunosensor for the detection of fluoroquinolone antibiotic residues in milk, *Journal of Agricultural and Food Chemistry* 59, 5036-5043.

Flores Abuxapqui, J. J., Suárez Hoil, G. J., Heredia Navarrete, M. R., Puc Franco, M. A., and Vivas Rosel, M. L. (1999) Four biochemical tests for identification of probable enteroinvasive *Escherichia coli* strains, *Rev Latinoam Microbiol* 41

Food Safety and Standards Authority of India (FSSAI).(2012) Manual of methods of analysis of foods, milk and milk products. Retrieved from:

<http://www.fssai.gov.in/portal/0/pdf/15Manuals/MILK AND MILK PRODUCTS.pdf>

Furusawa, N. (2003) Rapid high-performance liquid chromatographic determining technique of sulfamonomethoxine, sulfadimethoxine, and sulfaquinoxaline in eggs without use of organic solvents, *Analytica Chimica Acta* 481, 255-259.

Geng, P., Zhang, X., Meng, W., Wang, Q., Zhang, W., Jin, L., Feng, Z., and Wu, Z. (2008) Self-assembled monolayers-based immunosensor for detection of *Escherichia coli* using electrochemical impedance spectroscopy, *Electrochimica Acta* 53, 4663-4668.

Goeyens, L., Kindermans, N., Abu Yusuf, M., and Elskens, M. (1998) A room temperature procedure for the manual determination of urea in seawater, *Estuarine, Coastal and Shelf Science* 47, 415-418.

Guan, J.-G., Miao, Y.-Q., and Zhang, Q.-J. (2004) Impedimetric biosensors, *Journal of Bioscience and Bioengineering* 97, 219-226.

Guo, X., Lin, C.-S., Chen, S.-H., Ye, R., and Wu, V. C. (2012) A piezoelectric immunosensor for specific capture and enrichment of viable pathogens by quartz crystal microbalance sensor, followed by detection with antibody-functionalized gold nanoparticles, *Biosensors and Bioelectronics* 38, 177-183.

- Gutiérrez, M., Alegret, S., and del Valle, M. (2008) Bioelectronic tongue for the simultaneous determination of urea, creatinine and alkaline ions in clinical samples, *Biosensors and Bioelectronics* 23, 795-802.
- Haasnoot, W., Bienenmann-Ploum, M., and Kohen, F. (2003) Biosensor immunoassay for the detection of eight sulfonamides in chicken serum, *Analytica Chimica Acta* 483, 171-180.
- Haasnoot, W., Cazemier, G., Koets, M., and van Amerongen, A. (2003) Single biosensor immunoassay for the detection of five aminoglycosides in reconstituted skimmed milk, *Analytica Chimica Acta* 488, 53-60.
- Heering, W., Usleber, E., Dietrich, R., and Märtlbauer, E. (1998) Immunochemical screening for antimicrobial drug residues in commercial honey, *Analyst* 123, 2759-2762.
- Heo, J., and Hua, S. Z. (2009) An overview of recent strategies in pathogen sensing, *Sensors* 9, 4483-4502.
- Heyduk, E., and Heyduk, T. (2010) Fluorescent homogeneous immunosensors for detecting pathogenic bacteria, *Analytical Biochemistry* 396, 298-303.
- Holford, T. R. J., Holmes, J. L., Collyer, S. D., Davis, F., and Higson, S. P. J. (2013) Label-free impedimetric immunosensors for psoriasis—Increased reproducibility and sensitivity using an automated dispensing system, *Biosensors and Bioelectronics* 44, 198-203.
- IUPAC. Compendium of Chemical Terminology, 2nd ed. (the "Gold Book"). Compiled by A. D. McNaught and A. Wilkinson. Blackwell Scientific Publications, Oxford (1997). XML on-line corrected version: <http://goldbook.iupac.org> (2006) created by M. Nic, J. Jirat, B. Kosata; updates compiled by A. Jenkins. ISBN 0-9678550-9-8. doi:10.1351/goldbook.
- Jdanova, A., Poyard, S., Soldatkin, A., Jaffrezic-Renault, N., and Martelet, C. (1996) Conductometric urea sensor. Use of additional membranes for the improvement of its analytical characteristics, *Analytica Chimica Acta* 321, 35-40.
- Jenkins, D. M., and Delwiche, M. J. (2002) Manometric biosensor for on-line measurement of milk urea, *Biosensors and Bioelectronics* 17, 557-563.

Jensen, P. S., Bak, J., Ladefoged, S., and Andersson-Engels, S. (2004) Determination of urea, glucose, and phosphate in dialysate with Fourier transform infrared spectroscopy, *Spectrochimica Acta Part A: Molecular and Biomolecular Spectroscopy* 60, 899-905.

Jonker, J., Kohn, R., and Erdman, R. (1998) Using milk urea nitrogen to predict nitrogen excretion and utilization efficiency in lactating dairy cows, *Journal of Dairy Science* 81, 2681-2692.

Joshi, K. A., Tang, J., Haddon, R., Wang, J., Chen, W., and Mulchandani, A. (2005) A Disposable Biosensor for Organophosphorus Nerve Agents Based on Carbon Nanotubes Modified Thick Film Strip Electrode, *Electroanalysis* 17, 54-58.

Karplus, P. A., Pearson, M. A., and Hausinger, R. P. (1997) ChemInform Abstract: 70 Years of Crystalline Urease: What Have We Learned?, *ChemInform* 28.

Kawasaki, S., Fratamico, P. M., Horikoshi, N., Okada, Y., Takeshita, K., Sameshima, T., and Kawamoto, S. (2010) Multiplex real-time polymerase chain reaction assay for simultaneous detection and quantification of Salmonella species, Listeria monocytogenes, and Escherichia coli O157: H7 in ground pork samples, *Foodborne Pathogens and Disease* 7, 549-554.

Knecht, B. G., Strasser, A., Dietrich, R., Märtlbauer, E., Niessner, R., and Weller, M. G. (2003) Automated Microarray System for the Simultaneous Detection of Antibiotics in Milk, *Analytical Chemistry* 76, 646-654.

Koncki, R., Radomska, A., and Głąb, S. (2000) Potentiometric determination of dialysate urea nitrogen, *Talanta* 52, 13-17.

Kostić, T., Stessl, B., Wagner, M., Sessitsch, A., and Bodrossy, L. (2010) Microbial diagnostic microarray for food-and water-borne pathogens, *Microbial Biotechnology* 3, 444-454.

Krajewska, B. (2009) Ureases I. Functional, catalytic and kinetic properties: A review, *Journal of Molecular Catalysis B: Enzymatic* 59, 9-21.

Li, Y., Afrasiabi, R., Fathi, F., Wang, N., Xiang, C., Love, R., She, Z., and Kraatz, H.-B. (2014) Impedance based detection of pathogenic *E. coli* O157: H7 using a ferrocene-antimicrobial peptide modified biosensor, *Biosensors and Bioelectronics* 58, 193-199.



- Liao, W.-C., and Ho, J.-a. A. (2009) Attomole DNA electrochemical sensor for the detection of *Escherichia coli* O157, *Analytical Chemistry* 81, 2470-2476.
- Liu, B., Zhang, B., Cui, Y., Chen, H., Gao, Z., and Tang, D. (2011) Multifunctional gold–silica nanostructures for ultrasensitive electrochemical immunoassay of streptomycin residues, *ACS Applied Materials & Interfaces* 3, 4668-4676.
- Lu, L., Chee, G., Yamada, K., and Jun, S. (2013) Electrochemical impedance spectroscopic technique with a functionalized microwire sensor for rapid detection of food borne pathogens, *Biosensors and Bioelectronics* 42, 492-495.
- Luong, J. H. T., Groom, C. A., and Male, K. B. (1991) The potential role of biosensors in the food and drink industries, *Biosensors and Bioelectronics* 6, 547-554.
- Luppa, P. B., Sokoll, L. J., and Chan, D. W. (2001) Immunosensors—principles and applications to clinical chemistry, *Clinica Chimica Acta* 314, 1-26.
- Luzzana, M., and Giardino, R. (1999) Urea determination in milk by a differential pH technique, *Le Lait* 79, 261-267.
- Maalouf, R., Fournier-Wirth, C., Coste, J., Chebib, H., Saïkali, Y., Vittori, O., Errachid, A., Cloarec, J.-P., Martelet, C., and Jaffrezic-Renault, N. (2007) Label-free detection of bacteria by electrochemical impedance spectroscopy: comparison to surface plasmon resonance, *Analytical Chemistry* 79, 4879-4886.
- Maarit Niemi, R., Mentu, J., Siitonen, A., and Niemelä, S. I. (2003) Confirmation of *Escherichia coli* and its distinction from *Klebsiella* species by gas and indole formation at 44 and 44.5°C, *Journal of Applied Microbiology* 95, 1242-1249.
- Mach, K. E., Wong, P. K., and Liao, J. C. (2011) Biosensor diagnosis of urinary tract infections: a path to better treatment?, *Trends in Pharmacological Sciences* 32, 330-336.
- Magliulo, M., Simoni, P., Guardigli, M., Michelini, E., Luciani, M., Lelli, R., and Roda, A. (2007) A rapid multiplexed chemiluminescent immunoassay for the detection of *Escherichia coli* O157: H7, *Yersinia enterocolitica*, *Salmonella typhimurium*, and *Listeria monocytogenes* pathogen bacteria, *Journal of Agricultural and Food Chemistry* 55, 4933-4939.

Malhotra, B. D., Chaubey, A., and Singh, S. P. (2006) Prospects of conducting polymers in biosensors, *Analytica Chimica Acta* 578, 59-74.

Malitesta, C., Picca, R. A., Mazzotta, E., and Guascito, M. R. (2012) Tools for the Development of Electrochemical Sensors: an EQCM Flow Cell with Flow Focusing, *Electroanalysis* 24, 790-797.

Manual of methods of analysis of food, milk and milk products, Food Safety and Standards Authority of India, Ministry of Health and family welfare, Govt. of India, New Delhi, (2012) Online version Available: <http://www.fssai.gov.in/Portals/0/Pdf/15Manuals/MILKAND MILK PRODUCTS.pdf>.

Maxsignal Urea Enzymatic Assay Kit Manual. (2010) Catalog #:1051, BIOO Scientific, USA.

Min, J., and Baeumner, A. J. (2002) Highly Sensitive and Specific Detection of Viable Escherichia coli in Drinking Water, *Analytical Biochemistry* 303, 186-193.

Morishita, Y., Nakane, K., Fukatsu, T., Nakashima, N., Tsuji, K., Soya, Y., Yoneda, K., Asano, S., and Kawamura, Y. (1997) Kinetic assay of serum and urine for urea with use of urease and leucine dehydrogenase, *Clinical Chemistry* 43, 1932-1936.

Murtazina, N. R., Eremin, S. A., Mozoleva, O. V., Everest, S. J., Jim Brown, A., and Jackman, R. (2004) Fluorescent polarization immunoassay for sulphadiazine using a high specificity antibody, *International Journal of Food Science & Technology* 39, 879-889.

Noam N. Levey and Henry Chu, Virulent new strain of E. coli found in deadly European outbreak, (2011) Oct 26, Los Angeles Times, on-line version: <http://articles.latimes.com/2011/jun/03/world/la-fg-e-coli-20110603>

Noyhouzer, T., Kohen, R., and Mandler, D. (2009) A new approach for measuring the redox state and redox capacity in milk, *Analytical Methods* 1, 93-99.

Orsonneau, J.-L., Massoubre, C., Cabanes, M., and Lustenberger, P. (1992) Simple and sensitive determination of urea in serum and urine, *Clinical Chemistry* 38, 619-623.

- Park, I.-S., Kim, D.-K., Adanyi, N., Varadi, M., and Kim, N. (2004) Development of a direct-binding chloramphenicol sensor based on thiol or sulfide mediated self-assembled antibody monolayers, *Biosensors and Bioelectronics* 19, 667-674.
- Pedroso, M. M., Watanabe, A. M., Roque-Barreira, M. C., Bueno, P. R., and Faria, R. C. (2008) Quartz Crystal Microbalance monitoring the real-time binding of lectin with carbohydrate with high and low molecular mass, *Microchemical Journal* 89, 153-158.
- Petri, A., Gambicorti, T., and Salvadori, P. (2004) Covalent immobilization of chloroperoxidase on silica gel and properties of the immobilized biocatalyst, *Journal of Molecular Catalysis B: Enzymatic* 27, 103-106.
- Pieretti, B., Brunati, P., Pini, B., Colzani, C., Congedo, P., Rocchi, M., and Terramocci, R. (2010) Diagnosis of bacteriuria and leukocyturia by automated flow cytometry compared with urine culture, *Journal of Clinical Microbiology* 48, 3990-3996.
- Pirvutoiu, S., Dey, E., Bhand, S., Ciucu, A., Magearu, V., and Danielsson, B. (2002) Application of the enzyme thermistor for determination of mercury and other heavy metals using free and immobilised alcohol oxidase, *Romanian Biotechnological Letters* 7, 975-986.
- Pizzariello, A., Stredanský, M., Stredanská, S., and Miertuš, S. (2001) Urea biosensor based on amperometric pH-sensing with hematein as a pH-sensitive redox mediator, *Talanta* 54, 763-772.
- Que, X., Liu, B., Fu, L., Zhuang, J., Chen, G., and Tang, D. (2013) Molecular Imprint for Electrochemical Detection of Streptomycin Residues Using Enzyme Signal Amplification, *Electroanalysis* 25, 531-537.
- Queirós, R. B., de-los-Santos-Álvarez, N., Noronha, J., and Sales, M. (2013) A label-free DNA aptamer-based impedance biosensor for the detection of *E. coli* outer membrane proteins, *Sensors and Actuators B: Chemical* 181, 766-772.
- Radke, S. M., and Alocilja, E. C. (2004) Design and fabrication of a microimpedance biosensor for bacterial detection, *Sensors Journal, IEEE* 4, 434-440.

- Ram, S., Vajpayee, P., and Shanker, R. (2008) Rapid Culture-Independent Quantitative Detection of Enterotoxigenic *Escherichia coli* in Surface Waters by Real-Time PCR with Molecular Beacon, *Environmental Science & Technology* 42, 4577-4582.
- Ramanathan, K., and Danielsson, B. (2001) Principles and applications of thermal biosensors, *Biosensors and Bioelectronics* 16, 417-423.
- Rebe Raz, S., Bremer, M. G., Haasnoot, W., and Norde, W. (2009) Label-free and multiplex detection of antibiotic residues in milk using imaging surface plasmon resonance-based immunosensor, *Analytical Chemistry* 81, 7743-7749.
- Reeves, V. B. (1999) Confirmation of multiple sulfonamide residues in bovine milk by gas chromatography–positive chemical ionization mass spectrometry, *Journal of Chromatography B: Biomedical Sciences and Applications* 723, 127-137.
- Reis Lima, M., Fernandes, S. M., and Rangel, A. O. (2004) Enzymatic determination of urea in milk by sequential injection with spectrophotometric and conductometric detection, *Journal of Agricultural and Food Chemistry* 52, 6887-6890.
- Renny, E. F., Daniel, D. K., Krastanov, A. I., Zachariah, C. A., and Elizabeth, R. (2005) Enzyme Based Sensor for Detection of Urea in Milk, *Biotechnology & Biotechnological Equipment* 19, 198-201.
- Rompré, A., Servais, P., Baudart, J., de-Roubin, M.-R., and Laurent, P. (2002) Detection and enumeration of coliforms in drinking water: current methods and emerging approaches, *Journal of Microbiological Methods* 49, 31-54.
- Ruan, C., Yang, L., and Li, Y. (2002) Immunobiosensor chips for detection of *Escherichia coli* O157: H7 using electrochemical impedance spectroscopy, *Analytical Chemistry* 74, 4814-4820.
- Salman, S., Soundararajan, S., Safina, G., Satoh, I., and Danielsson, B. (2008) Hydroxyapatite as a novel reversible in situ adsorption matrix for enzyme thermistor-based FIA, *Talanta* 77, 490-493.

Samsonova, J., Bashkurov, M., Ivanova, N., Rubtsova, M. Y., and Egorov, A. (2005) ELISA of streptomycin in buffer and milk: Effect of reagents' structure and analysis format on assay performance, *Food and Agricultural Immunology* 16, 47-57.

Sassolas, A., Blum, L. J., and Leca-Bouvier, B. D. (2012) Immobilization strategies to develop enzymatic biosensors, *Biotechnology Advances* 30, 489-511.

Sauerbrey, G. (1959) Verwendung von Schwingquarzen zur Wägung dünner Schichten und zur Mikrowägung, *Z. Physik* 155, 206-222.

Settingington, E. B., and Alocilja, E. C. (2012) Electrochemical biosensor for rapid and sensitive detection of magnetically extracted bacterial pathogens, *Biosensors* 2, 15-31.

Settu, K., Liu, J.-T., Chen, C.-J., Tsai, J.-Z., and Chang, S. J. (2013) Concept for E. coli detection using interdigitated microelectrode impedance sensor, in *Engineering in Medicine and Biology Society (EMBC), 2013 35th Annual International Conference of the IEEE*, pp 1712-1715, IEEE.

Sharma, R., Rajput, Y. S., Kaur, S., and Tomar, S. K. (2008) A method for estimation of urea using ammonia electrode and its applicability to milk samples, *Journal of Dairy Research* 75, 466-470.

Shelton, D. R., Karns, J. S., Higgins, J. A., Van Kessel, J. A. S., Perdue, M. L., Belt, K. T., Russell-Anelli, J., and DebRoy, C. (2006) Impact of microbial diversity on rapid detection of enterohemorrhagic Escherichia coli in surface waters, *FEMS Microbiology Letters* 261, 95-101.

Shen, W., Li, Y., Chen, H., Horikawa, S., and Chin, B. A. (2010) A Biosensor System for the Detection of Salmonella Typhimurium Using Multiple Phage-based Magnetoelastic Biosensors, *MRS Online Proceedings Library* 1253.

Silva, M. S., Cavalcanti, I., Barroso, M. F., Sales, M. G., and Dutra, R. (2010) Gold electrode modified by self-assembled monolayers of thiols to determine DNA sequences hybridization, *Journal of Chemical Science* 122, 911-917.

Situ, C., Mooney, M. H., Elliott, C. T., and Buijs, J. (2010) Advances in surface plasmon resonance biosensor technology towards high-throughput, food-safety analysis, *TrAC Trends in Analytical Chemistry* 29, 1305-1315.

- Stoey, G., and Michailova, A. (2000) Quantitative determination of sulfonamide residues in foods of animal origin by high-performance liquid chromatography with fluorescence detection, *Journal of Chromatography A* 871, 37-42.
- Strasser, A., Dietrich, R., Usleber, E., and Märtlbauer, E. (2003) Immunochemical rapid test for multiresidue analysis of antimicrobial drugs in milk using monoclonal antibodies and hapten–glucose oxidase conjugates, *Analytica Chimica Acta* 495, 11-19.
- Sumana, G., Das, M., Srivastava, S., and Malhotra, B. D. (2010) A novel urea biosensor based on zirconia, *Thin Solid Films* 519, 1187-1191.
- Tiwari, A., Aryal, S., Pilla, S., and Gong, S. (2009) An amperometric urea biosensor based on covalently immobilized urease on an electrode made of hyper branched polyester functionalized gold nanoparticles, *Talanta* 78, 1401-1407.
- Trivedi, U., Lakshminarayana, D., Kothari, I., Patel, N., Kapse, H., Makhija, K., Patel, P., and Panchal, C. (2009) Potentiometric biosensor for urea determination in milk, *Sensors and Actuators B: Chemical* 140, 260-266.
- Ulman, A. (1996) Formation and Structure of Self-Assembled Monolayers, *Chemical Reviews* 96, 1533-1554.
- Velasco-Garcia, M. N., and Mottram, T. (2003) Biosensor technology addressing agricultural problems, *Biosystems Engineering* 84, 1-12.
- Verma, N., and Singh, M. (2003) A disposable microbial based biosensor for quality control in milk, *Biosensors and Bioelectronics* 18, 1219-1224.
- Verma, N., Kumar, R., and Kumar, M. (2012) Simple, qualitative cum quantitative, user friendly biosensor for analysis of Urea, *Advances in Applied Science Research* 3.
- Wang, Z., Li, N., Zhang, S., Zhang, H., Sheng, Y., and Shen, J. (2013) Production of antibodies and development of enzyme-linked immunosorbent assay for valnemulin in porcine liver, *Food Additives & Contaminants: Part A* 30, 244-252.

- Wu, J.-X., Zhang, S.-e., and Zhou, X.-p. (2010) Monoclonal antibody-based ELISA and colloidal gold-based immunochromatographic assay for streptomycin residue detection in milk and swine urine, *J. Zhejiang Univ. Sci. B* 11, 52-60.
- Xie, B., Ramanathan, K., and Danielsson, B. (2000) Mini/micro thermal biosensors and other related devices for biochemical/clinical analysis and monitoring, *TrAC Trends in Analytical Chemistry* 19, 340-349.
- Yakovleva, M., Bhand, S., and Danielsson, B. (2013) The enzyme thermistor—A realistic biosensor concept. A critical review, *Analytica Chimica Acta* 766, 1-12.
- Yang, D.-H., Bae, A.-H., Koumoto, K., Lee, S.-W., Sakurai, K., and Shinkai, S. (2005) In situ monitoring of polysaccharide–polynucleotide interaction using a schizophyllan-immobilized QCM device, *Sensors and Actuators B: Chemical* 105, 490-494.
- Yang, Y., Long, Y., Li, Z., Li, N., Li, K., and Liu, F. (2009) Real-time molecular recognition between protein and photosensitizer of photodynamic therapy by quartz crystal microbalance sensor, *Analytical Biochemistry* 392, 22-27.
- Yu, X., Lv, R., Ma, Z., Liu, Z., Hao, Y., Li, Q., and Xu, D. (2006) An impedance array biosensor for detection of multiple antibody–antigen interactions, *Analyst* 131, 745-750.
- Yu, X., Xu, D., and Cheng, Q. (2006) Label-free detection methods for protein microarrays, *Proteomics* 6, 5493-5503.
- Zemanick, E. T., Wagner, B. D., Sagel, S. D., Stevens, M. J., Accurso, F. J., and Harris, J. K. (2010) Reliability of quantitative real-time PCR for bacterial detection in cystic fibrosis airway specimens, *PLoS One* 5, e15101.
- Zhang, L., Liu, Y., and Chen, T. (2009) Label-free amperometric immunosensor based on antibody immobilized on a positively charged gold nanoparticle/l-cysteine-modified gold electrode, *Microchimica Acta* 164, 161-166.

## List of Publications

### List of publications counted in thesis:

1. Mishra, G. K., Mishra, R. K., and Bhand, S. (2010) Flow injection analysis biosensor for urea analysis in adulterated milk using enzyme thermistor, *Biosensors and Bioelectronics* 26, 1560-1564. (Output from chapter 2).
2. Mishra, G. K., and Bhand, S. (2012) FIA-EQCN biosensor for analysis of sulphadiazine residues in milk, in *Sixth International Conference on Sensing Technology (ICST), 2012*, pp 672-676, IEEE (Output from chapter 4).
3. Mishra, G.K., Sharma, A., Deshpande, K., and Bhand, S. (2014) Flow Injection Analysis Biosensor for Urea Analysis in Urine Using Enzyme Thermistor, *Applied Biochemistry and Biotechnology* 174, 998-1009 (Output from chapter 3).
4. Mishra, G. K.<sup>#</sup>, Sharma, A.<sup>#</sup>, and Bhand, S. (2014) Ultrasensitive detection of streptomycin using flow injection analysis-electrochemical quartz crystal nanobalance (FIA-EQCN) biosensor, *Biosensors and Bioelectronics*, In press, DOI: 10.1016/j.bios.2014.09.033 (Output from chapter 4).
5. Mishra, G. K., and Bhand, S. (2014) Biosensor for urea analysis in adulterated milk, *Indian Farming* 64, 115-117 (Output from chapter 2)
6. Mishra, G. K.<sup>#</sup>, Bacher, G.<sup>#</sup>, Roy, U., and Bhand, S. (2015) A label free impedemetric immunosensor for detection of *Escherichia coli* in water, *Chemical sensors*, 5-4 (Output from chapter 5).

### Other Publications:

1. Naik, P.P.<sup>#</sup>, Mishra, G.K.<sup>#</sup>, Danielsson, B., and Bhand, S., (2014) Android integrated urea biosensor for public health awareness, *Sensing and BioSensing Research*, In press, DOI: 10.1016/j.sbsr.2014.11.001.

<sup>#</sup> Authors with equal contribution

2. Mishra, R. K., Mishra, G. K., Dharma Teja, V., Danielsson, B., and Bhand, S. (2013) A visual colorimetric dual readout bioassay for determination of pesticide residues in drinking water, *Chemical sensors* 3-12.



### Conferences and Workshop Attended

1. Oral presentation at National Conference on Nano Functional Materials (NFM2014), BITS, Pilani India, 2014 entitled “A micro biosensor for label-free detection of *Salmonella* in water” Geetesh K Mishra, Gautam Bacher, Utpal Roy, and Sunil Bhand.
2. Presented a poster at Indo- UK International Workshop On Advanced Materials And Their Applications In Nanotechnology (AMAN 2014) Organized by BITS Pilani, KK Birla Goa Campus (May 17- 19, 2014) entitled “Impedometric immunosensor for bacterial detection” Geetesh K. Mishra , Gautam Bacher ,Utpal Roy and Sunil Bhand (2nd prize in poster presentation).
3. Presented a Poster at India-Japan workshop on biomolecular electronics & organic nanotechnology for environmental preservation (IJWBME 2013) organized by DTU New Delhi, 13-15 December 2013 entitled “Flow Injection Analysis biosensor for urea analysis in urine using Enzyme Thermistor” Geetesh K Mishra, Atul Sharma and Sunil Bhand.
4. Attended the International Conference on Emerging Technologies: Micro to Nano (ETMN 2013) on 23-24<sup>th</sup> February 2013.
5. Attended one-day workshop on IPR at BITS Pilani K.K. Birla Goa campus. (2012).

### Abstract accepted in conferences

1. Abstract accepted for poster presentation: Geetesh K. Mishra , Atul Sharma and Sunil Bhand “Ultrasensitive detection of streptomycin using Flow injection analysis-Electrochemical quartz crystal nanobalance (FIA-EQCN) biosensor” 24th Anniversary World Congress on Biosensors, May 27-30, 2014 Melbourne AUSTRALIA.
2. Abstract accepted for poster presentation: P.P. Naik, Geetesh K. Mishra, Bengt Danielsson and Sunil Bhand “ Android Integrated urea biosensor for public health awareness” 24th Anniversary World Congress on Biosensors, May 27-30, 2014 Melbourne AUSTRALIA.
3. Abstract accepted for Oral Presentation: Geetesh K Mishra and Sunil Bhand. FIA-EQCN biosensor for analysis of sulphadiazine residues in milk. Presented at 6th IEEE

International Conference on Sensing Technology, Special focus on sensors for agriculture and environmental monitoring ICST 2012, Dec. 18-21, 2012 Kolkata, India.

4. Abstract accepted for poster presentation: Geetesh Mishra, Souvik Pal, Sunil Bhand. Gold Nanoparticle based Optical Biosensor for Monitoring Streptomycin in Milk Samples at 5<sup>th</sup> International Symposium on Recent Advances in Food Analysis (RAFA 2011) 1 – 4, November 2011, Prague, Czech Republic.
5. Abstract accepted for poster presentation: Geetesh K Mishra, Rupesh K Mishra, and Sunil Bhand. Flow injection analysis biosensor for urea analysis in adulterated milk using enzyme thermistor at World Congress on Biosensors, Glasgow, UK, 2010.

### **Brief Biography of the candidate**

Name	Geetesh Kumar Mishra
Date of Birth	26-12-1984
Education	M.Sc. (Microbiology), 2007 Pt. Ravishankar Shukla University, Raipur (C.G.), India B.Sc. (Microbiology, Zoology, Chemistry), 2005 Devi Ahilya University, Indore (M.P.) India
Email ID	geeteshmishra26@gmail.com

#### **Research experience (5 Years and 8 months)**

1. Presently working as Project Fellow in Centre of Research Excellence in Waste Water and Energy Management (CORE WWEM) Project sanctioned by BITS, Pilani Rajasthan at BITS, Pilani-K.K. Birla Goa Campus, Goa. Co-PI: Prof. Sunil Bhand (October 2014 onwards).
2. Worked as Institute Research Scholar in the Department of Chemistry, BITS, Pilani-K. K. Birla Goa Campus, Goa. CPI: Prof. Sunil Bhand (July 2014 to September 2014).
3. Worked as Research Associate (National Agricultural Innovation Project, a consortium based project sponsored by ICAR, India and the World Bank at BITS, Pilani-K. K. Birla Goa Campus, Goa. CPI: Prof. Sunil Bhand (July 2011 to June 2014).
4. Worked as Senior Research Fellow (National Agricultural Innovation Project, a consortium based project sponsored by ICAR, India and the World Bank at BITS, Pilani-K. K. Birla Goa Campus, Goa. CPI: Prof. Sunil Bhand (March 2009 to June 2011).

#### **Research Publications**

07 publications in international journal, 01 publication in national journal.

### **Work Experience**

1. Worked as a Microbiologist in BSR-Apollo Hospitals, Bhilai C.G. (March 2008-February 2009), India.
2. Worked as a trainee technician in Apollo Hospitals, Bilaspur, C.G. (June 2007-November 2007), India.

### **Award and Honors**

2<sup>nd</sup> Prize in poster presentation at Indo- UK International Workshop on Advanced Materials and Their Applications in Nanotechnology (AMAN 2014).

### **Brief Biography of the Supervisor**

Name	Prof. Sunil Bhand
Date of Birth	17.03.1969
Present Position	Professor, Department of Chemistry, BITS, Pilani-KK Birla Goa Campus
Address	C-201 BITS, Pilani-KK Birla Goa Campus NH17B Bypass, Zuari Nagar Goa 403726 India
Email	sunilbhand@goa.bits-pilani.ac.in, sunil17_bhand@yahoo.com
Education	Ph.D., 1996 M.Sc., 1990 (First in University Merit)

#### **Post-Doctoral Experience**

Department of Pure and Applied Biochemistry  
Lund University Sweden 2001-2002,  
Short term visits 2003, 2004, 2005, 2007, 2008

#### **No. of Sponsored Research Projects**

##### **(a) Completed projects**

- i. Joint Indo-Swedish Project on Biosensors for Environmental analysis 2003-2005 funded by Swedish Research Council (Prof. B. Danielsson and Prof. Sunil Bhand as joint PIs) 35 lakhs.
- ii. CSIR Project 2006-2009 on biosensors for analysis of pesticides in sea water 14.6 lakhs.
- iii. Consortium PI for NAIP, ICAR New Delhi funded project on “Development of biosensors and micro techniques for analysis of pesticide residues, aflatoxin, heavy metals and bacterial contamination in milk.729 lakhs, in collaboration with IITD, NDRI and PU Patiala.
- iv. Consortium Co-PI, NAIP project on “Detection and mitigation of dairy pathogens and detection of adulterants using chemical biology” 45 lakhs.

**(b) Ongoing Project**

- i. Multi-institute Consortium Project entitled “Imprinted polymer for sensing and removal of selected antibiotic and pesticide residue” Project no. NFBSFARA/PHT-4007/2013-14. Funding Agency: National Funds for Basic and Strategic Research in Frontier Areas of Agricultural Science, ICAR, New Delhi, 125.25511 Lakh.
- ii. Centre of Research Excellence in Water, Waste water and Energy Management (CORE WWEM) funded by BITS, Pilani. Subproject title: Development of Field Deployable biosensor for analysis of bacterial contaminant in potable water. Rs. 41 lakh

**Honors and awards**

- i. Invited as Opponent to a Ph.D. Thesis for Linkoepping University Sept. 2011.
- ii. Best Poster award “Biosensors for arsenic analysis” 7<sup>th</sup> Intl Conference on Biogeochemistry of trace elements 2003 Uppsala Sweden.
- iii. UV Rao memorial awards for young scientists by Indian Chemical Society 1998.

**Publications**

- i. 06 Patents (03 International including 02 PCT and 01 Australian and 03 Indian) and 38 publications in international journals.
- ii. Membership of societies: Affiliate member IUPAC since 2000 IAEAC Switzerland, AAAS, USA, 2012.

**Reviewer for international journals**

Biosensors and Bioelectronics, Analytical Letters, Int Journal of Env Anal Chemistry, Applied Biochemistry and Biotechnology, J Agri food Chemistry.

**No of Ph.D. Students**

Completed 03, Registered 06,

**No of Conferences organized: 03**

*Appendix iv*  
**Reprint of Publications**



## Flow injection analysis biosensor for urea analysis in adulterated milk using enzyme thermistor

Geetesh K. Mishra, Rupesh K. Mishra, Sunil Bhand\*

Biosensor Lab., Chemistry Group, Birla Institute of Technology & Science, Pilani–KK Birla Goa Campus, NH17B Bypass, Zuari Nagar, Goa 403726, India

### ARTICLE INFO

#### Article history:

Received 14 April 2010

Received in revised form 28 July 2010

Accepted 29 July 2010

Available online 4 August 2010

#### Keywords:

Flow injection analysis

Enzyme thermistor

Adulterated milk

Urea

Immobilized urease

Control pore glass

### ABSTRACT

Urea in adulterated milk is one of the major health concern, it is especially harmful to pregnant women, children, and the sick. A sophisticated and reliable detection system is needed to replace current diagnostic tools for the urea in the milk. In this work, we report a flow injection analysis-enzyme thermistor (FIA-ET) bio-sensing system for monitoring of urea in adulterated milk. This biosensor was made of the covalently immobilized enzyme urease (Jack bean) on controlled pore glass (CPG) and packed into a column inside thermistor, which selectively hydrolysed the urea present in the sample. The specific heat registered from the hydrolysis of urea was found proportional to the concentration of urea present in the milk sample. The biosensor showed a linear range 1–200 mM, with % R.S.D. 0.96 for urea in 100 mM phosphate buffer, pH 7.2. Good recoveries were obtained (97.56–108.7%) for urea up to 200 mM in the spiked milk samples with % R.S.D. 0.95. In the adulterated milk, a simple filtration strategy and matrix matching technique was used to analyse urea. The response time of the sensor was evaluated for urea, which was 2 min, and it gives satisfactory output. A good comparison was observed between the urea concentrations measured through FIA-ET and the colorimetric method. These results indicate that utilizing this system could be very effective to detect low and high level of urea in adulterated milk. The immobilized urease column exhibited a good operational stability up to 180 days when used continuously at room temperature.

© 2010 Elsevier B.V. All rights reserved.

### 1. Introduction

Adulteration of natural milk with synthetic chemicals is a serious concern for human health. Milk is an excellent source of energy, protein, minerals and vitamins (Noyhouzer et al., 2009). In India, Urea [ $\text{CO}(\text{NH}_2)_2$ ] is commonly used as an adulterant for milk. Adulteration of milk with urea decreases the nutritive value of the milk. Urea is also a normal constituent of milk. The typical concentration of urea in milk is 18–40 mg/dL (Jonker et al., 1989). A cut-off limit for urea concentration in milk is normally accepted at 70 mg/dL. It also forms a major part (55%) of the nonprotein nitrogen of milk (Sharma et al., 2008). Urea being relatively cheap and rich in nitrogen is an economical choice to adulterate the milk. The effect of urea above cut-off limit in milk may cause indigestion, acidity, ulcers, cancers, malfunctions of kidney, etc. (Trivedi et al., 2009). Hence urea estimation in milk is of great significance.

Several conventional methods have been reported in recent years for urea analysis in milk, i.e. spectrophotometric and conductometric detection (Reis Lima et al., 2004), differential pH technique (Luzzana and Giardino, 1999). The conventional techniques as well

as current wet chemistry and analytical practices are time consuming and may require highly skilled workers and expensive equipment (Loung et al., 1991). The food and dairy industries need rapid, reliable and affordable techniques for quality control. The application of thermal biosensors in food analysis is a growing field with increasing demand for reliable sensors (Bhand et al., 2010). Numerous biosensors have been reported in recent years for milk urea analysis, such as manometric biosensor (Jenkins and Delwiche, 2002; Renny et al., 2005) and potentiometric biosensor (Verma and Singh, 2003; Trivedi et al., 2009). Some of these reported biosensors have very short detection limit and low operational stability, which renders them unfit for routine analysis. There is a need for economical, reliable, robust and reproducible biosensors specifically for urea analysis in milk. Thus, thermal biosensors are good alternative devices owing to their simplicity of operation and long term stability (Pirvutoiu et al., 2002).

Thermal biosensors are based on the measurement of heat, produced when a biological reaction takes place. The amount of reacted substrate is related to the heat produced through the specific enthalpy,  $\Delta H_r$ , of the reaction. An advantage of this principle as compared to other analytical tools like spectrophotometric and electrochemical methods is the universal detection principle which is combined with the specificity of the biological reactions (Bjarnason et al., 1998). Thermometric detection usually employs a

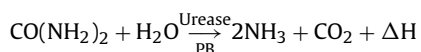
\* Corresponding author. Tel.: +91 832 2580332; fax: +91 832 2557033.

E-mail addresses: [sunil17.bhand@yahoo.com](mailto:sunil17.bhand@yahoo.com), [sgbhand@gmail.com](mailto:sgbhand@gmail.com) (S. Bhand).



different measurement scheme of temperature across the enzyme reactor in order to increase the common mode rejection ratio. As a result, thermal biosensors typically use flow injection-based analysis. In addition, control of the carrier solution and sample is straightforward using this continuous analysis scheme (Danielsson et al., 1976a). The method combines the advantage of the enzyme selectivity and the short analysis time, low reagent consumption, particularly when the enzymes are immobilized and used in a flow injection analysis (FIA) mode (Linhares et al., 1987). A large number of enzymatic reactions have been studied by this device among which urea and glucose detection were studied extensively in serum and different food stuffs (Danielsson et al., 1976b; Bjarnason et al., 1998; Salman et al., 2008). Recently cholesterol study, heavy metal study and fructose determination is also reported by this device (Raghvan et al., 1999; Pirvutoiu et al., 2002; Bhand et al., 2010). The objective of the present work is to demonstrate the application of enzyme thermistor for selective determination of adulterated milk urea using immobilized urease enzyme.

Herein we present a simple, economical and highly stable FIA-ET biosensor for analysis of urea in adulterated milk. We have successfully demonstrated an application for urea detection in milk which is first time by this instrument. The proposed biosensor can facilitate continuous analysis of milk urea in dairy industry. Another important feature of the presented biosensor is the lower detection limit and an excellent dynamic range of detection, 1–200 mM urea with a sample throughput of 30 within an hour. The biosensor comprise of immobilized enzyme Urease (Jack bean, EC 3.5.1.5) on controlled pore glass (CPG) which selectively hydrolyses urea present in the sample. The urea hydrolysis reaction is given below



## 2. Experimental

### 2.1. Biochemical and reagents

Enzyme urease (Jack beans lyophilized 5 U mg<sup>-1</sup>, EC 3.5.1.5), urea, sodium dihydrogen phosphate monohydrate, disodium hydrogen phosphate monohydrate, glutaraldehyde solution 25% and tri-ethanol amine were obtained from Merck, Germany. Amino silanized CPG spherical beads (Trisoperl, size 125–140 μm, pore size 50 nm) were purchased from VitraBio (Germany). All other chemicals used were GR grade. Maxsignal<sup>®</sup> urea enzymatic assay kit was purchased from BIOO SCIENTIFIC, USA.

### 2.2. Solution preparation

Phosphate buffer (PB) 100 mM, pH 7.2 was prepared by mixing 100 mM of sodium dihydrogen phosphate monohydrate and 100 mM of disodium hydrogen phosphate monohydrate in double distilled water. PB was degassed before analysis. A stock solution of urea (400 mM) was prepared by dissolving 2.4024 g in 100 mL of PB (100 mM, pH 7.2). Working solution of urea was prepared daily prior to use.

### 2.3. Enzyme immobilization

Enzyme immobilization was achieved by glutaraldehyde cross-linking on amine functionalized CPG beads (Weetall, 1976). In brief, urease was covalently immobilized on amino propyl CPG beads according to the following procedure: 352 mg of CPG was activated with 2.5% glutaraldehyde in 100 mM PB, pH 7.2. The reaction was allowed to take place for at least 1 h inside desiccators under reduced pressure. The product which changed its colour to brick

red was washed exhaustively with distilled water. Urease 200 mg (1000 U) dissolved in 1 mL PB was added to the wet activated CPG. The coupling was allowed to proceed for 30 min at room temperature and overnight at 4 °C under gentle shaking. The enzyme preparation was washed with buffer. Tri-ethanolamine (35 mg) was added to terminate all the unreacted groups on the matrix and then washed with 100 mM PB, pH 7.2. The immobilized urease was packed into a delrin column by a slurry packing method for the use in FIA mode.

### 2.4. Instrumentation/FIA-ET-system

The schematic set-up for FIA-ET biosensor for urea analysis is presented as Fig. 1. The set up consists of a peristaltic pump (Gilson Minipuls Evolution, France), an injection valve (type 50 from Rheodyne, Cotati, USA), sample loop (0.1 mL), enzyme thermistor, Wheatstone bridge equipped with a chopper-stabilized amplifier and data recorder. PTFE tubing (0.8 mm id) was used for connections. The carrier buffer was 100 mM PB, pH 7.2.

### 2.5. Procedure

For urea analysis, calibration standards were prepared by dilution of urea stock solution in 100 mM PB, pH 7.2. The immobilized urease column was mounted inside ET and was allowed to equilibrate with surrounding. Degassed carrier buffer was passed through the column initially at a higher flow rate (0.9 mL min<sup>-1</sup>). Subsequently, the flow rate was brought down to the optimum value of 0.5 mL min<sup>-1</sup> at which a stable baseline was achieved. Standards/spiked samples were injected and data were collected using a data acquisition system connected to the Wheatstone bridge. All measurements were carried out by injection of 0.1 mL sample at a flow rate of 0.5 mL min<sup>-1</sup>. After each sample analysis, the sample loop was thoroughly rinsed with PB. The milk samples were spiked with known amount of urea after appropriate filtration and dilution and injected in to the system.

## 3. Results and discussion

### 3.1. Optimization of the FIA biosensor system

#### 3.1.1. Ionic strength and pH of buffer

The influence of the ionic strength and pH on the activity of the enzyme urease was studied. Measurements were carried out in the flow system with varying ionic strength (10, 50, 100, 150 and 200 mM PB) and pH (6.8–7.8) for PB for 100 mM urea. The results are presented in Fig. 2a and b respectively. It is evident from Fig. 2a that with increase in the ionic strength of PB, response signal increases up to 100 mM, and then the signal starts decreasing. Thus further experiments were carried out with 100 mM PB. Fig. 2b, clearly suggests that urease exhibit maximum activity at pH 7.2 flow rate

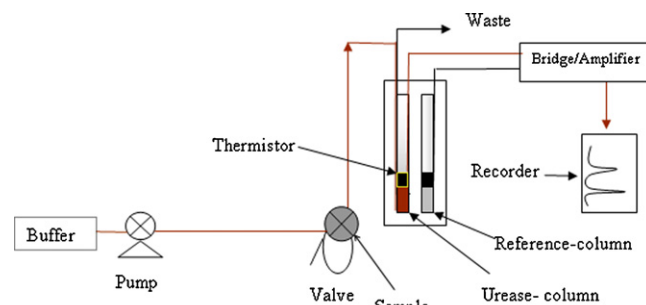
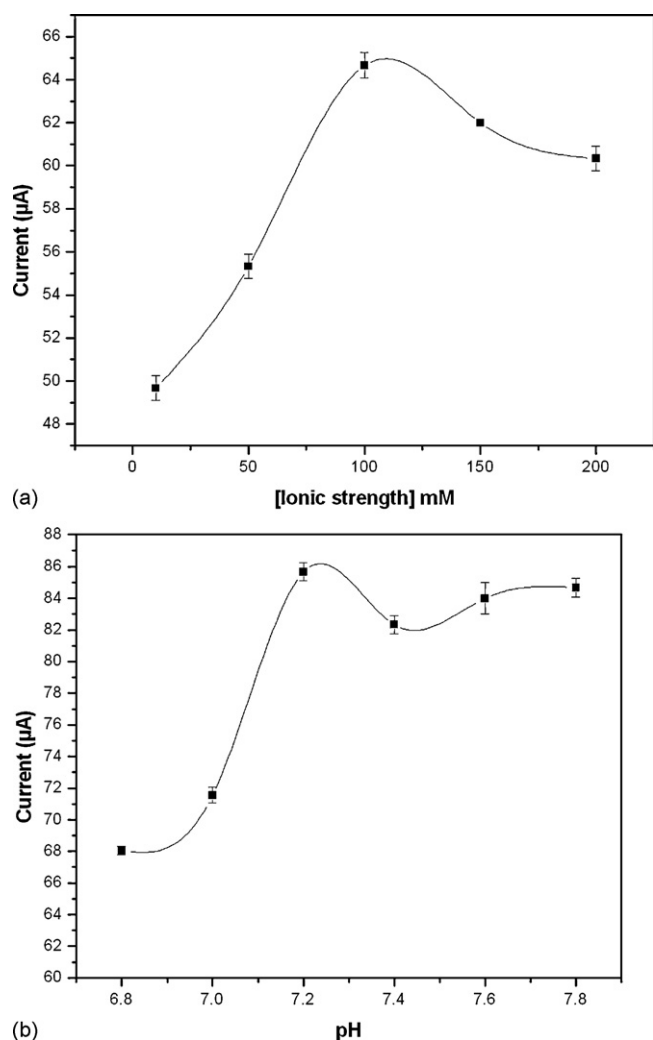


Fig. 1. Schematic set-up for flow injection analysis-enzyme thermistor (FIA-ET) biosensor for urea analysis.



**Fig. 2.** Effect of ionic strength of the PB on the response of FIA-ET biosensor for 0.1 mL injection of 100 mM urea, flow rate 0.5 mL min<sup>-1</sup>. Effect of pH of the phosphate buffer on the response of FIA-ET biosensor for 0.1 mL injection of 100 mM urea, flow rate 0.5 mL min<sup>-1</sup>.

0.5 mL min<sup>-1</sup> was found optimum to have sufficient contact time between the enzyme and the substrate.

### 3.1.2. Matrix matching

Commercial milk samples of different fat content (0.5%, 1.5%, and 3.5%) were purchased from local market of Goa, India. The matrix effect in the analysis of urea in milk samples was investigated. In FIA system, fat present in milk may lead to matrix related quenching and block the flow in FIA, which can decrease the device sensitivity or completely clog the column. Various sample pre-treatment techniques such as combination of centrifugation, filtration and dilution were tested to select the optimum pre-treatment procedure for milk urea analysis. Milk samples were centrifuged at 10,000 rpm for 10 min at room temperature. The centrifuged milk samples were diluted with PB to obtain different ratios of milk:PB and further spiked with known amount of urea.

It was observed that 1:4 dilution of milk and PB was most responsive for urea analysis. To obtain the calibration curve for urea in spiked milk samples, a simple strategy was worked out to remove the fat and also to obtain a suitable dilution to avoid clogging of the urease column. In brief, milk samples were centrifuged, diluted and filtered through 0.45 and 0.22 µm filter (Whatman, USA). Milk analysis was carried out within the same day after sample preparation.

### 3.1.3. Calibration of urea biosensor in PB

The immobilized urease column was kept inside the thermostat and allowed to equilibrate overnight. The buffer solution was filtered, degassed and pumped via FIA manifold, until a constant baseline is achieved. Urea standard solutions 0.1, 1, 10, 50, 100, 150, 200, 250 mM (1 mM urea solution corresponds to 60.6 ppm) were prepared in carrier buffer and injected in to the flow stream. Response signals were recorded using a data acquisition system connected to Wheatstone bridge and plotted as current (µA) vs. urea (mM). All samples were injected in triplicates. The Michaelis constant,  $K_M$  for urea was calculated using Lineweaver–Burk plot. The  $K_M$  was found to be 100 mM. A good linear response was obtained for urea hydrolysis in the range of 1–200 mM with minimum detection limit of 0.1 mM (6.06 ppm), which is presented in Fig. 3. Linear fit of data shows a good correlation between urea and immobilized urease ( $R^2 = 0.99$ , % R.S.D. = 0.96).

### 3.1.4. Calibration of urea biosensor in milk

Spiked milk urea standard solutions (0.1–250 mM) of different fat content (0.5%, 1.5% and 3.5%) were injected in to the flow stream, and response signals were recorded. All samples were injected in triplicates. The FIA-ET biosensor showed an excellent dynamic range for milk urea in the range 0.1–250 mM with a good linearity (1–200 mM). The results are presented in Fig. 3. ( $R^2 = 0.99$ , % R.S.D. = 0.95). An actual sensor signal recorded for triplicate measurement of 50 and 100 mM spiked milk urea samples is presented in Fig. 3.

### 3.1.5. Urea recovery from milk samples

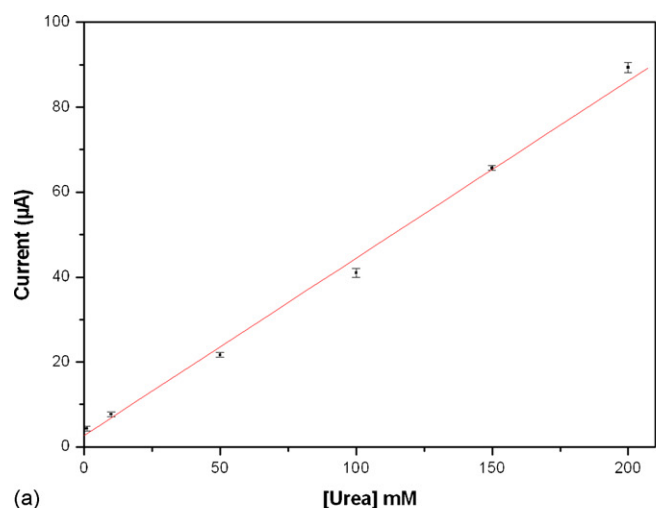
A known amount of urea standard solution was added to centrifuged, diluted and filtered milk and analysed in FIA-ET. Based on the response signal, recoveries were calculated. Table 1 shows the recovery results obtained for milk urea. Excellent recoveries in the range of 97.56–108.70% were obtained for urea in milk. This ensures the reproducibility of the presented biosensor.

### 3.1.6. Sensitivity, detection limit and dynamic range

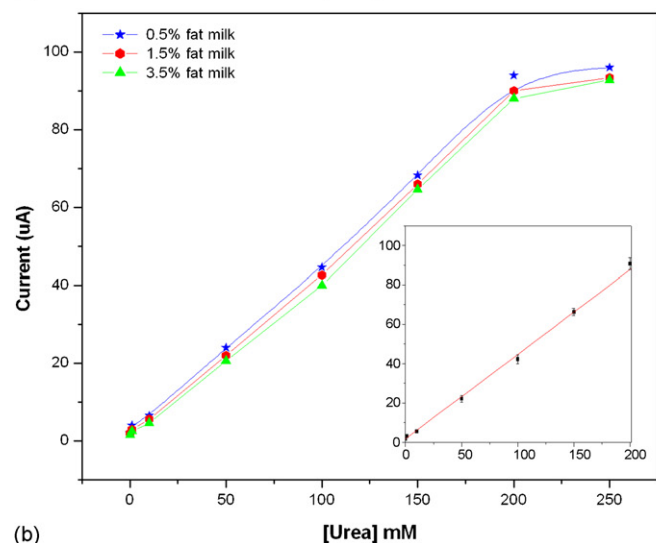
A broad linear range, 0.1–200 mM was obtained with the lower limit of detection 0.1 mM (6.06 ppm). The upper limit of detection as high as 200 mM was achieved with sensitivity of 4.17% mM<sup>-1</sup> for buffer urea. For milk urea, a broad linear range, 0.1–200 mM was obtained with the upper limit of detection 250 mM and sensitivity of the signal 4.58% mM<sup>-1</sup>. The reported heat of reaction for urea hydrolysis by urease is -61 kJ mol<sup>-1</sup>. In our case the calculated heat of reaction in diluted milk urea samples was found to be -46.81 kJ mol<sup>-1</sup>. The broad dynamic range obtained for milk urea makes the biosensor highly suitable for analysis of adulterated milk samples.

**Table 1**  
Determination of urea recovery from commercial milk samples spiked with known amount of urea using FIA-ET biosensor.

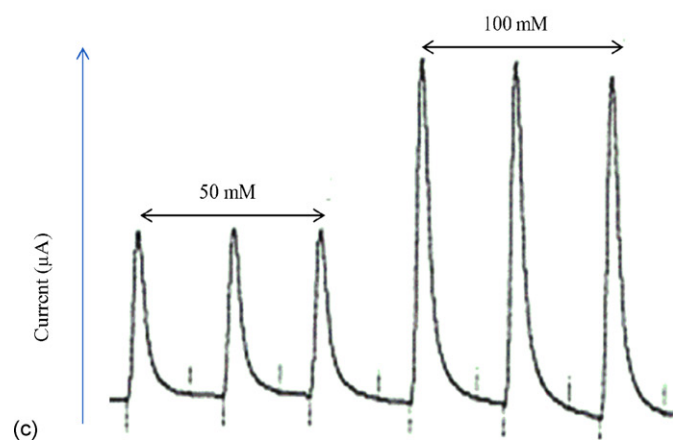
Sample	Added amount of urea (mM)	Recovered amount of urea (mM)	Recovery, %	Found ± S.D.	R.S.D. %
Milk 1	41	44.6	108.7	44.6 ± 0.4	0.89
Milk 2	41	42.6	103.9	42.6 ± 0.4	0.93
Milk 3	41	40	97.56	40.0 ± 0.5	1.25



(a)



(b)



(c)

**Fig. 3.** Calibration plot obtained for urea using urease column in 100 mM PB, pH 7.2 for 0.1 mL of sample injection, flow rate  $0.5 \text{ mL min}^{-1}$  at  $30^\circ\text{C}$ ,  $R^2 = 0.99$ , % R.S.D. = 0.96. Calibration plot obtained for urea using urease column in milk with 0.5%, 1.5% and 3.5% fat. (Inset: linear range obtained for 0.5% fat milk urea.  $R^2 = 0.99$ , % R.S.D. = 0.95). Response signal recorded for two different milk urea concentrations (50 mM and 100 mM) using FIA-ET biosensor. Urea dissolved in filtered milk samples, sample volume 0.1 mL, flow rate  $0.5 \text{ mL min}^{-1}$  acquired using data acquisition system with recorder.

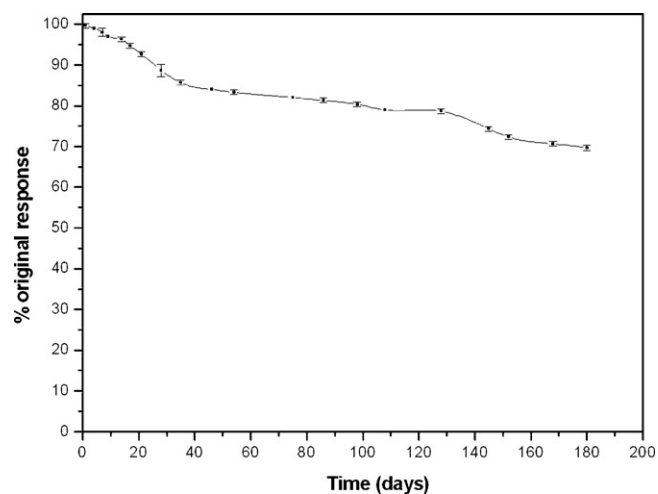


**Fig. 4.** Stability of urease column response to 0.1 mL, 100 mM urea using FIA-ET biosensor observed for continuous 180 days at  $30^\circ\text{C}$ . Samples were injected randomly during the period.

### 3.1.7. Response time and sample throughput

The response of the FIA-ET biosensor was highly reproducible with a variation coefficient less than 2.5% at  $30^\circ\text{C}$  and it was estimated from 20 repeated injection of 100 mM urea of 0.1 mL. Response time for urea hydrolysis by urease took about 2 min. Thus, up to 30 samples can be measured within an hour. Increased throughput can be achieved by reducing the sample injection volume down to 0.25 mL.

### 3.1.8. Operational stability

An excellent dynamic range is achieved while the sensor is continuous in use at room temperature. The operational stability of the system was continuously monitored over the period of 180 days. About 15 measurements were made every day for 0.1 mL, 100 mM urea. The operational stability is over the studied period is presented in Fig. 4. The immobilized urease inside the thermistor presented excellent stability, over the first 30 days the enzyme activity was found 90% of the original response and there was no appreciable loss of activity. However after a period of 45 days operation, about 16% decay in response was observed. Similarly the response was monitored after 75, 150 and for 180 days and signals recorded were respectively 82%, 73% and 70% of the original response.

### 3.1.9. Comparison of FIA-ET and commercially available colorimetric assay

The analytical features and figures of merit of the presented milk urea biosensor were compared with Maxsignal® Urea Enzymatic Assay Kit (BIO Scientific, USA). The kit measures the concentration of urea using the urease enzyme, which converts urea to ammonia. An alkaline hypochlorite solution is then added to the reaction mixture. The colour produced from the reaction is measured using a colorimetric multiplate reader at 620 nm. The limit of detection of urea in milk using the commercial kit is 40 ppm. The kit is designed to be used with a microplate reader. The kit is provided with reagents and a 96 well plate to perform the assay (catalogue no. #:1051 Ref.1051-01 BIO Scientific, USA). Spiked milk urea samples corresponding to 8, 25, 50, 100 and 200 ppm were analysed simultaneously using the FIA-ET and the colorimetric assay. The results obtained are presented in Fig. 5. For colorimetric measurements (Multilabel Plate Reader Victor X4, PerkinElmer, USA was deployed with 620 nm filter). The parameters such as detection range, analysis time, sensitivity, sample throughput and cost per sample were compared. The dynamic range and the upper limit of

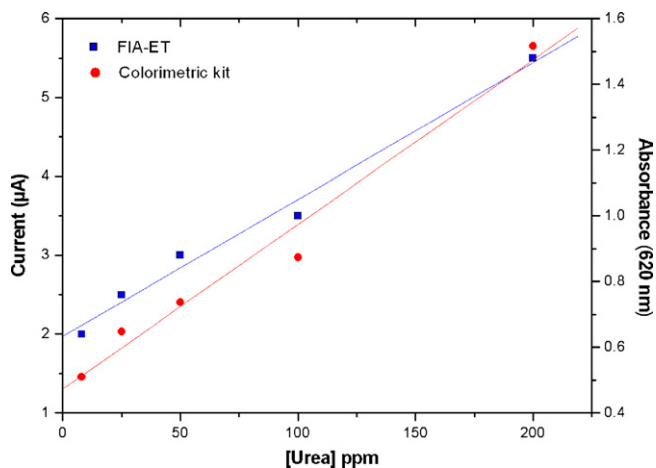


**Fig. 5.** Comparison of the results for milk urea concentration obtained with the FIA-ET biosensor and commercially available colorimetric plate assay (for FIA-ET  $R^2 = 0.99$  and for colorimetric kit  $R^2 = 0.98$ ).

detection for the milk urea using the kit were found much lower as against presented biosensor, which offers a manifold higher linear range 0.1–200 mM. The analysis time for the thermal biosensor is 2 min per sample with throughput of 30 h, whereas with commercial kit, up to 72 samples can be analysed within an hour. For FIA-ET biosensor, a higher sensitivity is observed. As many as 500 samples were analysed with the single urease column over the period of 180 days. The result suggests that the presented system is robust and suitable for urea determination in adulterated milk samples and can be easily adapted for routine analysis.

#### 4. Conclusions

A flow injection analysis-enzyme thermistor biosensor for detection of urea in adulterated milk is developed and demonstrated. The method was optimized and had been successfully applied to determine urea in adulterated milk samples. The biosensor is stable at room temperature for more than 180 days and

still in working condition with 30% loss of original response. Broad dynamic range (0.1–250 mM) of the sensor facilitates the urea analysis in milk. Reported method is highly reproducible, cost effective, reliable and robust. It fulfils the need of dairy processing plant for monitoring of milk urea.

#### Acknowledgements

This work is funded by National Agriculture Innovation Project (NAIP), ICAR and The World Bank Grant No. NAIP/C4/C30032. We offer our sincere thanks to Prof. Bengt Danielsson, Lund University, Sweden for providing enzyme thermistor at BITS, Pilani-KK Birla Goa Campus.

#### References

- Bhand, S.G., Soundararajan, S., Wärnmark, I.S., Milea, J.S., Dey, E.S., Yakovleva, M., Danielsson, B., 2010. *Anal. Chim. Acta* 668, 13–18.
- Bjarnason, B., Johansson, P., Johansson, G., 1998. *Anal. Chim. Acta* 372, 341–348.
- Danielsson, B., Mattiasson, B., Mosbach, K., 1976a. *Pure Appl. Chem.* 51, 1443–1457.
- Danielsson, B., Gadd, K., Mattiasson, B., Mosbach, K., 1976b. *Anal. Lett.* 9, 987–1001.
- Jenkins, D.M., Delwiche, M.J., 2002. *Biosens. Bioelectron.* 17, 557–563.
- Jonker, J.S., Kohn, R.A., Eradman, R.A., 1989. *J. Dairy Sci.* 81, 2681–2692.
- Linhares, P., Luque de Castro, M.D., Valcarcel, M., 1987. *Anal. Chim. Acta* 202, 199–205.
- Luzzana, M., Giardino, R., 1999. *Lait* 79, 261–267.
- Loung, J.H.T., Groom, C.A., Male, K.B., 1991. *Biosens. Bioelectron.* 6, 547–554.
- Maxsignal Urea Enzymatic Assay Kit Manual. Catalog #:1051, BIO Scientific, USA, 2010.
- Noyhouzer, T., Kohen, R., Mandler, D., 2009. *Anal. Methods* 1, 93–99.
- Pirvutoiu, S., Dey, E., Bhand, S., Ciucu, A., Magearu, B., Danielsson, B., 2002. *Roum. Biotechnol. Lett.* 7, 975–986.
- Raghvan, V., Ramanathan, K., Sundaram, P.V., Danielsson, B., 1999. *Clin. Chim. Acta* 289, 145–158.
- Reis Lima, M.J., Fernandes Silvia, M.V., Rangel Antonio, O.S.S., 2004. *J. Agric. Food Chem.* 52, 6887–6890.
- Renny, E.F., Daniel, D.K., Krastanov, A.I., Zachariah, C.A., Elizabeth, R., 2005. *Biotechnol. Biotechnol. Equip.* 19 (2), 198–201.
- Salman, S., Soundararajan, S., Safina, G., Satoh, I., Danielsson, B., 2008. *Talanta* 77, 490–493.
- Sharma, R., Rajput, Y.S., Kaur, S., Tomar, S.K., 2008. *J. Dairy Res.* 75, 466–470.
- Trivedi, U.B., Lakshminarayana, D., Kothari, I.L., Patel, N.G., Kapse, H.N., Makhija, K.K., Patel, P.B., Panchal, C.J., 2009. *Sens. Actuators B* 140, 260–266.
- Verma, N., Singh, M., 2003. *Biosens. Bioelectron.* 18, 1219–1224.
- Weetall, H.H., 1976. *Methods Enzymol.* 44, 134–148.

# *FIA-EQCN biosensor for analysis of sulphadiazine residues in milk*

Geetesh K. Mishra and Sunil Bhand\*

Biosensor Lab., Department of Chemistry,  
BITS, Pilani- K. K. Birla Goa Campus, Goa, 403726, India  
Emails: [geeteshmishra26@gmail.com](mailto:geeteshmishra26@gmail.com), [sgbhand@gmail.com](mailto:sgbhand@gmail.com)

\*Author for correspondence

**Abstract**— The widespread use of antibiotics within the farming industry is one of the factors that have been linked to the appearance of these residues in milk. A flow injection analysis-electrochemical quartz crystal nano-balance (FIA-EQCN) biosensor is presented for label free analysis of sulphadiazine residues in milk. The biosensor constituted a polyclonal antibody of sulphadiazine covalently immobilized to a gold coated quartz crystal mounted on a flow cell attached with FIA-EQCN setup. The biosensor showed linearity in the range 50 to 200  $\mu\text{g kg}^{-1}$ , with minimum detection limit of 10  $\mu\text{g kg}^{-1}$ ,  $R^2$  0.97 and % R.S.D. 0.83. Good recoveries were obtained (98.6–100.5%) for sulphadiazine in the spiked milk samples. A good correlation was observed between the sulphadiazine concentrations measured through FIA-EQCN and the commercial ELISA kit. These results indicate that utilizing this system could be very effective to detect low level of sulphadiazine residues in milk.

**Keywords**- Antibiotic residues; Flow injection analysis; Quartz crystal nanobalance; Milk; Sulphadiazine.

## I. INTRODUCTION

Antibiotics are one of the most important bioactive and chemotherapeutic group of compounds. In veterinary medicine antimicrobial drugs are routinely used to treat mastitis in dairy cows, but the efficiency of antibiotics as growth enhancers also has led to their use as supplements in animal feed. Sulphonamides are a family of chemotherapeutics that are widely used for therapeutic and prophylactic purposes in animal diseases. In the treatment of mastitis, sulphonamides are usually administered in the case of infections caused by gram-negative pathogens, e.g. *E. coli*. Toxicological data show that sulphonamides have antithyroid effects in both animals and humans [1]. Sulphadiazine (SDZ) is a member of the sulphonamide or sulpha drug family which play an important role in veterinary medicine by controlling many bacterial and protozoan diseases [2]. The occurrence of these antibiotic residues in food carries the risk of increasing the number of resistant bacteria and transferring antibiotic resistance genes to human pathogens. Apart from the consequences for public health, economic reasons have also led to a control of antimicrobial residues in food [3] Indiscriminate use of antibiotics may produce residues in milk, and subsequently induce allergic reactions in humans. In addition, antibiotics give rise to an increase in the antibiotic resistance of pathogenic bacteria, which may result in health hazards [4].

Early detection of contaminants in food requires sensitive and reliable analytical methods that should ideally be accessible to non-skilled users. Maximum residual level (MRL) for

sulfonamides has been established by the authorities to protect the consumer's health, e.g. against bacterial resistance. The European Commission (EC) has thus set up MRL for sulfonamides to 100  $\mu\text{g kg}^{-1}$  [5-6]. The widespread use of antibiotics outside human medicine is the cause of the alarming emergence in humans of bacteria that have acquired resistance to antimicrobials. This situation is causing a serious threat to the public health, as more and more infections can no longer be treated with the presently known antidotes [7]. Various analytical methods have been reported for the analysis of sulfonamides, such as high-performance liquid chromatography (HPLC) [8-9], gas chromatography-mass spectrometry (GC-MS) [10] and enzyme-linked immunosorbent assay (ELISA) [11]. HPLC and GC-MS are sensitive and specific but are very laborious and expensive. They are suitable for confirming but not for screening a large number of samples [12]. Apart from conventional techniques, biosensors based on Surface Plasmon Resonance (SPR) have also been reported addressing clinical, environmental, and food safety for antibiotic residue analysis [13-14].

As a sensitive surface mass sensor, Quartz Crystal Microbalance (QCM) has emerged as promising technique. The principle of QCM detection is based on the frequency changes of the crystal that is proportional to the mass changes on the crystal surface.

Because of its simplicity, convenience, and real time response, QCM has been increasingly used in many fields of biological studies [15]. One of its most popular applications is for immunoassay. The QCM immunosensor, which is generally based on specific recognition between immobilized and target molecules, exhibits extremely high detection sensitivity for biological macromolecules including proteins, microbes and whole living cells [16]. To implement a QCM immunosensor, antibody or antigen needs to be immobilized on the crystal surface to capture target molecules. Thus, the development of small ligands with high binding affinity and low cost is of great interest.

QCM biosensor integrated in a flow injection analysis (FIA) system has the advantage to work continuously and to monitor on-line label free binding of the analyte. Complicated and time-consuming drying procedures used in conventional ELISA are eliminated and a highly automated test performance can be achieved [17]. In addition, the binding results in a change of resonance frequency of the crystal and thus immunological marker, such as enzyme or fluorescence labeled tracers are not necessary. Such an FIA-EQCN system is suitable for rapid label free analysis of bio-specific

interactions. In this paper, an FIA-EQCN system was set up and used for analysis of SDZ residues in milk samples with immobilized polyclonal anti SDZ antibody (pAb-SDZ).

## II. EXPERIMENTAL

### A. Reagents and Solutions

Sodium dihydrogen phosphate monohydrate, disodium hydrogen phosphate monohydrate, glutaraldehyde solution 25%, sodium chloride, glycine and cystamine chloride were obtained from Merck (Germany). Anti-sulphadiazine polyclonal antibody Ig fraction isolated from sheep, sulphadiazine and sulphadiazine ELISA kit were purchased from Randox (UK). For sample handling, micropipettes (Eppendorf®, Germany) were used. Centrifugation of milk sample was done by minispin (Eppendorf®, Germany). Shaking and filtration of the samples were done by Spinix shaker (Tarsons, India). For preparing all the solutions, water produced in a Milli-Q system (Millipore, Bedford, MA, USA) was used. pH meter (Seven Multi Mettler Toledo, 8603, Switzerland) were used. All other chemicals used were of analytical grade and used as received.

### B. Apparatus

The experimental set-up used are presented as Figure 1A and 1B. FIA-EQCN system from Elchema (USA) was deployed as biosensor. The gold quartz crystal (10 MHz) was connected to the frequency-measuring unit, which contains a reference crystal with the same characteristics as the measuring crystal. The gold quartz crystal was placed in a plexiglass flow-cell, sandwiched between two O-rings, with its upper electrode in contact with the liquid and its lower electrode in air. The volume of the flow cell was 50  $\mu\text{l}$  ( $\text{O} = 8\text{mm}$  and height = 1 mm). A peristaltic pump (Gilson, France) was connected through a 6-port injection valve to the flow-cell. The pump was connected in such a way that it reduced the pressure exerted on the crystal. Samples were filled in a 100  $\mu\text{l}$  loop of the 6-port injection valve and injected into the carrier buffer. The output from the oscillator was measured by the frequency unit, which calculated the mass by using a conversion factor (1Hz equivalent to 1ng). A personal computer controlled the data acquisition. The flow cell was placed in a Faraday cage to shield the crystal from external electromagnetic sources.

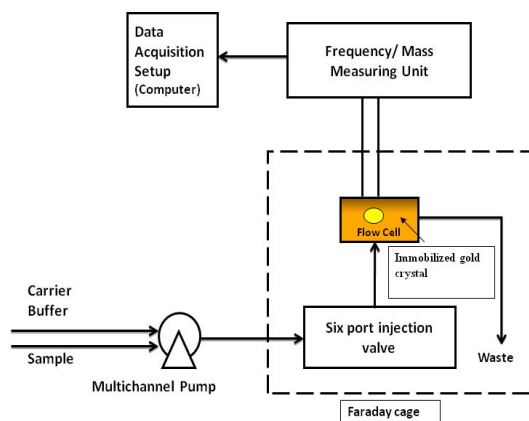


Figure 1. (A) Schematic of FIA-EQCN biosensor set-up.

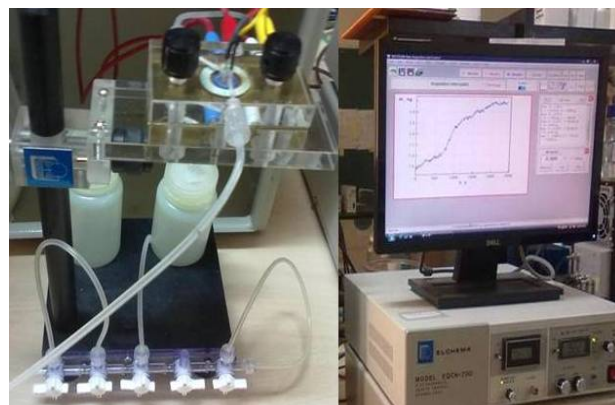


Figure 1. (B) Picture of flow cell used in FIA-EQCN biosensor with mass change read-out

### C. Solution preparation

Phosphate buffered saline (PBS) was prepared by dissolving appropriate amount of  $\text{Na}_2\text{HPO}_4$ ,  $\text{NaH}_2\text{PO}_4$  and  $\text{NaCl}$ . The pH of the buffer was adjusted to 7.4. For sulphadiazine standard solutions, appropriate amount were dissolved in PBS and further diluted to meet the calibration standards. For milk sample analysis, stock solution of 250  $\mu\text{g kg}^{-1}$  was prepared and further dilutions of the same milk gave the range of SDZ concentration as 200- 10  $\mu\text{g kg}^{-1}$ . All the solutions were stored at 4  $^\circ\text{C}$  when not in use.

### D. Immobilization protocol

The methodology employed for pAb immobilization was based on multilayer assembling on the gold surface of the piezoelectric transducer gold quartz crystal. The cleaned gold quartz crystal was incubated for 12 h in an aqueous solution with 15 mM cystamine. The crystal was then washed with double distilled water and was incubated in glutaraldehyde solution (2.5% v/v for 30 min.). Subsequently, the crystal was washed with PBS to remove residual glutaraldehyde molecules. The crystal was finally exposed to the pAb solution (1:500 dilutions, 10  $\mu\text{g/ml}$ ) for 1 h and then rinsed with PBS. To block remnant aldehyde groups the modified crystal surface was exposed to glycine solution (4% w/v for 30 min) and washed with PBS. Schematic presented as Figure 2.

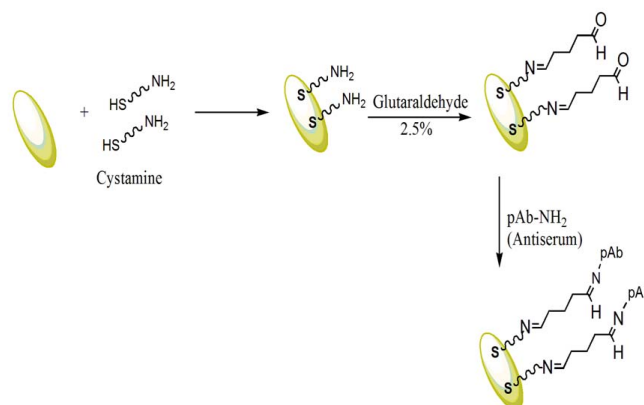


Figure 2. Schematic of immobilization procedure for coupling of SDZ-pAb to gold quartz crystal for FIA-EQCN biosensor.

### E. Experimental Procedure

The pAb-immobilized gold quartz crystal was mounted in the flow-cell via two-silicon rubber O-rings and rinsed with 100 mM L<sup>-1</sup> PBS (pH 7.4) continuously at a flow rate of 50  $\mu\text{L min}^{-1}$ . After a stable baseline was achieved, 100  $\mu\text{L}$  of standard sulphadiazine solutions were injected into the fluid system via the 6-port injection valve. The real time kinetic curves of mass change versus time were recorded

## III. RESULT AND DISCUSSION

### A. Optimization of the FIA-EQCN system

The influence of the ionic strength and pH of the working buffer on the mass binding activity of the pAb was studied. Measurements were carried out in the FIA-EQCN system with varying ionic strength (10, 50, 100, 150 and 200 mM) and pH (6.8–7.8) of PBS for 100  $\mu\text{g kg}^{-1}$  SDZ. Based on optimized experimental data further experiments were carried out with 100 mM PBS and pH 7.4 which exhibit maximum mass binding activity. Flow rate of 50  $\mu\text{L min}^{-1}$  was found optimum to have sufficient contact time between the immobilized pAb on gold quartz crystal and the analyte. Commercial milk of 3.5% fat content, was purchased from local market of Goa, India. The matrix effect of milk in SDZ analysis was investigated. In FIA system, fat present in milk may lead to matrix related quenching and block the flow in FIA, which can decrease the device sensitivity or completely clog the flow. Thus, various sample pre-treatment techniques such as combination of centrifugation, filtration, and dilution were tested to select the optimum pretreatment procedure for milk analysis. Milk samples were centrifuged at 10,000 rpm for 10 min at room temperature. The centrifuged milk samples were diluted with PBS to obtain different ratios of milk: PB and further spiked with known amount of SDZ. It was observed that 1:4 dilution of milk and PBS was most responsive for analysis. To obtain the calibration curve for SDZ in spiked milk samples, a simple strategy was worked out to remove the fat and also to obtain a suitable dilution to avoid clogging of the flow in FIA- EQCN system.

### B. Surface characterisation of immobilized gold crystal

The surface of the gold quartz crystal before and after coupling to SDZ-pAb were characterized by scanning electron microscopy (SEM) by Zeiss EVO-50 (Germany). Figure 3 shows the SEM micrograph of the bare gold quartz crystal and PAb immobilized gold quartz crystal at magnification 25 $\times$ .

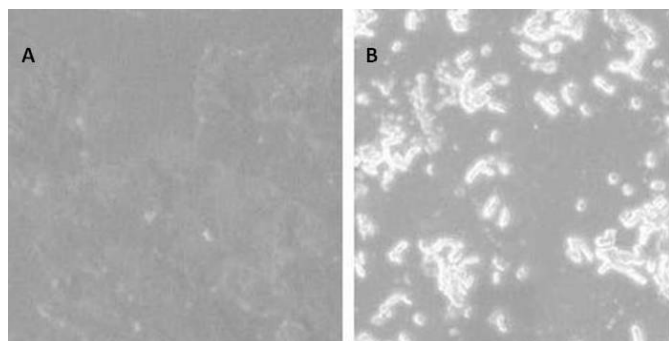


Figure 3. SEM image of gold crystal surface; (A) before pAb coupling and (B) after pAb coupling.

### C. Dose response curve of SDZ

The pAb immobilized gold quartz crystal was kept in a Plexiglas flow-cell, sandwiched between two O-rings and degassed PBS solution was pumped via FIA manifold, until a constant baseline is achieved. SDZ standard solutions from 10  $\mu\text{g kg}^{-1}$  to 200  $\mu\text{g kg}^{-1}$  were prepared in carrier buffer and injected in to the FIA-EQCN system. Response signals were recorded using a data acquisition system connected to resonator and plotted as mass change vs. Concentration of SDZ. All samples were injected in triplicates. A good linear response was obtained for SDZ binding in the range of 50–200  $\mu\text{g kg}^{-1}$  with minimum detection limit of 10  $\mu\text{g kg}^{-1}$ , which is presented in Figure 4. Linear fit of data shows a good correlation between immobilized pAb and SDZ ( $R^2 = 0.97$ , % R.S.D. = 0.83).

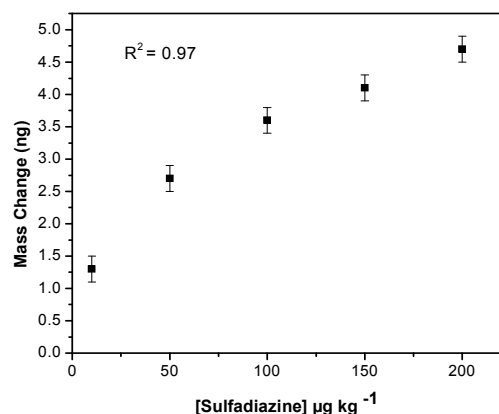


Figure 4. Calibration graph for different sulphadiazine concentrations obtained from FIA-EQCN Biosensor

### D. Recovery studies from milk samples

The potential application of the developed FIA-EQCN system for detection of SDZ in milk was tested. All milk samples were assumed as initially SDZ free. A known amount of SDZ standard solution was added to centrifuged, diluted and filtered milk and analyzed in FIA-EQCN system. Based on the response signal, recoveries were calculated. Table 1 shows the recovery results obtained for milk samples. Excellent recoveries in the range of 98.6–100.5% were obtained. This ensures the reproducibility of the presented biosensor.

TABLE I. RECOVERY STUDIES OF SULPHADIAZINE FROM SPIKED MILK SAMPLES

Added SDZ mean ( $\mu\text{g gm kg}^{-1}$ )(n= 3)	Found SDZ mean ( $\mu\text{g gm kg}^{-1}$ )(n=3)	Mean recovery % (n=3)	Found SD $\pm$ mean	% RSD mean
50	49.6	99.2	0.26 $\pm$ 46	0.96
100	98.6	98.6	0.40 $\pm$ 41	1.10
200	201	100.5	0.10 $\pm$ 01	0.21

### E. Cross reactivity

Cross-reactivity studies were performed in PBS using standard solutions of different sulfonamides. Most common sulfonamides like Sulphadiazine, Acetylsulfadiazine, Sulfathiazole, Sulfamethazine, Sulfaquinoxaline, and Sulfamethoxazole are tested for cross reactivity with sulphadiazine specific PAb. As shown in table 2, Very high cross-reactivity was obtained for sulphadiazine and acetyl sulphadiazine, which contains more related structure with sulphadiazine, are recognized by the antiserum with a cross-reactivity of 100% and 92%, respectively. Sulfathiazole and Sulfamethazine shows cross reactivity of 1.2% and 0.2% respectively. Sulfaquinoxaline and Sulfamethoxazole shows less than 0.1% cross reactivity.

TABLE II CROSS REACTIVITY OF SULFADIAZINE BIOSENSOR WITH OTHER SULPHONAMIDES

Sulphonamides	% Cross Reactivity
Sulfadiazine	100
Acetylsulfadiazine	92
Sulfathiazole	1.2
Sulfamethazine	0.2
Sulfaquinoxaline	<0.1
Sulfamethoxazole	<0.1

### F. Cross comparison and validation

The results obtained from the FIA-EQCN measurements were cross validated against commercial ELISA kit. Validation experiments against ELISA method confirmed the reliability of the FIA-EQCN biosensor test. In EQCN measurements, mass changes increases with increase in the concentration of SDZ whereas in the ELISA measurements, optical density of the reactant decreases with increase in the concentration. It is clear from the Figure 5 that one technique is supplementary to another technique as the results are inversely proportional. The obtained results from both the methods show good co-relation in terms of sensitivity and reproducibility. The % RSD obtained shows the difference of  $\pm 0.5\%$  by both methods. In addition, the methods show linearity in the same range as from 50 to 150  $\mu\text{g kg}^{-1}$ .

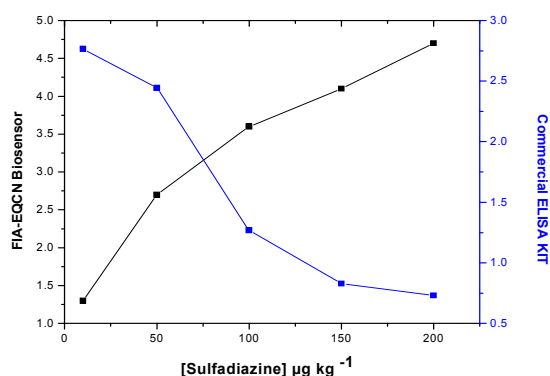


Figure 5. Comparison of the results for Sulphadiazine concentration obtained with the FIA-EQCN biosensor and commercially available ELISA kit

## IV. CONCLUSION

FIA-EQCN based biosensor approaches show promise, being capable of detection of antibiotics at levels below the MRL. A FIA-EQCN biosensor for analysis of SDZ residues in milk is developed and demonstrated. The method was optimized and had been successfully applied. The large detection range (10  $\mu\text{g kg}^{-1}$  to 200  $\mu\text{g kg}^{-1}$ ) of developed biosensor facilitates to analyze SDZ above MRL value. It has been possible to regenerate the sensor for multiple usages. The validation of the presented sensor supports that label-free approaches may become practical for routine analysis.

## ACKNOWLEDGEMENTS

This work is financially supported under NAIP Project No. C4/C30032 funded by ICAR (India) and the World Bank. G.K.M. thanks NAIP for Research Associate fellowshi. We offer our sincere thanks to Prof. Sudhir Chandra, IIT Delhi, India for facilitating SEM analysis.

## REFERENCES

- [1] M. N. Velasco-Garcia and T. Mottram, Biosensor technology addressing agricultural problems, *Biosystems Engineering*, 2003, 84 (1), 1–12.
- [2] Nailya R. Murtazina, Sergei A. Eremin, Olga V. Mozoleva, Sally J Everest, A Jim Brown, Roy Jackman, Fluorescent polarization immunoassay for sulphadiazine using a high specificity antibody, *International Journal of Food Science and Technology*, 2004, 39, 879–889.
- [3] F. Conzuelo, M. Gamella, S. Campuzano, D. G. Pinacho, A. J. Reviejo, M. P. Marco, J. M. Pingarron, Disposable and integrated amperometric immunosensor for direct determination of sulfonamide antibiotics in milk, *Biosensors and Bioelectronics*, 36, 2012, 81–88.
- [4] J. Raich-Montiu, J. Folch, R. Compañó, M. Granados, M.D. Prat, Analysis of trace levels of sulfonamides in surface water and soil samples by liquid chromatography-fluorescence, *J Chromatography A*, 2007, 1172(2), 186-93.
- [5] Commission Regulation (EEC) No. 675/92, 1992, Official Journal of the European Community L73/8 of 19 march 1992.
- [6] Commission Regulation (EU) No. 37/2010, 2009, Official Journal of the European Union L 15/1 of 22 December 2009.
- [7] H. Font, J. Adrian, R. Galve, M. Estevez, M. Castellari, M. Gratacos-Cubarsi, F. Sanchez-Baeza, M.P. Marco, Immunochemical assays for direct sulfonamide antibiotic detection in milk and hair samples using antibody derivatized magnetic nanoparticles, *J Agric. food chem.* 2008, 56: 736-743.
- [8] G. Stoev, A. Michailova, Quantitative determination of sulfonamide residues in foods of animal origin by high-performance liquid chromatography with fluorescence detection, *J. Chromatography. A*, 2000, 871,1-2, 37-42.
- [9] N. Furusawa, Rapid high-performance liquid chromatographic determining technique of sulfamonomethoxine, sulfadimethoxine, and sulfaquinoxaline in eggs without use of organic solvents, *Anal. Chim. Acta*, 2003, 481:2, 255-259.
- [10] V.B. Reeves, Confirmation of multiple sulfonamide residues in bovine milk by gas chromatography-positive chemical ionization mass spectrometry, *J. Chromatography. B*, 1999, 723:1-2, 127-137.
- [11] P. Cliquet, E. Cox, W. Haasnoot, E. Schacht, B.M. Goddeeris, Extraction procedure for sulfachloropyridazine in porcine tissues and detection in a sulfonamide-specific enzyme-linked immunosorbent assay (ELISA), *Anal. Chim. Acta*, 2003, 494:1-2, 21-28.
- [12] X. Wang, K. Li, D. Shi, X. Jin, N. Xiong, F. Peng, D. Peng, D. Bi, Development and validation of an immunochromatographic assay for rapid detection of sulfadiazine in eggs and chickens, *Journal of Chromatography B*, 2007, 847, 289–295.



- [13] C. Situ, M. H. Mooney, C. T. Elliott, J. Buijs, Advances in surface plasmon resonance biosensor technology towards high-throughput food-safety analysis, *Trends Anal. Chem.* 2010, 29, 1305–1315.
- [14] F. Fernández, D. G. Pinacho, F. Sánchez-Baeza, M. P. Marco, Portable surface plasmon resonance immunosensor for the detection of fluoroquinolone antibiotic residues in milk, *J. Agric. Food Chem.*, 2011, 59, 5036–5043.
- [15] Y. Yang, Y. Long, Z. Li, N. Li, K. Li, F. Liu, Real-time molecular recognition between protein and photosensitizer of photodynamic therapy by quartz crystal microbalance sensor, *Analytical Biochemistry*, 2009, 392, 22–27.
- [16] D.H. Yang, A.H. Bae, K. Koumoto, S.W. Lee, K. Sakurai, S. Shinkai, In situ monitoring of polysaccharide- polynucleotide interaction using a schizophyllan -immobilized QCM device, *Sens.Actuators, B: Chem.*, 2009, 105, 490.
- [17] Z. Hongwu, Z. Rui, C. Zhiyong, S. Di-Hua, L. Guoquan, QCM-FIA with PGMA coating for dynamic interaction study of heparin and antithrombin III, *Biosensors and Bioelectronics*, 2005, 21, 121–127.

## Flow Injection Analysis Biosensor for Urea Analysis in Urine Using Enzyme Thermistor

Geetesh K. Mishra · Atul Sharma ·  
Kanchanmala Deshpande · Sunil Bhand

Received: 14 January 2014 / Accepted: 19 May 2014 /  
Published online: 7 June 2014  
© Springer Science+Business Media New York 2014

**Abstract** There is a need for analytical methods capable of monitoring urea levels in urine for patients under clinical monitoring to appraise renal function. Herein, we present a practical method to quantify levels of urea in human urine samples using flow injection analysis-enzyme thermistor (FIA-ET) biosensor. The biosensor comprises a covalently immobilized enzyme urease (Jack bean) on aminated silica support, which selectively hydrolyzes the urea present in the sample. Under optimized conditions, the developed biosensor showed a linear response in the range of 10–1,000 mM,  $R^2=0.99$ , and response time of 90 s in 100 mM phosphate buffer (PB) (flow rate of 0.5 mL/min, sample volume of 0.1 mL, and pH 7.2). The urea-spiked human urine samples showed minimal matrix interference in the range of 10–1,000 mM. Recoveries were obtained (92.26–99.80 %) in the spiked urine samples. The reliability and reproducibility of the developed biosensor were found satisfactory with percent relative standard deviation (% RSD)=0.741. The developed biosensor showed excellent operational stability up to 30 weeks with 20 % loss in original response when used continuously at room temperature. These results indicate that the developed biosensor could be very effective to detect low and high levels of urea in urine samples.

**Keywords** Urea · Urine · Enzyme thermistor · Immobilized urease · Aminated silica gel

---

G. K. Mishra · A. Sharma · K. Deshpande · S. Bhand (✉)  
Biosensor Laboratory, Department of Chemistry, Birla Institute of Technology and Science, Pilani, KK Birla  
Goa Campus, Goa 403726, India  
e-mail: sunil17\_bhand@yahoo.com

G. K. Mishra  
e-mail: geeteshmishra26@gmail.com

A. Sharma  
e-mail: atulsharma407g@rediffmail.com

K. Deshpande  
e-mail: kanchi\_43@yahoo.com

*Present Address:*  
K. Deshpande  
Department of Chemistry, Goa University, Goa 403206, India

## Introduction

Determination of urea has numerous applications in a wide range of fields such as clinical diagnostics, environmental monitoring, and food science. However, the most important application of urea determination lies in clinical analysis to appraise renal functions. Being a waste product of the kidney, urea is an important biomarker that is routinely monitored to determine the functional ability of the renal system [1, 2]. The normal range of urea in urine and blood is between 8 and 20 mg/dL [3]. Elevated urea levels in serum and urine are indicative of renal dysfunction, urinary tract obstruction, dehydration, diabetes, shock, burns, and gastrointestinal bleeding. However, reduced urea level may cause hepatic failure, nephritic syndrome, and cachexia [4].

In recent years, several analytical methods such as reverse phase ultra-fast liquid chromatography [5], colorimetric method based on the reaction of urea and diacetylmonoxime derivatives [6], infrared spectrometry [7], and high performance liquid chromatography [8] have been utilized for urea determination. Furthermore, biosensor techniques such as potentiometry, conductimetry, amperometry, and coulometry have also been extensively studied for the detection of urea by urease-catalyzed hydrolysis products [9–12].

The growing demand for clinical diagnostics in relation to kidney diseases has stipulated the development of new methods for the rapid and accurate measurement of urea in samples like urine and serum. Thermal biosensors have been considered to be a practical alternative due to their robustness, simplicity, low cost, and extended stability. Another advantage of thermal biosensors is the universal detection principle that has been combined with the specificity of biological reactions. A number of enzymatic reactions for the analysis of urea, glucose, lactate, cholesterol, heavy metals, and fructose have been studied by thermal biosensors among which urea detection was studied extensively in serum and milk [13–18].

Recently, we have demonstrated a flow injection analysis-enzyme thermistor (FIA-ET) biosensor for urea adulteration in milk [19], which was for the first time studied by this instrument comprising urease (Jack bean, EC 3.5.1.5) immobilized on controlled pore glass (CPG). The objective of the present work is to demonstrate the application of the enzyme thermistor for the analysis of urea in urine samples. A low-cost amine-functionalized silica gel microparticle matrix was used as column material for the immobilization of urease. Herein, we present a highly stable, sensitive, and economical FIA-ET biosensor for the analysis of urea in urine samples. The presented biosensor can facilitate the regular and continuous monitoring of abnormal urea concentrations to keep track of the functional ability of the renal system. Another important feature of the presented biosensor is the lower detection limit (10 mM) and an excellent dynamic range of detection—10–1,000 mM urea with a sample throughput of more than 20 within an hour.

## Experimental

### Reagents and Materials

Enzyme urease (Jack beans lyophilized 5 U mg<sup>-1</sup>, EC 3.5.1.5), urea, sodium dihydrogen phosphate monohydrate, disodium hydrogen phosphate monohydrate, glutaraldehyde solution

25 %, and tri-ethanol amine were obtained from Merck, Germany. Functionalized silica gel (amino-3, ca. 1.4 mmol, particle size 40–83  $\mu\text{m}$ ) was procured from Across Organics, NJ, USA. All other chemicals used were of GR grade.

### Solution Preparation

Phosphate buffer (PB) 100 mM, pH 7.2, was prepared by mixing 100 mM of sodium dihydrogen phosphate monohydrate and 100 mM of disodium hydrogen phosphate monohydrate in double distilled water. PB was degassed before the analysis. A stock solution of urea (1,000 mM) was prepared by dissolving an appropriate amount of urea in 100 mL of PB (100 mM, pH 7.2). The working solution of urea was freshly prepared prior to use.

### Enzyme Column Preparation

Enzyme immobilization on amine-functionalized silica gel was achieved by glutaraldehyde cross-linking as reported earlier with slight modifications as presented in Fig. 1a. In brief, urease was covalently immobilized on amine-functionalized silica gel according to the following procedure: 250 mg aminated silica gel was activated with 2.5 % glutaraldehyde in 100 mM PB, pH 7.2. The reaction was allowed to take place for at least 1 h inside the desiccators, under reduced pressure. The activation of the aminated silica gel support was confirmed by the presence of a brick red color (formation of Schiff base). Activated silica gel was successively washed with double distilled water and PB. Urease 200 mg (1,000 IU) dissolved in 1 mL PB was added to the wet activated silica gel. The coupling reaction was allowed to proceed for 30 min at room temperature and overnight at 4 °C. The enzyme preparation was washed with PB. Tri-ethanolamine (200 mM) was added to terminate all the unreacted groups and then washed with 100 mM PB, pH 7.2. The immobilized urease was finally packed into a Delrin column by a slurry packing method.

### Instrumentation

The schematic setup for the FIA-ET biosensor for urea analysis is presented in Fig. 1b. The experimental setup consists of a peristaltic pump (Gilson Minipuls Evolution II, France), a six-port injection valve (Rheodyne, Cotati, USA), sample loop (0.1 mL), enzyme thermistor, Wheatstone bridge equipped with a chopper-stabilized amplifier, and Pico logger data recorder (Picotech, UK). PTFE tubings (0.8 mm i.d.) were used for the connection. PB (100 mM, pH 7.2) was used as the carrier buffer.

### Procedure

For urea analysis, calibration standards (10–1,000 mM) were prepared by dilution of urea stock solution (1,000 mM) in 100 mM PB, pH 7.2. The immobilized urease column was mounted inside the ET and was allowed to equilibrate with the surrounding. Degassed carrier buffer was passed at an optimum flow rate of 0.5 mL  $\text{min}^{-1}$  at which a stable baseline was achieved. Samples were injected and data collected using a data acquisition system connected to the Wheatstone bridge. All measurements were carried out by

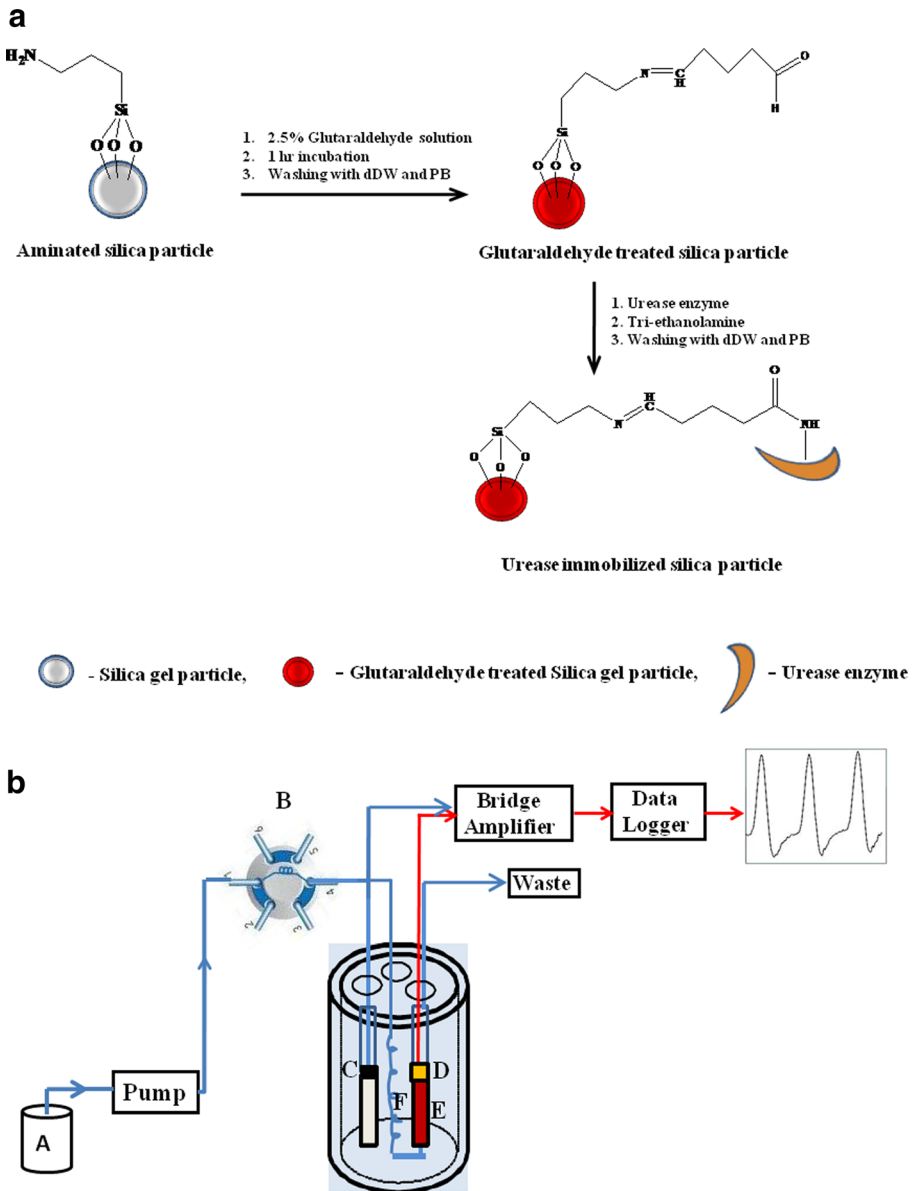


**Fig. 1** a Schematic representation of immobilization of enzyme urease to aminated silica matrix. b Schematic representation of the experimental setup of the FIA-ET biosensor for urea analysis in urine (A buffer reservoir, B injection valve, C reference probe, D thermistor, E immobilized urease column, F heat exchanger)

injection of 0.1 mL sample at a flow rate of 0.5 mL min<sup>-1</sup>. After each sample analysis, the sample loop was thoroughly rinsed with PB. The urine samples were spiked with a known amount of urea and, after matrix matching with appropriate dilutions, were injected into the FIA-ET system.

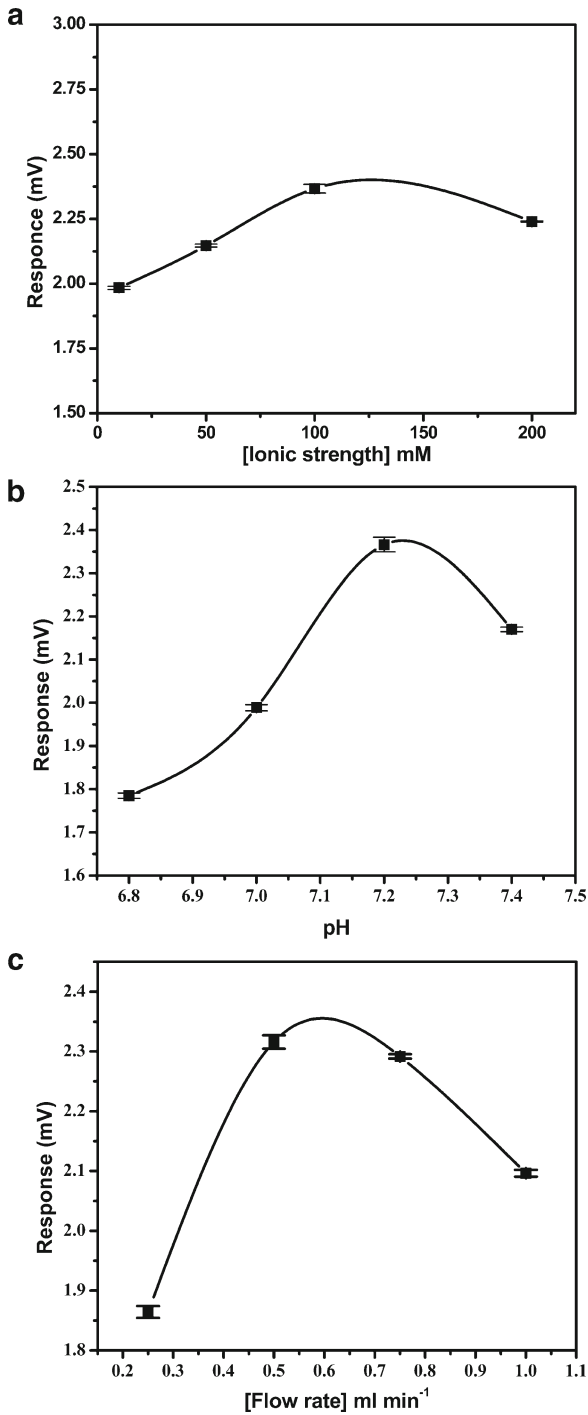


**Fig. 2** **a** Effect of ionic strength of PB on the response of the FIA-ET biosensor to 0.1 mL injection of 200 mM urea. **b** Effect of pH of PB on the response of the FIA-ET biosensor to 0.1 mL injection of 200 mM urea. **c** Effect of flow rate of PB on the response of the FIA-ET biosensor to 0.1 mL injection of 200 mM urea

## Result and Discussion

### Optimization of the FIA-ET Urea Biosensor

A series of experiments were performed to determine the influence of ionic strength and pH of PB, the flow rate and sample volume on the activity of enzyme urease, and the sensitivity of the biosensor. Measurements for optimization of the flow system were carried out with varying ionic strength (10, 50, 100, and 200 mM) and pH (6.8–7.4) for PB. Flow rates of 0.25, 0.5, 0.75, and 1.0 mL min<sup>-1</sup> and sample volumes of 0.05 and 0.1 mL were investigated against 200 mM urea. As presented in Fig. 2a–c, the results indicate that the performance of the FIA-ET was highly reproducible under optimized conditions of PB (ionic strength of 100 mM, pH 7.2, flow rate of 0.5 mL min<sup>-1</sup>, and sample volume of 0.1 mL).

### Matrix Matching

Urine samples from different individuals were collected and the matrix effect in the analysis of urea in the urine sample was investigated. Various measurements of ionic strength and pH of urine samples were performed for appropriate dilutions of urine with PB. It was observed that 1:4 dilution of the urine sample with PB was the most responsive for urea analysis. To obtain the calibration curve for urea in spiked urine samples, a simple dilution strategy was developed to avoid the effect of ionic strength and pH on the urease column. Urine analyses were carried out within the same day after sample preparation.

### Surface Characterization of the Silica Matrix

The surface morphology of the aminated silica matrix was characterized using a JEOL (JSM 6560 LV) Scanning Electron Microscope (SEM) operated at  $\times 400$  magnification and an accelerating voltage of 8 kV as presented in Fig. 3a(A, B). Figure 3a(A) shows the bare surface of the silica particle before the attachment of the enzyme molecule. Figure 3a(B) shows the enzyme molecule attached to the silica matrix. From both figures and enlargements, it is clearly distinct that the enzyme molecules are coupled to the silica matrix. Furthermore, Fourier transform infrared (FT-IR) spectroscopy was also applied to measure the surface properties of the aminated silica matrix coupled to the enzyme. The surface was characterized before and after immobilizing the enzyme to the silica particles. Spectra were recorded using IR Affinity 1 (SHIMADZU, Japan) with attenuated total reflectance (ATR) attachment Specac Diamond ATR AQUA using 40 scans at 4 cm<sup>-1</sup> resolution collected under vacuum condition. The ATR FT-IR spectra are shown in Fig. 3b. The insets in Fig. 3b(1a, 2a, 1b, 3a) show the results for amine-functionalized silica surface. In Fig. 3a(1a), the presence of two peaks at 2,963 and 2,858 cm<sup>-1</sup> represents the *as*CH<sub>2</sub> and *s*CH<sub>2</sub> vibration. In Fig. 3b(1b), four different peaks at 1,562, 1,506, 1,488, and 1,471 cm<sup>-1</sup> are due to the asymmetric and symmetric bending of primary amine. The presence of one peak at 669 cm<sup>-1</sup> with two associated peaks at 686 and 648 cm<sup>-1</sup> confirms the presence of –Si–C– bond in amine-functionalized silica (not shown in inset). In Fig. 3b(2a), the formation of Schiff base after treatment with glutaraldehyde is confirmed by the appearance of two different peaks at 1,702 for –C=N– of Schiff base and 1,651 cm<sup>-1</sup> –CO of free aldehyde group. In Fig. 3b(3a), the presence of peak at 1,641 cm<sup>-1</sup> is attributed to –C=O of peptide bond between immobilized urease enzyme and glutaraldehyde-activated silica particle. In Fig. 3b(3a), the presence of peaks at 1,528 and 1,477 cm<sup>-1</sup> with two associated peaks at 1,459 and 1,443 cm<sup>-1</sup> is due to asymmetric and symmetric bending vibration of –NH– of secondary amide. The peaks that appear at 1,234 and 1,076 cm<sup>-1</sup> are

due to  $-C-N-$  and  $-Si-O-Si$  bond. A broad band from  $3,257\text{ cm}^{-1}$  may be attributed to  $-NH-$  stretching vibration.

### Calibration of Urea Biosensor in PB

The packed column with immobilized urease enzyme was installed inside the thermistor and allowed to equilibrate with the carrier buffer. The filtered and degassed PB was pumped manifold via FIA until a constant baseline was achieved. Mock urea standard solutions in the range of 10–1,000 mM (1 mM urea corresponds to 60.06 ppm) were prepared in PB and injected into the flow stream. Response signals were recorded using a data logger acquisition system connected to the Wheatstone bridge and plotted as current (mV) vs. urea (mM). All samples were measured in triplicates. The Michaelis constant,  $K_M$ , for urea was calculated using Lineweaver–Burk plot and found to be 448 mM. A good linear response was obtained

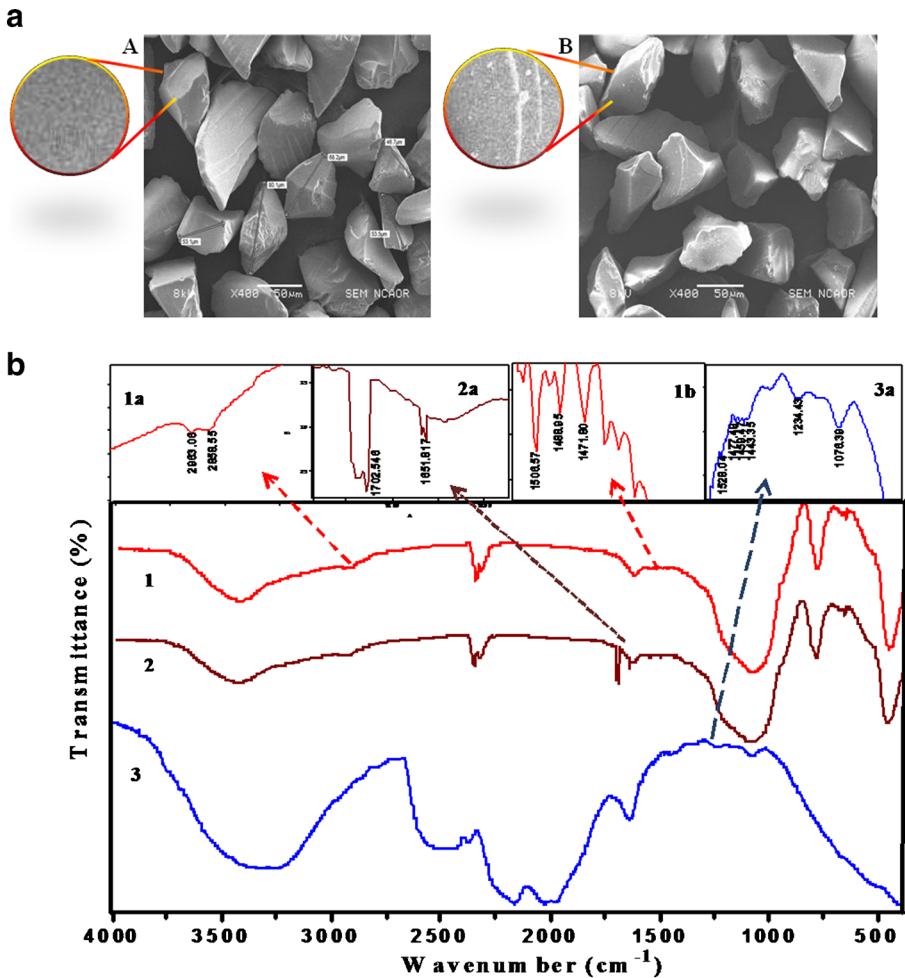


**Fig. 3** a SEM micrograph of the bare and enzyme-coupled silica matrix at magnification of  $\times 400$ . b FT-IR characterization of 1 aminated silica matrix, 2 glutaraldehyde-activated silica matrix, and 3 immobilized urease on silica matrix. Inset: 1a, 1b, 2a, and 3a represent the corresponding FT-IR characteristic peaks



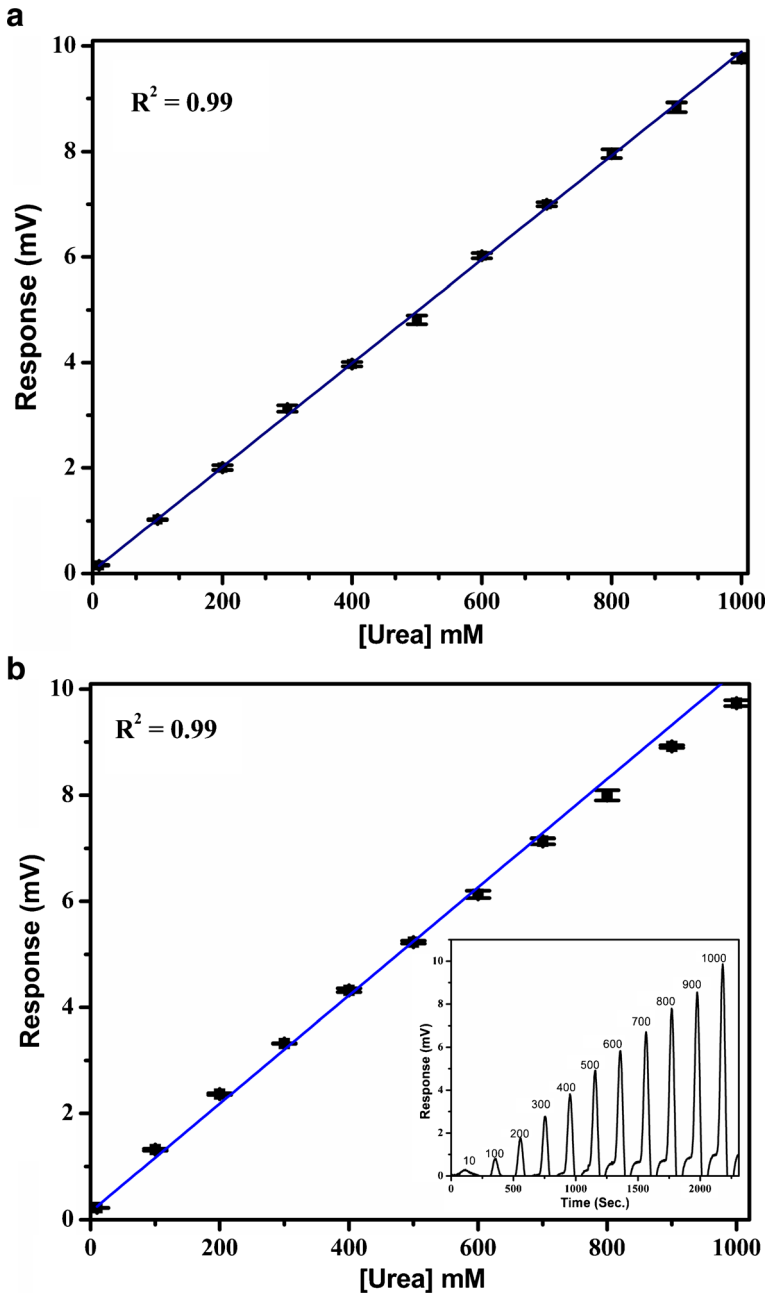


**Fig. 4** **a** Calibration plot obtained for urea using the FIA-ET biosensor in 100 mM PB, pH 7.2 for 0.1 mL of sample injection, flow rate of  $0.5 \text{ mL min}^{-1}$  at  $30 \text{ }^\circ\text{C}$ ,  $R^2=0.99$ , % RSD=0.02. **b** Calibration plot obtained for urea-spiked urine samples using the FIA-ET biosensor in 100 mM PB, pH 7.2 for 0.1 mL of sample injection, flow rate of  $0.5 \text{ mL min}^{-1}$  at  $30 \text{ }^\circ\text{C}$ ,  $R^2=0.99$ , % RSD=0.741. *Inset*: real-time response obtained from the FIA-ET urea biosensor for urea concentrations 10–1,000 mM

**Table 1** Comparison of the FIA-ET biosensor with other reported biosensor methods for the analysis of urea

S. no	Matrix	Transducer	Dynamic range	References
1	Urine	Thermal biosensor	10–1,000 mM	Present work
2	Urine, blood, water	Capacitance biosensor	0.1 pM–10 mM	[1]
3	Urine	Potentiometric bioelectronic tongue	1–1,000 mM	[2]
4	Blood	Potentiometric	1–1,000 mM	[20]
5	Blood, serum	Potentiometric	0.05–0.072 mM	[21]
6	Urine, blood	Colorimetric	0.17–0.44 M	[22]
7	Urine, blood	Amperometric	10–250 $\mu$ M	[23]
8	Urine	Enzyme-based biosensor	0–714.3 mM	[24]
9	Urine, serum	Enzyme-based biosensor	0–100 mM	[25]
10	Urine, serum	Amperometric biosensor	0.1–35 mM	[26]

for urea hydrolysis in the range of 10–1,000 mM, which is presented in Fig. 4a. Linear fit of data shows a good correlation between urea and immobilized urease ( $R^2=0.99$ , percent relative standard deviation (% RSD)=0.02).

#### Calibration of Urea Biosensor in Urine

Urine samples spiked with urea standard solutions (10–1,000 mM) were injected into the flow stream and the response signal was recorded. The FIA-ET biosensor showed an excellent dynamic range for urea present in spiked urine in the range of 10–1,000 mM with good linearity and the minimum detection limit was 10 mM. The results are presented as Fig. 4b ( $R^2=0.99$ , % RSD=0.960). Various biosensors reported in the literature for the analysis of urea are listed in Table 1. Most of the reported biosensors used urease as biorecognition element and have good detection range. However, the presented FIA-ET urea biosensor is capable of detecting urea in a urine sample in a broad dynamic range of

**Table 2** Determination of recovery from urine samples spiked with known amounts of urea using the FIA-ET urea biosensor

Urine samples	Urea added (mM) ( $n=3$ )	Urea found (mM) ( $n=3$ )	% Recovery	Mean $\pm$ SD	% RSD
Sample 1	0.5328	0.5219	97.97	0.97 $\pm$ 0.016	1.64
Sample 2	1.0237	0.9445	92.26	0.94 $\pm$ 0.012	1.28
Sample 3	2.0086	1.9767	98.41	1.97 $\pm$ 0.071	3.60
Sample 4	3.1277	2.9511	94.36	2.95 $\pm$ 0.016	0.54
Sample 5	3.9692	3.9613	99.80	3.96 $\pm$ 0.016	0.40
Sample 6	4.8124	4.7315	98.32	4.73 $\pm$ 0.022	0.46
Sample 7	6.0250	5.7695	95.76	5.77 $\pm$ 0.034	0.59
Sample 8	6.9983	6.7612	96.61	6.76 $\pm$ 0.021	0.31
Sample 9	7.9598	7.6810	96.50	7.68 $\pm$ 0.106	1.38
Sample 10	8.8393	8.5633	96.88	8.56 $\pm$ 0.123	0.14
Sample 11	9.7647	9.3846	96.11	9.38 $\pm$ 0.022	0.23

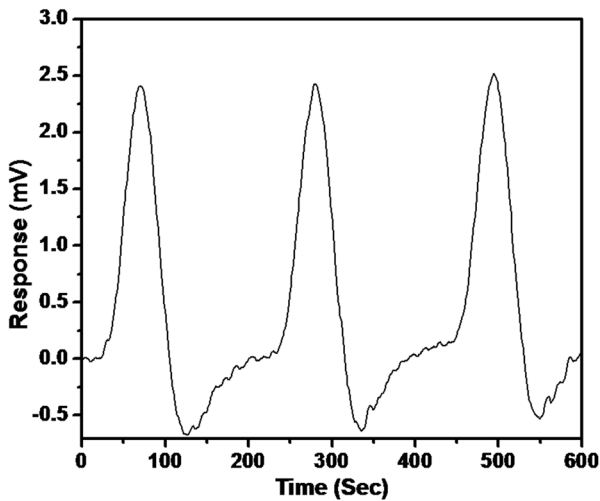


**Fig. 5** Real-time triplicate sensor signal recorded from the FIA-ET urea biosensor for 0.1 mL sample of 200 mM urea, flow rate of  $0.5 \text{ mL min}^{-1}$  at  $30 \text{ }^{\circ}\text{C}$

10–1,000 mM that covers the requirement of clinical industries to determine the functional ability of the renal system.

#### Recovery Studies from Spiked Urine Samples

A known amount of urea standard was spiked to a diluted urine sample and analyzed using the FIA-ET biosensor. Recoveries were calculated from the obtained response signal. Table 2 shows the recovery results obtained from urine urea. Excellent recoveries were obtained in the range of 92.26–99.80 % in the spiked urine samples. This ensures the reproducibility and sustainability of the developed biosensor.

#### Reliability and Reproducibility of the Urea Biosensor

In order to determine the reliability and reproducibility of the developed urea biosensor, several measurements were performed in triplicate. Figure 5 shows the real-time triplicate

**Table 3** Intraday and interday reliability of the FIA-ET urea biosensor

Intraday reliability				Interday reliability			
Urea concentration (mM)	Intraday mean (mV) ( $n=3$ )	Mean $\pm$ SD	% RSD	Day	Interday mean (mV) ( $n=3$ )	Mean $\pm$ SD	% RSD
100	1.3145	$1.31 \pm 0.017$	1.29	Day 1	2.3721	$2.37 \pm 0.021$	0.89
200	2.3664	$2.36 \pm 0.016$	0.67	Day 2	2.3605	$2.36 \pm 0.019$	0.80
500	5.2284	$5.22 \pm 0.026$	0.49	Day 3	2.3479	$2.34 \pm 0.015$	0.65
				Day 4	2.3518	$2.35 \pm 0.002$	0.10
				Day 5	2.3305	$2.33 \pm 0.002$	0.08

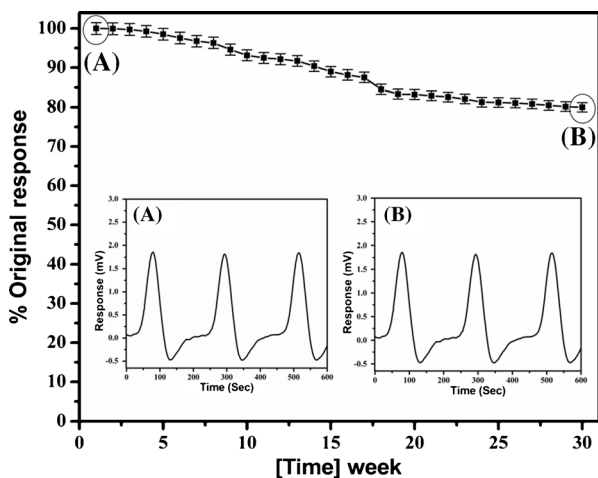


**Fig. 6** Operational stability of the sensor signal, response to 0.1 mL, 200 mM urea over the period of 30 weeks at room temperature. *Inset:* real-time triplicate sensor response obtained from the FIA-ET urea biosensor against 200 mM urea of the initial week and the 30th week of operation

sensor signal recorded from the FIA-ET urea biosensor on the urea-spiked urine sample. The obtained signal confirms the reproducibility of the sensor response. Table 3 presents the intraday and interday reliability of the developed biosensor.

#### Stability of the Sensor Signal

Stability of the sensor signal was investigated by making repetitive measurements over a period of 30 weeks. The sensor showed good operational stability when continuously monitored at room temperature. In an earlier reported work, CPG beads (125–140  $\mu\text{m}$  particle diameter and 50 nm pore size) were used as a column matrix. The column was stable up to 180 days at room temperature with about 70 % original response. In the present work, amine-functionalized silica gel microparticle (particle size 40–83  $\mu\text{m}$ ) was used as the column matrix to reduce the cost of the column and cost of per sample analysis. To check the stability of the sensor signal, about 20 measurements were made every week against 200 mM urea. The stability of the sensor signal is presented in Fig. 6. The sensor showed excellent stability over the initial 5 weeks with no appreciable loss of enzyme activity. After 15 weeks of continuous use, enzyme activity was found about 90 % of the original response. However, after a period of 20 weeks of operation, about 14 % decay in response was recorded. Similarly, the response was monitored within 25 and 30 weeks and signals recorded were 85 and 80 % of the original response, respectively. The presented urea biosensor is cost effective and shows good stability as reported earlier for the FIA-ET biosensor.

#### Conclusion

The FIA-ET biosensor for the analysis of urea in human urine samples is developed and demonstrated. A low-cost urease-immobilized aminated silica gel column matrix has been tested successfully, without compromising operational stability. This significantly reduces the cost of analysis per sample. A broad dynamic range has been obtained for urine urea analysis

(10–1,000 mM). The system has been automated for real-time analysis with a response time of 90 s. Results indicate that the developed biosensor is highly stable, simple, and economical. The method was optimized and had been successfully applied to determine urea levels in urine samples. The biosensor has been found to be stable at room temperature up to 30 weeks with 20 % loss of original response. The presented biosensor can facilitate the regular and continuous monitoring of abnormal urea concentrations to keep track of the functional ability of the renal system.

**Acknowledgments** This work is funded by the National Agriculture Innovation Project (NAIP) C4/C30032, ICAR, and The World Bank. We offer our sincere thanks to Prof. Bengt Danielsson, Acromed AB, Lund, Sweden for scientific interaction and providing the enzyme thermistor at BITS, Pilani-KK Birla Goa Campus. We also offer our sincere thanks to Dr. Rahul Mohan, NCAOR Goa for recording the SEM micrographs.

## References

1. Alizadeh, T., & Akbari, A. (2013). *Biosensors and Bioelectronics*, 43, 321–327.
2. Gutiérrez, M., Alegret, S., & Valle, M. D. (2007). *Biosensors and Bioelectronics*, 22, 2171–2178.
3. Ali, A., AlSalhi, M. S., Atif, M., Ansari, A. A., Israr, M. Q., Sadaf, J. R., et al. (2013). *Journal of Physics: Conference Series*, 414, 120–124.
4. Sumana, G., Das, M., Srivastava, S., & Malhotra, B. D. (2010). *Thin Solid Films*, 519, 1187–1191.
5. Czauderma, M., & Kowalczyk, J. (2012). *Czech Journal Animal Science*, 57(1), 19–27.
6. Goeyens, L., Kindermans, N., Yusuf, M. A., & Elskens, M. (1998). *Estuarine, Coastal and Shelf Science*, 47, 415–418.
7. Jensen, P. S., Bak, J., Ladefoged, S., & Andersson, S. (2004). *Spectrochimica Acta Part A*, 60, 899–905.
8. Clark, S., Francis, P. S., Conlan, X. A., & Barnett, N. W. (2007). *Journal of Chromatography A*, 161(1–2), 207–213.
9. Koncki, R., Radomska, A., & Glab, S. (2000). *Analytica Chimica Acta*, 418, 213–224.
10. Jdanova, S., Poyard, S., Soldatkin, A. P., Renault, N. J., & Martelet, C. (1996). *Analytica Chimica Acta*, 321, 35–40.
11. Pizzariello, A., Stredansky, M., Stredanska, S., & Stainslav, M. (2001). *Talanta*, 54, 763–772.
12. Adams, R. E., & Carr, P. W. (1978). *Analytical Chemistry*, 50, 944.
13. Danielsson, B., Mattiasson, B., & Mosbach, K. (1976). *Pure and Applied Chemistry*, 51, 1443–1457.
14. Bjarnason, B., Johansson, P., & Johansson, G. (1998). *Analytica Chimica Acta*, 372, 341–348.
15. Chen, Y., Andersson, A., Mecklenburg, M., Xie, B., & Zhou, Y. (2011). *Biosensors and Bioelectronics*, 29, 115–118.
16. Raghvan, V., Ramanathan, K., Sundaram, P. V., & Danielsson, B. (1999). *Clinica Chimica Acta*, 289, 145–158.
17. Pirvutoiu, S., Dey, E., Bhand, S., Ciucu, A., Magearu, B., & Danielsson, B. (2002). *Roumanian Biotechnology Letters*, 7, 975–986.
18. Bhand, S. G., Soundararajan, S., Wärmmark, I. S., Milea, J. S., Dey, E. S., Yakovleva, M., et al. (2010). *Analytica Chimica Acta*, 668, 13–18.
19. Mishra, G. K., Mishra, R. K., & Bhand, S. (2010). *Biosensors and Bioelectronics*, 26, 1560–1564.
20. Jha, S. K., Topkar, A., & D'Souza, S. F. (2008). *Journal of Biochemical and Biophysical Methods*, 70, 1145–1150.
21. Eggenstein, C., Borchardt, M., Diekmann, C., Grundig, B., Dumschat, C., Cammann, K., et al. (1999). *Biosensors & Bioelectronics*, 14, 33–41.
22. Verma, N., Minhas, R. K., & Kumar, S. (2012). *Advances in Applied Science Research*, 3(1), 135–141.
23. Pizzariello, A., Stredansky, M., Stredanska, S., & Miertus, S. (2001). *Talanta*, 54, 763–772.
24. Morishita, Y., Tsuji, K., Nakane, K., Soya, Y., Fukatsu, T., Yoneda, K., et al. (1997). *Clinical Chemistry*, 43(10), 1932–1936.
25. Orsonneau, J. L., Massoubre, C., Cabanes, M., & Lustenberger, P. (1992). *Clinical Chemistry*, 38(5), 619–623.
26. Tiwari, A., Aryal, S., Pilla, S., & Gong, S. (2009). *Talanta*, 78, 1401–1407.



ELSEVIER

Contents lists available at ScienceDirect

## Biosensors and Bioelectronics

journal homepage: [www.elsevier.com/locate/bios](http://www.elsevier.com/locate/bios)

# Ultrasensitive detection of streptomycin using flow injection analysis–electrochemical quartz crystal nanobalance (FIA-EQCN) biosensor

Geetesh K. Mishra<sup>1</sup>, Atul Sharma<sup>1</sup>, Sunil Bhand\*<sup>\*</sup>

Biosensor Lab, Department of Chemistry, BITS, Pilani – K. K. Birla Goa Campus, Zuarinagar 403726, Goa, India

## ARTICLE INFO

## Article history:

Received 15 May 2014

Received in revised form

5 September 2014

Accepted 11 September 2014

## Keywords:

Flow injection analysis

Quartz crystal nanobalance

Ultra-sensitive detection

Streptomycin

Milk

Antibiotic residue

## ABSTRACT

This work presents the development of an ultrasensitive biosensor for detection of streptomycin residues in milk samples using flow injection analysis–electrochemical quartz crystal nanobalance (FIA-EQCN) technique. Monoclonal antibody specific to streptomycin was immobilized on to the thiol modified gold quartz crystal surface. A broad dynamic range (0.3–300 ng/mL) was obtained for streptomycin with a good linearity in the range 0.3–10 ng/mL for PBS and 0.3–50 ng/mL for milk. The correlation coefficient ( $R^2$ ) of the biosensor was found to be 0.994 and 0.997 for PBS and milk respectively. Excellent recoveries were obtained from the streptomycin spiked milk samples in the range 98–99.33%, which shows the applicability of the developed biosensor in milk. The reproducibility of the developed biosensor was found satisfactory with % RSD ( $n=5$ ) 0.351. A good co-relation was observed between the streptomycin recoveries measured through the developed biosensor and the commercial ELISA kit. The analytical figures of merit of the developed biosensor confirm that the developed FIA-EQCN biosensor could be very effective for low-level detection of streptomycin in milk samples.

© 2014 Elsevier B.V. All rights reserved.

## 1. Introduction

Streptomycin (SRT), a member of aminoglycoside, finds wide application in modern agriculture and dairy for treatment of mastitis in cattle's (Haasnoot et al., 2003). Antibiotics such as aminoglycoside are being used either individually or in combination with other drugs for the treatment of inflammatory diseases or as feed additives. Monitoring of antibiotics is very important for safety of milk or milk products for human consumption. The presence of these residues even in minute amount can trigger potential health hazard such as allergic reactions in hypersensitive individuals, toxicity, or they can be act as potential carcinogens (Conzuelo et al., 2012). Antibiotics also give rise to an increase in the antibiotic resistance of pathogenic bacteria. Apart from the consequences for public health, economic reasons have also led to the control of antimicrobial residues in food. Milk contaminated with antibiotics may inhibit the starter cultures used in the production of other milk products (Ferguson et al., 2002). Several regulatory agencies have set the maximum residual limit (MRL) for antibiotics in milk for consumer protection. In particular,

European Union (EU) has fixed the limit at 200 ng/mL for SRT in milk whereas in The United States; the tolerance limit for SRT in milk is 125 ng/mL. The Codex committee has set a combined MRL of 200 ng/mL for SRT and dihydro-streptomycin (DHSRT) (Commission Regulation (EU) No. 37/2010, 2009; Baxter et al., 2001).

A wide range of analytical methods currently exists for the detection and quantitative measurements of SRT. Microbial inhibition assay (Currie et al., 1999), enzyme immunoassay (Abuknesha and Luk, 2005) and enzyme linked immuno-sorbent assay (ELISA) (Heering et al., 1998) are commonly employed as screening tests. Conventional analytical techniques such as liquid chromatography (Ye et al., 2008) and liquid chromatography-mass spectroscopy (Zhu et al., 2008) have been described for confirmatory analysis. Although the chromatographic techniques are sensitive and specific, they are restricted to confirmatory analysis being very laborious and expensive (Wang et al., 2006). Moreover, the long and tedious sample preparation involved prior to chromatographic analysis also limit sample throughput. An effective monitoring technique for regulation of these antibiotics require specific sensitivity, rapid, reliable and economical methods able to detect them at or below the MRL levels (Conzuelo et al., 2013).

Biosensors are a recent addition to analytical instrumentation capable of performing residues testing and offer the potential for rapid, quantitative high-throughput analysis. One such testimony

\* Corresponding author. Fax: +91 832 2557030/33.

E-mail addresses: [sunil17\\_bhand@yahoo.com](mailto:sunil17_bhand@yahoo.com), [sunilbhand@goa.bits-pilani.ac.in](mailto:sunilbhand@goa.bits-pilani.ac.in) (S. Bhand).<sup>1</sup> Authors with equal contribution.

for analysis of SRT in milk is Surface plasmon resonance (SPR) based optical biosensor (Baxter et al., 2001). Compared with expensive and complicated optical instrumentation of SPR, quartz crystal microbalance (QCM) is more suitable for wide generalization and applications. Owing to its simplicity, convenience, and real time response, QCM has been increasingly explored in many fields of biological studies (Yang et al., 2009a, 2009b). The principle of QCM is based on the frequency change of the crystal that is inversely proportional to the mass change on the crystal surface under appropriate conditions. The observed mass change can be correlated to the analyte binding on the surface of crystal. QCM has the advantages of minimal electrical requirements, adaptability to microfluidic techniques, inexpensive fabrication, utility in a flow cell, and label free detection. QCM biosensor integrated in a flow injection analysis (FIA-QCM) system has the advantages in terms of reproducibility, speed of analysis, control of contact time and concentration profiling in kinetic studies (Malitesta et al., 2012).

To implement a FIA-QCM biosensor, biomolecules need to be immobilized on the crystal surface to capture target analyte. Various immobilization methods including thiolation, silanization and immobilization via cross-linking are used for binding of the biomolecules on the crystal surface. Recently antibody immobilization by way of self-assembled monolayers (SAMs) of thiolated antibody, exploiting carboxyl-amine coupling of the antibody over the SAMs of different thiols or sulfide compounds have been demonstrated (Park et al., 2004).

In this study, we present for the first time an ultrasensitive detection of SRT antibiotic in milk samples using flow injection analysis-electrochemical quartz crystal nanobalance (FIA-EQCN) biosensor. The biosensor comprised monoclonal antibody specific to SRT (mAb-SRT) immobilized on the thiol modified gold crystal surface. The broad detection range (0.3–300 ng/mL) of developed biosensor facilitates ultra-sensitive detection of SRT in milk. The remarkable features of the developed FIA-EQCN biosensor are; its precision in reproducibility and reliability. Based on the state of the art, we could be able to achieve the sensitive detection of SRT as low as 0.3 ng/mL in milk using FIA-EQCN, which are summarized

in Table 1. This approach shows promising potential, being capable of detecting antibiotics at level below the MRL.

## 2. Materials and methods

### 2.1. Materials and Reagents

Anti-streptomycin monoclonal antibody-IgG fraction isolated from Mouse was purchased from M/s Abcam, Cambridge, UK. Streptomycin sulfate was procured from M/s MP Biomedicals, Santa Ana, California, USA and Streptomycin ELISA kit was procured from M/s Bioscientific Austin, Texas, USA. Sodium dihydrogen phosphate monohydrate, disodium hydrogen phosphate monohydrate, sodium chloride, 11-mercaptoundecanoic acid (11-MUA), 1-ethyl-3-[3-dimethylaminopropyl] carbodiimide hydrochloride (EDC), N-hydroxy succinimide (NHS), glutaraldehyde solution 25%, sodium chloride, glycine and cysteaminium chloride were obtained from M/s Merck KGaA, Darmstadt, Germany. L-cysteine hydrochloride was procured from M/s Himedia laboratory, Mumbai, India. Centrifugation of milk is carried out by minispin centrifuge and for sample handling micropipettes are used. Both are procured from M/s Eppendorf, Hamburg, Germany. All the solutions were prepared in 0.22  $\mu$ m membrane filtered Milli-Q system RO water, procured from M/s Millipore, Billerica, Massachusetts, USA. Seven Multi pH meter was used for pH measurements, procured from M/s Mettler Toledo, Greifensee, Switzerland. All other chemicals used were of analytical grade and used as received.

### 2.2. Instrumentation for FIA-EQCN biosensor

The experimental set-up used for present study is shown as Fig. 1. EQCN-700 system integrated with flow cell model FC-6 (M/s Elchema, Potsdam, New York, USA) was deployed for construction of FIA-EQCN biosensor. The gold quartz crystal (10 MHz, AT cut) was connected to the frequency-measuring unit, which contains a reference crystal with the same characteristics as the measuring crystal. The gold quartz crystal was placed in a plexiglass flow cell,

**Table 1**  
Comparison with earlier reported biosensors for streptomycin detection.

S. no.	Matrix	Detection limit	Detection technique	Reference	Year
1.	Milk	0.3 ng/mL	FIA-EQCN biosensor	Present work	2014
2.	Milk, Honey	7 pg/mL	Electrochemical	Que et al. (2013)	2013
3.	Honey	0.1 $\mu$ M	Aptasensor	Zhou et al. (2013)	2013
4.	Food	10 ng/g	HPLC	Benjing et al. (2012)	2012
5.	Food	5 pg/mL	Electrochemical immunoassay	Liu et al. (2011)	2011
6.	Honey	15.9 $\mu$ g/kg	Chemiluminescence immunoassay	Wutz et al. (2011)	2011
7.	Milk	4.5 $\mu$ g/L	Immunoassay	Bilandzić et al. (2011)	2011
8.	Milk	2 ng/mL and 20 ng/mL	ELISA and Immunochromatographic Assay	Wu et al. (2010)	2010
9.	Milk	100 $\mu$ g/mL	TLC/Bioautographic method	Kaya and Filazi (2010)	2010
10.	Milk	1.2 ng/mL	iSPR based Immunosensor	Raz et al. (2009)	2009
11.	Meat, Juice	0.1 $\mu$ g/mL	Solid-phase fluorescence immunoassay (SPFIA)	Pyun et al. (2008)	2008
12.	Milk	2.01 ng/mL	SMM-FIA	Ce et al. (2008)	2008
13.	Milk	3.0 ng/mL	ELISA	Samsonova et al. (2005)	2005
14.	Milk	5.06 $\mu$ g/L	Immunoassays	Knecht et al. (2004)	2004
15.	Milk, Honey	Milk 10 $\mu$ g/kg Honey 2 $\mu$ g/kg	LC-MS/MS	Bruijnsvoort et al. (2004)	2004
16.	Milk	3.2 ng/mL	Immunochemical rapid test	Strasser et al. (2003)	2003
17.	Milk	65 ng/mL	Immunoassay	Haasnoot et al. (2003)	2003
18.	Milk, Honey, Meat	Milk 30 $\mu$ g/kg Honey 15 $\mu$ g/kg Kidney 50 $\mu$ g/kg Muscle 70 $\mu$ g/kg	Optical biosensor	Ferguson et al. (2002)	2002
19.	Milk	4.1 ng/mL	Optical immunobiosensor	Baxter et al. (2001)	2001
20.	Milk	0.03 mg/kg	Solid-phase extraction/Fluorometric detection	Edder et al. (1999)	1999

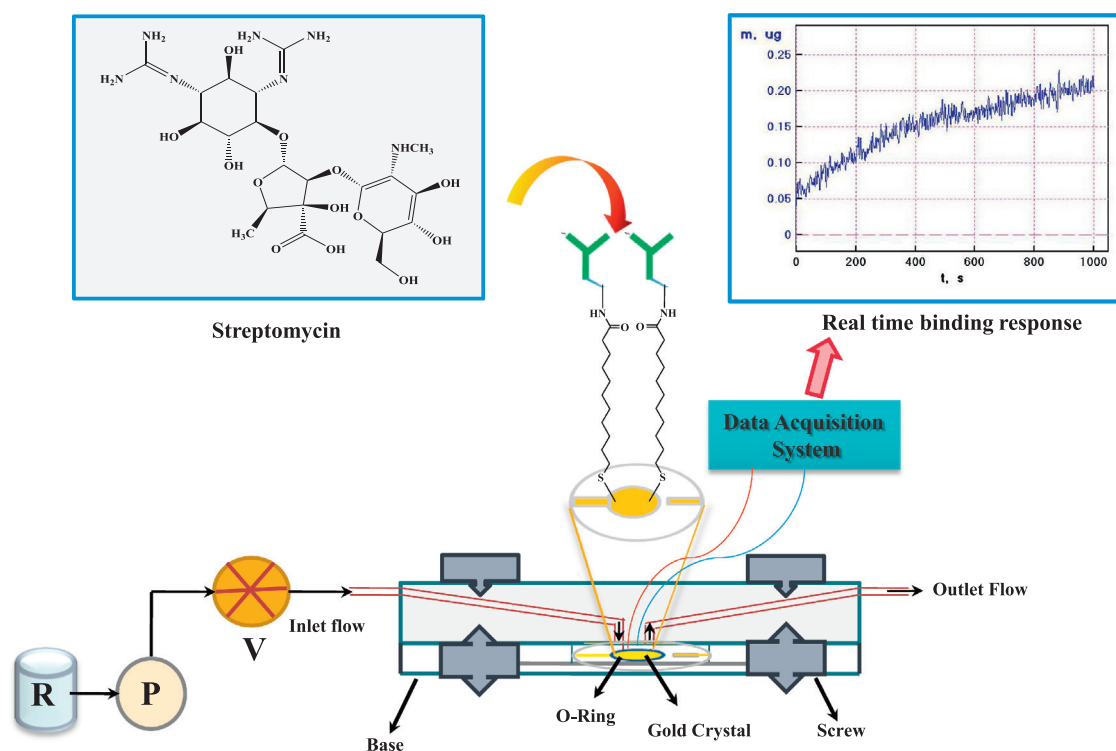


Fig. 1. Schematic of FIA-EQCN biosensor for analysis of streptomycin in milk. R – buffer reservoir, P – peristaltic pump, V – 6-port injection valve.

sandwiched between two O-rings, with its upper electrode in contact with the liquid and its lower electrode in air. The volume of the flow cell was 50  $\mu\text{L}$  ( $\varnothing=8$  mm and height=1 mm). A peristaltic pump (M/s Gilson Inc., Villiers-le-Bel, France) was connected through a 6-port Rheodyne injection valve (M/s, IDEX health and science, Oak Harbor, Washington, USA) to the flow-cell. Samples were filled in the 6-port injection valve and injected into the carrier buffer. The measurements of direct mass change were taken using Voltscan 5 software. The EQCN-700 system has inbuilt hardware and provides the data only as mass change. The inbuilt frequency unit, which calculated the mass by using a conversion factor (1 Hz equivalent to 1 ng approx.), measured the output from the oscillator. The calculation for conversion of 1 Hz to 1 ng is provided in the [Supplementary details](#). Though the output signal from the EQCN-700 system is in  $\mu\text{g}$  (auto calibrated), the mass change ( $\Delta m$ ) is converted in to ng to impart more clarity in calibration graph. A personal computer controlled the data acquisition. The flow cell was placed in a Faraday cage to shield the crystal from external electromagnetic sources.

### 2.3. Biosensor preparation

The methodology employed for preparation of biosensor for SRT analysis in milk was based on multilayer assembling on the surface of gold quartz crystal. In brief, a clean gold quartz crystal was immersed overnight in 4 mM ethanolic solution of 11-MUA under ambient condition. The gold quartz crystal was gently washed with absolute ethanol to remove unbound 11-MUA residues and dried with nitrogen stream before use. For coupling of the mAb-SRT antibody, the carboxyl group of SAM on modified electrode was activated by 1:1 EDC/NHS (100 mM each) mixture for 2 h. Subsequently, the crystal was washed with membrane filtered water to remove excess EDC/NHS. Finally, solution of 10 mg/mL (1:1000 in PBS) mAb-SRT was added carefully over the activated surface of SAM followed by overnight incubation

(8–12 h) at 4  $^{\circ}\text{C}$ . The coupled gold crystal was washed to remove unbound antibody and mounted on the flow cell to use in FIA mode.

### 2.4. Solution preparation

Phosphate buffer saline (PBS, 100 mM) was prepared by dissolving appropriate amount of  $\text{Na}_2\text{HPO}_4$  and  $\text{NaH}_2\text{PO}_4$  containing 137 mM NaCl and 2.7 mM KCl in membrane filtered RO water. The pH of the buffer was adjusted to 7.4 before use. For preparation of standards, known amount of SRT was dissolved in PBS and further diluted to meet the calibration standards. For analysis in milk, samples were centrifuged and diluted (1:4) in PBS. A stock solution of SRT (300 ng/mL) was prepared and further diluted to meet the calibration standards in the range of 0.001–300 ng/mL. All the solutions were freshly prepared before the experiment and stored at 4  $^{\circ}\text{C}$  when not in use. The commercial milk sample of 3.0% fat was procured from local market of Goa, India. The matrix effect on analysis of SRT in milk samples was investigated. In FIA system, fat present in the milk may lead to clogging of the fluidic channels and thus, can decrease the biosensor performance. To avoid such problems, a simple strategic approach was worked out to obtain the calibration curve for SRT in spiked milk samples. Combination of several sample pre-treatment techniques such as centrifugation, filtration, and dilution of milk with PBS was done for SRT analysis in milk. In brief, the milk samples were centrifuged at 6000 rpm for 20 min at room temperature and filtered with 0.22  $\mu\text{m}$  filter (Whatman, USA) and diluted with PBS to obtain different ratios of milk and PBS (1:2, 1:4, 1:6.1:8). A known amount of SRT was spiked in diluted milk samples and it was observed that 1:4 dilution of milk sample with PBS showed maximum binding for SRT with immobilized antibody on modified crystal surface.



### 3. Result and discussion

#### 3.1. Optimization of experimental variables

##### 3.1.1. Surface modification

Earlier reported protocols for SAMs were used for optimization of surface modification to immobilize mAb-SRT on gold quartz crystal, with slight modifications. 11-MUA (4 mM) (Park et al., 2004), cysteaminium chloride (10 mM) (Silva et al., 2010) and L-cysteine (10 mM) (Zhang et al., 2009) were tested. The concentrations of different surface modifiers and cross-linkers were optimized and mAb-SRT antibody was attached to the surface. The SAMs based on 11-MUA showed the maximum mass change against mAb-SRT coupled gold quartz crystal for SRT standard

which confirms the maximum binding. Thus, further experiments were carried out using 11-MUA. Fig. 2a represents the binding responses obtained with different SAM's.

##### 3.1.2. Antibody dilutions and binding capacity of the gold crystal

It is very important to optimize the concentration of antibody (bioreceptors), which critically affects their conjugation onto the electrodes as well as their ease of access toward analytes with minimum physical steric hindrance (Ahmed et al., 2013). To determine optimum antibody concentration and to check the maximum binding efficiency, different dilutions of mAb-SRT were injected into the FIA system on the SAMs modified crystal surface. The mAb-SRT antibody was diluted with PBS as 1:100, 1:500 and 1:1000. As shown in Fig. 2b, it was found that 1:1000 dilution of

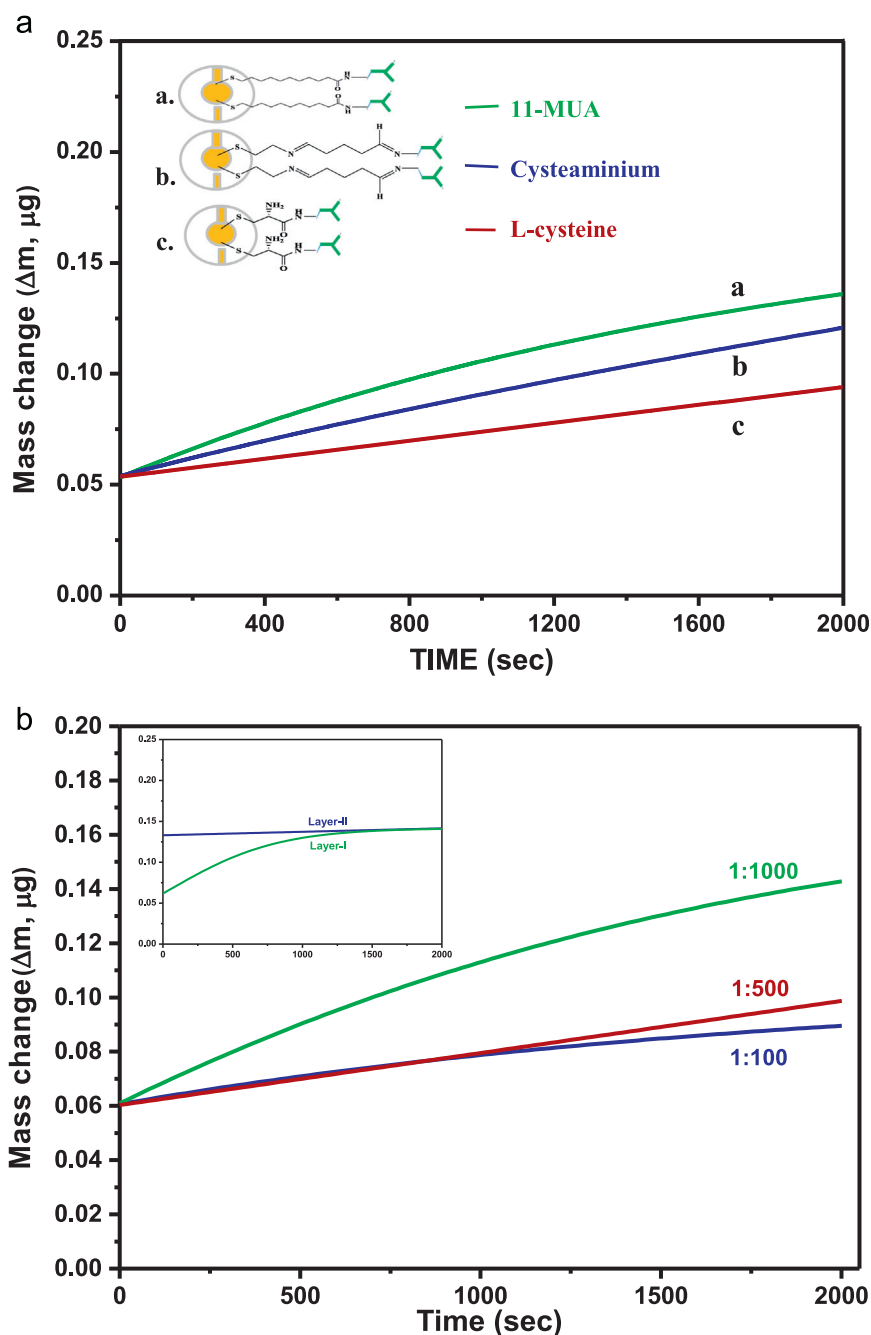


Fig. 2. (a) Optimization of different Self Assembled Monolayers. Inset: representation of different thiols attached to the gold quartz crystal. (b) Optimization of antibody dilutions for analysis of streptomycin. Inset: binding capacity of the gold crystal through different layers of antibody. Carrier buffer – PBS (100 mM), pH 7.4, flow rate 0.1 mL/min.

mAb-SRT showed the maximum binding on optimized monolayer surface. However, antibody dilution of 1:100 and 1:500 showed minimum binding which agrees with the hypothesis that too high a density of bioreceptors can actually hinder binding because of steric hindrance at high concentration. Recently, Holford et al. has also demonstrated that a high concentration of antibody decreased biosensor sensitivity, as it did not facilitate bioreceptor binding on the surface, probably due to steric hindrance (Holford et al., 2013). Hence, all the further experiments were carried out using 1:1000 dilutions. Simultaneously, experiments were carried out to study the maximum binding capacity of modified crystal with mAb-SRT. Optimized dilution of antibody solution in buffer was passed to the modified crystal surface and real time binding response was recorded. Saturation of the modified SAMs layer on crystal surface was observed during the second run of antibody as evident from Fig. 2b (inset).

### 3.1.3. Effect of influential parameters of FIA system

Different influential parameters like phosphate concentration, pH of the carrier buffer and flow rate of the FIA system were optimized before the experiment was performed. Measurements were carried out with different phosphate concentrations (10, 50, 100 and 200 mM) and pH (6.8–7.6) of PBS for 10 ng/mL SRT. It is evident from supplementary Fig. S1 that the 10 ng/mL SRT showed the maximum binding in 100 mM PBS, similarly, maximum binding was found at pH 7.4 as presented in supplementary Fig. S2. The effect of flow rate on SRT binding on modified crystal surface, immobilized with mAb-SRT was tested. The SRT standard (10 ng/mL) was passed over the mounted crystal in different flow rates (0.01, 0.1, 0.5 and 1 mL/min). As shown in supplementary Fig. S3, flow rate of 0.1 mL/min provides sufficient contact time for binding of SRT to immobilized mAb on gold crystal, thus gives the maximum response. These optimized parameters (phosphate concentration 100 mM, pH 7.4 and flow rate 0.1 mL/min) were used throughout the experiment.

### 3.2. Surface characterization of mAb-SRT immobilized gold crystal

Fourier Transform InfraRed (FT-IR) spectroscopy was applied to measure the surface properties of the AT-cut gold quartz crystal

coupled through 11-MUA SAMs via the carbodiimide cross-linking reaction. The surface was characterized before and after coupling of mAb-SRT at each step during the experiment. Spectra were recorded using IR Affinity-1 (M/s SHIMADZU Corp., Kyoto, Japan) with attenuated total reflectance (ATR) attachment Specac Diamond ATR AQUA. The spectra were recorded using 40 scans at  $4\text{ cm}^{-1}$  resolution collected under vacuum condition. The FT-IR spectra are shown in Fig. 3. FT-IR spectrum of bared gold surface is shown as Fig. 3(a). Spectrum of gold surface treated with 11-MUA is shown as Fig. 3(b) where it showed the C–H Stretches in asymmetric and symmetric mode at  $2925\text{ cm}^{-1}$  and  $2848\text{ cm}^{-1}$ . The broad region from  $2500\text{--}3500\text{ cm}^{-1}$  with out-of-plane bending for O–H at  $935\text{ cm}^{-1}$  confirming the presence of COOH group of 11-MUA. The broad region with asymmetric and symmetric Stretches at  $1676$  and  $1619\text{ cm}^{-1}$  confirm the presence of C=O of acid. Two-associated peak for C–H deformation(scissoring) was found to be at  $1488$  and  $1446\text{ cm}^{-1}$ . Three associated peak for long chain carbon of 11-MUA appears at  $684$ ,  $635$  and  $537\text{ cm}^{-1}$ . As shown in Fig. 3(c), after immobilization of Ab on gold crystal, new absorption bands appears at  $1645$  and  $1552\text{ cm}^{-1}$  which confirm the presence of amide bond (CO-NH) in between 11-MUA and mAb-SRT. The presented FT-IR spectra confirms the attachment of mAb-SRT to the modified surface of gold quartz crystal.

### 3.3. Biosensor performance in PBS and milk

The mAb-SRT immobilized gold quartz crystal was mounted in Plexiglas flow-cell and degassed PBS was passed until the constant baseline was achieved. Freshly prepared SRT standard in PBS (0.001–300 ng/mL) were injected into the FIA-EQCN system, starting from lower to higher concentration. The response signals of different concentration were recorded using the data acquisition system (DAQ-716) and plotted as mass change ( $\Delta m$ ) vs. concentrations. The obtained data from the Voltscan 5 software was treated using OriginPro 8 software and the data of best fit was plotted. In the developed FIA-EQCN biosensor, results were obtained as mass change resulting from the real time binding of SRT to the mAb-SRT immobilized via the SAMs on the quartz crystal. The mass change ( $\Delta m$ ) is converted in to ng to impart more clarity in the calibration graph. The background value (50 ng/mL) is

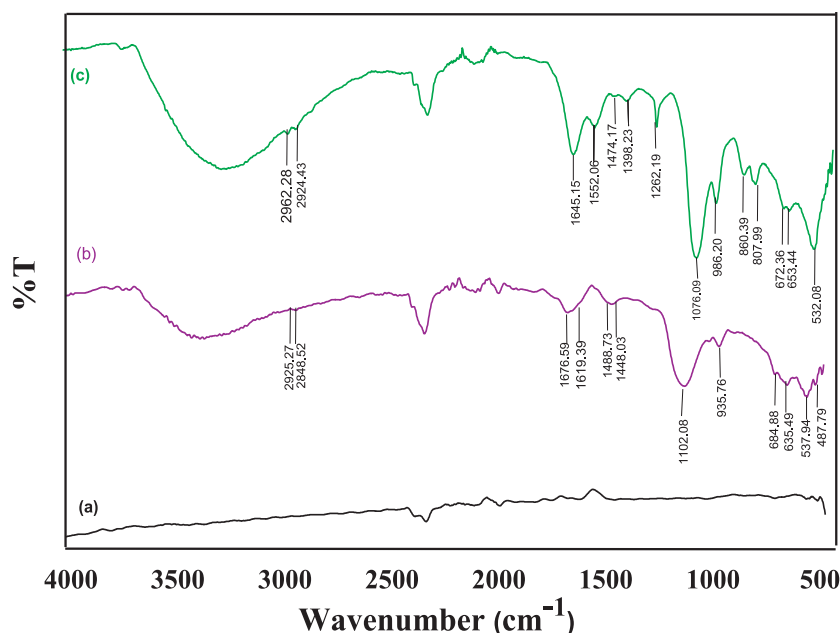
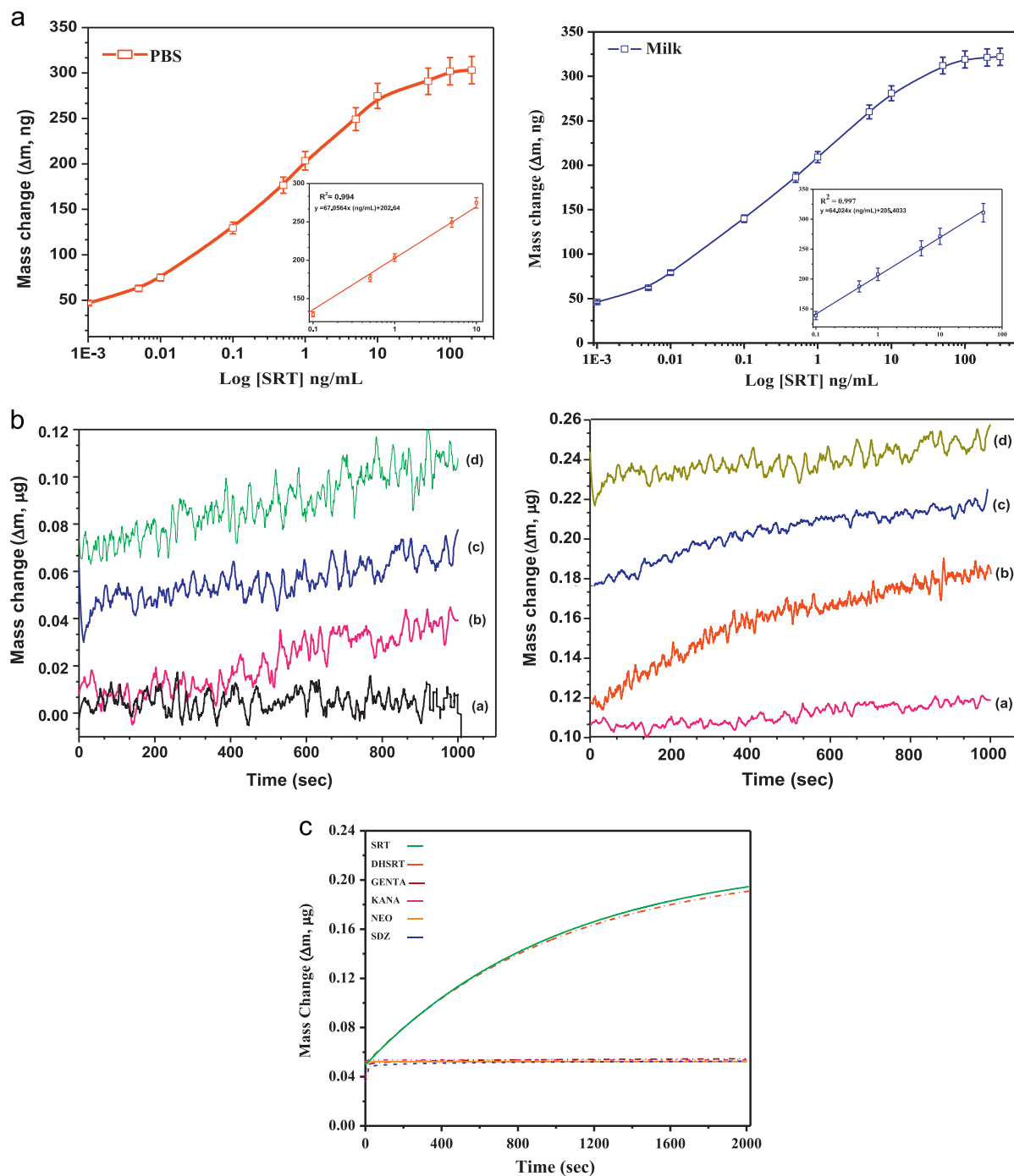


Fig. 3. FTIR characterization of immobilized antibody on modified gold crystal. The spectra's were recorded using 40 scans at  $4\text{ cm}^{-1}$  resolution collected under vacuum condition.



**Fig. 4.** (a) (i) Logarithmic representation of calibration graph for streptomycin analysis in PBS. Inset: linear fit data representation for streptomycin analysis in PBS. (ii) Logarithmic representation of calibration graph for streptomycin analysis in milk. Inset: linear fit data representation for streptomycin analysis in milk. (b) (i) Actual data graph for (a) response of functionalized gold crystal (b) response of mAb-SRT immobilized gold crystal (c) response of 0.001 ng/mL SRT spiked milk sample (d) response of 0.005 ng/mL SRT spiked milk sample. (ii) (a) Response of 0.01 ng/mL SRT spiked milk sample (b) response of 0.1 ng/mL SRT spiked milk sample (c) response of 0.05 ng/mL SRT spiked milk sample (d) response of 1 ng/mL SRT spiked milk sample. (c) Cross reactivity of streptomycin with other antibiotics. Carrier buffer – PBS (100 mM), pH 7.4, flow rate 0.1 mL/min.

exhibited from the interaction of the antibody coupled quartz crystal with the carrier buffer (PBS 100 mM, pH 7.4) at a flow rate of 0.1 mL/min. Good dynamic range was obtained for SRT in PBS from 0.3 to 300 ng/mL with linear range of 0.3–10 ng/mL. The correlation coefficient ( $R^2$ ) of the biosensor performance in PBS was 0.994 with % R.S.D. ( $n=3$ ) 0.23–2.13 and the linear equation was  $y = 67.0564x$  (ng/mL) + 202.64. Furthermore, the usefulness of the developed biosensor was also evaluated in the milk sample by analyzing 1:4 diluted milk with PBS. Known concentrations of SRT

(0.001–300 ng/mL) were spiked in the diluted milk samples to construct a calibration graph. A good dynamic range was obtained in SRT spiked milk from 0.3 to 300 ng/mL with linear range of 0.3–50 ng/mL. The correlation coefficient of the developed biosensor in milk was found to be 0.997, with % R.S.D. ( $n=3$ ) 0.13–1.10 and the linear equation was  $y = 64.024x$  (ng/mL) + 205.4033. Based on the calculation of baseline peak to peak noise root mean square (RMS) i.e. 6.7 and the sensitivity of the calibration curve i.e. 67.0564 ng/mL for PBS and 64.024 ng/mL for milk, the minimum

limit of detection for SRT in PBS and milk was determined as 0.3 ng/mL. The obtained results are presented as Fig. 4a(i) and (ii) for PBS and milk respectively. Sensitivity and the detection range of the developed biosensor is attributed to the affinity interaction between the antibodies and the antigen, since the specific monoclonal antibody against SRT was immobilized on the SAM surface which selectively graft the target analyte (SRT). To support the ultrasensitive detection of the developed biosensor, screen shot for real time binding of mAb-SRT to SRT (0.1 ng/mL and 1 ng/mL) have been provided in the supplementary section as supplementary Figs. S4 and S5 respectively. Actual readings were plotted for baseline of functionalized gold crystal and mAb-SRT immobilized crystal together with response of 0.001 and 0.005 ng/mL SRT and presented as Fig. 4b(i). For comparison, actual interaction data of 0.01, 0.1, 0.5 ng/mL and 1 ng/mL SRT spiked milk were also plotted and presented as Fig. 4b(ii). Obtained real time mass change ( $\Delta m$ ) and cumulative mass change values for baseline (functionalized gold crystal and mAb-SRT immobilized crystal) and SRT (0.001, 0.005, 0.01, 0.1, 0.5 and 1 ng/mL) spiked milk have also been included in the supplementary section as supplementary Table ST3. The dissociation constant ( $K_d$ ) for SRT spiked in PBS and milk with immobilized mAb-SRT on modified gold crystal was determined using ligand binding kinetics in sigma plot 11.0.0 and found to be  $1.33 \times 10^{-10}$  M and  $1.161 \times 10^{-10}$  M for PBS and milk respectively.

### 3.4. Cross reactivity

Cross-reactivity studies were performed to check the group specificity of the developed biosensor against the most structurally similar molecule dihydrostreptomycin (DHSRT) and other three non-targeted aminoglycosides namely gentamycin (GENTA), neomycin (NEO) and kanamycin (KANA). Apart from aminoglycosides, one sulfonamide e.g. sulphadiazine (SDZ) was also tested for cross reactivity, which is commonly used in veterinary medicine and may present in milk (Mishra and Bhand, 2012). Cross-reactivity was tested in 1:4 diluted milk samples using 10 ng/mL standard

solutions of above mentioned antibiotics. mAb-SRT immobilized crystal was fixed on flow cell and solutions of different antibiotics were passed individually through the FIA system at the flow rate of 0.1 mL/min. As shown in supplementary Table ST1, very high cross-reactivity was obtained for SRT and DHSRT (100% and 93.8% respectively) on mAb-SRT immobilized gold crystal, which contains more related structure with SRT. Other aminoglycosides e.g. GENTA, KANA and NEO showed no significant cross reactivity with mAb-SRT antibody and obtained results were less than 0.1% for all the three aminoglycosides. Similarly, no cross-reactivity was observed with SDZ. Fig. 4c shows the real time response for cross reactivity with different antibiotics. Obtained results demonstrate that there is no significant interference produced by any other non-targeted antibiotics, which may commonly be present in the milk. The results indicate the remarkable specificity of the developed FIA-EQCN biosensor.

### 3.5. Recovery studies from spiked milk samples

The potential application of developed FIA-EQCN biosensor has been tested for the detection of SRT in the diluted milk samples. Initially, all the milk samples were assumed to be free of SRT. Known amount of SRT (1 ng/mL) was spiked in the diluted milk samples from the prepared stock solution. Based on the response signals recorded from FIA-EQCN biosensor, recoveries were calculated. Supplementary Table ST2 shows the % recovery obtained for SRT spiked milk samples. The recoveries obtained (98–99.33%) from the developed biosensor indicates the potential application of the FIA-EQCN biosensor for the ultra-sensitive detection of SRT in milk sample

### 3.6. Precision of FIA-EQCN biosensor performance

Precision of developed biosensor was tested by determining intra and inter run analysis on the same modified gold quartz crystal immobilized with mAb-SRT antibody and with the diverse sets of immobilized crystals. A known amount of SRT

**Table 2**  
Analytical performance and validation of FIA-EQCN biosensor.

Repeatability of FIA-EQCN SRT biosensor on same crystal									
SRT concentration [ng/mL]	Response-1 ( $\Delta$ ng)	Response-2 ( $\Delta$ ng)	Response-3 ( $\Delta$ ng)	Response-4 ( $\Delta$ ng)	Response-5 ( $\Delta$ ng)	S.D. $\pm$ Mean (n=5)	% R.S.D.		
10	279.461	280.951	280.1	278.91	281.2	280.12 $\pm$ 0.9	0.351		
Reproducibility and performance of FIA-EQCN SRT biosensor on different crystals									
Sensors	SRT Concentration [ng/mL]	Response-1 ( $\Delta$ ng)	Response-2 ( $\Delta$ ng)	Response-3 ( $\Delta$ ng)	S.D. $\pm$ Mean (n=3)	% R.S.D.			
Sensor-1	10	279.40	280.94	280.10	280.15 $\pm$ 0.7	0.2781			
Sensor-2	10	280.65	281.20	279.64	280.496 $\pm$ 0.7	0.282			
Sensor-3	10	279.60	280.34	281.34	280.43 $\pm$ 0.8	0.310			
Sensor-4	10	281.56	280.40	280.00	280.654 $\pm$ 0.8	0.290			
Sensor-5	10	279.84	281.781	282.94	281.52 $\pm$ 1.5	0.5581			
Comparison of FIA-EQCN SRT biosensor with commercial kit									
Milk sample	SRT added [ng/mL]	SRT found (n=3)		Mean $\pm$ S.D. (n=3)		% RSD		% Recovery	
		FIA-EQCN	Commercial kit	FIA-EQCN	Commercial kit	FIA-EQCN	Commercial kit	FIA-EQCN	Commercial kit
Milk-1	10.0	10.03	10.02	10.03 $\pm$ 0.06	10.02 $\pm$ 0.1	0.601	1.60	100.3	100.2
Milk-2	10.0	9.971	9.871	9.971 $\pm$ 0.1	9.871 $\pm$ 0.1	1.502	1.31	99.70	98.70
Milk-3	10.0	10.02	10.06	10.02 $\pm$ 0.09	10.061 $\pm$ 0.1	0.901	1.781	100.21	100.61
Milk-4	10.0	10.13	10.11	10.13 $\pm$ 0.1	10.11 $\pm$ 0.1	1.381	1.281	101.30	101.10

concentration (10 ng/mL) was spiked in the diluted milk sample and successively analyzed for biosensor performance ( $n=5$ ). The baseline was corrected before each analysis and mass change ( $\Delta m$ ) was calculated based on the obtained responses. The biosensor showed a good reproducibility in  $\Delta m$  values with Standard deviation of  $280.13 \pm 0.9$  and calculated % R.S.D ( $n=5$ ) 0.351 within the same crystal. Similarly, the biosensor performance was tested on diverse sets of immobilized crystals. Satisfactory results were obtained for SRT analysis in diluted milk samples when analyzed using different sets of biosensor. The % R.S. D. ( $n=5$ ) was found in range of 0.2781–0.5581. The obtained results were summarized in the Table 2. These results indicate the precision and reproducibility of the biosensor thus can be used as potential tool for analysis of SRT in milk samples.

### 3.7. Validation of FIA-EQCN biosensor

The results obtained from the FIA-EQCN measurements were cross-validated against commercial ELISA kit. Different diluted milk samples were spiked with a known amount of SRT (10 ng/mL) and analyzed through the developed biosensor and commercial ELISA kit. Analysis was performed to determine % recovery for obtained results. The recoveries obtained from the FIA-EQCN biosensor (99.70–101.30%, % R.S.D. ( $n=3$ ) 0.601–1.502) was more or less similar to the results obtained from the ELISA kit (98.70–101.10%, % R.S.D. ( $n=3$ ) 1.281–1.781). It is evident from the Table 2 that the obtained results from both the methods show good co-relation in terms of sensitivity and reproducibility. The developed biosensor is reliable and as precise as the commonly used ELISA method.

## 4. Conclusion

A FIA-EQCN biosensor was developed and demonstrated for analysis of SRT residues in milk samples. Specific monoclonal antibody against SRT was immobilized on the gold crystals after SAMs formation. The developed biosensor could detect an ultra-trace level of (0.001 ng/mL) in milk samples. A good reproducibility was obtained with Standard deviation of  $280.13 \pm 0.9$  and calculated % R.S.D. ( $n=5$ ) 0.351 within the same crystal and % R.S. D. ( $i=5$ ) in range of 0.2781–0.5581 on diverse set of crystals. Precision of these results showed the reproducibility and reliability of the biosensor. The obtained recoveries (98–99.33%) for SRT spiked milk samples encourage the application of developed biosensor towards the quantification of SRT in milk sample. Validation of the presented biosensor against commercial ELISA kit (BioScientific, USA) also proves that developed biosensor provides much sensitive detection (0.3 ng/mL) as compare to the commercial kit (5 ng/mL). The developed biosensor could complete the analysis in less than 17 min. and exhibited a great potential for automated analysis. This approach may become practical for routine automated analysis for detection of SRT in milk samples.

## Acknowledgment

This work financially supported under NAIP Project no. C4/C30032 (ICAR) and partly under NFBSFARA Project no. PHT-4007/2013-14, funded by ICAR (India). G.K.M. thanks NAIP for Research Associate Fellowship and A.S. would like to thank NFBSFARA for

Senior Research Fellowship. Authors would like to thank the reviewers for their valuable inputs to improve the quality of manuscript.

## Appendix A. Supplementary information

Supplementary data associated with this article can be found in the online version at <http://dx.doi.org/10.1016/j.bios.2014.09.033>.

## References

- Abuknesha, R.A., Luk, C., 2005. *Analyst* 130, 964–970.
- Ahmed, A., Rushworth, J.V., Wright, J.D., Milner, P.A., 2013. *Anal. Chem.* 85, 12118–12125.
- Baxter, G.A., Ferguson, J.P., O'Connor, M.C., Elliott, C.T., 2001. *J. Agric. Food Chem.* 49 (7), 3204–3207.
- Benjing, C., Hongyan, Z., Baoxiang, L., Jing, G., Lihong, Q., 2012. *J. AOAC Int.* 95 (2), 523–527 (5).
- Bilandžić, N., Kolanović, B.S., Varenina, I., Jurković, Z., 2011. *Mljekarstvo* 61 (3), 260–267.
- Brujnsvoort, M.V., Ottink, S.J.M., Jonker, K.M., Boer, E.D., 2004. *J. Chromatogr. A* 1058, 137–142.
- Ce, Y.B., Songyang, L., Peng, Z., Hong, L.X., 2008. *Food Chem.* 106, 797–803.
- Commission Regulation (EU) No. 37/2010, 22 December 2009. *Off. J. Eur. Union* L15/1.
- Conzuelo, F., Gamella, M., Campuzano, S., Pinacho, G., Reviejo, A.J., Marco, M.P., Pingarrón, J.M., 2012. *Biosens. Bioelectron.* 36 (1), 81–88.
- Conzuelo, F., Campuzano, S., Gamella, M., Pinacho, D.G., Reviejo, A.J., Marco, M.P., Pingarrón, J.M., 2013. *Biosens. Bioelectron.* 50, 100–105.
- Currie, D., Lynas, L., Kennedy, D.G., McCaughey, M.J., 1999. *Food Addit. Contam.* 15, 651–660.
- Edder, P., Cominoli, A., Corvi, C., 1999. *J. Chromatogr. A* 830 (2), 345–351.
- Ferguson, J.P., Baxter, G.A., McEvoy, J.D.G., Stead, S., Rawlings, E., Sharman, M., 2002. *Analyst* 127, 951–956.
- Haasnoot, W., Ploum, M.B., Kohen, F., 2003. *Anal. Chim. Acta* 483 (1–2), 171–180.
- Heering, W., Usleber, E., Dietrich, R., Meartlbauer, E., 1998. *Analyst* 123, 2759–2762.
- Holford, T.R.J., Holmes, J.L., Collyer, S.D., Davis, F., Higson, S.P.J., 2013. *Biosens. Bioelectron.* 44, 198–203.
- Kaya, S.E., Filazi, A., 2010. *Kafkas Univ. Vet. Fak. Derg.* 16, S31–S35.
- Knecht, B.G., Strasser, A., Dietrich, R., Martlbauer, E., Niessner, R., Weller, M.G., 2004. *Anal. Chem.* 76, 646–654.
- Liu, B., Zhang, B., Cui, Y., Chen, H., Gao, Z., Tang, D., 2011. *ACS Appl. Mater. Interfaces* 3, 4668–4676.
- Malatesta, C., Picca, R.A., Mazzotta, E., Guascito, M.R., 2012. *Electroanalysis* 24, 790–797.
- Mishra, G.K., Bhand, S., 2012. In: *Proceedings of the IEEE Sixth International Conference on Sensing Technology (ICST)*, pp. 672–676.
- Park, I.S., Kim, D.K., Adanyi, N., Varadi, M., Kim, N., 2004. *Biosens. Bioelectron.* 19, 667–674.
- Pyun, C.W., El-Aty, A.M.A., Hashim, M.M.M., Shim, J.H., Lee, S.K., Choi, K.D., Park, K. H., Shin, H.C., Lee, C., 2008. *Biomed. Chromatogr.* 22, 254–259.
- Que, X., Liu, B., Fu, L., Zhuang, J., Chen, G., Tang, D., 2013. *Electroanalysis* 25 (2), 531–553.
- Raz, S.R., Bremer, M.G.E.G., Haasnoot, W., Norde, W., 2009. *Anal. Chem.* 81, 7743–7749.
- Samsonova, J.V., Bashkurov, M.L., Ivanova, N.L., Rubtsova, M.Y., Egorov, A.M., 2005. *Food Agric. Immunol.* 16 (1), 47–57.
- Silva, M.M.S., Cavalcanti, I., Barroso, M.F., Sales, M.G.F., Dutra, R.F., 2010. *J. Chem. Sci.* 122 (6), 911–917.
- Strasser, A., Dietrich, R., Usleber, E., Märtlbauer, E., 2003. *Anal. Chim. Acta* 495, 11–19.
- Wang, S., Zhang, H.Y., Wang, L., Duan, Z.J., Kennedy, I., 2006. *Food Addit. Contam.* 23 (4), 362–384.
- Wu, J.X., Zhang, S.E., Zhou, X.P., 2010. *J. Biomed. Biotechnol.* 11 (1), 52–60.
- Wutz, K., Niessner, R., Seidel, M., 2011. *Microchim. Acta* 173, 1–9.
- Yang, D.H., Bae, A.H., Koumoto, K., Lee, S.W., Sakurai, K., Shinkai, S., 2009a. *Sens. Actuators B: Chem.* 105, 490.
- Yang, Y., Long, Y., Li, Z., Li, N., Li, K., Liu, F., 2009b. *Anal. Biochem.* 392, 22–27.
- Ye, B., Li, S., Zuo, P., Li, X., 2008. *Food Chem.* 106, 797–803.
- Zhang, L., Liu, Y., Chen, T., 2009. *Microchim. Acta* 164, 161–166.
- Zhu, W.X., Yang, J.Z., Wei, W., Liu, Y.F., Zhang, S.S., 2008. *J. Chromatogr. A* 1207 (1–2), 29–37.
- Zhou, N., Wang, J., Zhang, J., Li, C., Tian, Y., Wang, J., 2013. *Talanta* 108, 109–116.



# Biosensor for Urea Analysis in adulterated milk

Geetesh K. Mishra<sup>1</sup> and Sunil Bhand<sup>2</sup>

Birla Institute of Technology & Science, Pilani-KK Birla Goa Campus, Goa 403 726

THE Indian Council of Medical Research in a report had mentioned that urea and detergents in milk caused severe health problems like indigestion, acidity, ulcers, cancers, malfunctions of kidney, etc. Hence, the demand for estimation of urea adulteration in milk is of great significance. According to the several survey on milk adulteration conducted by Food Safety and Standards Authority of India (FSSAI) in 2011-13 it was reported that around 65-70% of milk sample are adulterated with urea, detergents, water, skimmed milk etc. Several techniques are available to detect the levels of urea in milk but they are not capable enough to detect them in very low or very high level. Enzyme thermistor integrated with flow injection analysis system (FIA-ET) has been used for the development of the urea biosensor. As an open platform, enzyme thermistor provides enough scope for further development and innovations. The ET is usually based on an immobilized enzyme

column also called as the "immobilized enzyme reactor" placed in a flow-injection system.

The present study is aimed to analyze the adulteration of urea in packaged milk, supplied in local market of Goa, India. Seven leading brands have been selected randomly and milk samples of low fat content (3%) were collected. The survey was conducted using FIA-ET urea biosensor, commercially available colorimetric enzymatic urea assay kit and Association of Analytical Communities (AOAC) method for urea analysis in animal feed. The total no of seven samples analyzed in triplicate during measurement in which all samples were found within the permissible limit as per FSSAI. Urea recoveries are found in range for FIA-ET (98.96-105.15%), AOAC (98.93-105.13%) and kit (98.48-103.40%). The methods were also compared for their analytical performance, sensitivity, reproducibility and FIA-ET Biosensor found to be most suitable for analysis of urea adulterated milk samples.

## Experiment

### Enzyme Column Reactor

Enzyme immobilization on amine functionalized CPG beads was achieved by glutaraldehyde cross linking as reported earlier with slight modifications. In brief, enzyme urease was covalently immobilized on functionally modified CPG beads according to the following procedure: 352 mg of amine functionalized CPG was activated with 2.5% glutaraldehyde in 100 mM PB, pH 7.2 in a 2 ml capacity centrifuge tube. The reaction was allowed to take place for at least 1h inside the desiccators, under reduced pressure. The activation of amine functionalized CPG beads support was confirmed by presence of brick red color (i.e. formation of Schiff's base). Activated amine functionalized CPG beads were successively washed with double distilled water (ddH<sub>2</sub>O) and buffer (PB). Urease 200 mg (1000 IU) was dissolved in 1mL PB was added to the wet activated amine

---

*Milk, one of the most complete food available in nature for human consumption, contains all nutrients in balanced proportions to meet the demand of human health. Being a global food of supply chains, good quality milk is required for quality dairy products. The raw milk with adulterants is taken as defective and cannot be processed for dairy products. Adulteration of milk is a serious concern in the developing countries like India. Urea is a normal constituent of milk, serve as solid not fat (SNF) content found as commonly used adulterant in synthetic and natural milk. Normal concentration of urea in milk is 20-70 mg/dl. The most common reason given for adulteration is the difference between demand and supply of milk. In order to meet the demand, the suppliers usually adulterate the milk and increase the quantity. These adulterants are hazardous and cause irreversible damage to the organs.*

---



Pictorial representation of experimental set-up for FIA-ET biosensor for urea analysis in milk

functionalized CPG beads. The coupling reaction was allowed to proceed for 30 min at room temperature and overnight at 4°C with gentle shaking. The enzyme preparation was washed with buffer solution. Tri-ethanolamine (200 mM) was added to terminate the all unreacted groups and then washed with 100 mM PB, pH 7.2. The immobilized urease was finally packed into a delrin column by a slurry packing method for use.

**Milk sample collection:** Milk samples of different brands of low fat content (3.0%) were purchased from local market of Goa, India. The matrix effect in the analysis of urea in milk sample was investigated and appropriate dilutions of milk with buffer were made. During this work, it was observed that 1:6 dilution of milk sample with buffer was most appropriate for urea analysis. To obtain the calibration curve for urea in spiked milk samples, a simple dilution strategy worked out to avoid the effect of ionic strength and pH on urease column. In that, milk samples were centrifuged (at 6000 rpm for 20 min), diluted then filtered through 0.22 µm filter. Analysis for spiked milk samples were carried out within the same day after sample preparation.

**Instrumentation:** The experimental set up consists of a peristaltic pump (Gilson Minipuls Evolution II, France), an 6 port injection valve (Rheodyne, USA), sample loop

(0.1 mL), enzyme thermistor, Wheatstone bridge equipped with a chopper-stabilized amplifier (ET-2010-2, Omic Bioscience, Sweden) and Pico logger data recorder (Picotech, UK). PTFE tubing's (0.8 mm id) were used for the connection. 100 mM PB, pH 7.2 was used as the carrier buffer.

**Procedure for FIA-ET urea biosensor:** For urea analysis, calibration standards (1-500 mM) were prepared by dilution of urea stock solution (500 mM) in 100 mM PB, pH 7.2. The immobilized column was mounted inside ET and carrier buffer was passed at optimum flow rate of 0.5 mL/min at which a stable baseline was achieved. The spiked milk samples were injected and data were recorded in real time using a data acquisition system connected to the Wheatstone bridge. All measurements were carried out by injection of 0.1 mL sample at a flow rate of 0.5 mL/min. After each sample analysis, the sample loop was thoroughly rinsed with buffer. The milk samples spiked with known amount of urea were injected in to the FIA-ET system.

**Urea enzymatic assay kit:** To validate the earlier developed FIA-ET urea biosensor, the milk samples were analyzed by using commercial colorimetric kit. Urea measurement was performed as per the given protocol provided. The measurement of urea based on enzymatic hydrolysis by urease

enzyme which convert urea into ammonia. The colorimetric measurement was performed by using colorimetric multiplate reader (PerkinElmer, USA) at 620 nm.

**AOAC method:** The developed FIA-ET urea biosensor was further evaluated with AOAC approved method. Measurement was based on colorimetric reaction of *p*-Dimethyl amino benzaldehyde solution with milk sample denatured by trichloroacetic acid (24% w/v). All measurement was done using spectrophotometer at 420 nm.

**Recovery studies from spiked unknown milk samples:** A known amount of urea standard was spiked to diluted unknown milk sample and analyzed in FIA-ET biosensor. Recoveries were calculated from the obtained response signal. Table 1 shows the recovery results obtained for milk urea. Excellent recoveries were obtained in the range 98.96–105.15% in the spiked milk samples. This ensures the reliability of the developed biosensor, recovery studies were further validated with commercial kit and AOAC method found to be 98.48-103.40 and 98.93-105.13 % respectively. The results obtained confirm the reproducibility and sustainability of EIA-ET urea biosensor.

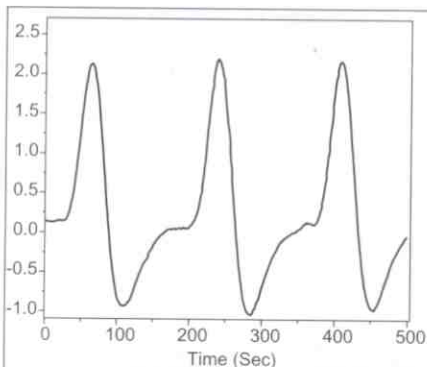
In order to determine the reliability and reproducibility of the developed urea biosensor, several measurements were performed in triplicate. As shown in the figures the real time triplicate sensor signal

**Table 1.** Recovery studies for urea from FIA-ET, Commercial Kit and AOAC method. Each sample done in triplicate, thrice in a day (total number of analysis is n=9)

Milk sample	Added Urea [mM]	Urea Found			% RSD			% Recovery		
		FIA-ET	Commercial Kit	AOAC	FIA-ET	Commercial Kit	AOAC	FIA-ET	Commercial Kit	AOAC
1	200	204.03	200.70	201.66	0.58	0.30	0.35	102.01	100.35	100.83
2	200	204.40	201.88	204.40	0.08	0.15	0.29	102.20	100.94	102.20
3	200	201.73	200.66	201.50	0.33	0.27	0.35	100.86	100.33	100.75
4	200	210.30	204.66	210.27	0.22	0.24	0.19	105.15	102.33	105.13
5	200	197.93	198.00	197.86	0.21	0.30	0.21	98.96	99.00	98.93
6	200	208.13	206.80	207.73	0.15	0.42	0.20	104.06	103.40	103.86
7	200	198.73	196.97	198.67	0.25	0.25	0.21	99.36	98.48	99.33

**Table 2.** Comparison of analytical features and figure of merit of all three method used FIA-ET, Commercial Kit and AOAC

Techniques	FIA-ET Biosensor	Commercial Enzymatic Assay Kit	AOAC method
Method	Thermal Biosensor-immobilized Enzyme based	Colorimetric-Enzyme based	Colorimetric/spectrophotometric
Stability	Up to 2 year	6 Months	Not mentioned
Format	Enzymatic	Enzymatic	Liquid/Chemical based
Instrument	Enzyme thermistor	Multiplate reader	Spectrophotometer
Sensitivity	1 mM	8 ppm	8 mM
Limit of detection	1 mM	20 ppm	25 mM
Precision	Intra/Inter-assay %C.V.'s typically <3%	Intra/Inter-assay %C.V.'s typically <3%	Intra/Inter-assay %C.V.'s typically <3%
R <sup>2</sup>	0.99	0.98	0.97



Real time triplicate sensor signal recorded from FIA-ET urea biosensor for 0.1mL sample of 200 mM urea, flow rate 0.5mL min<sup>-1</sup> at 30°C in spiked milk sample.

has been recorded from FIA-ET urea biosensor on urea spiked milk sample. The obtained signal confirms reproducibility of the sensor response. Table 2 represents the analytical figures of merit and

comparison of the developed biosensor with other used techniques.

### CONCLUSION

In the present study, based on the random sampling and analysis of commercial milk samples conclusion may be drawn that quality of packaged milk, supplied in local market of Goa, India are found to be as per standards of regulatory authorities and hence no urea adulteration is in practice. The results of the study shows that levels of urea in milk samples are found in minimal range (0.66-10.30mM), which is below the recommended levels as per FSSAI (11.6 mM). However, the present studies were conducted only for packaged milk samples of leading

brands in Goa. In the report, commercial colorimetric kit, AOAC method for urea analysis and earlier developed FIA-ET urea biosensor by the study group shows equally good results. These observations strongly suggest that the FIA-ET biosensor is sensitive, reliable and very robust analytical techniques that can be used to monitor the levels of urea in milk. Moreover, the commercial kit could detect urea levels as high as 1000 PPM (16.7 mM), whereas the FIA-ET biosensor can measure up to 500 mM urea in milk samples. The obtained result promises that the FIA-ET biosensor could be an effective analytical tool for routine analysis of milk samples for urea adulteration.

### SUMMARY

A study was done to analyze the adulteration of urea in packaged milk, supplied in the local market in Goa. Seven leading brands of milk were selected randomly. The total number of samples used in triplicate for urea analysis in animal feed. All samples were found within the permissible limit as per FSSAI (Food Safety and Standards Authority of India).

<sup>1</sup> Biomass Laboratory Department of Chemistry, <sup>2</sup> Professor





# A label free impedimetric immunosensor for detection of *Escherichia coli* in water

Geetesh K Mishra<sup>a,#</sup>, Gautam Bacher<sup>a,b,#</sup>, Utpal Roy<sup>c</sup>, Sunil Bhand<sup>a,\*</sup>

<sup>a</sup> Biosensor Lab, Department of Chemistry, BITS, Pilani-K.K. Birla Goa Campus, Goa 403726, India

<sup>b</sup> Department of EEE & I, BITS, Pilani-K.K. Birla Goa Campus, Goa 403726, India

<sup>c</sup> Department of Biological Sciences, BITS, Pilani-K.K. Birla Goa Campus, Goa 403726, India

<sup>#</sup> Authors with equal contribution

\* Author for correspondence: Sunil Bhand, email: sunilbhand@goa.bits-pilani.ac.in

Received 11 May 2014; Accepted 21 Jun 2014; Available Online 21 Jun 2014

## Abstract

In the presented work, a simple and sensitive impedimetric immunosensor based on silver (Ag) wire electrode for the detection of *Escherichia coli* microbial type culture collection-723 strain (*E. coli* MTCC 723) in water is reported. The sensor was constructed by functionalizing Ag-micro wire coupled with polyclonal antibodies of *E. coli* through self-assembled monolayers of cysteaminium. The biosensor detected the change in impedance caused by the presence of *E. coli* bacteria immobilized on Ag-micro wire electrodes. The antigen-antibody interaction was quantified by measuring impedance in the frequency range (1–100 Hz) at 10 mV applied potential. A dynamic range ( $10^2$  colony forming units/mL (CFU/mL) -  $10^8$  CFU/mL) for *E. coli* was obtained with 10 min analysis time. The limit of quantitation of the developed biosensor and lower limit of detection is  $10^2$  CFU/mL. The proposed method is useful for sensitive analysis of *E. coli* in water samples.

**Keywords:** Water; Bacteria; Label-free detection; Electrochemical impedance spectroscopy; Silver wire; Immunosensor

## 1. Introduction

Detection of contaminated water by pathogenic microorganism is an important concern for ensuring water safety, security and public health. A clean and treated water supply to each house may be the norm in Europe and North America, but in developing countries, access to both clean water and sanitation are not in the prime focus thus waterborne infections are common. Two and a half billion people have no access to improved sanitation, and more than 1.5 million children die each year from water borne diarrheal diseases [1]. According to the WHO, the mortality of water associated diseases exceeds 5 million people per year. From these, more than 50% are microbial intestinal infections [2]. *Escherichia coli* (*E. coli*) is a natural inhabitant of the intestinal tracts of humans and warm-blooded animals. The presence of this bacterium in water indicates that fecal contamination may have occurred and consumers might be exposed to enteric pathogens when consuming water. Hence, *E. coli* is often preferred as an indicator organism because it is specifically stands for fecal contamination [3]. Rapid and reliable detection of *E. coli* is critical for the management of the waterborne diseases threatening human lives worldwide. The occurrence of potential *E. coli* is extensively studied in water resources in the developing world, since it is an important health concern as a large population depends on both processed and unprocessed surface waters for drinking and domestic purposes [4]. Despite the potential public health threat from waterborne *E. coli*, there are no accepted methods for the rapid, accurate detection in surface waters. Current measures of microbial water quality rely exclusively on “indicators” of fecal pollution (e.g., fecal coliform bacteria or generic *E. coli*). However, there are no established correlations between the prevalence or concentration of these “indicators” and specific pathogens [5].

Conventional methods for bacterial identification usually involves various culturing techniques and different biochemical tests which are very time consuming and usually requires 2-4 days. Hence, there is a need for adequate monitoring technologies targeting representative pathogenic bacteria like *E. coli* at low levels within hours to prevent mortality and morbidity caused by waterborne outbreaks. The effective testing of bacteria requires methods of analysis that meet a number of challenging criteria. Analysis time and sensitivity are the most important limitations related to the usefulness of bacterial testing. An extremely selective detection methodology is also required, because low numbers of pathogenic bacteria are often present in a complex biological environment along with many other non-pathogenic bacteria [6]. Tedious and time consuming detection methods has prompted several groups in the recent years to develop other techniques to reduce the detection time like Polymerase Chain Reaction (PCR) and Enzyme Linked Immunosorbent Assay (ELISA). However, both techniques have limitations that exclude their widespread implementation. These limitations include accurate primer designing, requirement of specific labeled secondary antibody and their failure to distinguish spore viability [7-10]. Biosensor techniques are particularly attractive for the detection and identification of pathogenic organism since they have potential sensitivity and selectivity. They are easy to use, provides results in few minutes, require minimal reagents, and can be deployed in fields.

In recent years, several biosensors techniques have played important roles in detection of pathogenic bacteria in different matrices. Among them immuno-sensors and DNA-based biosensors are mostly used. A variety of immuno-sensors have been developed based on the antibody of the target bacteria, which utilizes fluorescence [11],

electrochemical impedance spectroscopy (EIS) [12,13], quartz crystal microbalance (QCM) [14] and surface plasmon resonance (SPR) [15]. However, these biosensors lack in practical applications because of their single use nature and instability of antibodies in unfavorable conditions. Moreover, DNA-based biosensors require efficient DNA extraction and need DNA amplification using PCR as bacterial cells contain a low copy number of DNA [16,17]. Among the reported biosensors, EIS has emerged as sensitive techniques for bacterial detection due to multiple advantages, such as fast response, low cost, and capability of miniaturization. EIS based sensors are particularly attractive since they allow label-free detection with high sensitivity [18]. In EIS, traditionally, macro sized metal rods or wires were used as electrodes immersed in the medium to measure impedance and it is suitable to analyze the electrical properties of the modified electrode, i.e. when an antibody coupled to the electrode reacts with the antigen of interest [19,20]. Radke *et al* reported an impedimetric biosensor with micro electromechanical systems (MEMS) technology integrated with biosensing methods to detect whole *E. coli* bacterial cells in food and water [21]. More recently, Queirós *et al* developed a label free DNA aptamer biosensor incorporated in a biochip and used for in situ detection of *E. coli* outer membrane protein in water samples [22]. These reported techniques support the fact that the EIS with label free approach is cost-effective because it does not require any labels, expensive instrumentation and allows portability.

The surface chemistry of the biosensor to immobilize biological receptors is an important factor affecting detection sensitivity and specificity. Various surface chemistry techniques has been developed for their applications as platforms for antibody-based biosensors. Self-assembled monolayer's (SAMs) have been investigated extensively since they provide a means for the molecular design on a bio-inert surface with specific functions. They were exploited to provide model surfaces for investigating cell behavior in bioanalysis. The design flexibility of the SAMs technique allows the immobilization of biological macromolecules and living organisms, such as cells, proteins, antibodies, and DNA, on different substrates. Thiol SAMs are widely used mainly on gold and silver surfaces due to their many advantages: they are resistant to nonspecific adsorption and form a well-ordered and dense monolayer structure that can easily be prepared on a surface by mild incubation for a sufficient time [6, 21, 23]. Recently, relatively new techniques such as microfluidics and nanoparticle-based magnetic separations have been integrated with EIS biosensors with the purpose of improving bacterial detection efficacy [24-26].

Recently, our group developed a practical and highly sensitive, cost effective, label-free impedimetric immunosensor with the help of two-electrode system for ultra sensitive detection of aflatoxin M1 (AFM1) in milk using impedimetric immunosensor based on functionalized Ag-wire electrode [27].

In this work, we demonstrate a simple, cost effective, label-free impedimetric immunosensor for detection of *E. coli* in water exploring earlier reported two-electrode system. To test the biosensor performance as a proof of concept for bacterial detection, a generic strain of *E. coli* MTCC 723 was used as a surrogate for the waterborne pathogen Enterotoxigenic *E. coli* (ETEC). The immunosensor is based on the use of *anti-E. coli* polyclonal antibodies immobilized on the

Ag-wire electrode surface. The antibody immobilization and its ability to selectively graft *E. coli* on the sensing surface were fully characterized by fluorescence microscopy techniques. The developed immunosensor is highly sensitive, allowing for the detection of  $10^2 - 10^8$  CFU/mL of *E. coli* bacteria. This detection range is attributed to the affinity interaction between the antibodies and the antigen (*E. coli*).

## 2. Experimental Details

### 2.1. Reagents and instrumentation

Ag-wire (diameter = 0.25 mm) and Bovine serum albumin (BSA) was procured from ACROS Organics, USA. Polyclonal antibody to *E. coli* raised from goat (2 mg/mL) (*pAb-E. coli*) and Fluorescein isothiocyanate (FITC) labeled polyclonal antibody against *E. coli* raised from rabbit (0.75 mg/ml) was purchased from AbCam, UK. Sodium dihydrogen phosphate monohydrate, disodium hydrogen phosphate monohydrate, sodium chloride, 11-mercaptoundecanoic acid (11-MUA), 1-ethyl-3-[3-dimethylaminopropyl] carbodiimide hydrochloride (EDC), N-hydroxy succinimide (NHS), ethyl alcohol 200 proof was purchased from TEDIA, USA. Glutaraldehyde solution 25%, sodium chloride, glycine and cysteaminium chloride were obtained from Merck (Germany). L-cysteine hydrochloride was procured from Himedia labs India. For sample handling, micropipettes (eppendorf®, Germany) were used. All the solutions were prepared in a 0.22  $\mu$ m membrane filtered Milli-Q system RO water (Millipore, Bedford, MA, USA), Seven Multi pH meter (Mettler Toledo, 8603, Switzerland) was used for pH measurements. All other chemicals used were of analytical grade and used as received. Certified ultra high pure nitrogen (99.9%), pH meter (Seven Multi Mettler Toledo, 8603, Switzerland) were used. Fluorescence images were taken on upright microscope (BX-51Olympus, Japan). Impedance measurements were carried out using IVIUM CompactStat impedance analyzer, Netherland. All the bacterial sample handling and dilutions were done under biosafety cabinet class II type B2 (NuAire, USA).

### 2.2. Preparation of buffers and other solutions

0.1 M phosphate buffered saline (PBS) was prepared by dissolving appropriate amount of  $\text{Na}_2\text{HPO}_4$ ,  $\text{NaH}_2\text{PO}_4$  containing 0.0027 M potassium chloride and 0.137 M sodium chloride. The pH of the buffer was adjusted to 7.4. All buffer solutions were stored at 4<sup>o</sup> C when not in use.

### 2.3. Experimental set-up

The experimental set-up consist of a pair of pre-functionalized Ag-wire electrode immersed in the single well of Nunc 384 polystyrene well plate (obtained through Sigma Aldrich, USA) (capacity 120  $\mu$ L/well) containing 90  $\mu$ L bacterial suspensions of different concentration. The operation of presented sensor was based on the pair of Ag-wire as an electrical transducer. The effective surface area of the Ag-wire electrode was calculated and found to be 7.85 mm<sup>2</sup>. The Ag-wire surface was functionalized with attached *pAb-E. coli* over the SAMs, to form a biological transducer. The binding of the bacterial cells to the biological transducer causes the change in impedance. This interaction was measured using two electrode set-up. The electrode set-up and the well plate were placed in a custom-made faraday cage to shield the electrodes from external electromagnetic sources. The schematic of

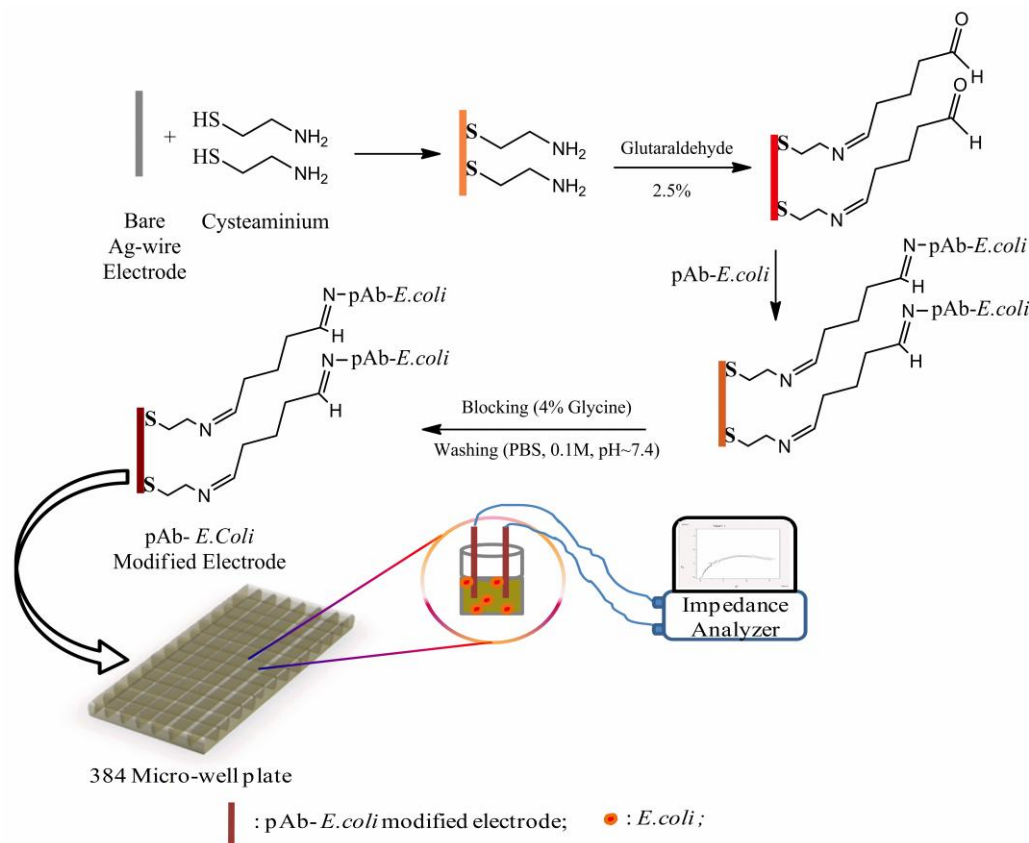


**Figure 1.** Schematic representation of Ag-wire electrode based impedimetric immunosensor with EIS measurement setup together with surface modification of Ag-wire electrode for immobilization of *E.coli* antibody.

experimental set-up is presented as Figure 1. In the presented set-up, the two pre-functionalized Ag-wire electrodes were dipped in to the micro well plate. The functionalized Ag-wire electrodes were connected to IVIUM CompactStat impedance analyzer in 4-Electrode mode controlled through software (IVIUM soft). In the 4-Electrode mode, the first electrode was configured as working electrode (working and sense electrode combined together) and second electrode was reference electrode (reference and counter combined together). The impedance change caused by antigen–antibody interactions at the electrode surface was measured at 1-100 KHz applied frequency and 10 mV applied potential.

#### 2.4. Immobilization of antibody to the Ag-wire surface

Initially the surfaces of the bare Ag-wire electrodes was washed ultrasonically in membrane filtered RO water for 5 min to remove inorganic particles. Following this, the electrodes were immersed into piranha solution (H<sub>2</sub>O<sub>2</sub>/H<sub>2</sub>SO<sub>4</sub>, 30/70 v/v) for 30 sec. The electrodes were washed with distilled water followed by drying under ultra pure nitrogen stream. This cleaning procedure was repeated before every step. The *pAb-E.coli* was covalently coupled on Ag-wire electrode through SAMs as described elsewhere [28] with some modifications. Firstly, the concentration of cysteaminium (CYST) was optimized and a set of clean Ag-wire electrode were immersed overnight into a solution of 10 mM CYST in 0.1 M phosphate buffer saline (PBS, pH 7.4) under ambient condition. The electrodes covered by SAMs were gently washed with RO water to remove any unbounded CYST residues. The electrodes were dried with nitrogen stream before use. For coupling the *pAb-E.coli*, the carboxyl group of SAMs on modified electrode was activated by incubated in

glutaraldehyde solution (2.5% v/v) for 30 min. Subsequently, the electrodes were washed with PBS to remove residual glutaraldehyde molecules. Finally, *pAb-E.coli* was attached to the electrode by carefully spreading the solution (1:1000 in PBS) over the activated surface followed by overnight incubation at 4 °C. To block reminiscent aldehyde groups the modified electrode surface was exposed to glycine solution (4% w/v) for 30 min and washed with PBS. The unused antibody coupled electrodes were washed and stored at 4 °C for future use. The schematic for immobilization of antibody to Ag-wire surface is presented in Figure 1 together with the schematic of experimental set-up.

#### 2.5. Bacterial culture and dilutions

The bacterial culture of *E. coli* (MTCC 723), *Salmonella infantis* (MTCC 1167) and *Streptococcus pyogenes* (MTCC 1928) used in the present study were procured from the microbial type culture collection and gene bank, IMTECH Chandigarh, India. The strains were grown aerobically for 16 h at 37 °C in Brain Heart Infusion broth, pH 7.40 ± 0.2 (BHI broth, Hi-Media, India). The bacterial cultures were maintained as frozen stock at -80 °C in BHI broth containing 15% (v/v) glycerol when not in use. The initial concentrations of the bacterial cultures were obtained using serial dilutions and plate counting methods. The concentration of *E. coli* (MTCC 723) is also confirmed by taking optical density at 600 nm (OD<sub>600</sub>) and found corresponding to bacteria concentration of 1.16 × 10<sup>9</sup> CFU/mL. The stock solution of bacterial concentration diluted serially in PBS to achieve the concentrations of calibration plot (1.16 × 10<sup>2</sup> to 1.16 × 10<sup>8</sup> CFU/mL).

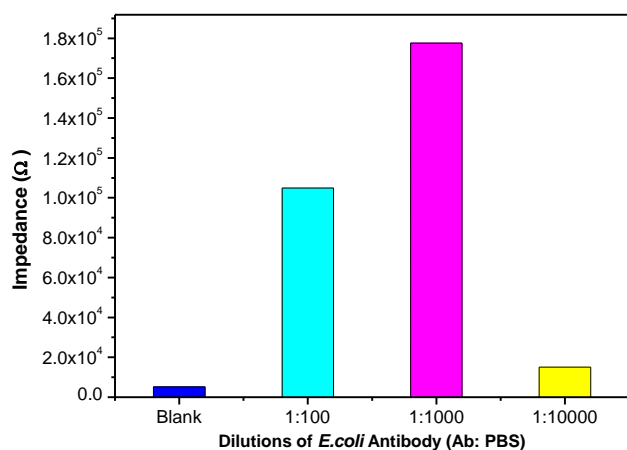


**Figure 2.** Impedance value at 10 Hz for dilutions of pAb-*E.coli* antibody with PBS (0.1 M, pH 7.4) for 10<sup>4</sup> CFU/mL *E.coli*.

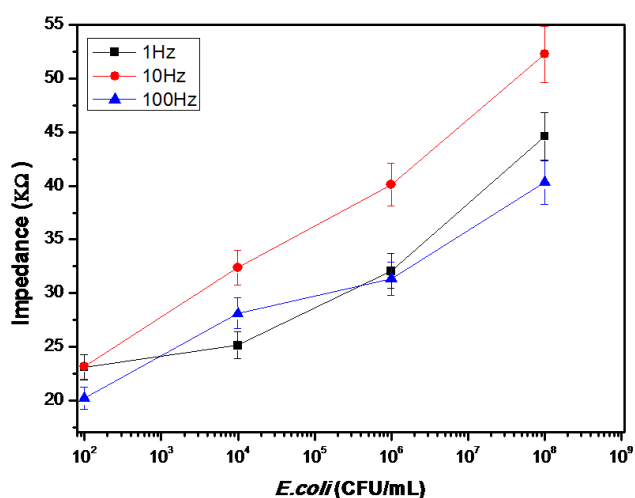


**Figure 3.** Impedance value for various concentration of *E.coli* at 1 Hz, 10 Hz and 100 Hz.

### 3. Results and Discussion

#### 3.1. Optimization of the immunosensor

##### 3.1.1. Optimization of antibody concentration

The binding of the *E.coli* and anti-*E.coli* antibody on the electrodes directly affects the sensitivity of the immunosensor. The amount of anti-*E.coli* antibody plays an important role in this process. The change in impedance of the immunosensor depends upon antigen- antibody binding and incubation time. Hence, the effect of both the parameters has been investigated. Several anti-*E.coli* dilution ratios with PBS were evaluated (1:100, 1:1000 and 1:10000) and the maximum change in impedance was recorded for dilution of 1:1000 as shown in Figure 2. Incubation time of 5 min was found to be optimal for impedance measurements. Thus, these optimized parameters were used for further investigations.

##### 3.1.2. Influence of applied frequency

Antigen-antibody interaction results in impedance change at the electrode and the electrode/electrolyte interface, known as interface impedance, which can be measured at different frequency ranges. The impedance measurement is conducted in the range of 1 Hz to 100 KHz. Since electrode impedance is dominated at low frequency, we have

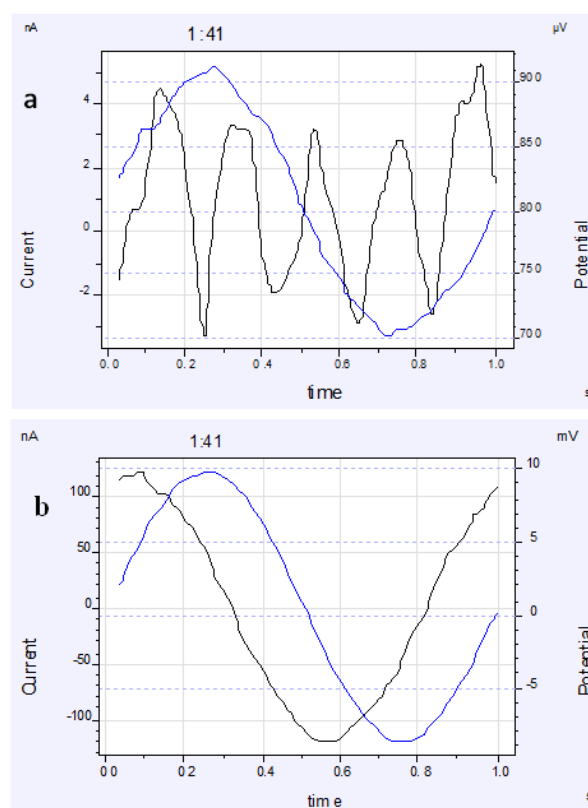


**Figure 4.** Voltage-current waveform at (a) 0.1 mV applied potential and (b) 10 mV applied potential.

investigated the impedance change at 1 Hz, 10 Hz and 100 Hz. Impedance change for antigen-antibody was found to be maximum at 10 Hz as shown in Figure 3. Thus 10 Hz was chosen for quantitative analysis of *E.coli* bacteria.

##### 3.1.3. Influence of applied potential

In impedance immunosensor the applied voltage/Potential should be quite small, usually 10 mV or lesser since the current voltage relationship is often linear for small perturbations [29]. The impedance measurement were conducted for different applied potential from 0.1 mV to 10 mV. It was observed that at low applied potential, the current voltage waveform is distorted, whereas a better response was found at 10 mV applied potential as depicted in Figure 4. Stable and non-distorted waveform at 10 mV, validate fruitful impedance measurement. Thus, this applied potential was chosen for impedance measurement for quantitative analysis of *E.coli* bacteria in water.

#### 3.2. Selection of SAMs for binding of *E.coli*

Well-established protocols for SAMs were used for optimization of surface modification to immobilize pAb-*E.coli* on the Ag-wire electrode surface, with slight modifications. 11-MUA [23], CYST [28] and L-cysteine [30] SAMs were tested for the immobilization of pAb-*E.coli* on the electrode surface. The concentrations of different surface modifiers and cross-linkers were optimized and pAb-*E.coli* antibody was attached to the surface. The SAM based on CYST showed the maximum % Impedance change for the binding of *E. coli* to pAb-*E.coli* antibody, thus the further experiments were carried out using CYST. Figure 5 represents the % Impedance change with respect to different *E.coli* concentrations obtained with different SAM's.

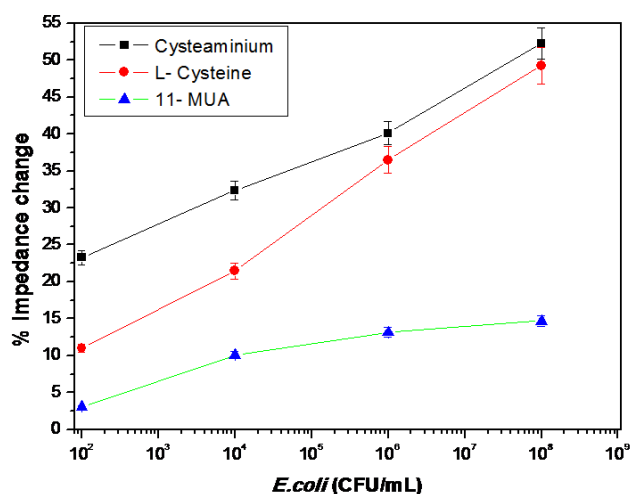


**Figure 5.** Percentage impedance change for different self-assembled monolayers (Cysteaminium, L-Cysteine and 11-MUA) for different concentrations of *E. coli* ( $10^2$ – $10^8$  CFU/mL). EIS: 1–100 KHz applied frequency and 10 mV applied potential.

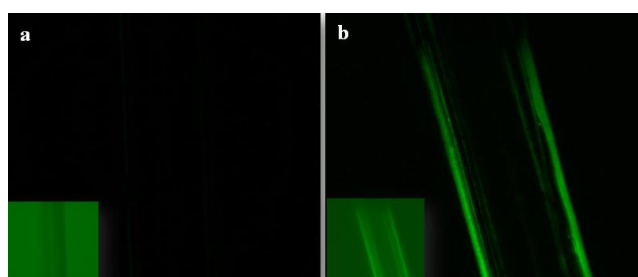


**Figure 6.** Surface characterization of pAb-*E. coli* modified electrodes using fluorescence microscopy (a) Image of control Ag-wire electrode, inset: non-subtracted background image of Ag-wire electrode (b) Image of pAb-*E. coli* coupled Ag-wire electrode attached with FITC labeled secondary *E. coli* antibody, inset: non-subtracted background image of Ag-wire electrode.

### 3.3. Surface characterization of pAb-*E. coli* modified electrodes

The binding of pAb-*E. coli* to Ag-wire electrodes was confirmed by fluorescence microscopy using IX71 inverted microscope (Olympus, Japan). Two functionalized Ag-wires (reference wire without pAb-*E. coli* and sample wire coupled with pAb-*E. coli*) were incubated with FITC labeled secondary antibody against *E. coli* (pAb-FITC) (1:1000) for 2 h at room temperature. Before excitation, both reference and the sample wire were rinsed with 0.1 M PBS to remove unbound pAb-FITC. Figure 6 (a) shows fluorescence image of reference and (b) the sample Ag wire, after excitation. It can be observed; the labeled secondary antibody specifically recognized the anti-*E. coli*, demonstrating an optimal immobilization of the primary capture antibodies to the activated SAM. The binding of the pAb-FITC to the pAb-*E. coli* of the thiolated Ag-wire is clearly distinguished from the fluorescence images.

### 3.4. EIS studies for bacterial binding

The antigen–antibody interaction of pAb-*E. coli* and *E. coli* Ag-wire electrode surface was studied using EIS. Figure 7 shows the impedance for different concentrations of *E. coli* ( $10^2$ – $10^8$  CFU/mL) in water resulted from interaction of antigen–antibody on functionalized electrode surface. EIS is a

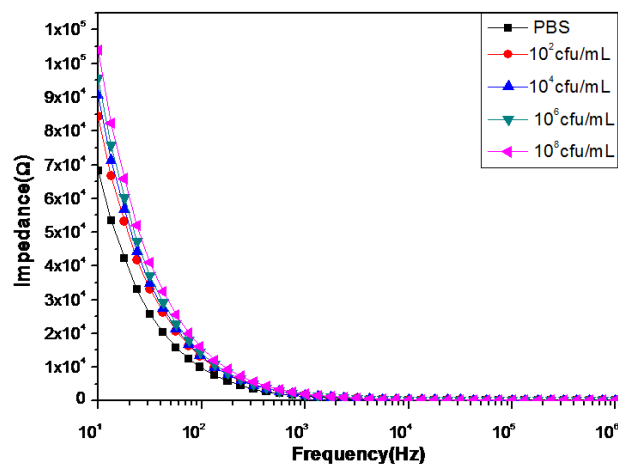


**Figure 7.** Impedance spectra for different concentrations of *E. coli* ( $10^2$ – $10^8$  CFU/mL) in water. EIS: 1–100 KHz applied frequency and 10 mV applied potential.

useful technique to capture such interaction. This interaction results in change of electrical properties such as capacitance and resistance at the electrode surface allowing for label-free biosensing [31]. The Impedance/capacitance change is commonly used as indicator of antigen–antibody interaction for non-faradic biosensor [32]. In the EIS measurement, pAb-*E. coli* interactions create a new charged layer as a capacitance that is in series with the double layer capacitance. A decreased double layer capacitance and increased impedance was observed at the lower frequency. This confirms that the change in impedance is resulting from binding of the antigen (*E. coli*). It is also clear from figure that the total impedance decreases linearly with the increasing frequency in the low frequency range from 10 Hz to 1 kHz, while it becomes independent of the frequency in the high frequency range from 1 kHz to 100 kHz. At low frequencies (<1 kHz), since the double layer capacitance offers essentially high impedance, it becomes the main component contributing to the total impedance, such that the medium resistance can be neglected. This region is defined as the double layer capacitive region in which the electrode impedance can be detected. When in the high frequency range (>1 kHz), the double layer capacitance almost offers no impedance, and its contribution to the total impedance is near zero. Thus, the only contribution to the total impedance at high frequencies is the medium resistance that is independent of the frequency. In the higher frequency region (10 Hz to 100 kHz) it was observed that impedance remains constant. A significant change was measurable in the low frequency region (10–1 kHz) with highest impedance change observed at 10 Hz.

### 3.5. Calibration of immunosensor for *E. coli* detection in water

The *E. coli* bacterial samples were spiked in water samples to meet the calibration standards. Before spiking the standards, water was filtered through the bacteriological membrane filter (0.22 μm) and tested for presence of any other *E. coli* strain i.e. *E. coli* O157:H7 using Singlepath® *E. coli* O157, a gold labeled immuno sorbent assay (GLISA) rapid test (obtained from Merck-Millipore, Germany). Impedance data were recorded for the functionalized electrodes after exposing it to increasing *E. coli* concentration ( $10^2$ – $10^8$  CFU/mL) in

**Table 1.** Analytical results for actual water samples analyzed using developed immunosensor.

Tested Samples	Impedance ( $\Omega$ )
Blank	$6.68 \times 10^4$
<i>E. coli</i> MTCC 723 $10^2$ CFU/mL	$8.42 \times 10^4$
<i>E. coli</i> MTCC 723 $10^4$ CFU/mL	$9.06 \times 10^4$
<i>E. coli</i> MTCC 723 $10^6$ CFU/mL	$9.57 \times 10^4$
<i>E. coli</i> MTCC 723 $10^8$ CFU/mL	$10.4 \times 10^4$
Water sample-I	$3.88 \times 10^4$
Water sample-II	$1.51 \times 10^4$
Water sample-III	$1.966 \times 10^4$
Water sample-IV	$2.056 \times 10^4$

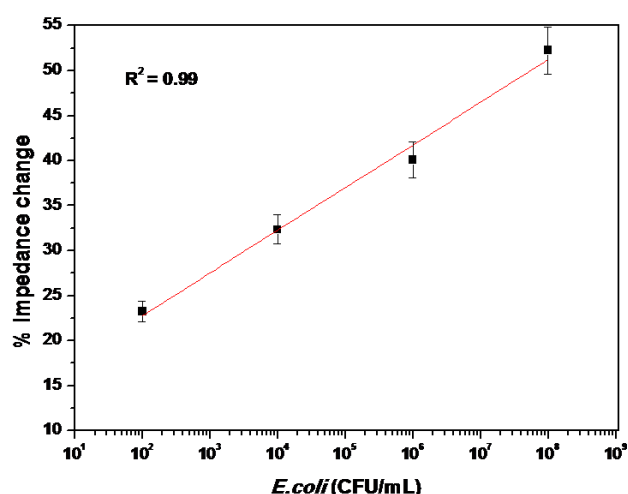


**Figure 8.** Calibration curve obtained for label-free impedimetric immunosensor for *E. coli* in water, linear range for *E. coli* detection  $10^2$ – $10^8$  CFU/mL with SD=0.802 and  $R^2=0.99$ . Limit of detection =  $10^2$  CFU/mL. EIS: 1–100 KHz applied frequency and 10 mV applied potential.

water. A frequency of 10 Hz at applied potential 10 mV was selected for analysis since at this frequency significant change in impedance response was observed. The specific interaction of pAb-*E. coli* and *E. coli* gave rise to an overall increase in impedance change from baseline response at the electrode/solution interface for *E. coli* concentrations. The % impedance change was calculated corresponding to different concentrations of *E. coli*. The resulting calibration curve in water is shown as Figure 8. A linear range for *E. coli* detection  $10^2$ – $10^8$  CFU/mL with SD=0.802 and  $R^2=0.99$  was achieved. Limit of detection (LOD) was  $10^2$  CFU/mL and sensitivity of the immunosensor is found to be 4.73. Actual water samples were tested for the presence of *E. coli* using the developed immunosensor and compared with the spiked water sample with different concentrations of *E. coli* (MTCC 723) as

presented in Table 1. For comparison the impedance value at 10 Hz were considered. All the tested water samples were found free of *E. coli*. Several examples of impedimetric immunosensor for the detection of different *E. coli* strains are reported in the literature. Lu *et al* achieved LOD of  $10^3$  CFU/mL for *E. coli* K12 using gold-tungsten micro-wire based three electrode EIS system with  $10^3$ – $10^8$  CFU/mL linear range [12]. Li *et al* achieved LOD of  $10^3$  CFU/mL of *E. coli* 0157:H7 using ferrocene-peptide conjugates based three-electrode EIS system with  $10^3$ – $10^7$  CFU/mL linear range [33]. The lowest LOD for *E. coli* 0157:H7 reported by Barreiros dos Santos *et al* is 2 CFU/mL using three electrode EIS system using gold disc as working electrode, they have achieved linear range of  $3 \times 10^3$ – $3 \times 10^4$  CFU/mL [13]. Settingington *et al* described a novel approach for detection of *E. coli* 0157:H7 using cyclic voltammetry in combination with immunomagnetic separation and achieved LOD of 6 CFU/mL from the pure culture in concentration range  $10^0$ – $10^2$  CFU/mL [34]. Among the reported EIS techniques, the immunosensor reported by us is rapid and low cost for detection of *E. coli* in water with a good linear range.

### 3.6. Sensing specificity of the immunosensor

The specificity of the immunosensor towards *E. coli* was tested against *Salmonella infantis* and *Streptococcus pyogenes* MTCC 1928. All the bacterial suspensions were taken at  $10^4$  CFU/mL. The impedance measurements were carried out at frequency range of 1 Hz to 100 KHz using EIS at 10 mV applied potential. In the optimized condition, the response signal for pAb-*E. coli* binding with bacterial suspension was measurable in 10 min. Results are presented as Nyquist plot in Figure 9. From the Nyquist plot, it is clear that the imaginary part (capacitive reactance) increased by 20% for binding of *E. coli* with pAb-*E. coli* as compared to *Salmonella infantis* and *Streptococcus pyogenes*. The response of *Salmonella infantis* and *Streptococcus pyogenes* towards pAb-*E. coli* can be attributed to non-specific adsorption on the Ag-wire electrode surface.

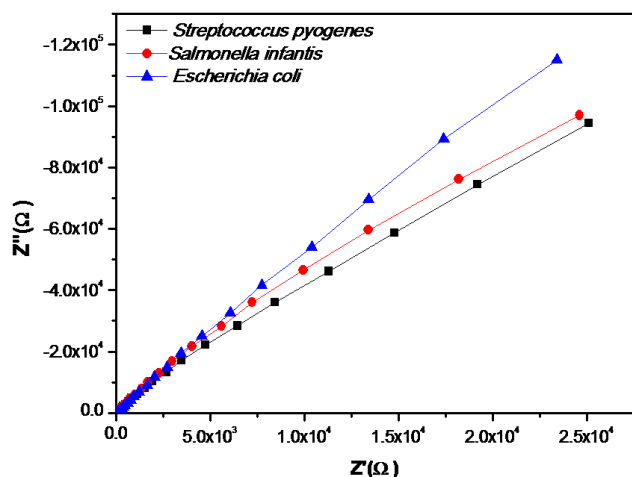


**Figure 9.** Nyquist plot for sensing specificity of the functionalized Ag-wire immunosensor validated for *E.coli* against *Salmonella infantis* and *Streptococcus pyogenes*. Concentrations of bacterial suspensions are  $10^4$  CFU/mL. EIS: 1-100 KHz applied frequency and 10 mV applied potential.

#### 4. Conclusions

In the presented work, a label free impedemetric immunosensor for rapid detection of *E.coli* MTCC 723 in water sample is developed and demonstrated. For biosensor development, polyclonal antibody against *E.coli* was immobilized over the SAMs of cysteaminium. Sensitivity and specificity of the developed immunosensor were evaluated by monitoring the changes in electrochemical impedance of the Ag-wire after bacterial cells were deposited on its surface. A linear trend of increasing impedance was obtained when the *E. coli* concentration increased from  $10^2$  to  $10^8$  CFU/mL. EIS analysis has proved that the developed immunosensor was able to detect  $10^2$  to  $10^8$  CFU/mL *E. coli* in water samples. The developed immunosensor is specific for detection of *E.coli*. The sensor does not require any additional reagents such as fluorescent or enzyme labels for sensor response and showed stable signals. Development of the presented immuno-sensor also supports that the label-free approaches may become practical for routine analysis of bacterial contamination in water.

#### Acknowledgements

This work is financially supported through Centre of Research Excellence in Water, Waste and Energy Management (CORE WWEM) funded by BITS, Pilani. G.B. would like to acknowledge Director, BITS Pilani-K.K. Birla Goa Campus.

#### References

1. A. Fenwick, Science 313 (2006) 1077.
2. J. P. S. Cabral, Int. J. Environ. Res. Public Health 7 (2010) 3657.

3. J. Min, A. J. Baeumner, Anal. Biochem. 303 (2002) 186.
4. S. Ram, P. Vajpayee, R. Shanker, Environ. Sci. Technol. 42 (2008) 4577.
5. D. R. Shelton, J. S. Karns, J. A. Higgins, J. A. S. Van Kessel, M. L. Perdue, K. T. Belt, J. Russell-Anelli, C. Deb Roy, FEMS Microbiol. Lett. 261 (2006) 95.
6. R. Maalouf, C. Fournier-Wirth, J. Coste, H. Chebib, Y. Saikali, O. Vittori, A. Errachid, J. P. Cloarec, C. Martelet and N. Jaffrezic-Renault, Anal. Chem. 79 (2007) 4879.
7. L. P. Mansfield, S. J. Forsythe, Food Microbiol. 18 (2001) 361.
8. W. Chen, G. Martinez, A. Mulchandani, Anal. Biochem. 280 (2000) 166.
9. H. P. Dwivedi, L. A. Jaykus, Crit. Rev. Microbiol. 37 (2011) 40.
10. J. J. Yu, L. D. Xiao and M. Yang, IEEE MEMS conferenc (2008) p. 272.
11. E. Heyduk, T. Heyduk, Anal. Biochem. 396 (2010) 298.
12. L. Lu, G. Chee, K. Yamada, S. Jun, Biosens. Bioelectron. 42 (2013) 492.
13. M. Barreiros dos Santos, J. P. Aguil, B. Prieto-Simón, C. Sporer, V. Teixeira, J. Samitier, Biosens. Bioelectron. 45 (2013) 174.
14. X. Guo, C. S. Lin, S. H. Chen, R. Ye, V. C. Wu, Biosens. Bioelectron. 38 (2012) 177.
15. H. Baccar, M. B. Mejri, I. Hafaiedh, T. Ktari, M. Aouni, A. Abdelghani, Talanta 82 (2010) 810.
16. W. C. Liao, J. A. Ho, Anal. Chem. 81 (2009) 2470.
17. J. Heo, S. Z. Hua, Sensors 9 (2009) 4483.
18. A. Bogomolova, E. Komarova, K. Reber, T. Gerasimov, O. Yavuz, S. Bhatt, M. Aldissi, Anal. Chem. 81 (2009) 3944.
19. C. Berggren, B. Bjarnason, G. Johansson, Biosens. Bioelectron. 13 (1998) 1061.
20. C. J. Felice, R. E. Madrid, J. M. Olivera, V. I. Rotger, M. E. Valentinuzzi, J. Microbiol. Methods 35 (1999) 37.
21. S. M. Radke, E. C. Alocilja, IEEE Sens. J. 4 (2004) 434.
22. R. B. Queirós, N. de-los-Santos-Álvarez, J. P. Noronha, M. G. F. Sales, Sens. Actuat. B 181 (2013) 766.
23. I-S Park, D-K Kim, N. Adanyi, M. Varadi, N. Kim, Biosens. Bioelectron. 19 (2004) 667.
24. M. Varshney, Y. Li, Biosens. Bioelectron. 22 (2007) 2408.
25. M. Varshney, Y. Li, B. Srinivasan, S. Tung, Sens. Actuat. B 128 (2007) 99.
26. D. A. Boehm, P. A. Gottlieb, S. Z. Hua, Sens. Actuat. B 126 (2007) 508.
27. G. Bacher, S. Pal, L. Kanungo, S. Bhand, Sens. Actuat. B 168 (2012) 223.
28. M. M. Pedroso, A. M. Watanabe, M. C. Roque-Barreira, P. R. Bueno, R. C. Faria, Microchem. J. 89 (2008) 153.
29. G. Barbero, A. L. Alexe-Ionescu, I. Lelidis, J. Appl. Phys. 98 (2005) 113703.
30. L. Zhang, Y. Liu, T. Chen, Microchim. Acta 164 (2009) 161.
31. J. G. Guan, Y. Q. Miao, Q. J. Zhang, J. Biosci. Bioeng. 97 (2004) 219.
32. J. S. Danielsa, N. Pourmand, Electroanalysis 19 (2007) 1239.
33. Y. Li, R. Afrasiabi, F. Fathi, N. Wang, C. Xiang, R. Love, Z. She, H. B. Kraatz, Biosens. Bioelectron. 58 (2014) 193.
34. E. B. Settingington, E. C. Alocilja, Biosensors 2 (2012) 15.

#### Cite this article as:

Geetesh K Mishra *et al.*: A label free impedemetric immunosensor for detection of *Escherichia coli* in water. *Chemical Sensors* 2015, 5: 4